Functional renormalization group approach to classical and quantum spin systems

Dissertation
zur Erlangung des Doktorgrades
der Naturwissenschaften

vorgelegt beim Fachbereich Physik
der Johann Wolfgang Goethe-Universität
in Frankfurt am Main

von
Jan Krieg
aus
Ludwigshafen am Rhein

Frankfurt (2019)
(D30)

vom Fachbereich Physik der
Johann Wolfgang Goethe-Universität
als Dissertation angenommen.

Dekan: Prof. Dr. Michael Lang

Gutachter: Prof. Dr. Peter Kopietz
Prof. Dr. Roser Valentí
Dr. Adam Rançon

Datum der Disputation: 06.12.2019

Contents

Abstract

The present thesis is primarily concerned with the application of the functional renormalization group (FRG) to spin systems. In the first part, we study the critical regime close to the Berezinskii-Kosterlitz-Thouless (BKT) transition in several systems. Our starting point is the dual-vortex representation of the two-dimensional XY model, which is obtained by applying a dual transformation to the Villain model. In order to deal with the integer-valued field corresponding to the dual vortices, we apply the lattice FRG formalism developed by Machado and Dupuis [Phys. Rev. E **82**, 041128 (2010)]. Using a Litim regulator in momentum space with the initial condition of isolated lattice sites, we then recover the Kosterlitz-Thouless renormalization group equations for the rescaled vortex fugacity and the dimensionless temperature. In addition to our previously published approach based on the vertex expansion [Phys. Rev. E **96**, 042107 (2017)], we also present an alternative derivation within the derivative expansion. We then generalize our approach to the $O(2)$ model and to the strongly anisotropic XXZ model, which enables us to show that weak amplitude fluctuations as well as weak out-of-plane fluctuations do not change the universal properties of the BKT transition.

In the second part of this thesis, we develop a new FRG approach to quantum spin systems. In contrast to previous works, our spin functional renormalization group (SFRG) does not rely on a mapping to bosonic or fermionic fields, but instead deals directly with the spin operators. Most importantly, we show that the generating functional of the irreducible vertices obeys an exact renormalization group equation, which resembles the Wetterich equation of a bosonic system. As a consequence, the non-trivial structure of the $\mathfrak{su}(2)$ algebra is fully taken into account by the initial condition of the renormalization group flow. Our method is motivated by the spin-diagrammatic approach to quantum spin system that was developed more than half a century ago in a seminal work by Vaks, Larkin, and Pikin (VLP) [Sov. Phys. JETP **26**, 188 (1968)]. By embedding their ideas in the language of the modern renormalization group, we avoid the complicated diagrammatic rules while at the same time allowing for novel approximation schemes.

As a demonstration, we explicitly show how VLP's results for the leading corrections to the free energy and to the longitudinal polarization function of a ferromagnetic Heisenberg model can be recovered within the SFRG. Furthermore, we apply our method to the spin-S Ising model as well as to the spin-S quantum Heisenberg model, which allows us to calculate the critical temperature for both a ferromagnetic and an antiferromagnetic exchange interaction. Finally, we present a new hybrid formulation of the SFRG, which combines features of both the pure and the Hubbard-Stratonovich SFRG that were published recently [Phys. Rev. B **99**, 060403(R) (2019)].

Chapter 1

Introduction

1.1 Overview

The purpose of the first chapter is to lay the foundation for the main part of this thesis. We start with an introduction to the renormalization group in Sec. 1.2, where we present an overview on its historical development as well as on its main concepts. In Sec. 1.3 we then give a short primer on the imaginary-time formalism, which will be a central building block in the development of the spin functional renormalization group in Ch. 3.

The second chapter is devoted to the Berezinskii-Kosterlitz-Thouless (BKT) transition, whose main features are illustrated in Sec. 2.1 in the context of the two-dimensional XY model. After introducing the Villain model as well as several of its dual representations in Sec. 2.2, we show in Sec. 2.3 how the functional renormalization group can be applied to the dual-vortex representation. The explicit derivation of the Kosterlitz-Thouless flow equations within the vertex expansion is given in Sec. 2.4, while in Sec. 2.5 we present an alternative derivation based on the derivative expansion. We then generalize our approach to the $O(2)$ model (Sec. 2.6) and to the strongly anisotropic XXZ model (Sec. 2.7), where we study the influence of amplitude and out-of-plane fluctuations on the BKT transition.

Finally, Ch. 3 is concerned with our work on the spin functional renormalization group (SFRG), which we briefly motivate in Sec. 3.1. We then construct the pure SFRG and apply it to the spin-S Ising model in Sec. 3.2. We end this section by discussing several possibilities for the initial condition of the renormalization group flow in quantum spin systems. In Sec. 3.3 we develop an alternative formulation of the SFRG and illustrate that this Hubbard-Stratonovich SFRG is closely connected to the spin-diagrammatic approach of Vaks, Larkin, and Pikin (VLP) [1–3]. We demonstrate the method by rederiving some results of VLP as well as by calculating the critical temperature of the spin-S quantum Heisenberg model. We conclude the chapter by developing a hybrid version of the pure and the Hubbard-Stratonovich SFRG in Sec. 3.4.

Note that throughout the thesis we will set $k_B = \hbar = 1$ to simplify the notation. Unless specifically stated otherwise, we will also assume (discrete) translational invariance in time and space.

1.2 Renormalization group

1.2.1 Historical overview

Perturbative renormalization

To understand the origins of the modern renormalization group, one has to go back to the early days of quantum field theory. This discipline was born 1927 when Dirac formulated a quantum theory of electrodynamics (aptly called quantum electrodynamics by him) by coupling the electric current density to a quantized version of the electromagnetic field, which he described as a system of quantized oscillators [4]. Within a leading-order perturbative calculation, this theory enabled Dirac to explain the phenomenon of spontaneous emission as well as photon scattering processes, resonance fluorescence, and non-relativistic Compton scattering of photons by electrons [5]. It quickly turned out, however, that higher-order terms are always riddled with infinities [6], since the corresponding Feynman diagrams involve closed loops which correspond to ultraviolet divergent integrals over arbitrarily high momenta. Nevertheless, as the leading-order results were good enough for the experimental accuracy at that time, it was possible to ignore this issue for a while [5].

Being unsolved for almost twenty years, a new impetus to tackle the problem of the ultraviolet divergences came from the experimental results of Lamb and Retherford, who showed that the $2S_{1/2}$ and the $2P_{1/2}$ states of hydrogen correspond to different energy levels [7]. While the Dirac equation predicted these states to be exactly degenerate, they found that the $2S_{1/2}$ state has a slightly higher energy with $\Delta E \approx 4.37 \times 10^{-6}$ eV (Lamb shift). Shortly after this observation had been discussed at the Shelter Island conference in 1947, Bethe managed to derive the Lamb shift by taking the interaction of the electron with the radiation field into account and effectively introducing an ultraviolet cutoff of the order of $m_e c^2$ [8]. Since most of the effect is due to photons of lower energy, the relative error of his result was below two per cent. About two years later, Kroll and Lamb [9] as well as French and

Weisskopf [10] managed to improve on this by calculating perturbatively the exact contribution to the Lamb shift up to lowest order in $e^2/\hbar c$. Although these authors managed to arrive at a finite result by subtracting the divergent terms, the methods to achieve this were "clumsy and unreliable" [5]. It was only through the work of Tomonaga, Schwinger, and Feynman that a reliable way of dealing with the infinities emerged, winning them the Physics Nobel prize in 1965; their approaches were subsequently unified by Dyson [11]. In essence, the idea consists of introducing counterterms at each order of the perturbative expansion in such a way that all infinities are cancelled; most importantly, the exact form of these counterterms can be fixed in quantum electrodynamics through a finite number of experimental measurements, which allows to calculate higher-order contributions to electromagnetic effects in an unambiguous way [11]. This method of perturbative renormalization marks the beginning of the modern renormalization group and will be described in more detail in Sec. 1.2.2.

Renormalization group

Although it was now possible to calculate observables like the Lamb shift or the g-factor of the electron perturbatively to a high precision, the situation was not really satisfying. On the one hand, there was evidence that the meson coupling constants[1] are of order unity, while on the other hand even in quantum electrodynamics there are domains in momentum space where the effective coupling can grow to infinity, making non-perturbative considerations necessary [14]. An important step in this direction was made by Stückelberg and Petermann [15, 16], who found that finite renormalization transformations of scattering-matrix elements form a Lie group and thus obey differential equations. Seemingly unaware of their work, Gell-Mann and Low [17] independently considered scale transformations in QED and showed that the electromagnetic coupling changes with the energy scale according to a differential equation, which in modern parlance is known as a beta function. These ideas were further developed by Bogolyubov and Shirkov [14]; the title of their paper "Charge Renormalization Group in Quantum Field Theory" marks the first appearance of the term renormalization group (RG).

Wilsonian RG

While these works resulted in useful techniques to analyze quantum field theories, their importance was not recognized for many years. The renormal-

[1] The concept of quarks was only developed more than a decade later in 1964 by Gell-Mann [12] and by Zweig [13].

ization group only seemed to provide information about the large-momentum regime; however, asymptotic freedom had not been discovered yet, so that the general consensus at this time was that all quantum field theories are strongly interacting in the short-distance limit. Without a good alternative to perturbation theory, it thus seemed that the renormalization group merely allowed for discussing, but not calculating, the asymptotic behaviour of quantum field theories in a physically uninteresting regime [18]. It was only in the beginning of the 1970s that Wilson provided a conceptual framework for the renormalization group and thus revolutionized the way we think about the scale dependence of physical theories [19–22]. In a seminal work [19, 20], he cast Kadanoff's "block spin" transformation [23] of an Ising ferromagnet into a differential form and subsequently generalized the approach to momentum space (see Sec. 1.2.3 for details). This allowed Wilson to connect the renormalization group to second-order phase transitions and to analyze the critical regime in a simple way.

Moreover, his work not only provided an extremely powerful technique to describe criticality in condensed matter systems, but it also had a significant impact on the interpretation of quantum field theories by comparing them with condensed matter systems. Since these systems are usually formulated on a lattice, the inverse lattice parameter $1/a$ acts as a ultraviolet cutoff. It is thus natural to interpret it as the energy scale where the model ceases to be meaningful; e.g., the Heisenberg model can only be expected to give a reasonable description of real magnetic materials at length scales much larger than a, while at shorter length scales it has to be superseded by a more fundamental theory. In this sense, the Heisenberg model constitutes an effective theory to describe the low-energy physics of the real material. By applying this point of view to quantum field theory, we see that the standard model should really be interpreted as an effective model; it constitutes the low-energy limit of some yet unknown physics. The necessity of introducing a finite ultraviolet cutoff Λ_0 that was hitherto seen as unphysical is easily explained by this: Λ_0 just represents the energy scale where the standard model ceases to be valid. Insisting on sending Λ_0 to infinity thus corresponds to the (rather bold) claim that our theory is valid at arbitrarily high energies. Furthermore, this point of view explains why the standard model is renormalizable (see Sec. 1.2.3 for details) [22, 24].

In addition to these conceptual points, Wilson also indirectly contributed to the discovery of asymptotic freedom in non-Abelian gauge theories by Gross and Wilczek [25] and by Politzer [26] by reviving the renormalization group formalism [18]. This led to the rehabilitation of quantum field theory, which was seen as suspect due to the apparent inevitability of a diverging coupling constant in the ultraviolet regime [27]. With respect to condensed matter physics, a very impressive practical contribution was Wilson's solution of the Kondo model using a formulation of the RG that combines its formal aspects with numerical calculations (today known as numerical renormalization group), which allowed him to arrive at quantitatively accurate results [28, 29]. While Anderson, Yuval, and Hamann [30] and Anderson [31] had previously succeeded in describing the weak-coupling regime of the Kondo model, Wilson's approach also covered the strong-coupling as well as the intermediate regime.

Functional RG

As mentioned above, Wilson's original idea [19] of implementing the renormalization procedure was based on Kadanoff's "block spin" transformation [23], where one groups nearby spins into so-called blocks and treats these blocks as single effective spins by averaging over their constituents. In practice, however, it is usually better to work in momentum space and to successively eliminate degrees of freedom whose wavevector lies inside a given interval; technically, Wilson realized this by dividing the momentum space into finite-sized spherical shells [20]. Shortly after the publication of Wilson's ideas, it was realized by Wegner and Houghton [32] that by making the momentum-space shells infinitely thin, one can derive an exact functional differential equation (Wegner-Houghton equation) that describes how the effective action of the model evolves with respect to the cutoff Λ. Conceptually, this was an important result; unfortunately, the momentum shell procedure can lead to technical complications due to the non-analyticity of a sharp momentum cutoff [33]. A significant improvement was made about ten years later by Polchinski, who formulated the renormalization group using functional integrals and introduced a general momentum cutoff [24]. Again a decade later, Wetterich [34] brought the functional renormalization group (FRG) into its modern form by introducing the average effective action. Defined as the Legendre transform of the generating functional of the connected Green functions, it generates the vertices that are irreducible with respect to the cutting of a single propagator line. Its behaviour under an infinitesimal change in the cutoff is given by the Wetterich equation, which nowadays usually constitutes the starting point for practical calculations in bosonic or fermionic systems [33].

1.2.2 Perturbative renormalization

Introduction

To shed more light on the technical details of perturbative renormalization, we will in the following demonstrate the concept by means of a simple example. As already mentioned in Sec. 1.2.1, the idea consists in renormalizing an ill-defined perturbative expansion via the introduction of suitable counterterms. Following Ref. [35], we consider an unspecified theory depending on a free parameter g_0, which we will call the bare coupling constant. We further assume that we are interested in calculating some function $F(x)$, which corresponds to an observable like a correlation function or the cross section of a scattering process. Expanding this function in powers of g_0 results in the general expression [up to a trivial redefinition of $F(x)$]

$$F(x) = g_0 + g_0^2 F_1(x) + g_0^3 F_2(x) + O(g_0^4). \tag{1.1}$$

The point is now that the coefficients in this Taylor expansion can be divergent; in practice, these divergences usually result from loop diagrams that correspond to ultraviolet-divergent integrals. A simple example is given by the integral

$$F_1(x) = \alpha \int_0^\infty \frac{dk}{k+x}, \tag{1.2}$$

which exhibits a logarithmic divergence as is common in renormalizable theories like the standard model. While the expansion (1.1) is then obviously pathological, this does not necessarily mean that a perturbative expansion of $F(x)$ is impossible; it might just be the case that expanding in the bare coupling g_0 is problematic. We therefore measure $F(x)$ experimentally at a single point $x = \mu$ and use the data to define the renormalized coupling constant g_{R},

$$F(\mu) = g_{\mathrm{R}}. \tag{1.3}$$

In order to replace the bare coupling constant in Eq. (1.1) by the renormalized one, we first have to ensure the existence of the expansion (1.1) by regularizing it. In general we thus write

$$F_\Lambda(x) = g_0 + g_0^2 F_{\Lambda,1}(x) + g_0^3 F_{\Lambda,2}(x) + O(g_0^4), \tag{1.4}$$

where Λ is an auxiliary parameter that deforms our theory such that all coefficients $F_{\Lambda,i}$ are well defined and we recover the original theory for $\Lambda \to \infty$. A simple choice would be

$$F_{\Lambda,1}(x) = \alpha \int_0^\Lambda \frac{dk}{k+x} = \alpha \ln\left(\frac{\Lambda + x}{x}\right), \tag{1.5}$$

where Λ acts as an ultraviolet cutoff. Note that in practice it is often advisable to use other schemes like dimensional regularization that preserve the symmetries of the theory at hand.

First- and second-order correction

Since the expansion (1.4) is well defined, we can now start the renormalization procedure. Since to leading order

$$F_\Lambda(x) = g_0 + O(g_0^2), \tag{1.6}$$

we directly see from condition (1.3) that

$$g_0 = g_\mathrm{R} + O(g_\mathrm{R}^2). \tag{1.7}$$

Up to this order it is trivial to take the limit $\Lambda \to \infty$ so that

$$F(x) = g_\mathrm{R} + O(g_\mathrm{R}^2). \tag{1.8}$$

The next-to-leading order is more interesting. Defining $\delta_2 g$ as the subleading term in the expansion

$$g_0 = g_\mathrm{R} + \delta_2 g + O(g_\mathrm{R}^3), \tag{1.9}$$

we can write

$$F_\Lambda(x) = g_\mathrm{R} + \delta_2 g + g_\mathrm{R}^2 F_{\Lambda,1}(x) + O(g_\mathrm{R}^3). \tag{1.10}$$

To fix the counterterm $\delta_2 g$, we set $x = \mu$ and again make use of condition (1.3) to find

$$\delta_2 g = -g_\mathrm{R}^2 F_{\Lambda,1}(\mu), \tag{1.11}$$

which immediately yields

$$F_\Lambda(x) = g_\mathrm{R} + g_\mathrm{R}^2 \left[F_{\Lambda,1}(x) - F_{\Lambda,1}(\mu)\right] + O(g_\mathrm{R}^3). \tag{1.12}$$

For the specific case (1.5) we can write this as

$$F_\Lambda(x) = g_\mathrm{R} + g_\mathrm{R}^2 \alpha \ln\left[\frac{(\Lambda + x)\mu}{(\Lambda + \mu)x}\right] + O(g_\mathrm{R}^3), \tag{1.13}$$

which is still well defined in the limit $\Lambda \to \infty$,

$$F(x) = g_\mathrm{R} + g_\mathrm{R}^2 \alpha \ln\left(\frac{\mu}{x}\right) + O(g_\mathrm{R}^3). \tag{1.14}$$

General remarks

Note that it is only possible to remove the cutoff in our second-order result (1.12) if the limit

$$\Delta F_1(x,\mu) = \lim_{\Lambda\to\infty} \left[F_{\Lambda,1}(x) - F_{\Lambda,1}(\mu)\right] \tag{1.15}$$

exists for all x. This is not always the case; a simple counterexample is given by

$$F_{\Lambda,1}(x) = \alpha \int_1^\Lambda dk\, \frac{k}{k+x}, \tag{1.16}$$

which diverges linearly. Setting $\mu = 0$ for simplicity so that our condition (1.3) becomes

$$F(0) = g_\mathrm{R}, \tag{1.17}$$

we find that

$$F_{\Lambda,1}(x) - F_{\Lambda,1}(\mu) = (\mu - x)\alpha \int_1^\Lambda dk\, \frac{k}{(k+x)(k+\mu)}. \tag{1.18}$$

Although the linear divergence has been weakened to a logarithmic one, we still cannot remove the cutoff. This is only possible if our theory contains another free parameter that we can then use to get rid of the remaining logarithmic divergence. Generalizing this point to higher orders in the perturbative renormalization, we find that there are two main possibilities: on the one hand, it might turn out that a finite number of free parameters is sufficient to remove, order by order, all divergences that appear. In this case we say that the theory is renormalizable; a specific example of this behaviour is quantum electrodynamics, where only two parameters (mass and electric charge) have to be renormalized [11]. On the other hand, it is possible that divergences in higher-order terms can only be removed by introducing an ever increasing number of free parameters. Since this necessitates an infinite number of experimental measurements to fully define the theory, we say that it is non-renormalizable. It therefore seems rather fortunate that the structure of the standard model is such that the theory is renormalizable; however, as we will see in Sec. 1.2.3, this follows naturally from a Wilsonian point of view.

1.2.3 Wilsonian renormalization group

Setup

While the Wilsonian RG is related to the perturbative renormalization as discussed in the previous section, it differs significantly in appearance as

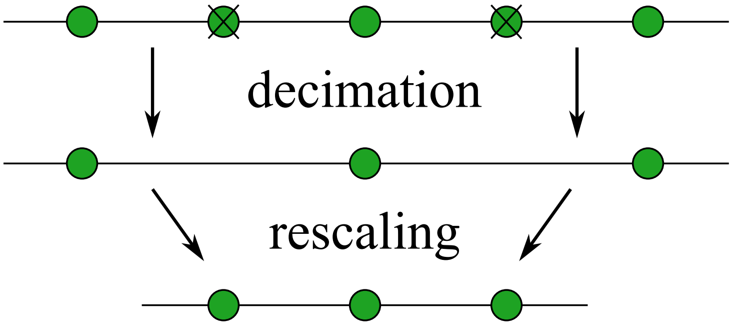

Figure 1.1: Schematic representation of Wilson's RG procedure in real space.

well as in its interpretation. The basic idea is to start from a microscopic model and to iteratively eliminate degrees of freedom. A single iteration of the Wilsonian RG consists of two steps: first we eliminate a subset of the degrees of freedom by integrating over them or by taking a partial trace (decimation). Intuitively, this has the effect of "zooming out" of the system. After the decimation has been performed, we then rescale all length scales such that the lattice parameter has again the original size. This rescaling is important since it makes it possible to encounter fixed points, where the system is invariant under the combined action of decimation and rescaling. A graphical representation of this procedure is shown in Fig. 1.1. While it is possible to perform the decimation and rescaling steps in real space (known as Migdal-Kadanoff RG [36, 37]), it is usually more efficient to work in momentum space. More explicitly, let us assume that we are interested in calculating the partition function [33]

$$\mathcal{Z}(\boldsymbol{g}) = \int D[\varphi]\, e^{-S[\varphi,\boldsymbol{g}]}, \tag{1.19}$$

where $S[\varphi, \boldsymbol{g}]$ is the action of the system under consideration. Here we have collected all coupling constants into the vector $\boldsymbol{g}$, while φ is a superfield that can comprise both bosonic and fermionic degrees of freedom. Furthermore, we perform an initial averaging over all microscopic fluctuations whose wavevectors $\boldsymbol{k}$ are larger than the UV cutoff Λ_0 [29]. In real space, this corresponds conceptually to dividing the system into regions of the size $(2\pi/\Lambda_0)^D$ and performing a statistical averaging over these regions. We thus rewrite Eq. (1.19) as

$$\mathcal{Z}(\boldsymbol{g}) = \int_0^{\Lambda_0} D[\varphi]\, e^{-S_{\Lambda_0}[\varphi,\boldsymbol{g}_{\Lambda_0}]}, \tag{1.20}$$

where the functional integral

$$\int_0^{\Lambda_0} D[\varphi] = \int D[\varphi^<_{\Lambda_0}] \tag{1.21}$$

by definition only involves fluctuations whose wavevectors fulfill $|\boldsymbol{k}| < \Lambda_0$. On a technical level, this can be done by separating the superfield φ into a long-distance part $\varphi^<_{\Lambda_0}$ and a microscopic part $\varphi^>_{\Lambda_0}$,

$$\varphi(\boldsymbol{k}) = \varphi^<_{\Lambda_0}(\boldsymbol{k}) + \varphi^>_{\Lambda_0}(\boldsymbol{k}). \tag{1.22}$$

Here $\varphi(\boldsymbol{k})$ are the Fourier components of the superfield φ and we use a sharp cutoff to realize the scale separation,

$$\begin{aligned} \varphi^<_{\Lambda_0}(\boldsymbol{k}) &= \Theta(\Lambda_0 - |\boldsymbol{k}|)\varphi(\boldsymbol{k}), \\ \varphi^>_{\Lambda_0}(\boldsymbol{k}) &= \Theta(|\boldsymbol{k}| - \Lambda_0)\varphi(\boldsymbol{k}). \end{aligned} \tag{1.23}$$

The important point is that Eq. (1.20) implicitly defines

$$e^{-S_{\Lambda_0}[\varphi^<_{\Lambda_0}, \boldsymbol{g}_{\Lambda_0}]} = \int_{\Lambda_0}^{\infty} D[\varphi]\, e^{-S[\varphi, \boldsymbol{g}]}, \tag{1.24}$$

where $S_{\Lambda_0}[\varphi^<_{\Lambda_0}, \boldsymbol{g}_{\Lambda_0}]$ characterizes our model at the microscopic scale Λ_0.

Decimation and rescaling

We are now in a position to define the decimation step of the RG procedure as

$$e^{-S_{\Lambda}[\varphi^<_{\Lambda}, \boldsymbol{g}_{\Lambda}]} = \int_{\Lambda}^{\Lambda_0} D[\varphi]\, e^{-S_{\Lambda_0}[\varphi^<_{\Lambda_0}, \boldsymbol{g}_{\Lambda_0}]}, \tag{1.25}$$

where we integrate over all fluctuations with wavevectors inside the momentum shell $\Lambda < |\boldsymbol{k}| < \Lambda_0$. All that is left to do is to properly rescale all variables. We therefore introduce the rescaled wavevector

$$\tilde{\boldsymbol{k}} = b\boldsymbol{k}, \tag{1.26}$$

where $b = \Lambda_0/\Lambda > 1$ is the step size of the RG transformation. In quantum systems we should also rescale the frequency as

$$\tilde{\omega} = b^z \omega, \tag{1.27}$$

where z is the dynamical critical exponent [33]. The rescaling of the superfield φ consists of two parts,

$$\tilde{\varphi}(\tilde{\boldsymbol{k}}) = b^{D_\varphi}\sqrt{Z_b}\varphi(\boldsymbol{k}). \tag{1.28}$$

Here D_φ is called the canonical (or engineering) dimension of φ, which can be easily derived by a dimensional analysis. The second factor $\sqrt{Z_b}$ arises due to interaction effects and is related to the anomalous dimension [33]. Finally, we express the action $S_\Lambda[\varphi_\Lambda^<, \boldsymbol{g}_\Lambda]$ in terms of the rescaled variables such that is has the same form as before the decimation step, which implicitly defines the rescaled coupling constants $\tilde{\boldsymbol{g}}_\Lambda$. We can therefore summarize the combined effect of decimation and rescaling as the RG transformation

$$\tilde{\boldsymbol{g}}_\Lambda = \mathcal{R}(b; \boldsymbol{g}_{\Lambda_0}). \tag{1.29}$$

However, since there is nothing special about the ultraviolet cutoff Λ_0, we can write this in the more general form

$$\tilde{\boldsymbol{g}}' = \mathcal{R}(b; \tilde{\boldsymbol{g}}), \tag{1.30}$$

which relates the coupling constants $\tilde{\boldsymbol{g}}$ at some scale Λ to the couplings constants $\tilde{\boldsymbol{g}}'$ at the lower scale $\Lambda' = \Lambda/b$. In general, $\mathcal{R}(b; \tilde{\boldsymbol{g}})$ is a complicated nonlinear function of the coupling constants. However, since a single RG transformation with the step size $b'' = b'b$ is by construction identical to two successive transformations with the step sizes b and b', we know that the functions $\mathcal{R}(b; \tilde{\boldsymbol{g}})$ fulfill the semigroup[2] property

$$\mathcal{R}(b'b; \tilde{\boldsymbol{g}}) = \mathcal{R}(b'; \mathcal{R}(b; \tilde{\boldsymbol{g}})). \tag{1.31}$$

Fixed points and universality

An important characteristic of the RG transformations $\mathcal{R}(b; \tilde{\boldsymbol{g}})$ is the existence of fixed points,

$$\tilde{\boldsymbol{g}}^* = \mathcal{R}(b; \tilde{\boldsymbol{g}}^*). \tag{1.32}$$

Since the correlation length ξ is rescaled as

$$\tilde{\xi} = \frac{\xi}{b} \tag{1.33}$$

under a single iteration of the Wilsonian RG and we require $\xi = \tilde{\xi}$ at a fixed point, it follows that there are exactly two classes of fixed points. One possibility is that the correlation length vanishes ($\xi = 0$); we then

[2]Since the Wilsonian RG involves the averaging over short-distance fluctuations, the transformation $\tilde{\boldsymbol{g}}_\Lambda$ cannot in general have an inverse; in this sense, the term renormalization group is a misnomer. Note that this argument does not apply to the modern FRG, where one introduces a regulator that depends continuously on the cutoff.

say that the fixed point is trivial. More interesting are critical fixed points where the correlation length diverges ($\xi = \infty$). These are encountered at a continuous phase transition, where fluctuations occur on all length scales. Setting $\tilde{\boldsymbol{g}} = \tilde{\boldsymbol{g}}^* + \delta\tilde{\boldsymbol{g}}$ and linearizing

$$\delta\tilde{\boldsymbol{g}}' = \tilde{\boldsymbol{g}}' - \tilde{\boldsymbol{g}}^* = \mathcal{R}(b;\tilde{\boldsymbol{g}}) - \mathcal{R}(b;\tilde{\boldsymbol{g}}^*) = \mathbf{R}(b;\tilde{\boldsymbol{g}}^*)\delta\tilde{\boldsymbol{g}} + O(\delta\tilde{\boldsymbol{g}}^2) \tag{1.34}$$

thus allows us to gain information about the critical regime by studying the quadratic matrix $\mathbf{R}(b;\tilde{\boldsymbol{g}}^*)$. In particular, it enables us to study the flow of the coupling constants close to the fixed point, which is closely related to the critical exponents that characterize a continuous phase transition [33]. On a technical level, we consider linear combinations of the coupling constants,

$$u_\alpha = \boldsymbol{v}_\alpha^{\mathrm{T}}\delta\tilde{\boldsymbol{g}} = \sum_i v_{\alpha,i}\delta\tilde{g}_i, \tag{1.35}$$

where the $\boldsymbol{v}_\alpha$ are left eigenvectors of $\mathbf{R}(b;\tilde{\boldsymbol{g}}^*)$. As a consequence, the scaling variables u_α do not mix under the linearized RG transformation (1.34). Using the semigroup property of the $\mathcal{R}(b;\tilde{\boldsymbol{g}})$, it is also straightforward to show that the eigenvalues $\lambda_\alpha(b)$ corresponding to the $\boldsymbol{v}_\alpha$ can be written as

$$\lambda_\alpha(b) = b^{y_\alpha}, \tag{1.36}$$

where the (in general real-valued) exponents y_α are independent of b. We thus arrive at the linearized flow equation of the scaling variables [33],

$$\partial_l u_\alpha = y_\alpha u_\alpha + O(u_\alpha^2), \tag{1.37}$$

where we have parametrized $b = e^l$. Since $u_\alpha^* = 0$ at the fixed point, the sign of y_α determines the qualitative behaviour of the flow of the scaling variables. For $y_\alpha > 0$ the associated scaling variable is called relevant, since it grows under the RG transformation. On the other hand, irrelevant scaling variables are related to a negative y_α. In the special case of $y_\alpha = 0$, the behaviour of the scaling variable is determined by the higher-order corrections in Eq. (1.37); this corresponds to marginally relevant and marginally irrelevant scaling variables, respectively.

As we will see in Ch. 2, this classification is directly useful for practical calculations as it allows us to study the critical regime by retaining only the relevant and marginal couplings. Furthermore, from a conceptual point of view, this shows how the phenomenon of universality[3] arises: while a microscopic model might depend on a large (possibly infinite) number of

[3]Universality refers to the fact that physical systems can exhibit the same critical behaviour although their underlying microscopic models are different.

coupling constants, it usually turns out that only a small number of them are relevant or marginal. In the critical regime close to a critical fixed point, almost all coupling constants flow to zero so that the macroscopic behaviour of the system can be characterized by a small number of parameters. With respect to quantum field theory, this also explains the renormalizability of the standard model by considering it as the long-distance limit of a more general theory [22]: since non-renormalizable couplings (i.e., irrelevant couplings with respect to an infrared fixed point) are strongly suppressed in the low energy regime, they can be neglected in this limit without significantly affecting the predictive power of the model. The seemingly fortunate fact that the perturbative renormalization procedure allowed to obtain finite results from quantum electrodynamics thus emerges in a natural way.

1.3 Imaginary-time formalism

In the following we will shift the focus away from the renormalization group and consider the imaginary-time formalism, which is also known as Matsubara formalism [38]. Since the functional renormalization group for spin operators as presented in Ch. 3 is formulated in terms of imaginary-time ordered Green functions, it seems appropriate to give a short introduction to this approach. The advantage of the Matsubara formalism is that it facilitates actual calculations by treating the statistical Boltzmann factor $e^{-\beta H}$ and the time-evolution operator e^{-itH} on the same footing. More specifically, in Sec. 3.2.1 it will allow us to write down the flow equation of the generating functional of connected spin correlators in a simple way. However, since experimentally only real times are relevant, results within the Matsubara formalism do not directly correspond to observables. In the present section, we will therefore motivate this approach by showing how imaginary-time ordered Green functions are related to physical quantities.

1.3.1 Experimental motivation

Linear response theory and retarded Green functions

In condensed matter physics, one is often interested in the response of a system to external perturbations driving it out of equilibrium. While working with many-body systems far from equilibrium is in general difficult, it is in many cases sufficient to assume weak perturbations and to linearize around the equilibrium state. This is achieved within linear response theory. As we will see, the corresponding response functions (magnetic susceptibility, thermal or electrical conductivity, etc.) are instances of retarded Green functions, which have a direct relation to imaginary-time ordered Green functions. Consider the Hamiltonian

$$H = H_0 + V(t), \tag{1.38}$$

where H_0 is the time-independent Hamiltonian of the system under consideration and $V(t)$ is a weak perturbation of the form

$$V(t) = Bf(t). \tag{1.39}$$

Here B is a quantum-mechanical operator and $f(t)$ is a scalar function modelling the external force acting on the system. We are thus interested in the effect of the time-dependent perturbation $V(t)$ on an observable A. Assuming that $V(t)$ is turned on at the time t_0, we define

$$\Delta \langle A(t) \rangle = \langle \tilde{A}(t) \rangle - \langle A(t_0) \rangle \,, \tag{1.40}$$

where the time evolution of $\tilde{A}$ is in the Heisenberg picture of the perturbed system,

$$\tilde{A}(t) = e^{iH(t-t_0)} A(t_0) e^{-iH(t-t_0)}, \tag{1.41}$$

while the expectation value $\langle \dots \rangle$ refers to the unperturbed system. It turns out that we can expand $\Delta \langle A(t) \rangle$ perturbatively in $V(t)$, which to leading order results in

$$\Delta \langle A(t) \rangle \approx -i \int_{t_0}^{t} dt' \, \langle [A(t), B(t')] \rangle \, f(t') \equiv \int dt' G^R_{AB}(t,t') f(t'). \tag{1.42}$$

Here we have defined the response function

$$G^R_{AB}(t,t') = -i\Theta(t-t') \, \langle [A(t), B(t')] \rangle \,, \tag{1.43}$$

which is known as the retarded Green function. Since the time evolution is now in the Heisenberg picture of the unperturbed system,

$$A(t) = e^{iH_0(t-t_0)} A(t_0) e^{-iH_0(t-t_0)}, \tag{1.44}$$

G^R_{AB} is independent of the perturbation $V(t)$ and can be evaluated fully within an equilibrium calculation.[4] The retarded Green function thus has direct physical relevance as it tells us how the system will react when it is slightly driven out of equilibrium, but it also has a clear microscopic interpretation in terms of the operators A and B.

[4]Conversely, this implies that static and dynamical properties of quantum-mechanical systems are intrinsically linked to each other: while for a classical system it is possible to treat the statics and the dynamics separately, this is in general not the case for quantum-mechanical systems unless all operators commute with each other [39].

Spectroscopy and spectral function

Another fundamental quantity in condensed matter physics is the spectral function ρ, which is related to the elementary excitations of the system. To give an idea of its physical relevance, consider a photoemission spectroscopy experiment, where we shine light with frequency ν on a metallic surface and measure the photocurrent $I_{\boldsymbol{p}}(\nu)$ of emitted electrons with momentum $\boldsymbol{p}$ and energy $\epsilon_{\boldsymbol{p}}$. In a simplified description, we can express the photocurrent as [40, 41]

$$I_{\boldsymbol{p}}(\nu) = 2\pi \sum_{\boldsymbol{k}} |M_{\boldsymbol{p},\boldsymbol{k}}|^2 \, \tilde{\rho}_{\boldsymbol{k}}(\epsilon_{\boldsymbol{p}} - \nu), \tag{1.45}$$

where the exact form of the matrix elements $M_{\boldsymbol{p},\boldsymbol{k}}$ depends on the electron-photon interaction. Since one can usually approximate $M_{\boldsymbol{p},\boldsymbol{k}}$ as a constant [40], the non-trivial functional dependence is encoded in [41]

$$\tilde{\rho}_{\boldsymbol{k}}(\omega) = \frac{1}{\mathcal{Z}} \sum_{m,n} |\langle E_m| \, c_{\boldsymbol{k}} \, |E_n\rangle|^2 \, e^{-\beta \tilde{E}_n} \delta[\omega - (\tilde{E}_n - \tilde{E}_m)], \tag{1.46}$$

where $|E_n\rangle = |E_n(N)\rangle$ is a simultaneous eigenstate of both the Hamiltonian H and the particle number operator N, while $\tilde{E}_n = E_n(N) - \mu N$ with the chemical potential μ. The form of $\tilde{\rho}_{\boldsymbol{k}}(\omega)$ is essentially dictated by Fermi's golden rule [42], where the fermionic annihilation operator $c_{\boldsymbol{k}}$ appears in the matrix element as the incoming photon removes an electron with momentum $\boldsymbol{k}$ from the system. The delta distribution ensures conservation of energy, while the Boltzmann factor

$$\frac{e^{-\beta \tilde{E}_n}}{\mathcal{Z}} = \frac{e^{-\beta(E_n(N) - \mu)}}{\mathrm{Tr}\left[e^{-\beta(H - \mu N)}\right]} \tag{1.47}$$

results from the finite temperature of the system. Besides the experimental relevance of $\tilde{\rho}_{\boldsymbol{k}}(\omega)$, its Fourier transform also has a simple microscopic interpretation,

$$\int d\omega e^{-i\omega t} \tilde{\rho}_{\boldsymbol{k}}(\omega) = \left\langle c^\dagger_{\boldsymbol{k}}(0) c_{\boldsymbol{k}}(t) \right\rangle . \tag{1.48}$$

We can therefore use $\tilde{\rho}_{\boldsymbol{k}}(\omega)$ to connect microscopic calculations on the theory side to experimental line spectra. However, as we will see in Sec. 1.3.2, a more convenient quantity to work with is the spectral function

$$\rho_{\boldsymbol{k}}(\omega) = (e^{\beta\omega} - \zeta)\tilde{\rho}_{\boldsymbol{k}}(\omega), \tag{1.49}$$

where the sign of $\zeta = \pm 1$ is usually chosen depending on whether we work with bosonic or fermionic operators. In general, we define the spectral function as

$$\rho_{AB}(\omega) = \frac{1}{\mathcal{Z}} \sum_{m,n} \langle E_n| B |E_m\rangle \langle E_m| A |E_n\rangle e^{-\beta \tilde{E}_n}(e^{\beta\omega} - \zeta)\delta[\omega - (\tilde{E}_n - \tilde{E}_m)], \tag{1.50}$$

where A and B are arbitrary operators. For example, the choice $A = B^\dagger = c_{\boldsymbol{k}}$ is connected to the single-particle correlator in Eq. (1.48) and describes photoemission spectroscopy as discussed above, while $A = B^\dagger = c_{\boldsymbol{k}} c_{\boldsymbol{k}'}$ refers to a microscopic two-particle correlator and corresponds to Auger electron spectroscopy. We can also write the spectral function in terms of correlators,

$$\int d\omega e^{-i\omega t} \rho_{AB}(\omega) = 2\pi \rho_{AB}(t) = \left\langle [A(t), B(0)]_{-\zeta} \right\rangle, \tag{1.51}$$

where the ζ subscript refers to the commutator or anticommutator, respectively. Comparing this expression with Eq. (1.43) shows the close relationship between ρ_{AB} and G^R_{AB}, which in frequency space takes the form

$$G^R_{AB}(\omega) = \int d\omega' \frac{\rho_{AB}(\omega')}{\omega - \omega' + i0^+}. \tag{1.52}$$

1.3.2 Wick rotation and Matsubara Green function

As we have seen in the previous subsection, the retarded Green function G^R_{AB} and the spectral function ρ_{AB} are central objects in the study of condensed matter systems, since they connect microscopic quantities like single-particle correlators to experimentally accessible observables. In the end, both can be expressed through correlators of the form

$$\langle A(t)B(0)\rangle = \frac{1}{\mathcal{Z}} \mathrm{Tr}\left[e^{-\beta(H-\mu N)} A(t)B(0)\right] = \frac{1}{\mathcal{Z}} \mathrm{Tr}\left[e^{-\beta\mathcal{H}} e^{i\mathcal{H}t} A e^{-i\mathcal{H}t} B\right], \tag{1.53}$$

where we have defined the grand-canonical Hamiltonian $\mathcal{H} = H - \mu N$. However, these real-time correlators at finite temperature are unfortunately inconvenient for practical calculations. An important technical point is that Wick's theorem, which tells us how to decompose time-ordered correlators of a non-interacting system, is only valid at $T = 0$ in the real-time formalism. In the context of the present work, the main obstacle is that the real-time formalism does not allow for an efficient formulation of the spin FRG developed in Ch. 3. To circumvent this problem, we analytically continue the time variable t in Eq. (1.53) to the complex plane. The correlator is then well defined as long as $\mathrm{Im}(t) \in [-\beta, 0]$, since $\mathcal{H} = \mathcal{H}^\dagger$ is bounded from below. For convenience, we write $t = -i\tau$ and choose $\tau \in [0, \beta]$, which is known as Wick rotation [43]. We can now introduce the Matsubara Green function

$$G^M_{AB}(\tau, \tau') = -\langle \mathcal{T} A(\tau) B(\tau') \rangle, \tag{1.54}$$

where the time evolution is in the imaginary-time Heisenberg picture,

$$A(\tau) = e^{\mathcal{H}\tau} A e^{-\mathcal{H}\tau}, \tag{1.55}$$

and the time-ordering symbol $\mathcal{T}$ sorts later times to the left,

$$\mathcal{T} A(\tau) B(\tau') = \begin{cases} A(\tau)B(\tau'), & \tau > \tau', \\ B(\tau')A(\tau), & \tau < \tau'. \end{cases} \tag{1.56}$$

More specifically, Eq. (1.54) refers to the bosonic Matsubara Green function, which corresponds to $\zeta = 1$ in Eqs. (1.49)–(1.51). While it is easy to define G^M_{AB} for general $\zeta = \pm 1$, we will in the present thesis only need the bosonic form since spin operators on different lattice sites commute. The Matsubara Green function is the main object of interest in the imaginary-time formalism. We first note that it is well defined as long as $-\beta < \tau - \tau' < \beta$ and that it obeys the Kubo-Martin-Schwinger boundary conditions,

$$G^M_{AB}(\beta, \tau') = G^M_{AB}(0, \tau'), \tag{1.57a}$$
$$G^M_{AB}(\tau, \beta) = G^M_{AB}(\tau, 0), \tag{1.57b}$$

which follow from the cyclicity of the trace. As a result, its Fourier transform

$$G^M_{AB}(i\omega_n) = \int_0^\beta d\tau e^{i\omega\tau} G^M_{AB}(\tau, 0) \tag{1.58}$$

is defined on the countably infinite set of (bosonic) Matsubara frequencies $\omega_n = 2\pi n/\beta$ with $n \in \mathbb{Z}$. It turns out that the Matsubara Green function in frequency space has a direct connection to the spectral function from the previous section via

$$G^M_{AB}(i\omega_n) = \int d\omega' \frac{\rho_{AB}(\omega')}{i\omega_n - \omega'}. \tag{1.59}$$

Together with

$$\left| \int d\omega \rho_{AB}(\omega) \right| = |\langle [A, B] \rangle| < \infty, \tag{1.60}$$

it follows that we can analytically continue $G^M_{AB}(i\omega_n) \to G^M_{AB}(i\omega)$ to the entire upper and lower half-plane, i.e., $\mathrm{Im}(i\omega) \neq 0$. Note that in the common case where $\rho_{AB}(\omega)$ acts as a probability distribution, the resulting function $G^M_{AB}(i\omega)$ can be identified with the Stieltjes transform of the spectral function. We also observe that, according to Eq. (1.59), $G^M_{AB}(i\omega)$ is holomorphic and vanishes for $|i\omega| \to \infty$ along any straight line in the upper or lower half-plane. These two conditions can be used in actual calculations to identify the correct analytic continuation of $G^M_{AB}(i\omega_n)$ [44]. Comparing the spectral representation (1.52) of G^R_{AB} with Eq. (1.59), we see that we can recover the retarded Green function via

$$G^R_{AB}(\omega) = G^M_{AB}(\omega + i0^+). \tag{1.61}$$

Furthermore, using Eq. (1.59) we can also express the spectral function as[5]

$$\rho_{AB}(\omega) = \frac{i}{2\pi}\left[G^M_{AB}(\omega + i0^+) - G^M_{AB}(\omega - i0^+)\right]. \tag{1.62}$$

We thus find that the knowledge of the analytic continuation of the Matsubara Green function gives us direct access to physically relevant quantities, which justifies the use of the imaginary-time formalism.

For completeness, we should mention that there is an alternative to the Matsubara approach called Keldysh formalism, which is especially useful in non-equilibrium situations (see, e.g., Ref. [45]). While it leads to a more complicated theory due to an artificial doubling of the degrees of freedom, it has the advantage of dealing directly with real-time Green functions. As a consequence, it avoids the additional step of analytically continuing to the real-frequency axis, in contrast to the Matsubara formalism. Since the analytic continuation of $G^M_{AB}(i\omega_n)$ is an ill-posed problem if the function is only known at a finite number of points to a finite precision, the Keldysh approach can be advantageous in situations where only numerical methods are feasible [46]. Due to the analytical nature of the present thesis, however, it is for our purpose more efficient to work completely within the Matsubara formalism.

[5] For real $\rho_{AB}(\omega)$ we can simplify Eq. (1.62) as $\rho_{AB}(\omega) = -\frac{1}{\pi}\mathrm{Im}\left[G^R_{AB}(\omega)\right]$. This is a general form of the well-known fluctuation-dissipation theorem, as it connects a correlator (fluctuation) to the imaginary part of a response function (dissipation).

Chapter 2

FRG approach to the Berezinskii-Kosterlitz-Thouless transition

2.1 Motivation

In the beginning of the 1970s, it was well known that long-range order through the spontaneous breaking of a continuous symmetry is not possible at finite temperature in one and two dimensions. This fact, which is formalized in the Mermin-Wagner theorem [47], is due to the increasingly strong effect of fluctuations in lower dimensions resulting from the massless Goldstone mode. The discovery of the Berezinskii-Kosterlitz-Thouless (BKT) transition was therefore completely unexpected as it constitutes a finite temperature continuous phase transition in a two dimensional system with continuous symmetry, something that was believed to be impossible due to the absence of long-range order. The solution to this apparent paradox is that the BKT transition does not break any symmetry, but is instead driven by topological defects. This possibility was first realized by Berezinskii [48, 49] and was developed further by Kosterlitz and Thouless [50, 51], whose correct description of the nature of the phase transition won them the Physics Nobel prize in 2016 as it highlighted the importance of topological concepts in the description of condensed matter systems.

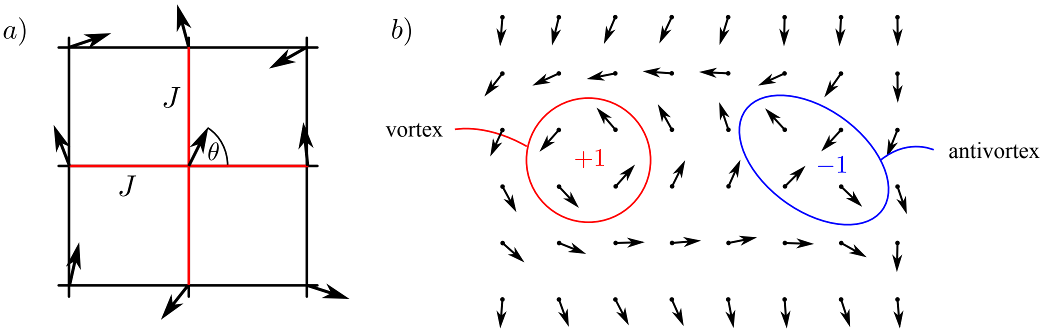

Figure 2.1: (a) Schematic representation of the XY model. The unit-length spins (arrows), parametrized by their polar angle θ, interact via a nearest-neighbour interaction J (shown in red for the center spin). (b) Configuration of the XY model with two topological defects. The vortex on the left has a vorticity of $q = 1$, while the antivortex on the right has a vorticity of $q = -1$. Together they form a vortex-antivortex pair with vanishing vorticity.

2.1.1 Introduction to the XY model

One of the original examples [48, 50] for a system exhibiting a BKT transition is the two-dimensional classical XY model with the Hamiltonian

$$H_{XY} = -J \sum_{i,\mu} \boldsymbol{s}_i \cdot \boldsymbol{s}_{i+\mu} = -J \sum_{i,\mu} \cos(\theta_{i+\mu} - \theta_i). \tag{2.1}$$

It consists of unit-length spins $\boldsymbol{s}_i = \boldsymbol{e}_x \cos\theta_i + \boldsymbol{e}_y \sin\theta_i$ located at the sites $\boldsymbol{r}_i$ of a square lattice with N sites and lattice spacing a, which interact via a nearest-neighbour interaction $J > 0$ (see Fig. 2.1a). The subscript $i + \mu$ refers to the lattice site $\boldsymbol{r}_i + \boldsymbol{a}_\mu$, where the vector $\boldsymbol{a}_\mu$ connects nearest-neighbour lattice sites in the direction $\mu \in \{x, y\}$. Since J is positive, it is obvious that the ground state of the system is ferromagnetic and thus spontaneously breaks the $U(1)$ symmetry of the Hamiltonian. On the other hand, for $T > 0$ the Mermin-Wagner theorem tells us that spontaneous symmetry breaking of a continuous symmetry is not possible in two dimensions [47]. Naively, this seems to exclude a classical continuous phase transition since long-range order is forbidden at any finite temperature. In order to understand why this conclusion is in fact wrong, it is useful to consider the continuum approximation of the system, which allows us to rigorously introduce the notion of topological defects in the XY model. Expanding the cosine in Eq. (2.1) to second order and taking the lattice spacing a to zero yields (up to a constant term)

$$H_{XY}^{\text{cont}} = \frac{J}{2} \int d^2r \, (\boldsymbol{\nabla}\theta)^2 \,, \tag{2.2}$$

where $\theta = \theta(\boldsymbol{r})$ is now a scalar field. This allows us to split the phase field θ into a spin-wave part θ^{sw} and a vortex part θ^{v},

$$\theta(\boldsymbol{r}) = \theta^{\mathrm{sw}}(\boldsymbol{r}) + \theta^{\mathrm{v}}(\boldsymbol{r}), \tag{2.3}$$

where $\theta^{\mathrm{v}}(\boldsymbol{r})$ is a local minimum of H_{XY}^{cont} and $\theta^{\mathrm{sw}}(\boldsymbol{r})$ is the so-called spin-wave deviation from it. This results in

$$H_{XY}^{\mathrm{cont}} = \frac{J}{2} \int d^2 r \left[(\boldsymbol{\nabla}\theta^{\mathrm{sw}})^2 + (\boldsymbol{\nabla}\theta^{\mathrm{v}})^2 \right], \tag{2.4}$$

where

$$\oint d\boldsymbol{r} \cdot \boldsymbol{\nabla}\theta^{\mathrm{sw}} = 0, \tag{2.5}$$

$$\oint d\boldsymbol{r} \cdot \boldsymbol{\nabla}\theta^{\mathrm{v}} = 2\pi q. \tag{2.6}$$

Here the integration is over an arbitrary closed contour and q is the integer-valued vorticity. Topological defects with $q > 0$ are called vortices, while antivortices have $q < 0$. For illustration, Fig. 2.1b shows a sample configuration of a vortex-antivortex pair with $q = \pm 1$ on a lattice. Note that vortex and spin-wave degrees of freedom are decoupled in the Hamiltonian (2.4). Retaining only the spin-wave part (which amounts to ignoring the periodicity of the phase), one can show that for all T this results in an algebraically decaying spin-spin correlation [51],

$$\langle \boldsymbol{s}_i \cdot \boldsymbol{s}_j \rangle \sim |\boldsymbol{r}_{ij}|^{-T/2\pi J}. \tag{2.7}$$

While spin waves are thus ultimately responsible for destroying any long-range order at low temperatures, they only result in an analytic contribution to the free energy and can therefore be neglected in a qualitative description of the BKT transition. For this reason, we will in the following concentrate on the effect of vortices in the system.

2.1.2 Role of vortices in the BKT transition

There is a simple argument in favor of a finite-temperature phase transition in the XY model. Consider a vortex with vorticity q centered at $\boldsymbol{r} = 0$. Its minimum energy configuration can be parametrized with the polar angle φ of $\boldsymbol{r}$ as

$$\theta^{\mathrm{v}}(\boldsymbol{r}) = q\varphi, \tag{2.8}$$

so that

$$|\nabla\theta^{\mathrm{v}}(\boldsymbol{r})| = \frac{q}{r}. \tag{2.9}$$

From Eq. (2.2) we see that the energy of this configuration is given by

$$H^{\mathrm{v}} = \frac{J}{2}\int d^2r \left(\frac{q}{r}\right)^2 = q^2\pi J \int_{r_0}^{R} dr \frac{1}{r} = q^2\pi J \ln\frac{R}{r_0}, \tag{2.10}$$

where r_0 is the radius of the vortex core (which of the order of the lattice spacing) and R is related to the system size. Obviously, H^{v} diverges in the thermodynamic limit where $R \to \infty$. However, at finite temperature we should actually consider the free energy. Since we have roughly $(R/r_0)^2$ possibilities to place the vortex core in the system, we can approximate the free energy shift that results from introducing a single vortex as

$$\Delta F = H^{\mathrm{v}} - TS^{\mathrm{v}} \approx q^2\pi J \ln\frac{R}{r_0} - T\ln\frac{R^2}{r_0^2} = \left(\frac{q^2\pi J}{2} - T\right)\ln\frac{R^2}{r_0^2}. \tag{2.11}$$

While $\Delta F > 0$ at low temperatures, we see that for sufficiently high temperatures the system energetically favors the creation of a single vortex. This argument thus indicates a phase transition at the critical temperature

$$T_c = \frac{\pi J}{2}, \tag{2.12}$$

above which free vortices and antivortices with $|q| = 1$ appear. Below T_c, topological defects are only possible in the form of bound vortex-antivortex pairs (cf. Fig. 2.1b), which at large separations d have the energy [cf. Eq. (2.10)]

$$H^{\mathrm{pair}} = 2q^2\pi J \ln\frac{d}{r_0}. \tag{2.13}$$

The intuitive picture (cf. Fig. 2.2) is then as follows: close to zero temperature, only tightly bound vortex-antivortex pairs arise. Increasing the temperature also increases the average size of the pairs, up to a point where the largest pair is broken up, which results in free vortices and antivortices. Note that our simple derivation of T_c above neglected the effect of having a finite number of vortex-antivortex pairs in the system. Since smaller pairs can lead to the screening of larger pairs, it facilitates the breaking of vortex-antivortex pairs and thus reduces the critical temperature. While it is possible to take this effect into account within a mean-field approach, we will not cover this here since we are mainly interested in the critical behaviour close to the BKT transition, where a mean-field approach will inevitably break down. In order to correctly describe the critical regime, we will in the following turn our attention to RG approaches.

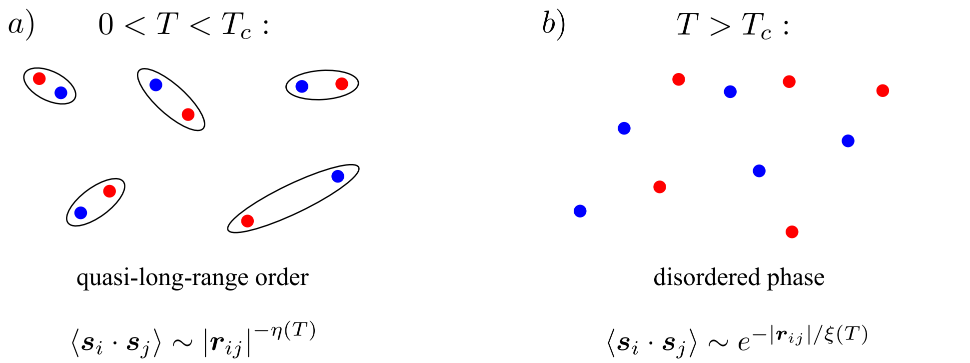

Figure 2.2: Intuitive picture of the BKT transition. (a) At low temperatures, the vortices (red dots) and antivortices (blue dots) only appear as bound pairs, which grow in size with increasing T. This dimerized behaviour of the topological defects results in an algebraically decaying spin-spin correlation, parametrized by the temperature-dependent anomalous dimension $\eta(T)$. Due to the corresponding infinite correlation length ξ, we call this phase quasi-long-range ordered. (b) Increasing the temperature beyond T_c breaks up the vortex-antivortex pairs and allows (anti)vortices to move around freely. Since this allows for much more efficient screening, the correlation length ξ becomes finite and the system is in the disordered phase.

2.1.3 Kosterlitz-Thouless real-space RG

Originally, the critical regime of the BKT transition was studied by Kosterlitz and Thouless within a real-space RG approach. Close to $\tau_l = \pi/2$ and $\tilde{y}_l = 0$, the resulting flow equations [51–53] are equivalent to

$$\partial_l \tilde{y}_l = (2 - \pi/\tau_l)\tilde{y}_l, \tag{2.14}$$

$$\partial_l \tau_l = \frac{\tilde{y}_l^2}{8\pi}, \tag{2.15}$$

where l is the scale parameter (given by the dimensionless lattice spacing in Ref. [52]), τ_l is related to T/J and $\tilde{y}_l$ is proportional to the vortex fugacity, whose initial condition depends on T/J in the XY model. The corresponding flow diagram is shown in Fig. 2.3. We see that for sufficiently small $\tilde{y}_l$ and τ_l (which translates to small T/J in the XY model), the flow terminates at a line of Gaussian fixed points where $\tilde{y}_l = 0$; this case corresponds to Fig. 2.2a. The behaviour changes as soon as we cross the separatrix; while $\tilde{y}_l$ will still initially decrease, it diverges for $l \to \infty$. This implies that the system is in the high-temperature phase in Fig 2.2b where free vortices are energetically

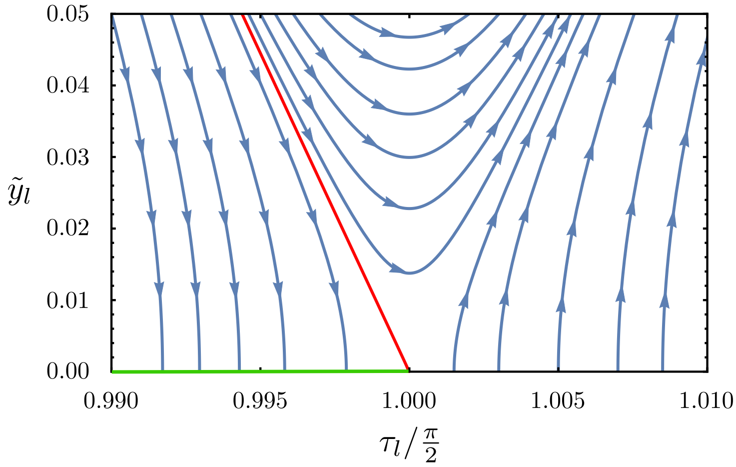

Figure 2.3: Flow diagram for the BKT transition in the neighborhood of $\tau_l = \pi/2, \tilde{y}_l = 0$, as described by the flow equations (2.14) and (2.15). To the left of the separatrix (red line), the system flows into the line of Gaussian fixed points (green line) at $\tilde{y}_l = 0, \tau_l \in [0, \pi/2]$, which corresponds to the quasi-long-range ordered phase at low temperatures. The disordered phase at high temperatures is found to the right of the separatrix, where the flow finally escapes to large $\tilde{y}_l$ and τ_l. (Figure reproduced from Ref. [54])

allowed, leading to a finite correlation length $\xi(T)$ of the form [52]

$$\xi(T) \underset{T \to T_c}{\sim} e^{C\sqrt{\frac{T_c}{T-T_c}}}, \tag{2.16}$$

where C is a non-universal number ($C \approx 1.5$ in the XY model). Since the singular part of the free energy F behaves as

$$F(T) \underset{T \to T_c}{\sim} \xi^{-2}(T) \tag{2.17}$$

above T_c, we find that the BKT transition is of infinite order in the Ehrenfest classification.

Note that the KT flow equations (2.14) and (2.15) have been derived in the limit of small $\tilde{y}_l$, which amounts to a very large, negative chemical potential of the vortices. In the XY model, this assumption is not strictly fulfilled: as we have noted at the end of Sec. 2.1.2, the density of vortices will be finite at the BKT transition, so that we cross the separatrix at a finite $\tilde{y}_l$. However, while this will certainly affect the numerical value of non-universal quantities, it does not change the universal behaviour of the phase transition. A good example of this fact is the discontinuous behaviour of τ_l^{-1} for $l \to \infty$

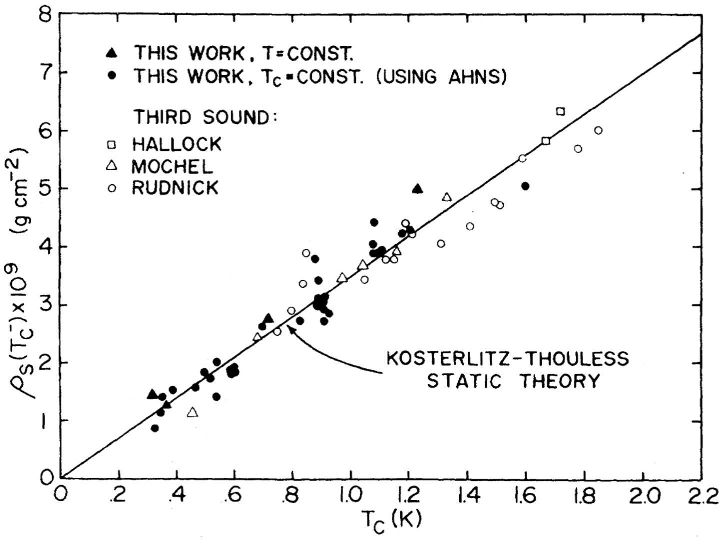

Figure 2.4: Experimental data on thin ^{4}He films for the discontinuity of the superfluid density $\rho_s(T)$ at the phase transition as a function of the critical temperature T_c. The solid line corresponds to the theoretical prediction in Eq. (2.19). (Reprinted figure with permission from D. J. Bishop and J. D. Reppy, Phys. Rev. Lett. **40**, 1727 (1978). Copyright 2019 by the American Physical Society.)

at T_c [55],

$$\lim_{l\to\infty}\left[\frac{1}{\tau_l(T_c^-)}-\frac{1}{\tau_l(T_c^+)}\right]=\frac{2}{\pi}. \tag{2.18}$$

In superfluid ^{4}He, we can identify the large l limit of τ_l^{-1} with $\rho_s(T)/(m^2T)$, where $\rho_s(T)$ is the superfluid density and m is the mass of a helium atom [56]. While neither T_c nor $\rho_s(T_c)$ are universal quantities on their own, Eq. (2.18) implies that the jump of the superfluid density at the phase transition is always proportional to T_c,

$$\rho_s(T_c^-)=\frac{2}{\pi}m^2T_c. \tag{2.19}$$

As can be seen in Fig. 2.4, the predicted universal behaviour is reproduced very well in experiments on thin ^{4}He films [57], which corroborates the theoretical description of the BKT transition by Kosterlitz and Thouless [51, 52]. Good agreement with theory is also seen in experiments on arrays of Josephson junctions [58] and in ultracold gases [59–61].

2.1.4 Previous FRG approaches to the BKT transition

As we have seen, Kosterlitz and Thouless correctly described the nature of the BKT transition. However, they used a rather uncommon real-space RG approach, which is not easily generalized to more complicated systems. It would therefore be desirable to reformulate their approach using a standard momentum regulator within the modern FRG formalism. This was first attempted by Gräter and Wetterich [62], who studied the $O(N)$-symmetric linear σ model in two dimensions within the derivative expansion. For $N = 2$, they generally found good agreement with the characteristics of the BKT transition; for instance, they estimated the anomalous dimension as $\eta(T_c) \approx 0.24$, which is very close to the exact result of $1/4$. In spite of that, their theory does not actually predict a phase transition at all, but rather a well-defined crossover: at low temperatures, they only found a line of quasi-fixed points with a large, but finite correlation length. Although the FRG flow almost stops at these quasi-fixed points, the finite mass of the amplitude mode very slowly decreases until the high-temperature regime is reached.

The same behaviour was found in subsequent FRG approaches to the two-dimensional $O(2)$ model, which also employed the derivative expansion [63–65]. While Jakubczyk, Dupuis, and Delamotte [64] managed to fine-tune the momentum regulator separately for each $T \leq T_c$ such that they encounter a line of true fixed points, yielding an accurate description of the universal jump of the superfluid density [cf. Eq. (2.19)], this fine-tuning is only justified if one assumes *a priori* that the $O(2)$ model in fact involves a BKT transition. However, as discussed in the paper by Jakubczyk and Metzner [65], it seems possible that the amplitude fluctuations in the $O(2)$ model do in fact reduce the BKT transition to a well-defined crossover: since the FRG calculations yield an exponentially large correlation length in the low-temperature region, it would be hard to distinguish from a truly infinite correlation length in numerical simulations or in experiments.

In another recent FRG approach to the $O(2)$ and the XY model in $D = 2$, Defenu et al. [66] decoupled the amplitude and phase fluctuations by hand. This enabled them to first solve the flow of the amplitude part and use it as input for the phase part; the latter is then solved with the help of the Kosterlitz-Thouless flow equations, which they do not derive within the FRG. While they generally find good agreement with BKT physics, similar to the previous FRG approaches [63–65], it seems unsatisfying not to consider amplitude and phase fluctuations simultaneously. Furthermore, they directly used the Kosterlitz-Thouless flow equations of the phase part, thus circumventing the problem of deriving them within the FRG formalism.

Our work in the present chapter thus serves two purposes: First, we show how to rederive the Kosterlitz-Thouless flow equations fully within an FRG approach, using a standard Litim cutoff in momentum space. In Sec. 2.4 we present the derivation within the vertex expansion and afterwards show an alternative route via the derivative expansion in Sec. 2.5. Secondly, we generalize our approach to the $O(2)$ model in Sec. 2.6, where we include weak amplitude fluctuations and show that they only lead to irrelevant additional couplings. Finally, in Sec. 2.7 we consider weak out-of-plane fluctuations and find that do not spoil the BKT transition either.

2.2 Villain model and dual transformations

2.2.1 Villain approximation

Since we are interested in the physics of the XY model described by the Hamiltonian (2.1), we would like to calculate the partition function

$$Z_{XY} = \prod_i \left(\int_0^{2\pi} \frac{d\theta_i}{2\pi} \right) e^{\frac{1}{\tau} \sum_{i,\mu} \cos(\Delta_\mu \theta_i)}, \tag{2.20}$$

where we have defined the dimensionless temperature

$$\tau = T/J \tag{2.21}$$

as well as the lattice derivative

$$\Delta_\mu \theta_i = \theta_{i+\mu} - \theta_i. \tag{2.22}$$

Since the cosine terms in the partition function (2.20) make it difficult to work directly with Z_{XY}, we employ the Villain approximation [67],

$$e^{\frac{1}{\tau}\cos(\Delta_\mu \theta_i)} \approx R_V(1/\tau) \sum_{n_{i\mu}=-\infty}^{\infty} \exp\left[-\frac{(\Delta_\mu \theta_i - 2\pi n_{i\mu})^2}{2\tau_V(1/\tau)} \right]. \tag{2.23}$$

To determine R_V and τ_V, we first expand both sides in a Fourier series,

$$\sum_{l=-\infty}^{\infty} I_l(1/\tau)\cos(l\theta_i) \approx R_V(1/\tau) \sqrt{\frac{\tau_V(1/\tau)}{2\pi}} \sum_{l=-\infty}^{\infty} e^{-l^2 \tau_V(1/\tau)/2} \cos(l\theta_i), \tag{2.24}$$

where the $I_l(x)$ are modified Bessel functions of the first kind,

$$I_l(x) \equiv \frac{1}{2\pi} \int_0^{2\pi} d\theta \, e^{x\cos\theta} \cos(l\theta). \tag{2.25}$$

Demanding equality for the two lowest Fourier coefficients $l = 0$ and $l = 1$ then results in

$$\tau_V(x) = 2\ln\frac{I_0(x)}{I_1(x)}, \tag{2.26}$$

$$R_V(x) = I_0(x)\sqrt{\frac{2\pi}{\tau_V(x)}}. \tag{2.27}$$

Intuitively, Eq. (2.23) amounts to a second-order expansion of the cosine around all its minima. This respects the periodicity of the cosine, which is crucial for the existence of the high-temperature phase due to vortices (cf. Sec. 2.1.1). Contrary to popular knowledge, the Villain approximation becomes exact in the limit of low as well as high temperatures [68]. Dropping the constant prefactor due to R_V, we arrive at the partition function of the Villain model,

$$Z_{\text{Villain}} = \prod_i \left(\int_0^{2\pi}\frac{d\theta_i}{2\pi}\right)\prod_{i,\mu}\left(\sum_{n_{i\mu}=-\infty}^{\infty}\right)\exp\left[-\sum_{i,\mu}\frac{(\Delta_\mu\theta_i - 2\pi n_{i\mu})^2}{2\tau_V(1/\tau)}\right]. \tag{2.28}$$

In the remainder of this section, we will derive several alternative representations of Z_{Villain} via exact duality transformations. To simplify the notation, we will from now on write τ instead of $\tau_V(1/\tau)$.

2.2.2 Current representation

We start by replacing the $n_{i\mu}$ variables in Eq. (2.28) by another set of integers $p_{i\mu}$ with the help of the identity

$$\sum_{n=-\infty}^{\infty} e^{-(x-2\pi n)^2/(2\tau)} = \sqrt{\frac{\tau}{2\pi}}\sum_{p=-\infty}^{\infty} e^{-\tau p^2/2 - ipx}, \tag{2.29}$$

which follows as a special case from the Poisson summation formula [69]

$$\sum_{n=-\infty}^{\infty} f(x-2\pi n) = \frac{1}{2\pi}\sum_{p=-\infty}^{\infty} e^{-ipx}\int_{-\infty}^{\infty} dx' e^{ipx'} f(x') \tag{2.30}$$

by setting $f(x) = e^{-x^2/(2\tau)}$. This results in

$$Z_{\text{Villain}} = \prod_i \left(\int_0^{2\pi}\frac{d\theta_i}{2\pi}\right)\prod_{i,\mu}\left(\sum_{p_{i\mu}=-\infty}^{\infty}\right)\exp\left[-\sum_{i,\mu}\left(\frac{\tau}{2}p_{i\mu}^2 + ip_{i\mu}\Delta_\mu\theta_i\right)\right], \tag{2.31}$$

where we have again dropped a constant prefactor. In order to get rid of the θ_i field, we rewrite [55]

$$-i\sum_{i,\mu} p_{i\mu}\Delta_\mu\theta_i = -i\sum_{i,\mu} p_{i\mu}(\theta_{i+\mu}-\theta_i) = i\sum_i \theta_i \boldsymbol{\Delta}\cdot\boldsymbol{p}_i, \tag{2.32}$$

where we have introduced the lattice divergence

$$\boldsymbol{\Delta}\cdot\boldsymbol{p}_i = \sum_\mu (p_{i\mu} - p_{i-\mu,\mu}), \tag{2.33}$$

so that $\boldsymbol{p}_i = (p_{i,x}, p_{i,y})$ can be interpreted as a current-like degree of freedom. This allows us perform the θ_i integrals,

$$Z_{\text{Villain}} = \prod_{i,\mu}\left(\sum_{p_{i\mu}=-\infty}^{\infty} \delta_{\boldsymbol{\Delta}\cdot\boldsymbol{p}_i,0}\right) e^{-\frac{\tau}{2}\sum_{i,\mu} p_{i\mu}^2}, \tag{2.34}$$

which has the effect of enforcing a local constraint of vanishing lattice divergence at each lattice site.

2.2.3 Dual-vortex representation

We have thus arrived at a representation of Z_{Villain} that is formulated purely in terms of discrete degrees of freedom. This is an important step, since we know that the BKT transition is driven by vortices, which are discrete quantities. However, the constraint of vanishing lattice divergence is inconvenient for actual calculations. It is more efficient to take it into account automatically by expressing $p_{i\mu}$ as the lattice curl of another field [55, 70, 71],

$$p_{i\mu} = \sum_\nu \epsilon_{\mu\nu}\Delta_\nu m_{i+\mu}, \tag{2.35}$$

where $\epsilon_{\mu\nu}$ is the Levi-Civita symbol and the integer field m_i lives on the dual lattice (see Fig. 2.5). Up to a constant prefactor,[1] the partition function now reads

$$Z_{\text{Villain}} = \prod_i \left(\sum_{m_i=-\infty}^{\infty}\right) e^{-S_{\text{dual}}[m]}, \tag{2.36}$$

[1]The partition function (2.36) is actually divergent, since $\omega_{\boldsymbol{k}=0} = 0$. This is due to the transformation (2.35), which only depends on differences of the m_i field. Strictly speaking, we should therefore fix the value of m_i at an arbitrary lattice site. However, since this choice does not affect the physics, it is more convenient to sum over all possible configurations, which results in Eq. (2.36).

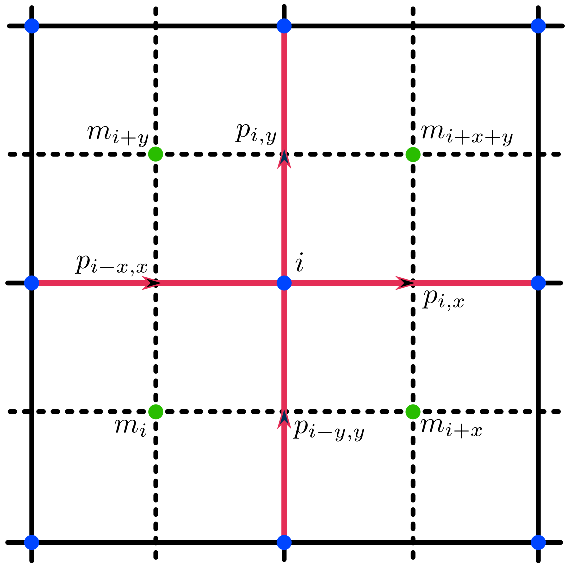

Figure 2.5: Schematic representation of the physical lattice (blue dots), the dual lattice (green dots), and of the related fields. The conserved currents $p_{i\mu}$ (red arrows) flow between sites of the physical lattice, while the m_i field defined in Eq. (2.35) lives on the dual lattice. (Figure reproduced from Ref. [54])

where the dual-vortex action is given by

$$S_{\text{dual}}[m] = \frac{\tau}{2} \sum_{i,\mu} (\Delta_\mu m_i)^2 = \frac{1}{2} \sum_{\boldsymbol{k}} \omega_{\boldsymbol{k}} \left| m_{\boldsymbol{k}} \right|^2 . \tag{2.37}$$

Here the Fourier components of the m_i field are defined as

$$m_{\boldsymbol{k}} = \frac{1}{\sqrt{N}} \sum_i e^{-i\boldsymbol{k}\cdot\boldsymbol{r}_i} m_i, \tag{2.38}$$

so that for the dimensionless dispersion we find

$$\omega_{\boldsymbol{k}} = 4\tau(1 - \gamma_{\boldsymbol{k}}) \tag{2.39}$$

with

$$\gamma_{\boldsymbol{k}} = \frac{1}{2} \sum_\mu \cos(k_\mu a), \tag{2.40}$$

the nearest-neighbour structure factor on a square lattice. The simple form of $S_{\text{dual}}[m]$ will make it an ideal starting point for our FRG approach.

2.2.4 Coulomb-gas representation

Nevertheless, let us perform one more duality transformation on Z_{Villain} to obtain the Coulomb-gas representation, as it will show the relation of the m_i field to the physical vortices. We therefore introduce an auxiliary continuous field ϕ_i and an integer field q_i by writing

$$Z_{\text{Villain}} = \prod_i \left(\int_{-\infty}^{\infty} d\phi_i \sum_{q_i=-\infty}^{\infty} \right) e^{-\frac{\tau}{2}\sum_{i,\mu}(\Delta_\mu \phi_i)^2 - 2\pi i \sum_i q_i \phi_i}. \tag{2.41}$$

The equivalence to Eq. (2.36) can be seen by using the distributional form of the Poisson summation formula (2.30),

$$\sum_{q=-\infty}^{\infty} e^{-2\pi i q\phi} = \sum_{m=-\infty}^{\infty} \delta(\phi - m), \tag{2.42}$$

so that the ϕ_i integrals become trivial due to the delta distributions. On the other hand, we can first perform the Gaussian integral over ϕ_i, which yields (up to a constant factor)

$$Z_{\text{Villain}} = \prod_i \left(\sum_{q_i=-\infty}^{\infty} \right) \delta\left(\sum_i q_i \right) e^{-\frac{1}{2}\sum_{ij} V_{ij} q_i q_j}. \tag{2.43}$$

Here the delta distribution[2] ensures charge neutrality of the system and the interaction V_{ij} is defined as

$$V_{ij} = \frac{(2\pi)^2}{N} \sum_{\boldsymbol{k}\neq 0} \frac{e^{i\boldsymbol{k}\cdot(\boldsymbol{r}_i - \boldsymbol{r}_j)}}{\omega_{\boldsymbol{k}}} \to a^2 \int_{-\pi/a}^{\pi/a} dk_x \int_{-\pi/a}^{\pi/a} dk_y \frac{e^{i\boldsymbol{k}\cdot(\boldsymbol{r}_i - \boldsymbol{r}_j)}}{\omega_{\boldsymbol{k}}}, \tag{2.44}$$

where the latter expression refers to the thermodynamic limit. Since $\omega_{\boldsymbol{k}} \approx \tau a^2 k^2$ for small momenta, it is obvious that the integral in Eq. (2.44) is infrared divergent. This behaviour is due to the finite on-site interaction

$$V_0 = \frac{(2\pi)^2}{N} \sum_{\boldsymbol{k}\neq 0} \frac{1}{\omega_{\boldsymbol{k}}}, \tag{2.45}$$

which diverges for an infinite system. We therefore introduce the regularized interaction $\tilde{V}_{ij}$ by subtracting the problematic on-site term,

$$\tilde{V}_{ij} = V_{ij} - V_0 = \frac{(2\pi)^2}{N} \sum_{\boldsymbol{k}\neq 0} \frac{e^{i\boldsymbol{k}\cdot(\boldsymbol{r}_i - \boldsymbol{r}_j)} - 1}{\omega_{\boldsymbol{k}}}, \tag{2.46}$$

[2] The appearance of the delta distribution without an enclosing integral is due to the divergence of the partition function (2.36) (cf. footnote 1). In practice, we can thus interpret it as a Kronecker delta.

which is still well defined in the thermodynamic limit. The partition function (2.43) is unchanged under the replacement $V_{ij} \to \tilde{V}_{ij}$,

$$Z_{\text{Villain}} = \prod_i \left(\sum_{q_i=-\infty}^{\infty} \right) \delta\left(\sum_i q_i \right) e^{-\frac{1}{2}\sum_{ij} \tilde{V}_{ij} q_i q_j}, \tag{2.47}$$

as the additional term in the action

$$\frac{1}{2}\sum_{ij} \tilde{V}_{ij} q_i q_j = \frac{1}{2}\sum_{ij} V_{ij} q_i q_j - \frac{V_0}{2}\left(\sum_i q_i \right)^2 \tag{2.48}$$

vanishes due to the enforced charge neutrality. Comparing the large-distance behaviour of the regularized interaction,

$$\tilde{V}_{ij} \sim -\ln\left(\frac{|\boldsymbol{r}_i - \boldsymbol{r}_j|}{a} \right), \tag{2.49}$$

with the energy of a vortex-antivortex pair [cf. Eq. (2.13)],

$$H^{\text{pair}} = 2q^2\pi J \ln\left(\frac{|\boldsymbol{r}_i - \boldsymbol{r}_j|}{r_0} \right), \tag{2.50}$$

we see that we can interpret the partition function (2.47) as describing a system of interacting (anti)vortices, where q_i gives the vorticity of a topological defect at the lattice site $\boldsymbol{r}_i$. Since we can equally interpret the q_i as interacting electrical charges in two dimensions, the form of Z_{Villain} in Eq. (2.47) is also called Coulomb-gas representation. We thus find that the m_i field in Eq. (2.36) is related to the physical vortices by a duality transformation; therefore, we refer to the m_i as dual vortices.

2.3 FRG on the dual-vortex model

2.3.1 Technical preliminaries

Before we apply the FRG to the dual-vortex representation (2.36) of Z_{Villain}, let us first give a technical overview of the definitions we will use and the resulting exact relations. We consider a general deformation S_λ of the full action S_{dual}, which depends continuously on the cutoff λ via a regulator R_λ. The generating functional of the scale-dependent connected Green functions $\mathcal{G}_\lambda$ is then defined via

$$e^{\mathcal{G}_\lambda[h]} = \prod_i \left(\sum_{m_i=-\infty}^{\infty} \right) e^{-S_\lambda[m] + \sum_i h_i m_i}. \tag{2.51}$$

Taking derivatives of $\mathcal{G}_\lambda$ with respect to the source field h_i yields the scale-dependent connected Green functions of the integer field m_i; e.g.,

$$\delta_{h_i}\mathcal{G}_\lambda[h] = \langle m_i \rangle_{\lambda,h} = \bar{m}_{\lambda,i}[h], \tag{2.52}$$

$$\delta_{h_j}\delta_{h_i}\mathcal{G}_\lambda[h] = \langle m_i m_j \rangle_{\lambda,h} - \langle m_i \rangle_{\lambda,h} \langle m_j \rangle_{\lambda,h}\,, \tag{2.53}$$

where the scale- and source field-dependent expectation value of an arbitrary functional $F[m]$ is defined by

$$\langle F[m] \rangle_{\lambda,h} = \frac{\prod_i \left(\sum_{m_i=-\infty}^{\infty}\right) e^{-S_\lambda[m]+\sum_i h_i m_i} F[m]}{\prod_i \left(\sum_{m_i=-\infty}^{\infty}\right) e^{-S_\lambda[m]+\sum_i h_i m_i}}. \tag{2.54}$$

Inverting the relation between the h_i and the $\bar{m}_{\lambda,i}[h]$ allows us to introduce the generating functional of the irreducible vertices Γ_λ as the subtracted Legendre transform

$$\Gamma_\lambda[\bar{m}] = \sum_i h_{\lambda,i}[\bar{m}]\bar{m}_i - \mathcal{G}_\lambda[h_\lambda[\bar{m}]] - \frac{1}{2}\sum_{\boldsymbol{k}} R_\lambda(\boldsymbol{k}) \left|\bar{m}_{\boldsymbol{k}}\right|^2, \tag{2.55}$$

so that the irreducible vertices are defined by

$$\Gamma_\lambda^{(n)}(\boldsymbol{k}_1, \ldots, \boldsymbol{k}_n) = \delta_{\bar{m}_{\boldsymbol{k}_n}} \cdots \delta_{\bar{m}_{\boldsymbol{k}_1}} \Gamma_\lambda[\bar{m}]\Big|_{\bar{m}=0}. \tag{2.56}$$

Since the full action $S_{\text{dual}}[m]$ is parity symmetric with respect to the field m_i, we assume that the regulator R_λ is chosen such that this also holds for the deformed action $S_\lambda[m]$; as a consequence, all irreducible n-point vertices with n odd vanish identically. It is easy to show that $\Gamma_\lambda[\bar{m}]$ obeys the Wetterich equation

$$\partial_\lambda \Gamma_\lambda[\bar{m}] = \frac{1}{2}\sum_{\boldsymbol{k}} \frac{\partial_\lambda R_\lambda(\boldsymbol{k})}{\Gamma^{(2)}_{\lambda,\boldsymbol{k},-\boldsymbol{k}}[\bar{m}] + R_\lambda(\boldsymbol{k})}, \tag{2.57}$$

where

$$\Gamma^{(2)}_{\lambda,\boldsymbol{k},\boldsymbol{k}'}[\bar{m}] = \delta_{\bar{m}_{\boldsymbol{k}}}\delta_{\bar{m}_{\boldsymbol{k}'}}\Gamma_\lambda[\bar{m}]. \tag{2.58}$$

Differentiating the Wetterich equation twice then yields the flow equation of the two-point irreducible vertex,

$$\partial_\lambda \Gamma_\lambda^{(2)}(\boldsymbol{k}) = \frac{1}{2N}\sum_{\boldsymbol{q}} \dot{G}_\lambda(\boldsymbol{q})\Gamma_\lambda^{(4)}(\boldsymbol{k}, -\boldsymbol{k}, \boldsymbol{q}, -\boldsymbol{q}). \tag{2.59}$$

Here $\dot{G}_\lambda$ is the single-scale propagator,

$$\dot{G}_\lambda(\boldsymbol{k}) = -\left[G_\lambda(\boldsymbol{k})\right]^2 \partial_\lambda R_\lambda(\boldsymbol{k}), \tag{2.60}$$

which depends on the propagator

$$G_\lambda(\boldsymbol{k}) = \frac{1}{N}\sum_{ij} e^{i\boldsymbol{k}\cdot(\boldsymbol{r}_i-\boldsymbol{r}_j)}\, \delta_{h_j}\delta_{h_i}\mathcal{G}_\lambda[h]\Big|_{\boldsymbol{m}=0} = \left[\Gamma^{(2)}_\lambda(\boldsymbol{k}) + R_\lambda(\boldsymbol{k})\right]^{-1}. \tag{2.61}$$

The exact flow equations of higher-order irreducible vertices are derived analogously by taking derivatives of the Wetterich equation; the irreducible four-point vertex, e.g., flows according to

$$\begin{aligned}
\partial_\lambda\Gamma^{(4)}_\lambda(\boldsymbol{k}_1,\boldsymbol{k}_2,\boldsymbol{k}_3,\boldsymbol{k}_4) &= \frac{1}{2N}\sum_{\boldsymbol{q}}\dot{G}_\lambda(\boldsymbol{q})\Gamma^{(6)}_\lambda(\boldsymbol{k}_1,\boldsymbol{k}_2,\boldsymbol{k}_3,\boldsymbol{k}_4,\boldsymbol{q},-\boldsymbol{q}) \\
-\frac{1}{N}\sum_{\boldsymbol{q}}\Big[\dot{G}_\lambda(\boldsymbol{q})&\Gamma^{(4)}_\lambda(\boldsymbol{k}_1,\boldsymbol{k}_2,\boldsymbol{q},-\boldsymbol{q}-\boldsymbol{k}_1-\boldsymbol{k}_2)G_\lambda(-\boldsymbol{q}-\boldsymbol{k}_1-\boldsymbol{k}_2) \\
&\times\Gamma^{(4)}_\lambda(\boldsymbol{q}+\boldsymbol{k}_1+\boldsymbol{k}_2,-\boldsymbol{q},\boldsymbol{k}_3,\boldsymbol{k}_4) + (\boldsymbol{k}_2\leftrightarrow\boldsymbol{k}_3) + (\boldsymbol{k}_2\leftrightarrow\boldsymbol{k}_4)\Big].
\end{aligned} \tag{2.62}$$

A graphical representation of these flow equations up to sixth order is shown in Fig. 2.6.

2.3.2 Initial condition within the lattice FRG

We are now in a position to set up the FRG. As mentioned above, we will work within the dual-vortex representation of the Villain model [see Eq. (2.36)], where the dual-vortex action is given by

$$S_{\text{dual}}[m] = \frac{\tau}{2}\sum_{i,\mu}(\Delta_\mu m_i)^2 = \frac{1}{2}\sum_{\boldsymbol{k}}\omega_{\boldsymbol{k}}\left|m_{\boldsymbol{k}}\right|^2. \tag{2.63}$$

Due to the quadratic dependence of S_{dual} on the integer field m_i, this representation is also known as the discrete Gaussian model [73–75]. Since a Gaussian theory describes a trivial system of non-interacting entities, the non-trivial aspects that are responsible for the BKT transition are encoded in the discreteness of the m_i. This prevents us from applying the usual FRG methods, which are tailored to path integrals [33]. Instead, we will rely on the lattice FRG formalism developed by Machado and Dupuis [76], where the deformed action is given by

$$S_\lambda[m] = \frac{1}{2}\sum_{\boldsymbol{k}}\left[\omega_{\boldsymbol{k}} + R_\lambda(\boldsymbol{k})\right]\left|m_{\boldsymbol{k}}\right|^2 \tag{2.64}$$

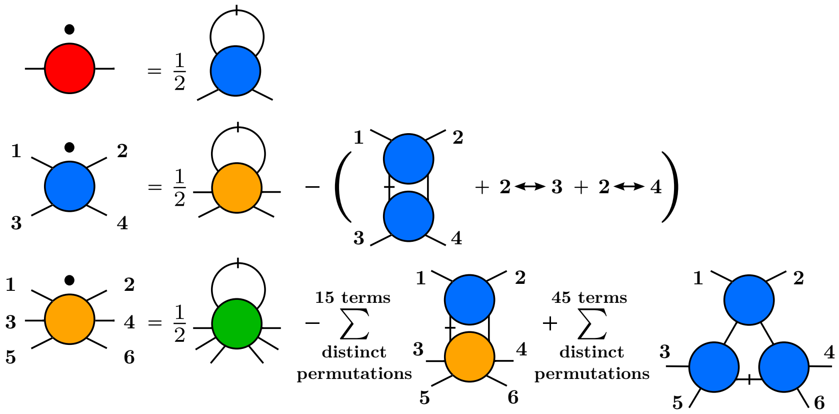

Figure 2.6: Graphical representation of the exact flow equations of the irreducible n-point vertices $\Gamma_\lambda^{(n)}$ with $n = 2$ [see Eq. (2.59)], $n = 4$ [see Eq. (2.62)], and $n = 6$ (see Ref. [72]). Solid lines denote the propagator G_λ defined in Eq. (2.61), while slashed solid lines represent the single-scale propagator $\dot{G}_\lambda$ given in Eq. (2.60). The dotted vertices on the left-hand side refer to their scale-derivative $\partial_\lambda \Gamma_\lambda^{(n)}$. We have labelled the external momenta by integers, omitting them where there is no danger of ambiguity. (Figure reproduced from Ref. [54])

with the Litim regulator [77]

$$R_\lambda(\boldsymbol{k}) = (\lambda - \omega_{\boldsymbol{k}})\Theta(\lambda - \omega_{\boldsymbol{k}}). \tag{2.65}$$

Choosing this regulator has two advantages: on the one hand, it only modifies the dispersion at long wavelengths and thus follows the intuitive picture where we integrate out high-energy modes during the FRG flow. On the other hand, at the initial scale

$$\lambda_0 = \max_{\boldsymbol{k}} \omega_{\boldsymbol{k}} = 8\tau \tag{2.66}$$

the dual vortices on different lattice sites are completely decoupled,

$$S_{\lambda_0}[m] = \frac{\lambda_0}{2} \sum_{\boldsymbol{k}} |m_{\boldsymbol{k}}|^2 = \frac{\lambda_0}{2} \sum_i m_i^2, \tag{2.67}$$

so that the initial condition reduces to a single-site problem; this is the main feature of the lattice FRG [76]. As a result, the scale-dependent generating functional of the connected Green functions introduced in Eq. (2.51) simplifies at the initial scale to

$$\mathcal{G}_{\lambda_0}[h] = \sum_i \ln \left[\sum_{m_i=-\infty}^{\infty} e^{-\frac{\lambda_0}{2} m_i^2 + h_i m_i} \right] = \sum_i \ln \vartheta_3 \left(\frac{i h_i}{2}, e^{-\lambda_0/2} \right), \tag{2.68}$$

where the theta-function $\vartheta_3(z,q)$ is defined as [78]

$$\vartheta_3(z,q) = \sum_{m=-\infty}^{\infty} q^{m^2} e^{2imz} = 1 + 2\sum_{m=1}^{\infty} q^{m^2}\cos(2mz) \tag{2.69}$$

and exists as long as $|q| < 1$. We can bring this into a more intuitive form by using Jacobi's identity [69]

$$\vartheta_3(z, e^{-\pi x}) = \frac{1}{\sqrt{x}} e^{-z^2/(\pi x)} \vartheta_3\left(\frac{z}{ix}, e^{-\pi/x}\right). \tag{2.70}$$

This results in

$$\mathcal{G}_{\lambda_0}[h] = \sum_i \left[\frac{h_i^2}{2\lambda_0} + \ln\sqrt{\frac{2\pi}{\lambda_0}} + \ln\vartheta_3\left(\frac{\pi h_i}{\lambda_0}, y_0\right)\right], \tag{2.71}$$

where we have introduced the vortex fugacity at scale λ_0,

$$y_0 = e^{-2\pi^2/\lambda_0} = e^{-\pi^2/(4\tau)}. \tag{2.72}$$

In the limit of low temperatures where no vortices are present ($y_0 = 0$), the last term in Eq. (2.71) vanishes and $\mathcal{G}_{\lambda_0}[h]$ describes a free (Gaussian) system. A finite value of y_0 thus takes the discreteness of the m_i field into account, which reflects a finite density of vortices. At this point it turns out to be useful to generalize our model by considering y_0 as an independent variable; the dual-vortex model is then recovered by using the relation (2.72). Since we can show *a posteriori* that the universal aspects of the BKT transition can be discussed within a neighborhood of $y_0 = 0$, we expand

$$\vartheta_3\left(\frac{\pi h_i}{\lambda_0}, y_0\right) = 1 + 2y_0\cos\left(\frac{2\pi h_i}{\lambda_0}\right) + O(y_0^4). \tag{2.73}$$

The expectation value of m_i as a function of the source field then reads

$$\langle m_i\rangle_{\lambda_0,h} = \bar{m}_{\lambda_0,i}[h] = \frac{\delta\mathcal{G}_{\lambda_0}[h]}{\delta h_i} = \frac{h_i}{\lambda_0} - \frac{4\pi y_0}{\lambda_0}\sin\left(\frac{2\pi h_i}{\lambda_0}\right) + O(y_0^2), \tag{2.74}$$

so that

$$h_{\lambda_0,i}[\bar{m}] = \lambda_0\bar{m}_i + 4\pi y_0\sin(2\pi\bar{m}_i) + O(y_0^2). \tag{2.75}$$

As a consequence, the generating functional of the irreducible vertices [see Eq. (2.55)] has the initial form

$$\Gamma_{\lambda_0}[\bar{m}] = -N\ln\sqrt{\frac{2\pi}{\lambda_0}} + \frac{1}{2}\sum_{\boldsymbol{k}}\omega_{\boldsymbol{k}}\left|\bar{m}_{\boldsymbol{k}}\right|^2 - 2y_0\sum_i\cos(2\pi\bar{m}_i) + O(y_0^2). \tag{2.76}$$

2.3.3 Continuum limit

So far we have formulated everything on a lattice, which has allowed us to make use of the lattice FRG formalism in order to derive the initial condition (2.76) for $\Gamma_\lambda[\bar{m}]$. For the discussion of the critical regime and the derivation of the Kosterlitz-Thouless RG equations, however, it will be useful to switch to the continuum limit, where

$$\omega_{\boldsymbol{k}} = c_0 k^2 + O(k^4) \tag{2.77}$$

with

$$c_{\Lambda_0} = \tau a^2. \tag{2.78}$$

We accordingly parametrize the cutoff via

$$\lambda = c_{\Lambda_0} \Lambda^2 \tag{2.79}$$

and rescale the regulator $R_\lambda(\boldsymbol{k})$ by an appropriate wave-function renormalization factor $c_\Lambda / c_{\Lambda_0}$, so that

$$R_\Lambda(\boldsymbol{k}) = c_\Lambda(\Lambda^2 - k^2)\Theta(\Lambda^2 - k^2). \tag{2.80}$$

Here the scale-dependent coupling c_Λ is defined via the long-wavelength expansion of the flowing irreducible two-point vertex,

$$\Gamma_\Lambda^{(2)}(\boldsymbol{k}) = r_\Lambda + c_\Lambda k^2 + O(k^4). \tag{2.81}$$

Within this parametrization, the propagator is given by

$$G_\Lambda(\boldsymbol{k}) = \left[\Gamma_\Lambda^{(2)}(\boldsymbol{k}) + R_\Lambda(\boldsymbol{k})\right]^{-1} = \begin{cases} (r_\Lambda + c_\Lambda \Lambda^2)^{-1}, & k < \Lambda, \\ (r_\Lambda + c_\Lambda k^2)^{-1}, & k > \Lambda, \end{cases} \tag{2.82}$$

while the single-scale propagator reads

$$\dot{G}_\Lambda(\boldsymbol{k}) = -\left[G_\Lambda(\boldsymbol{k})\right]^2 \partial_\Lambda R_\Lambda(\boldsymbol{k}) = -\frac{[2c_\Lambda \Lambda + (\partial_\Lambda c_\Lambda)(\Lambda^2 - k^2)]\Theta(\Lambda^2 - k^2)}{(r_\Lambda + c_\Lambda \Lambda^2)^2}. \tag{2.83}$$

From simple power counting we find that r_Λ is a relevant coupling at the Gaussian fixed-point manifold with a scaling dimension of two, while c_Λ is a marginal coupling. This generalizes to higher-order irreducible vertices: expanding the irreducible n-point vertex with $n \in \mathbb{Z}^+$ as

$$\Gamma_\Lambda^{(2n)}(\boldsymbol{k}, -\boldsymbol{k}, 0, \ldots, 0) = u_\Lambda^{(2n)} + \frac{1}{2} c_\Lambda^{(2n)} a^2 k^2 + O(\boldsymbol{k}^4), \tag{2.84}$$

it turns out that the couplings

$$u_\Lambda^{(2n)} = \Gamma_\Lambda^{(2n)}(0,\ldots,0) \tag{2.85}$$

are all relevant with the same scaling dimension, while the couplings

$$c_\Lambda^{(2n)} = a^{-2} \lim_{k\to 0} \partial_k^2 \Gamma_\Lambda^{(2n)}(\boldsymbol{k}, -\boldsymbol{k}, 0, \ldots, 0) \tag{2.86}$$

are all marginal (couplings due to higher-order terms in k are irrelevant). To derive the Kosterlitz-Thouless RG equations, we thus have to keep track of a countably infinite number of relevant and marginal couplings. In the following section we will do this within the vertex expansion, while in Sec. 2.5 we will present an alternative derivation within the derivative expansion by using a generalization of the LPA'.

2.4 Kosterlitz-Thouless flow equations from the vertex expansion

2.4.1 General strategy

For a non-trivial system like the Villain model, it is of course impossible to keep track of an infinite number of couplings in an exact way. We therefore start with a few remarks about the strategy that we will use in this section and the approximations we will be making. Let us first write down the initial condition for the generating functional of the irreducible vertices in the continuum limit [cf. Eq. (2.76)],

$$\begin{aligned}\Gamma_{\Lambda_0}[\bar{m}] &= -N \ln \sqrt{\frac{\pi}{4\tau}} + \frac{1}{2}\sum_{\boldsymbol{k}} \omega_{\boldsymbol{k}} \, |\bar{m}_{\boldsymbol{k}}|^2 - 2y_0 \sum_i \cos(2\pi \bar{m}_i) + O(y_0^2) \\ &= N\Gamma_{\Lambda_0}^{(0)} + \frac{1}{2}\sum_{\boldsymbol{k}} (r_{\Lambda_0} + c_{\Lambda_0} k^2) \, |\bar{m}_{\boldsymbol{k}}|^2 + \sum_{n=2}^{\infty} \frac{u_{\Lambda_0}^{(2n)}}{(2n)!} \sum_i \bar{m}_i^{2n} + O(y_0^2),\end{aligned} \tag{2.87}$$

where

$$\Gamma_{\Lambda_0}^{(0)} = -\ln \sqrt{\frac{\pi}{4\tau}} - 2y_0, \tag{2.88a}$$

$$r_{\Lambda_0} = u_{\Lambda_0}^{(2)} = (2\pi)^2 2y_0, \tag{2.88b}$$

$$c_{\Lambda_0} = \tau a^2, \tag{2.88c}$$

$$u_{\Lambda_0}^{(2n)} = (-1)^{n+1} (2\pi)^{2n} 2y_0. \tag{2.88d}$$

Since we have chosen the regulator such that at the initial scale the system reduces to a single-site problem, we see that the expansion of Γ_{Λ_0} in the initial vortex fugacity amounts to an expansion of the initial value of the relevant couplings $u^{(2n)}_{\Lambda_0}$ in y_0, which to leading order depend linearly on the initial vortex fugacity. This continues to hold during the flow: defining the flowing vortex fugacity y_Λ via

$$\Gamma^{(2)}_\Lambda(0) = u^{(2)}_\Lambda = r_\Lambda = (2\pi)^2 2y_\Lambda \tag{2.89}$$

so that $y_{\Lambda_0} = y_0 + O(y_0^2)$, the flowing relevant couplings $u^{(2n)}_\Lambda$ will to leading order depend linearly on y_Λ. Furthermore, for $n \geq 2$ we will find that the marginal couplings $c^{(2n)}_\Lambda$, which initially vanish, will to leading order be proportional to y_Λ^2. These facts will allow us to simplify the flow equations of the relevant and marginal couplings by expanding the right-hand side to leading order in y_Λ, which makes it possible to solve the infinite hierarchy of flow equations analytically. Consider the exact flow equation of the irreducible two-point vertex,

$$\partial_\Lambda \Gamma^{(2)}_\Lambda(\boldsymbol{k}) = \frac{1}{2N} \sum_{\boldsymbol{q}} \dot{G}_\Lambda(\boldsymbol{q}) \Gamma^{(4)}_\Lambda(\boldsymbol{k}, -\boldsymbol{k}, \boldsymbol{q}, -\boldsymbol{q}). \tag{2.90}$$

From the considerations above it is clear that to leading order in y_Λ and neglecting irrelevant couplings, we can ignore the dependence of $\Gamma^{(4)}_\Lambda$ on the loop-momentum $\boldsymbol{q}$. This results in the simpler flow equation

$$\partial_\Lambda \Gamma^{(2)}_\Lambda(\boldsymbol{k}) = \frac{1}{2N} \sum_{\boldsymbol{q}} \dot{G}_\Lambda(\boldsymbol{q}) \Gamma^{(4)}_\Lambda(\boldsymbol{k}), \tag{2.91}$$

where we have defined

$$\Gamma^{(2n)}_\Lambda(\boldsymbol{k}) = \Gamma^{(2n)}_\Lambda(\boldsymbol{k}, -\boldsymbol{k}, 0, \ldots, 0), \quad n \in \mathbb{Z}^+. \tag{2.92}$$

Dropping all contributions which are at least of the order of y_Λ^3, we can simplify the flow equations of the irreducible four- and six-point vertices in a similar way, which results in [cf. Eq. (2.62)]

$$\begin{aligned}\partial_\Lambda \Gamma^{(4)}_\Lambda(\boldsymbol{k}) = \frac{1}{N} \sum_{\boldsymbol{q}} \dot{G}_\Lambda(\boldsymbol{q}) \Big[&\frac{1}{2} \Gamma^{(6)}_\Lambda(\boldsymbol{k}) - G_\Lambda(\boldsymbol{q}) \Gamma^{(4)}_\Lambda(\boldsymbol{k}) \Gamma^{(4)}_\Lambda(0) \\ &- 2G_\Lambda(\boldsymbol{k}+\boldsymbol{q}) [\Gamma^{(4)}_\Lambda(\boldsymbol{k})]^2 \Big]\end{aligned} \tag{2.93}$$

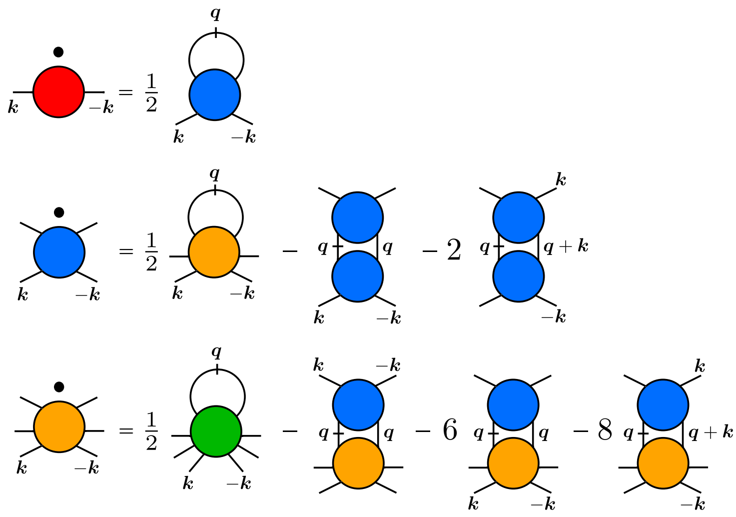

Figure 2.7: Graphical representation of the approximate flow equations of the irreducible vertices $\Gamma_\Lambda^{(2)}(\boldsymbol{k})$, $\Gamma_\Lambda^{(4)}(\boldsymbol{k})$, and $\Gamma_\Lambda^{(6)}(\boldsymbol{k})$ as given in Eqs. (2.91), (2.93), and (2.94), respectively. External legs without labels carry vanishing momentum. (Figure reproduced with modifications from Ref. [54])

and (cf. Fig. 2.6)

$$\partial_\Lambda \Gamma_\Lambda^{(6)}(\boldsymbol{k}) = \frac{1}{N}\sum_{\boldsymbol{q}} \dot{G}_\Lambda(\boldsymbol{q})\bigg[\frac{1}{2}\Gamma_\Lambda^{(8)}(\boldsymbol{k}) - G_\Lambda(\boldsymbol{q})\Gamma_\Lambda^{(4)}(\boldsymbol{k})\Gamma_\Lambda^{(6)}(0) \\ - 6G_\Lambda(\boldsymbol{q})\Gamma_\Lambda^{(4)}(0)\Gamma_\Lambda^{(6)}(\boldsymbol{k}) - 8G_\Lambda(\boldsymbol{q}+\boldsymbol{k})\Gamma_\Lambda^{(4)}(\boldsymbol{k})\Gamma_\Lambda^{(6)}(\boldsymbol{k})\bigg]. \tag{2.94}$$

In Fig. 2.7 we show a graphical representation of these approximate flow equations.

2.4.2 Flow of the relevant couplings

To begin with, let us concentrate on the flow of the relevant couplings $u_\Lambda^{(2n)}$, which are defined as the momentum-independent part of the irreducible $2n$-point vertices. Since all $\Gamma_\Lambda^{(2n)}$ with $n \in \mathbb{Z}^+$ are at least of the order of y_Λ, we see that to leading order in the flowing vortex fugacity it is sufficient to keep only the first term in the flow equations. This results in the infinite hierarchy

$$\partial_\Lambda u_\Lambda^{(2n)} = \frac{A_\Lambda}{2} u_\Lambda^{(2n+2)}, \quad n \in \mathbb{Z}^+, \tag{2.95}$$

where A_Λ is given by

$$A_\Lambda = \frac{1}{N}\sum_{\boldsymbol{q}} \dot{G}_\Lambda(\boldsymbol{q}) = -\frac{a^2\left(\Lambda^3 c_\Lambda + \frac{1}{4}\Lambda^4 \partial_\Lambda c_\Lambda\right)}{2\pi(r_\Lambda + c_\Lambda \Lambda^2)^2} = -\frac{a^2\left(1 + \frac{1}{4}\Lambda \frac{\partial_\Lambda c_\Lambda}{c_\Lambda}\right)}{2\pi c_\Lambda \Lambda[1 + r_\Lambda/(c_\Lambda\Lambda^2)]^2}$$
$$= -\frac{a^2\left[1 + O(y_\Lambda^2)\right]}{2\pi c_\Lambda \Lambda[1 + O(y_\Lambda)]^2} = -\frac{1}{2\pi\tau_l\Lambda} + O(y_\Lambda). \tag{2.96}$$

Here we have used that $\partial_\Lambda c_\Lambda$ is of the order of y_Λ^2, which we will show explicitly in Sec. 2.4.3, and we have introduced the scale-dependent dimensionless temperature τ_l,

$$\tau_l = \frac{c_\Lambda}{a^2}, \tag{2.97}$$

which is a function of the logarithmic scale parameter $l = \ln(\Lambda_0/\Lambda)$. With the logarithmic scale derivative $\partial_l = -\Lambda\partial_\Lambda$ we can now write down the infinite hierarchy of coupled flow equations of the relevant couplings as

$$\partial_l u_\Lambda^{(2n)} = \frac{u_\Lambda^{(2n+2)}}{4\pi\tau_l} + O(y_\Lambda^2), \quad n \in \mathbb{Z}^+, \tag{2.98}$$

with the initial condition

$$u_{\Lambda_0}^{(2n)} = (-1)^{n+1}(2\pi)^{2n} 2y_0, \tag{2.99}$$

which obeys the recurrence relation $u_{\Lambda_0}^{(2n+2)} = -(2\pi)^2 u_{\Lambda_0}^{(2n)}$. The obvious ansatz of generalizing this relation to arbitrary Λ,

$$u_\Lambda^{(2n+2)} = -(2\pi)^2 u_\Lambda^{(2n)}, \tag{2.100}$$

is in fact compatible with the flow equations, which subsequently decouple as

$$\partial_l u_\Lambda^{(2n)} = -\frac{\pi}{\tau_l} u_\Lambda^{(2n)} + O(y_\Lambda^2), \quad n \in \mathbb{Z}^+. \tag{2.101}$$

Note that relation (2.100) or the equivalent statement

$$u_\Lambda^{(2n)} = (-1)^{n+1}(2\pi)^{2n} 2y_\Lambda \tag{2.102}$$

amount to the ansatz

$$U_\Lambda(\bar{m}) = \frac{1}{N}\,\Gamma_\Lambda[\bar{m}]\big|_{\bar{m}_i=\bar{m}} = \Gamma_\Lambda^{(0)} + 2y_\Lambda - 2y_\Lambda\cos(2\pi\bar{m}) \tag{2.103}$$

for the effective potential, which we will encounter again in Sec. 2.5 in the context of the derivative expansion. In order to derive the Kosterlitz-Thouless

RG equations, we are mainly interested in the irreducible two-point vertex. We therefore set $n = 1$ in Eq. (2.101) to obtain the flow of the vortex fugacity,

$$\partial_l y_\Lambda = -\frac{\pi}{\tau_l} y_\Lambda + O(y_\Lambda^2). \tag{2.104}$$

Since y_Λ is a relevant coupling with a scaling dimension of two, we should introduce the rescaled vortex fugacity

$$\tilde{y}_l = \frac{(2\pi)^3 2 y_\Lambda}{c_\Lambda \Lambda^2} = -\frac{u_\Lambda^{(4)}}{2\pi c_\Lambda \Lambda^2}, \tag{2.105}$$

which obeys the flow equation

$$\partial_l \tilde{y}_l = (2 - \eta_l - \pi/\tau_l)\tilde{y}_l + O(\tilde{y}_l^2). \tag{2.106}$$

As we will later show that the flowing anomalous dimension

$$\eta_l = \frac{\partial_l \tau_l}{\tau_l} \tag{2.107}$$

of the dual-vortex field $\bar{m}_{\boldsymbol{k}}$ is of the order of $\tilde{y}_l^2$, we recover the first Kosterlitz-Thouless RG equation from Sec. 2.1.3,

$$\partial_l \tilde{y}_l = (2 - \pi/\tau_l)\tilde{y}_l + O(\tilde{y}_l^2). \tag{2.108}$$

2.4.3 Flow of the marginal couplings

The remaining step is now to solve the infinite hierarchy of flow equations of the marginal couplings. We start by writing down the flow equation of τ_l,

$$\partial_\Lambda \tau_l = \frac{A_\Lambda}{4} c_\Lambda^{(4)}, \tag{2.109}$$

which follows from the long-wavelength expansion of Eq. (2.91). Using the same approximation of A_Λ as before [see Eq. (2.96)], we find to leading order in the vortex fugacity

$$\partial_l \tau_l = \frac{c_\Lambda^{(4)}}{8\pi\tau_l}. \tag{2.110}$$

Since the structure of the flow equations of the marginal couplings is more complicated than in the case of the relevant couplings, let us first consider the flow equation of $c_\Lambda^{(4)}$ in detail. From the Taylor expansion of Eq. (2.93) we see that

$$\partial_\Lambda c_\Lambda^{(4)} = \frac{A_\Lambda}{2} c_\Lambda^{(6)} - 5 B_\Lambda^0 u_\Lambda^{(4)} c_\Lambda^{(4)} - 2 B_\Lambda'' \left(u_\Lambda^{(4)}\right)^2, \tag{2.111}$$

where the coefficients B^0_Λ and B''_Λ are defined via

$$B_\Lambda(k) = \frac{1}{N}\sum_{\boldsymbol{q}} \dot{G}_\Lambda(\boldsymbol{q}) G_\Lambda(\boldsymbol{q}+\boldsymbol{k}) = B^0_\Lambda + \frac{k^2 a^2}{2} B''_\Lambda + O(k^4). \tag{2.112}$$

Within our cutoff scheme, we can analytically evaluate them to leading order in y_Λ as

$$B^0_\Lambda = -\frac{a^2\left(\Lambda^3 c_\Lambda + \frac{1}{4}\Lambda^4 \partial_\Lambda c_\Lambda\right)}{2\pi(r_\Lambda + c_\Lambda \Lambda^2)^3} = -\frac{a^2}{2\pi c_\Lambda^2 \Lambda^3} + O(y_\Lambda), \tag{2.113}$$

$$B''_\Lambda = \frac{c_\Lambda^2 \Lambda^3}{2\pi(r_\Lambda + c_\Lambda \Lambda^2)^4} = \frac{1}{2\pi c_\Lambda^2 \Lambda^5} + O(y_\Lambda), \tag{2.114}$$

so that

$$\partial_l c^{(4)}_\Lambda = \frac{c^{(6)}_\Lambda}{4\pi\tau_l} - \frac{5u^{(4)}_\Lambda c^{(4)}_\Lambda}{2\pi\tau_l c_\Lambda \Lambda^2} + \frac{1}{\pi}\left(\frac{u^{(4)}_\Lambda}{c_\Lambda \Lambda^2}\right)^2 = \frac{c^{(6)}_\Lambda}{4\pi\tau_l} + \frac{5c^{(4)}_\Lambda \tilde{y}_l}{\tau_l} + 4\pi\tilde{y}_l^2, \tag{2.115}$$

where we have used the definition (2.105) of $\tilde{y}_l$. However, as we have mentioned before in Sec. 2.4.1, all $c^{(2n)}_\Lambda$ with $n \geq 2$ are of the order of $\tilde{y}_l^2$. This allows us to drop the second term in the flow equation of $c^{(4)}_\Lambda$, which thus reads

$$\partial_l c^{(4)}_\Lambda = \frac{c^{(6)}_\Lambda}{4\pi\tau_l} + 4\pi\tilde{y}_l^2 + O(\tilde{y}_l^3). \tag{2.116}$$

To get an idea of the general structure, let us also consider the flow equations of the marginal couplings $c^{(6)}_\Lambda$ and $c^{(8)}_\Lambda$ explicitly. From Eq. (2.94) we see that

$$\partial_\Lambda c^{(6)}_\Lambda = \frac{A_\Lambda}{2} c^{(8)}_\Lambda - 8u^{(4)}_\Lambda u^{(6)}_\Lambda B''_\Lambda, \tag{2.117}$$

since all other terms containing either $c^{(4)}_\Lambda$ or $c^{(6)}_\Lambda$ are of the order of y^3_Λ. With our leading-order results for A_Λ and B''_Λ given above as well as the recurrence relation (2.102), we can write the flow equation as

$$\partial_l c^{(6)}_\Lambda = \frac{c^{(8)}_\Lambda}{4\pi\tau_l} - (4\pi)^3\tilde{y}_l^2 + O(\tilde{y}_l^3). \tag{2.118}$$

Writing down the flow equation of $\Gamma^{(8)}_\Lambda(\boldsymbol{k})$, one can analogously show that

$$\partial_\Lambda c^{(8)}_\Lambda = \frac{A_\Lambda}{2} c^{(10)}_\Lambda - \left[12u^{(4)}_\Lambda u^{(8)}_\Lambda + 20(u^{(6)}_\Lambda)^2\right] B''_\Lambda, \tag{2.119}$$

which to leading order in the vortex fugacity reads

$$\partial_l c_\Lambda^{(8)} = \frac{c_\Lambda^{(10)}}{4\pi\tau_l} + (4\pi)^5 \tilde{y}_l^2 + O(\tilde{y}_l^3). \tag{2.120}$$

Comparing Eqs. (2.116), (2.118), and (2.120), we see that they have the form

$$\partial_l c_\Lambda^{(2n)} = \frac{c_\Lambda^{(2n+2)}}{4\pi\tau_l} + (-1)^n (4\pi)^{2n-3} \tilde{y}_l^2 + O(\tilde{y}_l^3). \tag{2.121}$$

It turns out that this expression is in fact valid for all $n \geq 2$ (see Appendix A.1 for the explicit derivation) and thus constitutes an infinite hierarchy of coupled flow equations. Though this system of differential equations is more complicated than the one for the relevant couplings in Eq. (2.98), we can solve it analogously with the ansatz

$$c_\Lambda^{(2n+2)} = -(4\pi)^2 c_\Lambda^{(2n)}, \quad n \geq 2, \tag{2.122}$$

which implies

$$c_\Lambda^{(2n)} = (-1)^n (4\pi)^{2n-4} c_\Lambda^{(4)}, \quad n \geq 2. \tag{2.123}$$

This decouples the flow equations as

$$\partial_l c_\Lambda^{(2n)} = -\frac{4\pi}{\tau_l} c_\Lambda^{(2n)} + (-1)^n (4\pi)^{2n-3} \tilde{y}_l^2 + O(\tilde{y}_l^3). \tag{2.124}$$

To simplify this further, it is convenient to parametrize

$$c_\Lambda^{(2n)} = (-1)^n (4\pi)^{2n-3} \tilde{c}_l \tilde{y}_l^2, \quad n \geq 2. \tag{2.125}$$

Inserting this into the flow equation of $c_\Lambda^{(2n)}$ and using Eq. (2.108) to replace $\partial_l \tilde{y}_l$ results in

$$\partial_l \tilde{c}_l = 1 - \tilde{c}_l \left(4 + \frac{2\pi}{\tau_l}\right) + O(\tilde{y}_l). \tag{2.126}$$

From this expression we readily see that $\tilde{c}_l$ is of order unity; as a result, the $c_\Lambda^{(2n)}$ with $n \geq 2$ are of the order of $\tilde{y}_l^2$, justifying our previous approximations. To leading order in the vortex fugacity we thus have to take care of three independent couplings, which flow according to

$$\partial_l \tilde{y}_l = (2 - \pi/\tau_l)\tilde{y}_l, \tag{2.127a}$$

$$\partial_l \tau_l = \frac{\tilde{c}_l \tilde{y}_l^2}{2\tau_l}, \tag{2.127b}$$

$$\partial_l \tilde{c}_l = 1 - \tilde{c}_l \left(4 + \frac{2\pi}{\tau_l}\right). \tag{2.127c}$$

However, in the vicinity of the line of Gaussian fixed points at $\tilde{y}_l = 0$ and $\tau_l \leq \pi/2$, the third coupling $\tilde{c}_l$ will rapidly converge to

$$\tilde{c}_l = \frac{1}{4 + \frac{2\pi}{\tau_l}}, \tag{2.128}$$

so that

$$\partial_l \tau_l = \frac{\tilde{y}_l^2}{8\tau_l + 4\pi} + O(\tilde{y}_l^3). \tag{2.129}$$

Close to the BKT transition temperature for vanishing vortex fugacity, $\tau_l \approx \tau_* = \pi/2$, we therefore recover the second Kosterlitz-Thouless RG equation from Sec. 2.1.3,

$$\partial_l \tau_l = \frac{\tilde{y}_l^2}{8\pi} + O(\tilde{y}_l^3). \tag{2.130}$$

Solving this flow equation together with

$$\partial_l \tilde{y}_l = (2 - \pi/\tau_l)\tilde{y}_l + O(\tilde{y}_l^2) \tag{2.131}$$

then results in the well-known flow diagram shown in Fig. 2.3. Note that since y_Λ is a relevant coupling, there is some freedom in defining the rescaled coupling $\tilde{y}_l$. While Eq. (2.131) is unaffected by this, a rescaling of $\tilde{y}_l$ would change the prefactor on the right-hand side of Eq. (2.130), which is thus non-universal. Finally, let us point out a technical subtlety regarding the flow equation of $\tilde{y}_l$: while it is certainly consistent for general τ_l to neglect the second-order term in the vortex fugacity, this is not true for the interesting region close to $\tau_* = \pi/2$, where the coefficient of the linear $\tilde{y}_l$ term can become arbitrarily small. In that case, our result in Eq. (2.131) should be understood as the second-order mixed term in a double expansion in $\tilde{y}_l$ and in $\tau - \tau_*$, which implies that we also have to take the $\tilde{y}_l^2$ term at $\tau = \tau_*$ into account to be consistent. However, in Appendix A.2 we show that including the next-to-leading-order term yields

$$\partial_l \tilde{y}_l = \left(2 - \frac{\pi}{\tau_l}\right)\tilde{y}_l + \frac{8\tau_l + 5\pi}{8\,(\tau_l + \pi)\,(2\tau_l + \pi)}\left(2 - \frac{\pi}{\tau_l}\right)\tilde{y}_l^2 + O(\tilde{y}_l^3). \tag{2.132}$$

It follows that Eq. (2.131) is indeed correct to second order in the double expansion in $\tilde{y}_l$ and in $\tau - \tau_*$.

2.5 Alternative derivation within the derivative expansion

2.5.1 Parametrization of $\Gamma_\Lambda[\bar{m}]$

As we have seen in the last section, working within the vertex expansion amounts to taking an infinite number of relevant and marginal couplings into account and solving the corresponding infinite hierarchy of flow equations. The analytic solution to this was helped by the internal structure of the infinite sets of couplings $\{u_\Lambda^{(2n)}\}$ and $\{c_\Lambda^{(2n)}\}$; this structure can be traced back to the cosine term in the initial condition (2.87) of $\Gamma_\Lambda[\bar{m}]$, which relates higher-order couplings via its Taylor expansion. While we were successful in deriving the Kosterlitz-Thouless flow equations in Sec. 2.4, it nevertheless seems inefficient to renormalize the prefactor of a cosine function by working with its infinite number of Taylor coefficients. We will therefore show in the present section how we can recover the flow equations of τ_l and $\tilde{y}_l$ from the derivative expansion. This expansion strategy has been very successful to calculate the critical exponents of $O(N)$-symmetric scalar models [79]. Intuitively, an expansion in gradients of the field $\bar{m}_i$ is justified by the fact that we are interested in the long-wavelength properties of the system.[3]

We start by parametrizing the generating functional of the irreducible vertices as

$$\Gamma_\Lambda[\bar{m}] = \sum_i U_\Lambda(\bar{m}_i) + \frac{1}{2}\sum_i c_\Lambda(\bar{m}_i)\left(\boldsymbol{\nabla}_{\boldsymbol{r}_i}\bar{m}_i\right)^2, \tag{2.133}$$

so that for a space-independent field configuration

$$\Gamma_\Lambda[\bar{m}]\big|_{\bar{m}_i=\bar{m}} = N U_\Lambda(\bar{m}), \tag{2.134}$$

$$\left.\frac{\delta^2\Gamma_\Lambda[\bar{m}]}{\delta\bar{m}_{\boldsymbol{k}}\delta\bar{m}_{-\boldsymbol{k}}}\right|_{\bar{m}_i=\bar{m}} = U_\Lambda''(\bar{m}) + c_\Lambda(\bar{m})k^2. \tag{2.135}$$

Here $U_\Lambda(\bar{m})$ is the effective potential and $c_\Lambda(\bar{m})$ is the field-dependent wave-function renormalization factor, whose field-independent part corresponds to

$$c_\Lambda(\bar{m}=0) = c_\Lambda = \tau_l a^2. \tag{2.136}$$

In contrast to the usual approach, it is for our purpose more convenient to work directly with $\bar{m}$ instead of $\bar{m}^2/2$. Comparing our parametrization of

[3] While $\Gamma_\Lambda[\bar{m}]$ can contain non-analyticities in the physical limit $\Lambda \to 0$, this is not the case for finite Λ where long-wavelength fluctuations are suppressed by the regulator.

$\Gamma_\Lambda[\bar{m}]$ with its initial value (2.87), we find that

$$U_{\Lambda_0}(\bar{m}) = -\ln\sqrt{\frac{\pi}{4\tau}} - 2y_0\cos(2\pi\bar{m}) + O(y_0^2) \tag{2.137}$$

$$c_{\Lambda_0}(\bar{m}) = c_{\Lambda_0} = \tau a^2. \tag{2.138}$$

Note that neither the local potential approximation (LPA) nor its common improvement LPA' (see, e.g., Ref. [33]) would be sufficient for our system, since we know from Sec. 2.3.3 that all Taylor coefficients of $c_\Lambda(\bar{m})$ are marginal and have to be taken into account. As a result, we need to compute the flow of both $U_\Lambda(\bar{m})$ and $c_\Lambda(\bar{m})$.

2.5.2 Derivation of the flow equations of $U_\Lambda(\bar{m})$ and $c_\Lambda(\bar{m})$

Flow equation of the effective potential

Let us first consider the effective potential, whose flow equation can be simply read off from the Wetterich equation (2.57) as

$$\partial_\Lambda U_\Lambda(\bar{m}) = \frac{1}{2N}\sum_{\boldsymbol{k}} \frac{\partial_\Lambda R_\Lambda(\boldsymbol{k})}{U''_\Lambda(\bar{m}) + c_\Lambda(\bar{m})k^2 + R_\Lambda(\boldsymbol{k})}. \tag{2.139}$$

Since the regulator is given by [cf. Eq. (2.80)]

$$R_\Lambda(\boldsymbol{k}) = c_\Lambda(\Lambda^2 - k^2)\Theta(\Lambda^2 - k^2), \tag{2.140}$$

it will be useful to introduce the shorthand $G^<_\Lambda$ as the low-momentum part ($k < \Lambda$) of the propagator,

$$G^<_\Lambda(\bar{m}, k) = \frac{1}{U''_\Lambda(\bar{m}) + [c_\Lambda(\bar{m}) - c_\Lambda]\,k^2 + c_\Lambda\Lambda^2}. \tag{2.141}$$

With the flowing anomalous dimension $\eta_l = \partial_l \ln\tau_l$ we can then write the flow equation of $U_\Lambda(\bar{m})$ as

$$\begin{aligned}\partial_l U_\Lambda(\bar{m}) &= -\frac{a^2\Lambda^2}{4\pi}\int_0^1 dx x G^<_\Lambda(\bar{m}, \Lambda x)\left[2\Lambda^2 c_\Lambda + (\partial_\Lambda c_\Lambda)\Lambda^3(1-x^2)\right] \\ &= -\frac{a^2\Lambda^2}{4\pi}\frac{c_\Lambda}{c_\Lambda(\bar{m}) - c_\Lambda}\left\{\frac{\eta_l}{2} + \left[1 - \frac{\eta_l}{2}\left(1 + \frac{c_\Lambda\Lambda^2 + U''_\Lambda(\bar{m})}{[c_\Lambda(\bar{m}) - c_\Lambda]\Lambda^2}\right)\right]\right. \\ &\qquad\left.\times\ln\left(1 + \frac{[c_\Lambda(\bar{m}) - c_\Lambda]\Lambda^2}{c_\Lambda\Lambda^2 + U''_\Lambda(\bar{m})}\right)\right\}.\end{aligned} \tag{2.142}$$

Flow equation of the wave-function renormalization factor

Next we evaluate the flow equation of the field-dependent wave-function renormalization factor, which is given by

$$c_\Lambda(\bar{m}) = \frac{1}{2} \lim_{\boldsymbol{k}\to 0} \partial_k^2 \left. \frac{\delta^2 \Gamma_\Lambda[\bar{m}]}{\delta \bar{m}_{\boldsymbol{k}} \delta \bar{m}_{-\boldsymbol{k}}} \right|_{\bar{m}_i = \bar{m}} . \tag{2.143}$$

We therefore need the second derivative of the Wetterich equation with respect to the field,

$$\begin{aligned} \partial_\Lambda \left. \frac{\delta^2 \Gamma_\Lambda[\bar{m}]}{\delta \bar{m}_{\boldsymbol{k}} \delta \bar{m}_{-\boldsymbol{k}}} \right|_{\bar{m}_i = \bar{m}} &= \frac{1}{2} \sum_{\boldsymbol{q}} \dot{G}_\Lambda(\bar{m}, \boldsymbol{q}) \Gamma_\Lambda^{(4)}(\bar{m}, \boldsymbol{k}, -\boldsymbol{k}, \boldsymbol{q}, -\boldsymbol{q}) \\ &\quad - \sum_{\boldsymbol{q}} \dot{G}_\Lambda(\bar{m}, \boldsymbol{q}) G_\Lambda^{(2)}(\bar{m}, \boldsymbol{k}+\boldsymbol{q}) \left[\Gamma_\Lambda^{(3)}(\bar{m}, \boldsymbol{k}, \boldsymbol{q}, -\boldsymbol{k}-\boldsymbol{q}) \right]^2 . \end{aligned} \tag{2.144}$$

The irreducible four-point vertex is for a space-independent field configuration given by

$$\Gamma_\Lambda^{(4)}(\bar{m}, \boldsymbol{k}, -\boldsymbol{k}, \boldsymbol{q}, -\boldsymbol{q}) = \frac{1}{N} \left[U_\Lambda''''(\bar{m}) + c_\Lambda''(\bar{m})(k^2 - 4\boldsymbol{k}\cdot\boldsymbol{q} + q^2) \right] , \tag{2.145}$$

so that

$$\frac{1}{2} \lim_{\boldsymbol{k}\to 0} \partial_k^2 \Gamma_\Lambda^{(4)}(\bar{m}, \boldsymbol{k}, -\boldsymbol{k}, \boldsymbol{q}, -\boldsymbol{q}) = \frac{c_\Lambda''(\bar{m})}{N} . \tag{2.146}$$

As a consequence, we can write the $\Gamma_\Lambda^{(4)}$ contribution to the flow equation of $c_\Lambda(\bar{m})$ as

$$\frac{1}{2} \sum_{\boldsymbol{q}} \dot{G}_\Lambda(\bar{m}, \boldsymbol{q}) \frac{1}{2} \partial_k^2 \left. \Gamma_\Lambda^{(4)}(\bar{m}, \boldsymbol{k}, -\boldsymbol{k}, \boldsymbol{q}, -\boldsymbol{q}) \right|_{k=0} = -\frac{c_\Lambda c_\Lambda''(\bar{m}) a^2 \Lambda^3}{4\pi} I_\Lambda^{(4)}(\bar{m}), \tag{2.147}$$

where we have defined

$$I_\Lambda^{(4)}(\bar{m}) = \int_0^1 dx x \left[G_\Lambda^<(\bar{m}, \Lambda x) \right]^2 \left[2 - \eta_l (1 - x^2) \right] . \tag{2.148}$$

For the irreducible three-point vertex we find

$$\Gamma_\Lambda^{(3)}(\bar{m}, \boldsymbol{k}, \boldsymbol{q}, -\boldsymbol{k}-\boldsymbol{q}) = \frac{1}{\sqrt{N}} \left[U_\Lambda'''(\bar{m}) + (k^2 + \boldsymbol{k}\cdot\boldsymbol{q} + q^2) c_\Lambda'(\bar{m}) \right] . \tag{2.149}$$

Due to the $\boldsymbol{k}$ dependence in the propagator in Eq. (2.144) we need the derivatives

$$\partial_k \, \Gamma^{(3)}_\Lambda(\bar{m}, \boldsymbol{k}, \boldsymbol{q}, -\boldsymbol{k}-\boldsymbol{q})\Big|_{k=0} = \frac{c'_\Lambda(\bar{m}) q \cos\phi}{\sqrt{N}}, \tag{2.150}$$

$$\partial_k^2 \, \Gamma^{(3)}_\Lambda(\bar{m}, \boldsymbol{k}, \boldsymbol{q}, -\boldsymbol{k}-\boldsymbol{q})\Big|_{k=0} = \frac{2c'_\Lambda(\bar{m})}{\sqrt{N}}, \tag{2.151}$$

where ϕ is defined via $\boldsymbol{k}\cdot\boldsymbol{q} = kq\cos\phi$. We thus get

$$\partial_k \left[\Gamma^{(3)}_\Lambda(\bar{m}, \boldsymbol{k}, \boldsymbol{q}, -\boldsymbol{k}-\boldsymbol{q})\right]^2\Big|_{k=0} = \frac{2c'_\Lambda(\bar{m}) q\cos\phi}{N}\left[U'''_\Lambda(\bar{m}) + q^2 c'_\Lambda(\bar{m})\right], \tag{2.152}$$

$$\partial_k^2 \left[\Gamma^{(3)}_\Lambda(\bar{m}, \boldsymbol{k}, \boldsymbol{q}, -\boldsymbol{k}-\boldsymbol{q})\right]^2\Big|_{k=0} = \frac{2c'_\Lambda(\bar{m})}{N}\left[\left(2+\cos^2\phi\right) q^2 c'_\Lambda(\bar{m}) + 2U'''_\Lambda(\bar{m})\right]. \tag{2.153}$$

We also need the derivatives of the propagator with respect to k, which for $q < \Lambda$ are given by

$$\partial_k \, G^{(2)}_\Lambda(\bar{m}, \boldsymbol{k}+\boldsymbol{q})\Big|_{k=0} = -2q\cos\phi\,[c_\Lambda(\bar{m}) - c_\Lambda]\,[G^<_\Lambda(\bar{m}, q)]^2\,, \tag{2.154}$$

$$\begin{aligned}\partial_k^2 \, G^{(2)}_\Lambda(\bar{m}, \boldsymbol{k}+\boldsymbol{q})\Big|_{k=0} = 2\,[G^<_\Lambda(\bar{m}, q)]^2 \Big\{ & 4q^2\cos^2\phi\,[c_\Lambda(\bar{m}) - c_\Lambda]^2\, G^<_\Lambda(\bar{m}, q) \\ & - [c_\Lambda(\bar{m}) - c_\Lambda] - \Lambda c_\Lambda \cos^2\phi\,\delta(\Lambda - q)\Big\}.\end{aligned} \tag{2.155}$$

Putting these expressions together, we find that the three $\Gamma^{(3)}_\Lambda$ contributions to the flow of $c_\Lambda(\bar{m})$ read

$$\begin{aligned}& -\sum_{\boldsymbol{q}} \dot{G}_\Lambda(\bar{m}, \boldsymbol{q}) G^{(2)}_\Lambda(\bar{m}, \boldsymbol{q}) \frac{\partial_k^2}{2}\left[\Gamma^{(3)}_\Lambda(\bar{m}, \boldsymbol{k}, \boldsymbol{q}, -\boldsymbol{k}-\boldsymbol{q})\right]^2\Big|_{k=0} \\ & = \frac{c_\Lambda c'_\Lambda(\bar{m}) a^2 \Lambda^3}{2\pi} I^{(1)}_\Lambda(\bar{m}),\end{aligned} \tag{2.156}$$

$$\begin{aligned}& -\sum_{\boldsymbol{q}} \dot{G}_\Lambda(\bar{m}, \boldsymbol{q})\, \partial_k G^{(2)}_\Lambda(\bar{m}, \boldsymbol{k}+\boldsymbol{q})\Big|_{k=0} \partial_k \left[\Gamma^{(3)}_\Lambda(\bar{m}, \boldsymbol{k}, \boldsymbol{q}, -\boldsymbol{k}-\boldsymbol{q})\right]^2\Big|_{k=0} \\ & = -\frac{c_\Lambda c'_\Lambda(\bar{m})\,[c_\Lambda(\bar{m}) - c_\Lambda]\, a^2\Lambda^5}{\pi} I^{(2)}_\Lambda(\bar{m}),\end{aligned} \tag{2.157}$$

$$\begin{aligned}& -\sum_{\boldsymbol{q}} \dot{G}_\Lambda(\bar{m}, \boldsymbol{q}) \frac{\partial_k^2}{2}\, G^{(2)}_\Lambda(\bar{m}, \boldsymbol{k}+\boldsymbol{q})\Big|_{k=0} \left[\Gamma^{(3)}_\Lambda(\bar{m}, 0, \boldsymbol{q}, -\boldsymbol{q})\right]^2 \\ & = \frac{c_\Lambda\,[c_\Lambda(\bar{m}) - c_\Lambda]\, a^2\Lambda^3}{2\pi} I^{(3)}_\Lambda(\bar{m}) - \frac{c_\Lambda^2 a^2 \Lambda^3}{4\pi}\left[c'_\Lambda(\bar{m})\Lambda^2 + U'''_\Lambda(\bar{m})\right]^2 [G^<_\Lambda(\bar{m}, \Lambda)]^4\,,\end{aligned} \tag{2.158}$$

where the momentum integrals are given by

$$I_\Lambda^{(1)}(\bar{m}) = \int_0^1 dx x \left[G_\Lambda^<(\bar{m}, \Lambda x)\right]^3 \Big[2 - \eta_l(1 - x^2)\Big] \left[\frac{5}{2} c'_\Lambda(\bar{m}) x^2 \Lambda^2 + 2U'''_\Lambda(\bar{m})\right], \tag{2.159}$$

$$I_\Lambda^{(2)}(\bar{m}) = \int_0^1 dx x^3 \left[G_\Lambda^<(\bar{m}, \Lambda x)\right]^4 \Big[2 - \eta_l(1 - x^2)\Big] \Big[c'_\Lambda(\bar{m}) x^2 \Lambda^2 + U'''_\Lambda(\bar{m})\Big], \tag{2.160}$$

$$\begin{aligned} I_\Lambda^{(3)}(\bar{m}) = \int_0^1 dx x \left[G_\Lambda^<(\bar{m}, \Lambda x)\right]^4 \Big[2 - \eta_l(1 - x^2)\Big] \Big[c'_\Lambda(\bar{m}) x^2 \Lambda^2 + U'''_\Lambda(\bar{m})\Big]^2 \\ \times \Big[2\left[c_\Lambda(\bar{m}) - c_\Lambda\right] x^2 \Lambda^2 G_\Lambda^<(\bar{m}, \Lambda x) - 1\Big]. \end{aligned} \tag{2.161}$$

Putting everything together, we arrive at the flow equation

$$\begin{aligned} \partial_l c_\Lambda(\bar{m}) = \frac{c_\Lambda a^2 \Lambda^2}{4\pi} \Bigg[& - 2c'_\Lambda(\bar{m}) \Lambda^2 I_\Lambda^{(1)}(\bar{m}) + 4c'_\Lambda(\bar{m}) \left[c_\Lambda(\bar{m}) - c_\Lambda\right] \Lambda^4 I_\Lambda^{(2)}(\bar{m}) \\ & - 2\left[c_\Lambda(\bar{m}) - c_\Lambda\right] \Lambda^2 I_\Lambda^{(3)}(\bar{m}) + c''_\Lambda(\bar{m}) \Lambda^2 I_\Lambda^{(4)}(\bar{m}) \\ & + \frac{c_\Lambda \Lambda^2 \left[c'_\Lambda(\bar{m}) \Lambda^2 + U'''_\Lambda(\bar{m})\right]^2}{\left[U''_\Lambda(\bar{m}) + c_\Lambda(\bar{m}) \Lambda^2\right]^4} \Bigg]. \end{aligned} \tag{2.162}$$

Since it is straightforward to evaluate the integrals $I_\Lambda^{(n)}(\bar{m})$ analytically, we actually know the flow equation of $c_\Lambda(\bar{m})$ in closed form, which should be solved together with the flow equation (2.142) of $U_\Lambda(\bar{m})$. Note that both flow equations are exact within our ansatz (2.133) for $\Gamma_\Lambda[\bar{m}]$. By evaluating the initial condition $\Gamma_{\Lambda_0}[\bar{m}]$ numerically, we can therefore compute the flow of $\tilde{y}_l$ and τ_l without assuming that the vortex fugacity is small. However, in the present context we are mainly interested in rederiving the Kosterlitz-Thouless RG equations, which we will do in the following.

2.5.3 Recovering the Kosterlitz-Thouless RG equations

Flow equation of $\tilde{y}_l$

We start with the effective potential, whose flow equation is given in Eq. (2.142). Using the fact that $c_\Lambda(\bar{m}) = c_\Lambda + O(y_\Lambda^2)$, we can expand this expression as

$$\partial_l U_\Lambda(\bar{m}) = -\frac{a^2 \Lambda^2 (1 - \eta_l/4)}{4\pi \left[1 + \frac{U''_\Lambda(\bar{m})}{c_\Lambda \Lambda^2}\right]} + O(y_\Lambda^2) = -\frac{a^2 \Lambda^2}{4\pi} \left[1 - \frac{U''_\Lambda(\bar{m})}{c_\Lambda \Lambda^2}\right] + O(y_\Lambda^2), \tag{2.163}$$

where in the second step we have also used $U''_\Lambda = O(y_\Lambda)$ and $\eta_l = O(y_\Lambda^2)$. Inserting the ansatz [cf. Eq. (2.103)]

$$U_\Lambda(\bar{m}) = \Gamma_\Lambda^{(0)} + 2y_\Lambda - 2y_\Lambda \cos(2\pi\bar{m}) \tag{2.164}$$

on the right-hand side of this flow equation yields

$$\partial_l U_\Lambda(\bar{m}) = \frac{\pi}{\tau_l} 2y_\Lambda \cos(2\pi\bar{m}) - \frac{a^2\Lambda^2}{4\pi} + O(y_\Lambda^2), \tag{2.165}$$

so that

$$\partial_l y_\Lambda = \frac{\partial_l U''_\Lambda(0)}{2(2\pi)^2} = -\frac{\pi}{\tau_l} y_\Lambda + O(y_\Lambda^2). \tag{2.166}$$

Rewriting this in terms of the rescaled vortex fugacity

$$\tilde{y}_l = \frac{(2\pi)^3 2y_\Lambda}{c_\Lambda \Lambda^2} \tag{2.167}$$

then gives

$$\partial_l \tilde{y}_l = (2 - \pi/\tau_l)\tilde{y}_l + O(\tilde{y}_l^2), \tag{2.168}$$

in exact agreement with our result (2.108) from the last section.

Flow equation of τ_l

In the same spirit we can also expand the flow equation (2.162) of $c_\Lambda(\bar{m})$ to leading order in y_Λ. With $c_\Lambda(\bar{m}) = c_\Lambda + O(y_\Lambda^2)$ and $U_\Lambda(\bar{m}) = O(y_\Lambda)$ we find

$$\partial_l \tau_l(\bar{m}) = \frac{1}{4\pi}\left[\frac{\tau''_l(\bar{m})}{\tau_l} + \frac{[U'''_l(\bar{m})]^2}{\tau_l^2 a^4 \Lambda^4}\right] + O(y_\Lambda^3), \tag{2.169}$$

where we have defined $\tau_l(\bar{m}) = c_\Lambda(\bar{m})/a^2$. From our ansatz (2.164) for the effective potential it follows that

$$U'''_\Lambda(\bar{m}) = -(2\pi)^3 2y_\Lambda \sin(2\pi\bar{m}) = -\tau_l a^2 \Lambda^2 \tilde{y}_l \sin(2\pi\bar{m}), \tag{2.170}$$

so that we have to solve

$$\partial_l \tau_l(\bar{m}) = \frac{\tau''_l(\bar{m})}{4\pi\tau_l} + \frac{\tilde{y}_l^2}{4\pi}\sin^2(2\pi\bar{m}). \tag{2.171}$$

This can be done with the ansatz

$$\tau_l(\bar{m}) = \tau_l + \tilde{c}_l \frac{\tilde{y}_l^2}{4\pi} \sin^2(2\pi\bar{m}), \tag{2.172}$$

which leads to

$$\partial_l \tau_l + \left[\frac{\partial_l \tilde{c}_l}{\tilde{c}_l} + 2 \frac{\partial_l \tilde{y}_l}{\tilde{y}_l} \right] \frac{\tilde{c}_l \tilde{y}_l^2}{4\pi} \sin^2(2\pi\bar{m}) = \frac{\tilde{c}_l \tilde{y}_l^2}{2\tau_l} \cos(4\pi\bar{m}) + \frac{\tilde{y}_l^2}{4\pi} \sin^2(2\pi\bar{m}). \tag{2.173}$$

For $\bar{m} = 0$ this simplifies to

$$\partial_l \tau_l = \frac{\tilde{c}_l \tilde{y}_l^2}{2\tau_l}, \tag{2.174}$$

while for $\bar{m} = 1/4$ we have

$$\partial_l \tilde{c}_l = 1 - \frac{4\pi \tilde{c}_l}{\tau_l} - 2\tilde{c}_l \frac{\partial_l \tilde{y}_l}{\tilde{y}_l} = 1 - \tilde{c}_l \left(4 + \frac{2\pi}{\tau_l} \right), \tag{2.175}$$

where we have inserted the flow equation (2.168) of $\tilde{y}_l$. The fact that these flow equations of τ_l and $\tilde{c}_l$ solve Eq. (2.173) for any $\bar{m}$ justifies our ansatz for $\tau_l(\bar{m})$ above. All in all, we end up with a set of three coupled flow equations,

$$\partial_l \tilde{y}_l = (2 - \pi/\tau_l)\tilde{y}_l, \tag{2.176a}$$

$$\partial_l \tau_l = \frac{\tilde{c}_l \tilde{y}_l^2}{2\tau_l}, \tag{2.176b}$$

$$\partial_l \tilde{c}_l = 1 - \tilde{c}_l \left(4 + \frac{2\pi}{\tau_l} \right), \tag{2.176c}$$

which are identical to the flow equations (2.127a)–(2.127c) from the last section where we have used the vertex expansion.

2.6 Effect of weak amplitude fluctuations on the BKT transition

2.6.1 Including density fluctuations in the dual-vortex model

Villain approximation of the $O(2)$ model

Having understood how to derive the Kosterlitz-Thouless flow equations within the modern FRG formalism, we are now in a position to assess the effect of weak amplitude fluctuations on the BKT transition. As already discussed in Sec. 2.1.4, previous FRG studies [62–65] yielded the unexpected result that these fluctuations become massless in the long-distance limit, so that the correlation length is always finite and the BKT transition is replaced by a well-defined crossover. However, these studies did not explicitly introduce vortices, which are known to be the relevant degrees of freedom at the BKT transition. In the following, we will therefore analyze the effect of amplitude fluctuations within a generalization of our dual-vortex FRG as developed in the previous sections.

For this purpose, we consider the $O(2)$ model with the action

$$S[\psi] = \frac{U}{2T}\sum_i \left(|\psi_i|^2 - \alpha^2\right)^2 + \frac{J}{2T}\sum_{i,\mu} |\psi_{i+\mu} - \psi_i|^2 \,, \tag{2.177}$$

where ψ_i represents a complex field on a square lattice with lattice parameter a. We can understand Eq. (2.177) as the action of a bosonic field close to a classical continuous phase transition, where it is sufficient to retain only the zero-frequency mode. The first term in the action is then related to a repulsive contact interaction between the bosons with interaction strength $U > 0$, while the second term represents the kinetic energy due to the finite exchange interaction $J > 0$. The parameter α depends to the chemical potential and is assumed to be positive definite, so that the interaction term has the form of a Mexican-hat potential with radius α. The XY model corresponds to the limit $U \to \infty$ where the field can only take values on the brim of the Mexican hat. In order to evaluate the effect of weak amplitude fluctuations, we thus assume that U is sufficiently large; more specifically, writing the complex field in density-phase notation,

$$\psi_i = \sqrt{\rho_i}e^{i\theta_i}, \tag{2.178}$$

we assume that $U\bar{\rho}^2/T \gg 1$, where $\bar{\rho} = \langle \rho_i \rangle$ is the expectation value of the density field ρ_i. On a technical level, the relation to the XY model is more clearly seen by expressing the action in terms of ρ_i and θ_i,

$$S[\rho,\theta] = \frac{U}{2T}\sum_i \left(\rho_i - \alpha^2\right)^2 + \frac{J}{2T}\sum_{i,\mu}\left[\rho_i + \rho_{i+\mu} - 2\sqrt{\rho_i\rho_{i+\mu}}\cos(\theta_{i+\mu} - \theta_i)\right]. \tag{2.179}$$

In the limit $U \to \infty$, the first term fixes the density field to a constant value so that only the phase-dependent cosine with constant prefactor remains, while for general U we find that the density field allows for fluctuations of the effective exchange coupling $\sqrt{\rho_i\rho_{i+\mu}}J$. We thus have to generalize our derivation of the dual-vortex model in Sec. (2.2) to take this additional field dependence into account. We start with the Villain approximation

$$\exp\left[\frac{J\sqrt{\rho_i\rho_{i+\mu}}}{T}\cos(\Delta_\mu\theta_i)\right] \approx R_{V,i\mu}\sum_{n_{i\mu}=-\infty}^{\infty}\exp\left[-\frac{(\Delta_\mu\theta_i-2\pi n_{i\mu})^2}{2\tau_{V,i\mu}}\right], \tag{2.180}$$

where the coefficients now read

$$R_{V,i\mu} = R_V(\sqrt{\rho_i\rho_{i+\mu}}/\tau), \tag{2.181a}$$
$$\tau_{V,i\mu} = \tau_V(\sqrt{\rho_i\rho_{i+\mu}}/\tau), \tag{2.181b}$$

with $\tau = T/J$; the functions R_V and τ_V are in turn given in Eqs. (2.26) and (2.27).

Dual-vortex picture with weak density fluctuations

For the next steps it will be useful to separate the phase part of the partition function,

$$\begin{aligned} Z_{\text{amp}} = &\prod_i\left(\int_0^\infty d\rho_i\right)Z_{\text{eff}}[\rho] \\ &\times\exp\left[-\frac{U}{2T}\sum_i\left(\rho_i-\alpha^2\right)^2-\frac{2J}{T}\sum_i\rho_i+\sum_{i,\mu}\ln R_{V,i\mu}\right], \end{aligned} \tag{2.182}$$

where

$$Z_{\text{eff}}[\rho] = \prod_i\left(\int_0^{2\pi}\frac{d\theta_i}{2\pi}\right)\prod_{i,\mu}\left(\sum_{n_{i\mu}=-\infty}^{\infty}\right)\exp\left[-\sum_{i,\mu}\frac{(\Delta_\mu\theta_i-2\pi n_{i\mu})^2}{2\tau_{V,i\mu}}\right]. \tag{2.183}$$

It is then straightforward to apply the same duality transformations that we have used for the XY model between Eqs. (2.28) and (2.34) to derive the current representation; the fact that $\tau_{V,i\mu}$ is now position dependent does not pose any problem and we get

$$Z_{\text{eff}}[\rho] = \exp\left[\frac{1}{2}\sum_{i,\mu}\ln\tau_{V,i\mu}\right]\prod_{i,\mu}\left(\sum_{p_{i\mu}=-\infty}^{\infty}\delta_{\boldsymbol{\Delta}\cdot\boldsymbol{p}_i,0}\right)\exp\left[-\frac{1}{2}\sum_{i,\mu}\tau_{V,i\mu}p_{i\mu}^2\right], \tag{2.184}$$

with the lattice divergence

$$\boldsymbol{\Delta}\cdot\boldsymbol{p}_i = \sum_\mu(p_{i\mu}-p_{i-\mu,\mu}). \tag{2.185}$$

The final duality transformation from the current-field $p_{i\mu}$ to the dual-vortex field m_i is given by (cf. Sec. 2.2.3)

$$p_{i\mu} = \sum_{\nu} \epsilon_{\mu\nu} \Delta_\nu m_{i+\mu}. \tag{2.186}$$

Inserting this into $Z_{\mathrm{eff}}[\rho]$ results in the more complicated exponent

$$-\frac{1}{2}\sum_{i,\mu} \tau_{V,i\mu} p_{i\mu}^2 = -\frac{1}{2}\sum_{i,\mu} \tau_{V,i\mu} (\Delta_{\bar{\mu}} m_{i+\mu})^2, \tag{2.187}$$

where $\bar{\mu}$ is the complement of μ so that $\mu + \bar{\mu} = x + y$. For a given configuration of the density field, the spatial dependence of $\tau_{V,i\mu}$ breaks the translational invariance so that the right-hand side of Eq. (2.187) is non-diagonal in Fourier space. To render the model more tractable and to make contact with our previous work in Sec. 2.4, we introduce the relative fluctuations $\tilde{\rho}_i$ of the density field,

$$\rho_i = \bar{\rho}(1 + \tilde{\rho}_i), \tag{2.188}$$

and expand our action in the density fluctuations $\tilde{\rho}_i$. For $\tau_{V,i\mu}$ we find

$$\tau_{V,i\mu} \approx \tau_V^{(0)} + \tau_V^{(1)} \frac{\tilde{\rho}_{i+\mu} + \tilde{\rho}_i}{2} + \frac{1}{2}\tau_V^{(2)} \tilde{\rho}_i^2 \tag{2.189}$$

with the coefficients

$$\tau_V^{(0)} = \tau_V\left(\frac{\bar{\rho}}{\tau}\right), \quad \tau_V^{(1)} = \frac{\bar{\rho}}{\tau}\tau_V'\left(\frac{\bar{\rho}}{\tau}\right), \quad \tau_V^{(2)} = \left(\frac{\bar{\rho}}{\tau}\right)^2 \tau_V''\left(\frac{\bar{\rho}}{\tau}\right). \tag{2.190}$$

In the expansion we have additionally approximated $\tilde{\rho}_{i+\mu} \approx \tilde{\rho}_i$ in the second-order term. This is sufficient since we are eventually interested in the leading-order contributions due to the density fluctuations; the only reason to include the second-order term at all is that it allows us to extend the integrals over the density fluctuations $\tilde{\rho}_i$ to the entire real axis, which simplifies the calculations. With this expansion of $\tau_{V,i\mu}$ we find that Eq. (2.187) becomes

$$-\frac{1}{2}\sum_{i,\mu} \tau_{V,i\mu} p_{i\mu}^2 = -\frac{1}{2}\sum_{i} M_i \left[\tau_V^{(0)} + \tau_V^{(1)}\tilde{\rho}_i + \frac{1}{2}\tau_V^{(2)}\tilde{\rho}_i^2\right], \tag{2.191}$$

where

$$M_i = \frac{1}{2}\sum_{\mu}\left[(\Delta_\mu m_i)^2 + (\Delta_\mu m_{i+\bar{\mu}})^2\right]. \tag{2.192}$$

In the same manner we can expand the logarithm of $\tau_{V,i\mu}$ as

$$\frac{1}{2}\sum_{i,\mu}\ln\tau_{V,i\mu}\approx\kappa_V^{(0)}+\kappa_V^{(1)}\sum_i\tilde{\rho}_i+\frac{1}{2}\kappa_V^{(2)}\sum_i\tilde{\rho}_i^2, \tag{2.193}$$

where $\kappa_V^{(0)}$ amounts to a trivial constant contribution and

$$\kappa_V^{(1)}=\frac{\tau_V^{(1)}}{\tau_V^{(0)}},\quad \kappa_V^{(2)}=\frac{\tau_V^{(2)}}{\tau_V^{(0)}}-\left(\frac{\tau_V^{(1)}}{\tau_V^{(0)}}\right)^2. \tag{2.194}$$

Finally, we also need the expansion of $R_{V,i\mu}$,

$$R_{V,i\mu}\approx R_V^{(0)}+R_V^{(1)}\frac{\tilde{\rho}_{i+\mu}+\tilde{\rho}_i}{2}+\frac{1}{2}R_V^{(2)}\tilde{\rho}_i^2, \tag{2.195}$$

with coefficients

$$R_V^{(0)}=R_V\left(\frac{\bar{\rho}}{\tau}\right),\quad R_V^{(1)}=\left(\frac{\bar{\rho}}{\tau}\right)R_V'\left(\frac{\bar{\rho}}{\tau}\right),\quad R_V^{(2)}=\left(\frac{\bar{\rho}}{\tau}\right)^2R_V''\left(\frac{\bar{\rho}}{\tau}\right), \tag{2.196}$$

so that its logarithm has the expansion

$$\sum_{i,\mu}\ln R_{V,i\mu}\approx L_V^{(0)}+2L_V^{(1)}\sum_i\tilde{\rho}_i+L_V^{(2)}\sum_i\tilde{\rho}_i^2, \tag{2.197}$$

where the constant $L_V^{(0)}$ can again be neglected and

$$L_V^{(1)}=\frac{R_V^{(1)}}{R_V^{(0)}},\quad L_V^{(2)}=\frac{R_V^{(2)}}{R_V^{(0)}}-\left(\frac{R_V^{(1)}}{R_V^{(0)}}\right)^2. \tag{2.198}$$

We then find that the full partition function of our model, formulated in terms of the dual-vortex field m_i and the density fluctuations $\tilde{\rho}_i$, reads

$$\begin{aligned}Z_{\mathrm{amp}}=&\prod_i\left(\int_{-\infty}^{\infty}d\tilde{\rho}_i\sum_{m_i=-\infty}^{\infty}\right)\\&\times\exp\left\{-\sum_i\left[\frac{1}{2}u\tilde{\rho}_i^2+v\tilde{\rho}_i+\frac{1}{2}M_i\left(\tau_V^{(0)}+\tau_V^{(1)}\tilde{\rho}_i+\frac{1}{2}\tau_V^{(2)}\tilde{\rho}_i^2\right)\right]\right\},\end{aligned} \tag{2.199}$$

where the dimensionless coefficients u and v are defined as

$$u=\frac{U\bar{\rho}^2}{T}-2L_V^{(2)}-\kappa_V^{(2)}\approx\frac{U\bar{\rho}^2}{T}, \tag{2.200}$$

$$v=\frac{2\bar{\rho}}{\tau}+\frac{U\bar{\rho}(\bar{\rho}-\alpha^2)}{T}-2L_V^{(1)}-\kappa_V^{(1)}. \tag{2.201}$$

Our assumption of weak amplitude fluctuations thus translates to the requirement $u \gg 1$. Considering the order of magnitude of the remaining coefficients, we find that close to the BKT transition $\bar{\rho}/\tau$ is of order unity, which thus also holds for the $\tau_V^{(i)}$. Regarding the coefficient v we note that

$$v = -\frac{1}{2}\tau_V^{(1)} \langle M_i \rangle + O(u^{-1}), \tag{2.202}$$

which follows easily from the identity $\langle \tilde{\rho}_i \rangle = 0$. Since the expectation value of M_i is at most of order unity below the BKT transition, this is therefore also true for v.

Effective dual-vortex model

We now take advantage of the fact that the action in Eq. (2.199) is quadratic in $\tilde{\rho}_i$, which allows us to integrate out the density fluctuations exactly. Up to a constant prefactor, this results in the following effective theory for the dual-vortex field m_i,

$$\begin{aligned} Z_{\mathrm{amp}} = \prod_i \left(\sum_{m_i=-\infty}^{\infty} \right) \\ \times \exp\left\{ -\frac{1}{2}\sum_i \left[\tau_V^{(0)} M_i + \ln\left(1 + \frac{\tau_V^{(2)}}{2u} M_i\right) - \frac{\left(v + \frac{\tau_V^{(1)}}{2} M_i\right)^2}{u + \frac{\tau_V^{(2)}}{2} M_i} \right] \right\}. \end{aligned} \tag{2.203}$$

We first note that for large M_i we have

$$\tau_V^{(0)} M_i + \ln\left(1 + \frac{\tau_V^{(2)}}{2u} M_i\right) - \frac{\left(v + \frac{\tau_V^{(1)}}{2} M_i\right)^2}{u + \frac{\tau_V^{(2)}}{2} M_i} \sim \left[\tau_V^{(0)} - \frac{\left(\tau_V^{(1)}\right)^2}{2\tau_V^{(2)}} \right] M_i, \tag{2.204}$$

so that our partition function is only well defined if

$$\tau_V^{(0)} - \frac{\left(\tau_V^{(1)}\right)^2}{2\tau_V^{(2)}} > 0. \tag{2.205}$$

Fortunately, this inequality is always fulfilled (this would not be true if we had neglected $\tau_V^{(2)}$). We also find that close to the BKT transition, the left-hand side of Eq. (2.205) is of order unity so that the sums over m_i are effectively cut off at $M_i \approx 1$. This allows us to approximate our partition function by

$$Z_{\text{amp}} = \prod_i \left(\sum_{m_i=-\infty}^{\infty} \right) \exp\left[-\frac{\tau'}{2} \sum_i M_i + \frac{(\tau_V^{(1)})^2}{8} \sum_i \frac{M_i^2}{u + \frac{\tau_V^{(2)}}{2} M_i} \right], \tag{2.206}$$

where the effective dimensionless temperature τ' is defined as

$$\tau' = \tau_V^{(0)} + \frac{\tau_V^{(2)}}{2u} - \frac{v\tau_V^{(1)}}{u} \approx \tau_V^{(0)}. \tag{2.207}$$

Since $u \gg 1$, we may also expand

$$\exp\left[\frac{(\tau_V^{(1)})^2}{8} \sum_i \frac{M_i^2}{u + \frac{\tau_V^{(2)}}{2} M_i} \right] \approx 1 + \frac{(\tau_V^{(1)})^2}{8u} \sum_i M_i^2. \tag{2.208}$$

With the dimensionless coupling constant

$$g = \frac{3\left(\tau_V^{(1)}\right)^2}{u} \ll 1 \tag{2.209}$$

we can then write

$$Z_{\text{amp}} = \prod_i \left(\sum_{m_i=-\infty}^{\infty} \right) \exp\left[-\frac{\tau'}{2} \sum_i M_i \right] \left(1 + \frac{g}{4!} \sum_i M_i^2 \right). \tag{2.210}$$

In momentum space this becomes

$$\begin{aligned} Z_{\text{amp}} = \prod_i \left(\sum_{m_i=-\infty}^{\infty} \right) \exp\left[-\frac{1}{2} \sum_{\boldsymbol{k}} \omega_{\boldsymbol{k}} |m_{\boldsymbol{k}}|^2 \right] \\ \times \left[1 + \frac{g}{4!N} \sum_{\boldsymbol{k}_1\boldsymbol{k}_2\boldsymbol{k}_3\boldsymbol{k}_4} \delta_{\boldsymbol{k}_1+\boldsymbol{k}_2+\boldsymbol{k}_3+\boldsymbol{k}_4,0} V_{\boldsymbol{k}_1,\boldsymbol{k}_2,\boldsymbol{k}_3,\boldsymbol{k}_4} m_{\boldsymbol{k}_1} m_{\boldsymbol{k}_2} m_{\boldsymbol{k}_3} m_{\boldsymbol{k}_4} \right], \end{aligned} \tag{2.211}$$

where the dispersion $\omega_{\boldsymbol{k}} = 4\tau'(1-\gamma_{\boldsymbol{k}})$ is defined in analogy to Eq. (2.39) and $V_{\boldsymbol{k}_1,\boldsymbol{k}_2,\boldsymbol{k}_3,\boldsymbol{k}_4}$ describes the momentum dependence of the fully symmetrized quartic interaction due to amplitude fluctuations,

$$V_{\boldsymbol{k}_1,\boldsymbol{k}_2,\boldsymbol{k}_3,\boldsymbol{k}_4} = \frac{1}{3} \left[\tilde{V}_{\boldsymbol{k}_1,\boldsymbol{k}_2;\boldsymbol{k}_3,\boldsymbol{k}_4} + \tilde{V}_{\boldsymbol{k}_1,\boldsymbol{k}_3;\boldsymbol{k}_2,\boldsymbol{k}_4} + \tilde{V}_{\boldsymbol{k}_1,\boldsymbol{k}_4;\boldsymbol{k}_3,\boldsymbol{k}_2} \right], \tag{2.212}$$

where

$$\begin{aligned} \tilde{V}_{\boldsymbol{k}_1,\boldsymbol{k}_2;\boldsymbol{k}_3,\boldsymbol{k}_4} = \frac{1}{4} \sum_{\mu\nu\in\{x,y\}} \left(e^{i\boldsymbol{k}_1\cdot\boldsymbol{a}_\mu} - 1 \right) \left(e^{i\boldsymbol{k}_2\cdot\boldsymbol{a}_\mu} - 1 \right) \left(1 + e^{i(\boldsymbol{k}_1+\boldsymbol{k}_2)\cdot(\boldsymbol{a}_x+\boldsymbol{a}_y-\boldsymbol{a}_\mu)} \right) \\ \times \left(e^{i\boldsymbol{k}_3\cdot\boldsymbol{a}_\nu} - 1 \right) \left(e^{i\boldsymbol{k}_4\cdot\boldsymbol{a}_\nu} - 1 \right) \left(1 + e^{i(\boldsymbol{k}_3+\boldsymbol{k}_4)\cdot(\boldsymbol{a}_x+\boldsymbol{a}_y-\boldsymbol{a}_\nu)} \right). \end{aligned} \tag{2.213}$$

2.6.2 Effect of the quartic interaction on the KT flow equations

Due to the similarity of Eq. (2.211) to the partition function (2.36) of the original dual-vortex model, we set up the FRG in the same way as we did in Sec. 2.3 for our analysis of the XY model. To that end, we replace

$$\frac{1}{2}\sum_{\boldsymbol{k}} \omega_{\boldsymbol{k}} |m_{\boldsymbol{k}}|^2 \to \frac{1}{2}\sum_{\boldsymbol{k}} \left[\omega_{\boldsymbol{k}} + R_\lambda(\boldsymbol{k})\right] |m_{\boldsymbol{k}}|^2, \tag{2.214}$$

where the Litim regulator is defined as

$$R_\lambda(\boldsymbol{k}) = \zeta_\lambda(\lambda - \omega_{\boldsymbol{k}})\Theta(\lambda - \omega_{\boldsymbol{k}}). \tag{2.215}$$

Here the scale-dependent prefactor initially fulfills $\zeta_{\lambda_0} = 1$; its behaviour during the flow will be specified later on. The initial value of the cutoff, $\lambda_0 = \max_{\boldsymbol{k}} \omega_{\boldsymbol{k}}$, is again chosen such that the dispersion becomes constant. The cutoff-dependent generating functional of the connected correlation functions [cf. Eq. (2.51)] is then initially given by

$$\begin{aligned} e^{\mathcal{G}_{\lambda_0}[h]} &= \left[1 + \frac{g}{4!N} \sum_{\boldsymbol{k}_1\boldsymbol{k}_2\boldsymbol{k}_3\boldsymbol{k}_4} \delta_{\boldsymbol{k}_1+\boldsymbol{k}_2+\boldsymbol{k}_3+\boldsymbol{k}_4,0} V_{\boldsymbol{k}_1,\boldsymbol{k}_2,\boldsymbol{k}_3,\boldsymbol{k}_4} \frac{\delta}{\delta h_{-\boldsymbol{k}_1}} \frac{\delta}{\delta h_{-\boldsymbol{k}_2}} \frac{\delta}{\delta h_{-\boldsymbol{k}_3}} \frac{\delta}{\delta h_{-\boldsymbol{k}_4}}\right] \\ &\quad \times \prod_i \left(\sum_{m_i=-\infty}^{\infty} \exp\left[-\frac{\lambda_0}{2} m_i^2 + h_i m_i\right]\right). \end{aligned} \tag{2.216}$$

Here we have used the fact that we may replace the Fourier coefficients of the dual-vortex field $m_{\boldsymbol{k}}$ by the derivative with respect to the corresponding Fourier coefficient of the source field $h_{-\boldsymbol{k}}$, which allows us to pull the non-trivial terms out of the m_i sums. Reusing our earlier results (2.71) and (2.73) for the second line,

$$\sum_{m_i=-\infty}^{\infty} \exp\left[-\frac{\lambda_0}{2} m_i^2 + h_i m_i\right] = \sqrt{\frac{2\pi}{\lambda_0}} \exp\left[\frac{h_i^2}{2\lambda_0} + 2y_0 \cos\left(\frac{2\pi h_i}{\lambda_0}\right) + O(y_0^4)\right], \tag{2.217}$$

it is then trivial to evaluate the derivatives with respect to the source field. Up to a constant term, we find

$$\begin{aligned} \mathcal{G}_{\lambda_0}[h] &= \sum_i \frac{h_i^2}{2\lambda_0} + 2y_0 \sum_i \cos\left(\frac{2\pi h_i}{\lambda_0}\right) + \frac{g}{4\lambda_0^3 N} \sum_{\boldsymbol{k}} |h_{\boldsymbol{k}}|^2 \sum_{\boldsymbol{q}} V_{\boldsymbol{k},-\boldsymbol{k},\boldsymbol{q},-\boldsymbol{q}} \\ &\quad + \frac{g}{4!\lambda_0^4 N} \sum_{\boldsymbol{k}_1\boldsymbol{k}_2\boldsymbol{k}_3\boldsymbol{k}_4} \delta_{\boldsymbol{k}_1+\boldsymbol{k}_2+\boldsymbol{k}_3+\boldsymbol{k}_4,0} V_{\boldsymbol{k}_1,\boldsymbol{k}_2,\boldsymbol{k}_3,\boldsymbol{k}_4} h_{\boldsymbol{k}_1} h_{\boldsymbol{k}_2} h_{\boldsymbol{k}_3} h_{\boldsymbol{k}_4} + O(y_0^2, y_0 g, g^2). \end{aligned} \tag{2.218}$$

Inverting the relation

$$\bar{m}_i = \frac{\delta \mathcal{G}_{\lambda_0}[h]}{\delta h_i} \tag{2.219}$$

perturbatively, it is straightforward to show that the initial condition for the average effective action [cf. Eq. (2.55)] is to first order in y_0 and g given by

$$\begin{aligned}\Gamma_{\lambda_0}[\bar{m}] = {} & \frac{c_0}{2} \sum_{\boldsymbol{k}} k^2 \left|\bar{m}_{\boldsymbol{k}}\right|^2 - 2y_0 \sum_i \cos(2\pi \bar{m}_i) \\ & - \frac{g}{4!N} \sum_{\boldsymbol{k}_1\boldsymbol{k}_2\boldsymbol{k}_3\boldsymbol{k}_4} \delta_{\boldsymbol{k}_1+\boldsymbol{k}_2+\boldsymbol{k}_3+\boldsymbol{k}_4,0} V_{\boldsymbol{k}_1,\boldsymbol{k}_2,\boldsymbol{k}_3,\boldsymbol{k}_4} \bar{m}_{\boldsymbol{k}_1} \bar{m}_{\boldsymbol{k}_2} \bar{m}_{\boldsymbol{k}_3} \bar{m}_{\boldsymbol{k}_4},\end{aligned} \tag{2.220}$$

where

$$c_0 = \tau' a^2 - \frac{g a^2}{\lambda_0} \tag{2.221}$$

and we have expanded

$$\omega_{\boldsymbol{k}} = \tau' a^2 k^2 + O(k^4), \tag{2.222}$$

$$\frac{g}{2\lambda_0 N} \sum_{\boldsymbol{q}} V_{\boldsymbol{k},-\boldsymbol{k},\boldsymbol{q},-\boldsymbol{q}} = \frac{g a^2 k^2}{\lambda_0} + O(k^4). \tag{2.223}$$

In analogy to our FRG approach to the XY model we now set $\lambda = \tau' a^2 \Lambda$. Due to the g-dependent term in Eq. (2.221), it is then convenient to define the wave-function renormalization factor as

$$\zeta_\lambda = \frac{c_\Lambda + \frac{g a^2}{\lambda_0}}{c_0 + \frac{g a^2}{\lambda_0}}, \tag{2.224}$$

which leads to

$$R_\lambda(\boldsymbol{k}) = \left(c_\Lambda + \frac{g a^2}{\lambda_0}\right) \left(\Lambda^2 - k^2\right) \Theta\left(\Lambda^2 - k^2\right). \tag{2.225}$$

This differs from the regulator (2.80) in the XY model by a g-dependent correction, which thus also appears in the flow equations of the relevant and the marginal couplings via the functions A_Λ and $B_\Lambda(\boldsymbol{k})$, see Eqs. (2.96) and (2.112). However, in our derivation of the KT flow equations in Sec. 2.4 we have neglected y_Λ-dependent corrections to these functions, so that it is consistent to neglect g-dependent corrections as well. This leaves us with evaluating the effect of the finite quartic interaction in the initial average effective action (2.220) on the KT flow equations. In a qualitative way, this is most easily done by considering the long-wavelength expansion

$$\tilde{V}_{\boldsymbol{k}_1,\boldsymbol{k}_2;\boldsymbol{k}_3,\boldsymbol{k}_4} \approx \sum_{\mu\nu\in\{x,y\}} (\boldsymbol{k}_1 \cdot \boldsymbol{a}_\mu)(\boldsymbol{k}_2 \cdot \boldsymbol{a}_\mu)(\boldsymbol{k}_3 \cdot \boldsymbol{a}_\nu)(\boldsymbol{k}_4 \cdot \boldsymbol{a}_\nu), \tag{2.226}$$

which implies that the interaction vertex $V_{\boldsymbol{k}_1,\boldsymbol{k}_2,\boldsymbol{k}_3,\boldsymbol{k}_4}$ is of fourth order in the external momenta. As already mentioned in Sec. 2.3.3, this translates to an irrelevant coupling with scaling dimension -2, which does not affect the KT flow equations close to the line of Gaussian fixed points in a qualitative way. To see more explicitly how this comes about, we make the ansatz that the momentum dependence of the quartic interaction $V_{\boldsymbol{k}_1,\boldsymbol{k}_2,\boldsymbol{k}_3,\boldsymbol{k}_4}$ does not change during the flow. We thus parametrize the vertex as

$$-\frac{g_\Lambda}{4!N} \sum_{\boldsymbol{k}_1\boldsymbol{k}_2\boldsymbol{k}_3\boldsymbol{k}_4} \delta_{\boldsymbol{k}_1+\boldsymbol{k}_2+\boldsymbol{k}_3+\boldsymbol{k}_4,0} V_{\boldsymbol{k}_1,\boldsymbol{k}_2,\boldsymbol{k}_3,\boldsymbol{k}_4} \bar{m}_{\boldsymbol{k}_1} \bar{m}_{\boldsymbol{k}_2} \bar{m}_{\boldsymbol{k}_3} \bar{m}_{\boldsymbol{k}_4}, \tag{2.227}$$

where we identify $g_{\Lambda_0} = g$. This allows us to show analytically (see Appendix A.3.1 for technical details) that the rescaled coupling

$$\tilde{g}_l = \frac{c_\Lambda \Lambda^2}{2\pi} g_\Lambda \tag{2.228}$$

obeys the flow equation

$$\partial_l \tilde{g}_l = -2\tilde{g}_l - 4\tau_l \tilde{y}_l^2. \tag{2.229}$$

For $\tau_l \approx \pi/2$ and $\tilde{y}_l \ll 1$, the flow quickly converges to its asymptotic behaviour

$$\tilde{g}_l \underset{l\to\infty}{\sim} -2\tau_l \tilde{y}_l^2, \tag{2.230}$$

which is independent of its initial value $\tilde{g}_0 \propto g$ (see Fig. 2.8). While the flow equation of $\tilde{y}_l$ is not affected by a finite $\tilde{g}_l$, we show in Appendix A.3.2 that it results in a correction to the flow equation of τ_l,

$$\partial_l \tau_l = \frac{\tilde{y}_l^2}{8\pi} \left(1 + \frac{16}{3}\right). \tag{2.231}$$

However, since we can absorb this additional factor by appropriately redefining the rescaled vortex fugacity $\tilde{y}_l$, it does not affect the universal properties of the phase transition. We thus conclude that weak amplitude fluctuations are indeed innocuous and do not spoil the BKT transition.

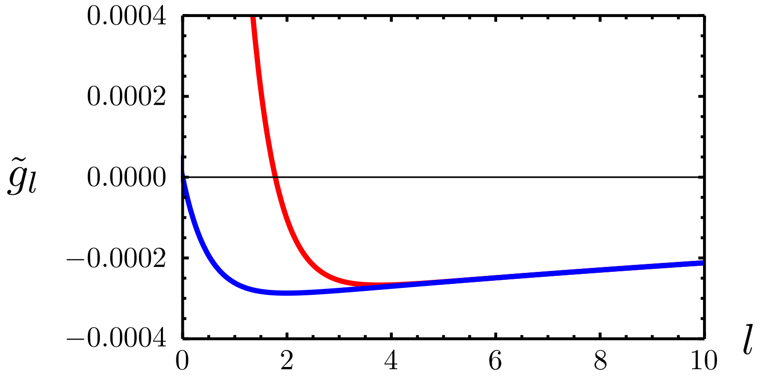

Figure 2.8: Typical flow of the rescaled irrelevant coupling $\tilde{g}_l$ defined in Eq. (2.228) as a function of the logarithmic scale parameter $l = \ln(\Lambda_0/\Lambda)$. The shown curves only differ by their initial condition for $\tilde{g}_l$: the upper (red) curve corresponds to $\tilde{g}_0 = 0.01$ (implying finite amplitude fluctuations), while the lower (blue) curve corresponds to $\tilde{g}_0 = 0$ as in the XY model. Both curves were computed by solving the flow equations (2.130), (2.131), and (2.229) numerically with $\tilde{y}_0 = 0.01$ and $\tau' = 0.99\tau_* = 0.99\pi/2$. Clearly both flows converge for large l, so that the initial value of $\tilde{g}_l$ and, as a consequence, the presence of weak amplitude fluctuations do not qualitatively affect the BKT transition. (Figure reproduced from Ref. [54])

2.7 Effect of weak out-of-plane fluctuations on the BKT transition

While the effect of amplitude fluctuations is one possible way for real systems to deviate from the XY model, it is for sure not the only one. Another evident generalization is the strongly anisotropic XXZ model, where the classical spins of unit length are allowed to point slightly out of the xy plane. Since the effect of out-of-plane fluctuations on the vortices driving the BKT transition is not *a priori* obvious, it is interesting to analyze this situation. We therefore consider the Hamiltonian of the XXZ model given by

$$H_{\mathrm{XXZ}} = -J \sum_{i,\mu} \boldsymbol{s}_i \cdot \boldsymbol{s}_{i+\mu} + \frac{U}{2} \sum_i \left(\vartheta_i - \frac{\pi}{2} \right)^2 , \tag{2.232}$$

which generalizes the Hamiltonian (2.1) of the XY model. Here $\boldsymbol{s}_i = (\sin\vartheta_i \cos\varphi_i, \sin\vartheta_i \sin\varphi_i, \cos\vartheta_i)$ denotes a classical spin of unit length at lattice site i and the coupling U parametrizes the easy-plane anisotropy. While taking the limit $U \to \infty$ would result in the XY model, we will in the following assume $U/T \gg 1$ so that weak out-of-plane fluctuations are possible.

The partition function for our XXZ model is

$$Z_{\mathrm{XXZ}} = \prod_i \left(\int d\Omega_i \right) \exp \Bigg[\frac{J}{T} \sum_{i,\mu} \left[\cos\vartheta_{i+\mu} \cos\vartheta_i + \sin\vartheta_{i+\mu} \sin\vartheta_i \cos(\Delta_\mu \varphi_i) \right] - \frac{U}{2T} \sum_i \left(\vartheta_i - \frac{\pi}{2} \right)^2 \Bigg], \tag{2.233}$$

where $\int d\Omega_i = \int_0^\pi d\vartheta_i \sin\vartheta_i \int_0^{2\pi} d\varphi_i$ is a shorthand for the integral over the unit sphere. In analogy to our treatment of the XY and the $O(2)$ model, we now apply the Villain approximation to the φ_i-dependent part of Z_{XXZ},

$$\exp\left[\frac{J}{T} \sin\vartheta_{i+\mu} \sin\vartheta_i \cos(\Delta_\mu \varphi_i) \right] \approx R_{V,i\mu} \sum_{n_{i\mu}=-\infty}^{\infty} \exp\left[- \frac{(\Delta_\mu \varphi_i - 2\pi n_{i\mu})^2}{2\tau_{V,i\mu}} \right], \tag{2.234}$$

where the coefficients are given by

$$R_{V,i\mu} = R_V(\sin\vartheta_{i+\mu} \sin\vartheta_i / \tau), \tag{2.235a}$$

$$\tau_{V,i\mu} = \tau_V(\sin\vartheta_{i+\mu} \sin\vartheta_i / \tau). \tag{2.235b}$$

Here $\tau = T/J$ and the functions R_V and τ_V have been defined in Eqs. (2.26) and (2.27). This results in the partition function

$$Z_{\mathrm{XXZ}} = \prod_i \left(\int_0^\pi d\vartheta_i \sin\vartheta_i \right) Z_{\mathrm{eff}}[\vartheta] \times \exp\left[- \frac{U}{2T} \sum_i \left(\vartheta_i - \frac{\pi}{2} \right)^2 + \frac{J}{T} \sum_{i,\mu} \cos\vartheta_{i+\mu} \cos\vartheta_i + \sum_{i,\mu} \ln R_{V,i\mu} \right], \tag{2.236}$$

where

$$Z_{\mathrm{eff}}[\vartheta] = \prod_i \left(\int_0^{2\pi} d\varphi_i \right) \prod_{i,\mu} \left(\sum_{n_{i\mu}=-\infty}^{\infty} \right) \exp\left[- \frac{(\Delta_\mu \varphi_i - 2\pi n_{i\mu})^2}{2\tau_{V,i\mu}} \right]. \tag{2.237}$$

Again performing the duality transformations between Eqs. (2.28) and (2.34) then yields a current representation of $Z_{\mathrm{eff}}[\vartheta]$ similar to Eq. (2.184). We proceed in the same spirit as in Sec. 2.6.1 by defining

$$\vartheta_i = \frac{\pi}{2} + \tilde{\vartheta}_i \tag{2.238}$$

and expanding $\tau_{V,i\mu}$ as well as the cosine terms to second order in $\tilde{\vartheta}_i$, which is certainly justified for $U/T \gg 1$. With

$$\tau_{V,i\mu} = \tau_V^{(0)} - \tau_V^{(1)} \frac{\tilde{\vartheta}_{i+\mu}^2 + \tilde{\vartheta}_i^2}{2} + O\left(\tilde{\vartheta}_i^4\right) \tag{2.239}$$

and

$$\tau_V^{(0)} = \tau_V\left(\frac{1}{\tau}\right), \quad \tau_V^{(1)} = \frac{1}{\tau}\tau_V'\left(\frac{1}{\tau}\right), \tag{2.240}$$

we find

$$Z_{\text{eff}}[\vartheta] = \exp\left[\frac{1}{2}\sum_{i\mu}\ln\tau_{V,i\mu}\right]\prod_i\left(\sum_{m_i=-\infty}^{\infty}\right)\exp\left[-\frac{\tau_V^{(0)}}{2}\sum_i M_i + \frac{\tau_V^{(1)}}{2}\sum_i\tilde{\vartheta}_i^2 M_i\right], \tag{2.241}$$

where m_i is the familiar dual-vortex field and M_i is again defined as

$$M_i = \frac{1}{2}\sum_\mu\left[(\Delta_\mu m_i)^2 + (\Delta_\mu m_{i+\bar{\mu}})^2\right]. \tag{2.242}$$

Since expanding $\ln R_{V,i\mu}$ and $\ln\tau_{V,i\mu}$ as well as the integral measure $\sin\vartheta_i$ to second order in $\tilde{\vartheta}_i$ only results in terms of the form $\tilde{\vartheta}_i^2$ with coefficients of order unity, we can take their effect into account by introducing the dimensionless coupling

$$u = \frac{U}{T} + O(1) \gg 1. \tag{2.243}$$

In total we thus arrive at

$$Z_{\text{XXZ}} = \prod_i\left(\int_{-\infty}^{\infty}d\tilde{\vartheta}_i\sum_{m_i=-\infty}^{\infty}\right)\exp\left[-\frac{\tau_V^{(0)}}{2}\sum_i M_i - \frac{1}{2}\sum_{ij}A_{ij}\tilde{\vartheta}_i\tilde{\vartheta}_j\right], \tag{2.244}$$

where the matrix elements A_{ij} are given by

$$A_{ij} = \delta_{ij}\left(u - \tau_V^{(1)}M_i\right) - \frac{1}{\tau}\sum_\mu\left(\delta_{j,i+\mu} + \delta_{j,i-\mu}\right) \tag{2.245}$$

and we have extended the $\tilde{\vartheta}_i$ integration to the entire real line. Since $\tau_V^{(1)}$ is always negative, we note that the partition function (2.244) is well defined. Performing the Gaussian integrals over the out-of-plane fluctuations $\tilde{\vartheta}_i$ yields

$$Z_{\text{XXZ}} = \prod_i\left(\sum_{m_i=-\infty}^{\infty}\right)\exp\left[-\frac{\tau_V^{(0)}}{2}\sum_i M_i - \frac{1}{2}\ln\det\mathbf{A}\right], \tag{2.246}$$

where $[\mathbf{A}]_{ij} = A_{ij}$. Since the off-diagonal part of $\mathbf{A}$ does not contribute to first order in $1/u$, we may write the second term in the action as

$$\ln \det \mathbf{A} = \sum_i \ln \left[u - \tau_V^{(1)} M_i + O\left(u^{-1}\right) \right] = N \ln u - \frac{\tau_V^{(1)}}{u} \sum_i M_i + O\left(u^{-2}\right), \tag{2.247}$$

which results in

$$Z_{\mathrm{XXZ}} = \prod_i \left(\sum_{m_i=-\infty}^{\infty} \right) \exp\left[-\frac{\tau'}{2} \sum_i M_i \right]. \tag{2.248}$$

Up to the renormalization of the dimensionless temperature,

$$\tau' = \tau_V^{(0)} - \frac{\tau_V^{(1)}}{u}, \tag{2.249}$$

the partition function (2.248) is identical to the dual-vortex representation (2.36) of the XY model. Let us also consider the next-to-leading-order correction in $1/u$. In this case, the off-diagonal part of $\mathbf{A}$ only contributes an irrelevant constant term, which after expanding $\ln \det \mathbf{A}$ leads to a constant rescaling of the partition function. On the other hand, the second-order contribution from the diagonal part of $\mathbf{A}$ is proportional to M_i^2 and thus depends on the dual-vortex field m_i. To second order in $1/u$ we therefore find

$$Z_{\mathrm{XXZ}} = \prod_i \left(\sum_{m_i=-\infty}^{\infty} \right) \exp\left[-\frac{\tau'}{2} \sum_i M_i \right] \left(1 + \frac{g}{4!} \sum_i M_i^2 \right), \tag{2.250}$$

where the dimensionless coupling g is defined as

$$g = \frac{6\left(\tau_V^{(1)}\right)^2}{u^2}. \tag{2.251}$$

Comparing Eq. (2.250) with the effective dual-vortex representation (2.210) of the $O(2)$ model, it is clear that weak out-of-plane fluctuations lead to the same effective theory as weak amplitude fluctuations do. Our discussion in Sec. 2.6.2 about the effect of weak amplitude fluctuations on the BKT transition thus applies directly to weak out-of-plane fluctuations. We therefore conclude that the strongly anisotropic XXZ model also exhibits a phase transition, whose universal properties are identical to the BKT transition in the XY model.

Chapter 3

Spin functional renormalization group

3.1 Motivation

In the first half of this thesis, we have exclusively dealt with classical spins that can be described by vectors in three-dimensional Euclidean space. While classical spin systems are conceptually rather easy to understand, they can already lead to highly non-trivial emergent phenomena. A good example is the XY model as discussed in Ch. 2, featuring a phase transition of infinite order driven by vortices that themselves are emergent entities. On a technical level, this is reflected by the various representations of the partition function derived in Sec. 2.2, which are connected by duality transformations.

In terms of complexity and richness of physical phenomena, however, classical spin systems do not come close to quantum spin systems, which encompass exotic behaviour such as fractional excitations and resonating valence bonds [80]. A quantum-mechanical spin $\boldsymbol{S} = (S^x, S^y, S^z)$ cannot be easily visualized: in contrast to the Cartesian components of a classical spin which are real numbers, the S^α are operators acting on a Hilbert space. Mathematically, they are elements of the Lie algebra $\mathfrak{su}(2)$ satisfying the commutation relation

$$\left[S^\alpha, S^\beta\right] = i\epsilon^{\alpha\beta\gamma} S^\gamma, \tag{3.1}$$

where $\epsilon^{\alpha\beta\gamma}$ is the three-dimensional Levi-Civita symbol. The crucial difference between this spin algebra and the algebra of bosonic or fermionic ladder operators consists in the appearance of the spin component S^γ on the right-hand side of Eq. (3.1). For this reason, we cannot directly transfer the usual construction of a path integral for bosonic or fermionic fields to spin systems.

While it is indeed possible to define spin coherent states and use them to construct a path integral formulation of quantum-mechanical spins [81], it is rather uncommon to see this approach in actual calculations. In fact, modern many-body techniques are often tailored towards bosonic or fermionic field theories; this is also true for the FRG [33]. Although in one dimension the Bethe ansatz provides a way to work directly on the level of spin operators and wavefunctions [82], it is therefore quite common to map spin systems to a bosonic or fermionic field theory, which is then handled by one of the many available many-body techniques. For ordered magnets where the low-energy excitations are renormalized spin waves, one can apply the Holstein-Primakoff [83] or the Dyson-Maleev [84, 85] transformation and expand in powers of the inverse spin number $1/S$. This approach is unfortunately not applicable to systems without long-range magnetic order; in this case, one may represent the spin operators in terms of Schwinger bosons [86, 87], Abrikosov pseudofermions [88, 89], or Majorana fermions [90–93]. While these methods have been successfully used to describe spin systems, they all have their own shortcomings: using Majorana fermions leads to a redundancy in Hilbert space, whereas both the Abrikosov pseudofermion and the Schwinger boson approach introduce unphysical states which have to projected out, which can only be done approximately for non-trivial systems.

There is, however, another method by Vaks, Larkin, and Pikin (VLP) [1–3] that was developed in the 1960s. While their spin-diagrammatic approach is formulated directly in terms of the physical spin operators, it also makes use of diagrammatic many-body techniques based on spin correlators and the Matsubara formalism. VLP's starting point is a generalized Wick theorem for isolated spin operators [1, 3], which allows them to systematically expand the irreducible[1] spin vertices in powers of the inverse range $1/r_0$ of the ferromagnetic exchange interaction. Although this approach is conceptually close to the usual diagrammatic techniques for bosons or fermions and was further developed by other people [3, 94–96], it never gained widespread popularity, probably due to the more complicated Wick theorem for spin operators that results in rather cumbersome diagrammatic rules.

In the present chapter, we will show how to formulate the FRG in terms of the physical spin operators. This allows us to retain the advantages of the VLP approach such as dealing directly with the physical Hilbert space and being conceptually close to the more familiar many-body techniques for bosons and fermions, while replacing the complicated diagrammatic rules by the well-known expansion of the Wetterich equation. Although we will later

[1]The spin vertices are irreducible with respect to the cutting of a single line of the effective exchange interaction.

show that our spin FRG (SFRG) allows us to recover VLP's $1/r_0$ expansion via a simple truncation of the corresponding Wetterich equation, the SFRG by no means restricted to this approach. With the Wetterich equation being an exact flow equation of the generating functional of the irreducible vertices, it not only allows for novel approximation schemes, but it also enables us to describe the critical behaviour of spin systems. Furthermore, we will in fact formulate the SFRG for three different generating functionals of irreducible vertices: while we can define irreducibility either with respect to the cutting of a single spin propagator or exchange interaction line, we will also construct a hybrid approach which combines these two notions of irreducibility by treating the transversal and the longitudinal part of the spin correlators separately. Depending on the system at hand, we can then choose the most suitable formulation of the SFRG.

Finally, while we will in the present chapter mainly consider the quantum Heisenberg model, it is straightforward to generalize our SFRG formalism to any Hamiltonian which can be written in terms of local operators satisfying a non-trivial algebra such as Hubbard X-operators [97]. A specific example of this is given by our recent work on the Kondo model [98], where we derive a generalized Wetterich equation for both the conduction electrons and the impurity spin. Using a simple truncation of the average effective action, this allows us to derive Anderson's one-loop "poor man's scaling" equations for the Kondo model [30, 31] with an arbitrary impurity spin.

3.2 Pure SFRG

3.2.1 Derivation of the Wetterich equation for quantum spin systems

In the following we will show how to construct the SFRG for the quantum Heisenberg model, which is defined by the Hamiltonian

$$H = -\frac{1}{2}\sum_{ij} V_{ij}\boldsymbol{S}_i \cdot \boldsymbol{S}_j - h_0 \sum_i S_i^z. \tag{3.2}$$

Here the subscripts i and j label the N lattice sites $\boldsymbol{r}_i$ of an arbitrary D-dimensional lattice, $V_{ij} = V(\boldsymbol{r}_i - \boldsymbol{r}_j)$ represents an arbitrary exchange coupling, and h_0 measures an external magnetic field in units of energy. The spin operators $\boldsymbol{S}_i$ fulfill the commutation relation (3.1) and are normalized such that $\boldsymbol{S}_i^2 = S(S+1)$. To set up the FRG, we replace the exchange coupling V_{ij} by the continuous deformation V_{ij}^{Λ}, which is parametrized by the deformation parameter $\Lambda \in [0,1]$. We choose the deformed exchange interaction such that for $\Lambda = 0$ the system is sufficiently simple to allow for a controlled calculation of the spin correlators, while for $\Lambda = 1$ we recover the full Heisenberg model, $V_{ij}^{\Lambda=1} = V_{ij}$.

The Λ-dependent generating functional of the connected spin correlators can then be written as

$$\mathcal{G}_\Lambda[\boldsymbol{h}] = \ln \mathrm{Tr}\left[e^{-\beta H_0} \mathcal{T} e^{\int_0^\beta d\tau \left[\sum_i \boldsymbol{h}_i(\tau)\cdot \boldsymbol{S}_i(\tau) - \mathcal{V}_\Lambda(\tau) \right]} \right], \tag{3.3}$$

in full analogy to bosonic systems [41]. Here

$$H_0 = -h_0 \sum_i S_i^z \tag{3.4}$$

is the free part of the Hamiltonian, $\mathcal{T}$ denotes the time-ordering symbol in imaginary time, the $\boldsymbol{h}_i(\tau)$ are arbitrary time-dependent source fields, and

$$\mathcal{V}_\Lambda(\tau) = -\frac{1}{2} \sum_{ij} V_{ij}^\Lambda \boldsymbol{S}_i(\tau) \cdot \boldsymbol{S}_j(\tau) \tag{3.5}$$

is the deformed interaction part of the Hamiltonian. The time dependence of all operators is in the interaction picture with respect to H_0,

$$\boldsymbol{S}_i(\tau) = e^{\tau H_0} \boldsymbol{S}_i e^{-\tau H_0}. \tag{3.6}$$

Taking the nth derivative of $\mathcal{G}_\Lambda[\boldsymbol{h}]$ with respect to the source fields and setting $\boldsymbol{h}_i(\tau) = \bar{\boldsymbol{h}}_\Lambda$ afterwards yields the connected n-point spin correlators; e.g., the first derivative of the generating functional gives the local magnetic moment at the lattice site $\boldsymbol{r}_i$,

$$\langle \boldsymbol{S}_i(\tau) \rangle_\Lambda = \left. \frac{\delta \mathcal{G}_\Lambda[\boldsymbol{h}]}{\delta \boldsymbol{h}_i(\tau)} \right|_{\boldsymbol{h}=\bar{\boldsymbol{h}}_\Lambda}, \tag{3.7}$$

while the second derivative generates the spin propagator,

$$\begin{aligned} G^{\alpha\alpha'}_{\Lambda,ij}(\tau,\tau') &= \langle \mathcal{T}[S_i^\alpha(\tau) S_j^{\alpha'}(\tau')] \rangle_\Lambda - \langle S_i^\alpha(\tau) \rangle_\Lambda \langle S_j^{\alpha'}(\tau') \rangle_\Lambda \\ &= \left. \frac{\delta^2 \mathcal{G}_\Lambda[\boldsymbol{h}]}{\delta h_i^\alpha(\tau) \delta h_j^{\alpha'}(\tau')} \right|_{\boldsymbol{h}=\bar{\boldsymbol{h}}_\Lambda}. \end{aligned} \tag{3.8}$$

Here the scale-dependent uniform field configuration $\bar{\boldsymbol{h}}_\Lambda = \bar{h}_\Lambda \boldsymbol{e}_z$ is related to the flowing minimum of the Legendre transform of $\mathcal{G}_\Lambda[\boldsymbol{h}]$ as we will show later on.[2] While it is guaranteed that $\bar{\boldsymbol{h}}_\Lambda$ vanishes for $\Lambda = 1$ so that we recover

[2]Instead of evaluating the connected n-point spin correlators at $\boldsymbol{h} = \bar{\boldsymbol{h}}_\Lambda$, we could have equally well defined them to be evaluated at $\boldsymbol{h} = 0$. The advantage of the former choice, however, is that the connected spin correlators are then directly related to the irreducible vertices as defined in Eq. (3.23). This is easily seen from Eqs. (3.12), (3.14), (3.21), and (3.23); in essence, since the irreducible n-point vertices are defined as the nth derivative of the generating functional of the irreducible vertices $\Gamma_\Lambda[\boldsymbol{M}]$ evaluated at its minimum $\boldsymbol{M} = \bar{\boldsymbol{M}}_\Lambda$ instead of $\boldsymbol{M} = 0$, they depend on $\mathcal{G}_\Lambda[\boldsymbol{h}]$ and its derivatives evaluated at $\bar{\boldsymbol{h}}_\Lambda$.

the physical connected spin correlators [see Eq. (3.26)], it will in general be non-zero during the flow. Note that spin operators on different lattice sites commute with each other, which mirrors the behaviour of bosonic ladder operators. As a consequence, the imaginary-time-ordered spin propagator $G^{\alpha\alpha'}_{\Lambda,ij}(\tau,\tau')$ has the same analytical properties as the bosonic Matsubara Green function that we discussed in Sec. 1.3. Most importantly, this implies that we can obtain physical observables like the dynamical spin structure factor by Fourier transforming the connected spin correlators to frequency space and analytically continuing the Matsubara frequencies to just above or below the real axis. From this we can already see the close connection between our SFRG and the usual FRG of bosonic field theories.

To derive an exact flow equation of the generating functional of the connected spin correlators, we simplify differentiate Eq. (3.3) with respect to Λ,

$$\partial_\Lambda \mathcal{G}_\Lambda[\boldsymbol{h}] = \frac{1}{2}\int_0^\beta d\tau \sum_{ij,\alpha} (\partial_\Lambda V^\Lambda_{ij}) \left[\frac{\delta^2 \mathcal{G}_\Lambda[\boldsymbol{h}]}{\delta h^\alpha_i(\tau)\delta h^\alpha_j(\tau)} + \frac{\delta \mathcal{G}_\Lambda[\boldsymbol{h}]}{\delta h^\alpha_i(\tau)} \frac{\delta \mathcal{G}_\Lambda[\boldsymbol{h}]}{\delta h^\alpha_j(\tau)} \right]. \tag{3.9}$$

This expression corresponds to an infinite hierarchy of coupled flow equations for the connected n-point spin correlators

$$G^{\alpha_1\ldots\alpha_n}_{\Lambda,i_1\ldots i_n}(\tau_1,\ldots,\tau_n) = \left. \frac{\delta^n \mathcal{G}_\Lambda[\boldsymbol{h}]}{\delta h^{\alpha_1}_{i_1}(\tau_1)\ldots\delta h^{\alpha_n}_{i_n}(\tau_n)} \right|_{\boldsymbol{h}=\bar{\boldsymbol{h}}_\Lambda}, \tag{3.10}$$

which is explicitly given by

$$\begin{aligned} \partial_\Lambda G^{\alpha_1\ldots\alpha_n}_{\Lambda,i_1\ldots i_n}(\tau_1,\ldots,\tau_n) &= \frac{1}{2}\int_0^\beta d\tau \sum_{ij,\alpha} (\partial_\Lambda V^\Lambda_{ij}) \Bigg[G^{\alpha_1\ldots\alpha_n\alpha\alpha}_{\Lambda,i_1\ldots i_n ij}(\tau_1,\ldots,\tau_n,\tau,\tau) \\ &+ \sum_{m=0}^{n} \mathcal{S}_{1,\ldots,m;m+1,\ldots,n} \left\{ G^{\alpha_1\ldots\alpha_m\alpha}_{\Lambda,i_1\ldots i_m i}(\tau_1,\ldots,\tau_m,\tau) G^{\alpha_{m+1}\ldots\alpha_n\alpha}_{\Lambda,i_{m+1}\ldots i_n j}(\tau_{m+1},\ldots,\tau_n,\tau) \right\} \Bigg] \\ &+ \int_0^\beta d\tau \sum_i G^{\alpha_1\ldots\alpha_n z}_{\Lambda,i_1\ldots i_n i}(\tau_1,\ldots,\tau_n,\tau)\partial_\Lambda \bar{h}_\Lambda. \end{aligned} \tag{3.11}$$

Here we have introduced the symmetrization operator $\mathcal{S}_{1,\ldots,m;m+1,\ldots,n}$, which symmetrizes the expression to its right with respect to the exchange of all labels [33]. The last term in Eq. (3.11) arises due to the fact that the spin correlators are evaluated at $\boldsymbol{h}_i(\tau) = \bar{\boldsymbol{h}}_\Lambda$; the flow equation of $\bar{h}_\Lambda$ will be derived later on [see Eqs. (3.24) and (3.26)]. A graphical representation of the exact flow equation (3.11) is shown in Fig. 3.1.

However, it is well known from FRG calculations for bosonic and fermionic systems that it is often more efficient to work with the average effective action,

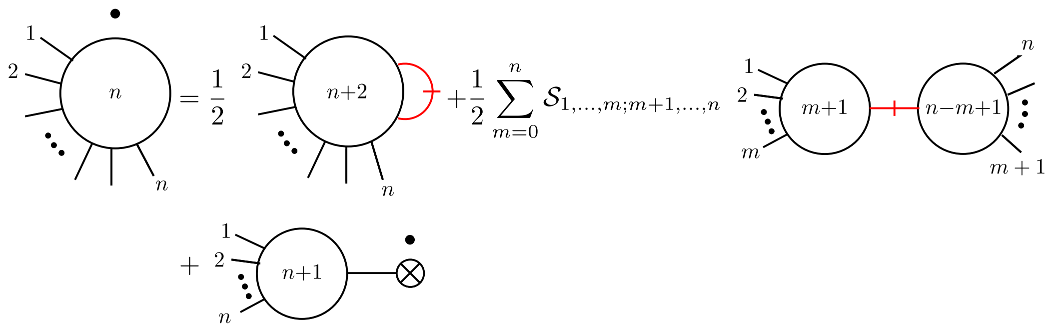

Figure 3.1: Graphical representation of the exact flow equation (3.11) of the connected n-point spin correlator $G^{\alpha_1\ldots\alpha_n}_{\Lambda,i_1\ldots i_n}(\tau_1,\ldots,\tau_n)$. The dot above the diagrams represents the derivative ∂_Λ, the red slashed lines denote the derivative $\partial_\Lambda V^\Lambda_{ij}$ of the deformed exchange coupling, and the flowing magnetic field $\bar{h}_\Lambda$ is symbolized by a crossed circle. (Figure reproduced with modifications from Ref. [99])

which generates all vertices which are irreducible with respect to the cutting of a single propagator line [33, 79, 100]. We therefore introduce the generating functional of the irreducible spin vertices, $\Gamma_\Lambda[\boldsymbol{M}]$, which we define in the usual way as the subtracted Legendre transform of the generating functional $\mathcal{G}_\Lambda[\boldsymbol{h}]$,

$$\Gamma_\Lambda[\boldsymbol{M}] = \int_0^\beta d\tau \sum_i \boldsymbol{h}_i(\tau)\cdot\boldsymbol{M}_i(\tau) - \mathcal{G}_\Lambda[\boldsymbol{h}] - \frac{1}{2}\int_0^\beta d\tau \sum_{ij} R^\Lambda_{ij}\boldsymbol{M}_i(\tau)\cdot\boldsymbol{M}_j(\tau). \tag{3.12}$$

Here the regulator

$$R^\Lambda_{ij} = V_{ij} - V^\Lambda_{ij} \tag{3.13}$$

is defined such that it vanishes at $\Lambda = 1$ and the source fields $\boldsymbol{h}_i(\tau)$ appearing on the right-hand side of Eq. (3.12) are to be understood as functionals of the local magnetization $\boldsymbol{M}_i(\tau)$ by inverting the relation

$$\boldsymbol{M}_i(\tau) = \langle \boldsymbol{S}_i(\tau)\rangle_{\Lambda,\boldsymbol{h}} = \frac{\delta\mathcal{G}_\Lambda[\boldsymbol{h}]}{\delta\boldsymbol{h}_i(\tau)}. \tag{3.14}$$

The first derivative of $\Gamma_\Lambda[\boldsymbol{M}]$ with respect to the local magnetization $\boldsymbol{M}_i(\tau)$ thus reads

$$\frac{\delta\Gamma_\Lambda[\boldsymbol{M}]}{\delta\boldsymbol{M}_i(\tau)} = \boldsymbol{h}_i(\tau) - \sum_j R^\Lambda_{ij}\boldsymbol{M}_j(\tau), \tag{3.15}$$

while the Hessian matrix $\mathbf{\Gamma}''_\Lambda[\boldsymbol{M}]$ of $\Gamma_\Lambda[\boldsymbol{M}]$ can be written as

$$[\mathbf{\Gamma}''_\Lambda[\boldsymbol{M}]]_{\alpha i\tau,\alpha' j\tau'} = \Gamma^{\alpha\alpha'}_{\Lambda,ij}(\tau,\tau';\boldsymbol{M}) = \frac{\delta^2\Gamma_\Lambda[\boldsymbol{M}]}{\delta M_i^\alpha(\tau)\delta M_j^{\alpha'}(\tau')}$$
$$= \left[\mathbf{G}_\Lambda^{-1}[\boldsymbol{h}] - \mathbf{R}_\Lambda\right]_{\alpha i\tau,\alpha' j\tau'}. \tag{3.16}$$

Here $\mathbf{G}_\Lambda^{-1}[\boldsymbol{h}]$ is the inverse of the spin-propagator matrix in the presence of the source fields,

$$[\mathbf{G}_\Lambda[\boldsymbol{h}]]_{\alpha i\tau,\alpha' j\tau'} = G^{\alpha\alpha'}_{\Lambda,ij}(\tau,\tau';\boldsymbol{h}) = \frac{\delta^2\mathcal{G}_\Lambda[\boldsymbol{h}]}{\delta h_i^\alpha(\tau)\delta h_j^{\alpha'}(\tau')}, \tag{3.17}$$

and $\mathbf{R}_\Lambda$ is the regulator matrix

$$[\mathbf{R}_\Lambda]_{\alpha i\tau,\alpha' j\tau'} = \delta_{\alpha,\alpha'}\delta(\tau-\tau')R^\Lambda_{ij}. \tag{3.18}$$

Differentiating Eq. (3.12) with respect to the deformation parameter Λ, replacing $\partial_\Lambda\mathcal{G}_\Lambda[\boldsymbol{h}]$ by its flow equation (3.9), and using the relation (3.16) we then find

$$\partial_\Lambda\Gamma_\Lambda[\boldsymbol{M}] = \frac{1}{2}\,\mathrm{Tr}\left\{(\mathbf{\Gamma}''_\Lambda[\boldsymbol{M}] + \mathbf{R}_\Lambda)^{-1}\,\partial_\Lambda\mathbf{R}_\Lambda\right\}. \tag{3.19}$$

However, since $\Gamma_\Lambda[\boldsymbol{M}]$ will in general have a minimum at a finite scale-dependent uniform field configuration $\boldsymbol{M}_i(\tau) = \bar{\boldsymbol{M}}_\Lambda = \bar{M}_\Lambda\boldsymbol{e}_z$ that is implicitly defined by

$$\left.\frac{\delta\Gamma_\Lambda[\boldsymbol{M}]}{\delta M_i^\alpha(\tau)}\right|_{\boldsymbol{M}=\boldsymbol{M}_\Lambda} = 0, \tag{3.20}$$

we should actually consider the shifted generating functional

$$\tilde{\Gamma}_\Lambda[\boldsymbol{\eta}] = \Gamma_\Lambda[\bar{\boldsymbol{M}}_\Lambda + \boldsymbol{\eta}], \tag{3.21}$$

where $\boldsymbol{\eta}_i(\tau) = \boldsymbol{M}_i(\tau) - \bar{\boldsymbol{M}}_\Lambda$ measures the distance to the minimum of the average effective action. Together with Eq. (3.19) we thus arrive at the Wetterich equation [34] for quantum spin systems,

$$\partial_\Lambda\tilde{\Gamma}_\Lambda[\boldsymbol{\eta}] = \partial_\Lambda\Gamma_\Lambda[\boldsymbol{M}]|_{\boldsymbol{M}\to\bar{\boldsymbol{M}}_\Lambda+\boldsymbol{\eta}} + \int_0^\beta\sum_i\frac{\delta\tilde{\Gamma}_\Lambda[\boldsymbol{\eta}]}{\delta\eta_i^z(\tau)}\partial_\Lambda\bar{M}_\Lambda$$
$$= \frac{1}{2}\,\mathrm{Tr}\left\{\left(\tilde{\mathbf{\Gamma}}''_\Lambda[\boldsymbol{\eta}] + \mathbf{R}_\Lambda\right)^{-1}\partial_\Lambda\mathbf{R}_\Lambda\right\} + \int_0^\beta\sum_i\frac{\delta\tilde{\Gamma}_\Lambda[\boldsymbol{\eta}]}{\delta\eta_i^z(\tau)}\partial_\Lambda\bar{M}_\Lambda. \tag{3.22}$$

This flow equation is formally identical to the Wetterich equation for bosonic systems [33], which can be traced back to the identical analytical properties of imaginary-time-ordered spin correlators and bosonic Matsubara Green functions as already mentioned above. We note that our derivation of Eq. (3.22) makes no mention of path integrals at any point, in contrast to the usual construction of the FRG in terms of complex-valued or Berezin integrals [33]. The fact that the derivation of exact FRG flow equations does not depend on a path-integral formulation was already noticed by Pawlowski [101] and was subsequently applied to classical spin systems and bosonic quantum lattice models [76, 102–106].

It is now straightforward to derive the infinite hierarchy of flow equations for the irreducible vertices

$$\tilde{\Gamma}^{\alpha_1\ldots\alpha_n}_{\Lambda,i_1\ldots i_n}(\tau_1,\ldots,\tau_n) = \left.\frac{\delta^n \tilde{\Gamma}_\Lambda[\boldsymbol{\eta}]}{\delta\eta^{\alpha_1}_{i_1}(\tau_1)\ldots\delta\eta^{\alpha_n}_{i_n}(\tau_n)}\right|_{\boldsymbol{\eta}=0} \tag{3.23}$$

by expanding Eq. (3.22) around $\boldsymbol{\eta} = 0$. Of special interest is the first-order coefficient since it yields an exact flow equation for the flowing magnetization $\bar{M}_\Lambda$,

$$\begin{aligned}&\int_0^\beta d\tau' \sum_j \tilde{\Gamma}^{zz}_{\Lambda,ij}(\tau,\tau')\partial_\Lambda \bar{M}_\Lambda \\ &= -\frac{1}{2}\int_0^\beta d\tau_1 \int_0^\beta d\tau_2 \sum_{i_1 i_2,\alpha_1\alpha_2} \dot{G}^{\alpha_1\alpha_2}_{\Lambda,i_1 i_2}(\tau_1,\tau_2)\tilde{\Gamma}^{\alpha_2\alpha_1 z}_{\Lambda,i_2 i_1 i}(\tau_2,\tau_1,\tau).\end{aligned} \tag{3.24}$$

Here we have defined the single-scale propagator

$$\dot{G}^{\alpha\alpha'}_{\Lambda,ij}(\tau,\tau') = -\left[\mathbf{G}_\Lambda[\bar{\boldsymbol{h}}_\Lambda]\left(\partial_\Lambda \mathbf{R}_\Lambda\right)\mathbf{G}_\Lambda[\bar{\boldsymbol{h}}_\Lambda]\right]_{\alpha i\tau,\alpha' j\tau'} \tag{3.25}$$

and we have used that the irreducible one-point vertex vanishes by construction. Together with Eq. (3.15), this fact also allows us to connect the flowing magnetization $\bar{\boldsymbol{M}}_\Lambda$ to the flowing uniform field configuration $\boldsymbol{h}_i(\tau) = \bar{\boldsymbol{h}}_\Lambda$ via

$$\bar{\boldsymbol{h}}_\Lambda = \sum_j R^\Lambda_{ij}\bar{\boldsymbol{M}}_\Lambda. \tag{3.26}$$

As a consequence, the derivative $\partial_\Lambda \bar{h}_\Lambda$ appearing in Eq. (3.11) can be directly expressed through the flow equation (3.24) of $\bar{M}_\Lambda$.

Finally, let us point out a subtlety in our formalism that is related to the appearance of the equal-time combination $\boldsymbol{S}_i(\tau)\cdot\boldsymbol{S}_j(\tau)$ under the time-ordering symbol [see Eqs. (3.3) and (3.5)]. Writing the scalar product in terms of the fundamental spin operators,

$$\boldsymbol{S}_i(\tau)\cdot\boldsymbol{S}_j(\tau) = S^x_i(\tau)S^x_j(\tau) + S^y_i(\tau)S^y_j(\tau) + S^z_i(\tau)S^z_j(\tau), \tag{3.27}$$

it is clear that the operators commute with each other so that there is no ambiguity regarding their time ordering. However, in practice it is often useful to express S_i^x and S_i^y in terms of the spin ladder operators

$$S_i^{\pm} = \frac{1}{\sqrt{2}}(S_i^x \pm i S_i^y). \tag{3.28}$$

Rewriting Eq. (3.27) in terms of S_i^+ and S_i^- we now have to introduce an infinitesimal shift,

$$\boldsymbol{S}_i(\tau) \cdot \boldsymbol{S}_j(\tau) = S_i^+(\tau + 0^{\pm}) S_j^-(\tau) + S_i^-(\tau + 0^{\pm}) S_j^+(\tau) + S_i^z(\tau) S_j^z(\tau), \tag{3.29}$$

where both choices of 0^+ and 0^- are equally valid. While the formal appearance of the Wetterich equation (3.22) stays unchanged, the regulator matrix is now given by

$$[\mathbf{R}_\Lambda]_{\alpha i \tau, \alpha' j \tau'} = \delta_{\alpha,\alpha'} \delta(\tau - \tau' - 0^{\pm}) R_{ij}^{\Lambda}. \tag{3.30}$$

Note that in the quantum Heisenberg model we can circumvent this subtlety by redefining the deformed exchange interaction V_{ij}^{Λ} such that $V_{ii}^{\Lambda} = 0$, since spin operators on different sites always commute with each other and an on-site interaction only amounts to a constant shift in the Hamiltonian. However, as the SFRG formalism is not restricted to the Heisenberg model and similar subtleties can also appear in a more complicated fashion, it will be instructive to consider the general case of a finite on-site interaction. We will come back to this point in Sec. 3.3.3 where we explicitly evaluate the flow equations of the quantum Heisenberg model.

3.2.2 Initial condition of isolated spins in the Ising model

As the construction of the SFRG given above is rather technical, let us demonstrate the main concepts by considering the spin-S Ising model,

$$H = -\frac{1}{2} \sum_{ij} V_{ij} S_i^z S_j^z - h_0 \sum_i S_i^z. \tag{3.31}$$

Since all S_i^z operators commute with each other, we can neglect their time dependence; for example, the generating functional of the connected spin correlators then reads

$$\mathcal{G}_\Lambda[h^z] = \ln \mathrm{Tr} \left[e^{-\beta H_0} e^{\beta \left(\sum_i h_i^z S_i^z - \mathcal{V}_\Lambda \right)} \right], \tag{3.32}$$

where

$$\mathcal{V}_\Lambda = -\frac{1}{2}\sum_{ij} V_{ij}^{\Lambda} S_i^z S_j^z. \tag{3.33}$$

For simplicity, we choose the deformation scheme $V_{ij}^{\Lambda} = \Lambda V_{ij}$ where the deformed exchange interaction initially vanishes, $V_{ij}^{\Lambda=0} = 0$. Our SFRG formalism then corresponds to the lattice FRG for classical spin systems developed by Machado and Dupuis [76], which we have already used in Ch. 2 to study the BKT transition. At $\Lambda = 0$, calculating $\mathcal{G}_\Lambda[h^z]$ reduces to a single-site problem that can be solved analytically,

$$\mathcal{G}_0[h^z] = \sum_i \ln \mathrm{Tr}\left[e^{\beta(h_0+h_i^z)S_i^z}\right] = \sum_i B\left(\beta(h_0+h_i^z)\right), \tag{3.34}$$

where

$$B(y) = \ln\left[\frac{\sinh\left[(S+1/2)y\right]}{\sinh(y/2)}\right]. \tag{3.35}$$

Taking the first derivative of $\mathcal{G}_0[h^z]$ then results in

$$M_i^z[h^z] = \langle S_i^z \rangle_{\Lambda,h^z} = \frac{\partial \mathcal{G}_0[h^z]}{\partial(\beta h_i^z)} = b\left(\beta(h_0+h_i^z)\right), \tag{3.36}$$

where

$$b(y) = B'(y) = \left(S+\frac{1}{2}\right)\coth\left[\left(S+\frac{1}{2}\right)y\right] - \frac{1}{2}\coth\left(\frac{y}{2}\right) \tag{3.37}$$

is the well-known Brillouin function. Higher-order connected spin correlators are derived analogously by successively differentiating the Brillouin function,

$$G^{(n)}_{0,i_1\ldots i_n}[h^z] = \frac{\partial^n \mathcal{G}_0[h^z]}{\partial(\beta h_i^z)^n} = \delta_{i_1,i_2}\cdots\delta_{i_1,i_n} b^{(n-1)}\left(\beta(h_0+h_i^z)\right). \tag{3.38}$$

To derive the initial condition for the average effective action $\Gamma_\Lambda[M^z]$, we need to invert the relation (3.36) between M_i^z and h_i^z, which amounts to finding the inverse function to $b(y)$. Unfortunately, it is not possible to invert the Brillouin function analytically for general spin S [107]. Nevertheless, we may expand $\Gamma_\Lambda[M^z]$ in a Taylor series around its minimum at $\bar{M}_\Lambda^z$, which is determined by the condition

$$\left.\frac{\delta \Gamma_\Lambda[M^z]}{\delta M_i^z}\right|_{M^z=\bar{M}_\Lambda^z} = 0. \tag{3.39}$$

To simplify the following calculations, we set $h_0 = 0$ and assume that there is no spontaneous breaking of the rotational symmetry so that $\bar{M}^z_\Lambda = 0$. We may then expand the average effective action as

$$\Gamma_\Lambda[M^z] = \sum_{n=0}^{\infty} \frac{1}{n! N^{n-1}} \sum_{\boldsymbol{k}_1 \ldots \boldsymbol{k}_n} \delta_{\boldsymbol{k}_1 + \ldots + \boldsymbol{k}_n, 0} \Gamma^{(n)}_\Lambda(\boldsymbol{k}_1, \ldots, \boldsymbol{k}_n) M^z_{\boldsymbol{k}_1} \ldots M^z_{\boldsymbol{k}_n}, \quad (3.40)$$

where

$$M^z_{\boldsymbol{k}} = \sum_i e^{-i\boldsymbol{k}\cdot\boldsymbol{r}_i} M^z_i \quad (3.41)$$

are the Fourier coefficients of the local magnetization M^z_i. By taking derivatives of the exact relation (3.16) and setting $M^z_i = 0$ afterwards, we can express the irreducible vertices $\Gamma^{(n)}_\Lambda$ through the connected spin correlators $G^{(m)}_\Lambda$ with $m \leq n$. Since we know the connected spin correlators at $\Lambda = 0$ from Eq. (3.38), this allows us to derive the initial condition $\Gamma^{(n)}_0$ for the irreducible vertices. For example, the irreducible two-point vertex is initially given by

$$\Gamma^{(2)}_0(\boldsymbol{k}) = \frac{1}{b'} - \beta V_{\boldsymbol{k}}, \quad (3.42)$$

where $b' = S(S+1)/3$ is the first derivative of $b(y)$ at $y = 0$, $V_{\boldsymbol{k}}$ is the Fourier transform of the exchange interaction, and we have used the notation

$$\Gamma^{(2)}_0(\boldsymbol{k}, \boldsymbol{k}') = \delta_{\boldsymbol{k}, -\boldsymbol{k}'} \Gamma^{(2)}_0(\boldsymbol{k}'). \quad (3.43)$$

Let us here also write down the irreducible four-point vertex,

$$\Gamma^{(4)}_0(\boldsymbol{k}_1, \boldsymbol{k}_2, \boldsymbol{k}_3, \boldsymbol{k}_4) = -\delta_{\boldsymbol{k}_1 + \boldsymbol{k}_2 + \boldsymbol{k}_3 + \boldsymbol{k}_4, 0} \frac{b'''}{(b')^4}, \quad (3.44)$$

where $b''' = [1 - (2S+1)^4]/120$ is the third derivative of the Brillouin function at vanishing external field.

3.2.3 Critical temperature of the spin-S Ising model within the vertex expansion

As a simple way to quantitatively compare our SFRG with established methods, we will in the following compute the critical temperature T_c of the spin-S Ising model with nearest-neighbour interaction on a D-dimensional hypercubic lattice within the vertex expansion. Its Hamiltonian is given by

$$H = -V \sum_{\langle ij \rangle} S^z_i S^z_j, \quad (3.45)$$

where we sum over all distinct pairs of nearest neighbors. Since T_c is determined by the condition $\Gamma^{(2)}_{\Lambda=1}(0) = 0$, we have to evaluate the flow of the irreducible two-point vertex. In the simplest approximation we replace $\Gamma^{(2)}_{\Lambda}(\boldsymbol{k}) \approx \Gamma^{(2)}_{0}(\boldsymbol{k})$, which according to Eq. (3.42) yields the mean-field result

$$T_{c0} = b'|V_0| = \frac{S(S+1)}{3} 2D|V| \tag{3.46}$$

for the critical temperature, where $V_0 = V_{\boldsymbol{k}=0} = 2DV$. We can improve on this result by considering the exact flow equation of the irreducible two-point vertex,

$$\partial_\Lambda \Gamma^{(2)}_{\Lambda}(\boldsymbol{k}) = \frac{\beta}{2N} \sum_{\boldsymbol{q}} \dot{G}_\Lambda(\boldsymbol{q}) \Gamma^{(4)}_{\Lambda}(-\boldsymbol{q}, \boldsymbol{q}, -\boldsymbol{k}, \boldsymbol{k}), \tag{3.47}$$

which can be derived by expanding the Wetterich equation (3.22) in the usual way [33]. Here we have introduced the single-scale propagator

$$\dot{G}_\Lambda(\boldsymbol{k}) = -G^2_\Lambda(\boldsymbol{k}) \partial_\Lambda R_\Lambda(\boldsymbol{k}), \tag{3.48}$$

which is defined in terms of the regularized spin propagator

$$G_\Lambda(\boldsymbol{k}) = \frac{1}{\Gamma^{(2)}_{\Lambda}(\boldsymbol{k}) + \beta R_\Lambda(\boldsymbol{k})} \tag{3.49}$$

and the regulator

$$R_\Lambda(\boldsymbol{k}) = (1 - \Lambda) V_{\boldsymbol{k}}. \tag{3.50}$$

The irreducible four-point vertex that appears in Eq. (3.47) obeys the exact flow equation

$$\begin{aligned} \partial_\Lambda \Gamma^{(4)}_{\Lambda}(\boldsymbol{k}_1, \boldsymbol{k}_2, \boldsymbol{k}_3, \boldsymbol{k}_4) &= \frac{\beta}{2N} \sum_{\boldsymbol{q}} \dot{G}_\Lambda(\boldsymbol{q}) \Gamma^{(6)}_{\Lambda}(-\boldsymbol{q}, \boldsymbol{q}, \boldsymbol{k}_1, \boldsymbol{k}_2, \boldsymbol{k}_3, \boldsymbol{k}_4) \\ &- \frac{\beta}{2N} \mathcal{S}_{\boldsymbol{k}_1,\boldsymbol{k}_2;\boldsymbol{k}_3,\boldsymbol{k}_4} \sum_{\boldsymbol{q}} \dot{G}_\Lambda(\boldsymbol{q}) \Gamma^{(4)}_{\Lambda}(-\boldsymbol{q}, \boldsymbol{q} - \boldsymbol{k}_1 - \boldsymbol{k}_2, \boldsymbol{k}_1, \boldsymbol{k}_2) G_\Lambda(\boldsymbol{q} - \boldsymbol{k}_1 - \boldsymbol{k}_2) \\ &\times \Gamma^{(4)}_{\Lambda}(-\boldsymbol{q} + \boldsymbol{k}_1 + \boldsymbol{k}_2, \boldsymbol{q}, \boldsymbol{k}_3, \boldsymbol{k}_4), \end{aligned} \tag{3.51}$$

which in turn depends on the irreducible six-point vertex. We close this infinite hierarchy of flow equations by approximating $\Gamma^{(6)}_{\Lambda}$ by its initial value

$$\Gamma^{(6)}_{0}(\boldsymbol{k}_1, \boldsymbol{k}_2, \boldsymbol{k}_3, \boldsymbol{k}_4, \boldsymbol{k}_5, \boldsymbol{k}_6) = \delta_{\boldsymbol{k}_1+\boldsymbol{k}_2+\boldsymbol{k}_3+\boldsymbol{k}_4+\boldsymbol{k}_5+\boldsymbol{k}_6,0} \left[-\frac{b^{(5)}}{(b')^6} + 10 \frac{(b''')^2}{(b')^7} \right], \tag{3.52}$$

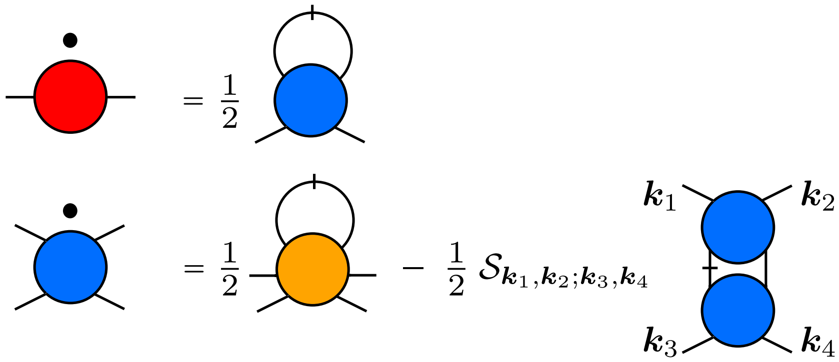

Figure 3.2: Graphical representation of the exact flow equations (3.47) and (3.51) of the irreducible vertices $\Gamma_\Lambda^{(2)}$ and $\Gamma_\Lambda^{(4)}$, respectively. The dot over the diagrams denotes the derivative ∂_Λ, the colored circles symbolize the irreducible vertices $\Gamma_\Lambda^{(n)}$, solid lines represent the regularized spin propagator $G_\Lambda(\boldsymbol{k})$, and slashed solid lines represent the single-scale propagator $\dot{G}_\Lambda(\boldsymbol{k})$. Note the formal similarity to the flow equations of the irreducible vertices in the dual-vortex model as shown in Fig. 2.6.

where $b^{(n)}$ is the nth derivative of $b(y)$ at $y = 0$. A graphical representation of the flow equations (3.47) and (3.51) is shown in Fig. 3.2. To keep the calculation simple, we also replace the flowing irreducible four-point vertex by its zero-momentum part. This has the advantage that the momentum dependence of the irreducible two-point vertex, which we there parametrize as

$$\Gamma_\Lambda^{(2)}(\boldsymbol{k}) = \Sigma_\Lambda - \beta V_{\boldsymbol{k}}, \tag{3.53}$$

does not change during the flow. The resulting set of coupled flow equations reads

$$\partial_\Lambda \Sigma_\Lambda = \frac{\beta}{2N} \sum_{\boldsymbol{q}} \dot{G}_\Lambda(\boldsymbol{q}) \Gamma_\Lambda^{(4)}, \tag{3.54}$$

$$\partial_\Lambda \Gamma_\Lambda^{(4)} = \frac{\beta}{2N} \sum_{\boldsymbol{q}} \dot{G}_\Lambda(\boldsymbol{q}) \left[\Gamma_0^{(6)} - 6 \left(\Gamma_\Lambda^{(4)} \right)^2 G_\Lambda(\boldsymbol{q}) \right], \tag{3.55}$$

where

$$\dot{G}_\Lambda(\boldsymbol{k}) = \frac{V_{\boldsymbol{k}}}{\left[\Sigma_\Lambda - \beta\Lambda V_{\boldsymbol{k}}\right]^2}, \quad G_\Lambda(\boldsymbol{k}) = \frac{1}{\Sigma_\Lambda - \beta\Lambda V_{\boldsymbol{k}}}, \tag{3.56}$$

and the exchange interaction $V_{\boldsymbol{k}}$ can be written in terms of the nearest-neighbor structure factor $\gamma_{\boldsymbol{k}}$ for a D-dimensional hypercubic lattice with lattice parameter a,

$$V_{\boldsymbol{k}} = V_0 \gamma_{\boldsymbol{k}} \quad \text{with} \quad \gamma_{\boldsymbol{k}} = \frac{1}{D} \sum_{i=1}^{D} \cos(k_i a). \tag{3.57}$$

It is straightforward to solve these flow equations in the thermodynamic limit, where the momentum sums are replaced by integrals over the first Brillouin zone. While it is not possible to evaluate the integrals analytically in higher dimensions, it is straightforward to calculate them numerically for various values of $\Lambda V_0/\Sigma_\Lambda$ and interpolate the result. This allows us to integrate the flow equations of Σ_Λ and $\Gamma_\Lambda^{(4)}$ efficiently for any value of the spin S.

The results for the critical temperature T_c at various values of D and S are shown in Table 3.1 and Table 3.2, respectively. We find good quantitative agreement with the accepted results, except for $D = 2$ where our truncation incorrectly predicts $T_c = 0$. This can be understood by noting that our truncation strategy amounts to an expansion of the effective potential $U_\Lambda(\bar{M}^z) = \Gamma_\Lambda[M^z]|_{M_i^z = \bar{M}^z}$ up to the sixth order in $\bar{M}^z$. While fluctuations of the magnetization field are suppressed in higher dimensions, they can be rather strong in one and two dimensions where our truncation overestimates their effect. This can be seen explicitly for the special case $S = 1/2$, which was studied numerically by Machado and Dupuis within the local potential approximation [76]. Taking the full effective potential into account, they obtain a finite T_c for $D = 2$, while their prediction for $D = 3$ is of a similar accuracy as our result.

3.2.4 Critical temperature of the spin-S Ising model within the $1/D$ expansion

While the vertex expansion as discussed above yields in general quantitatively good results for T_c, it becomes increasingly difficult in higher dimensions to compute the momentum integrals on the right-hand of the flow equations to a sufficiently high accuracy. In this section we will therefore develop an alternative approximation strategy, which has the additional advantage that it is almost fully analytical. The basic idea is to use our SFRG formalism to generate an expansion of the irreducible two-point vertex in powers of $1/D$, which we can then use to compute the critical temperature. Let us again write down the exact flow equation of $\Gamma_\Lambda^{(2)}(\boldsymbol{k})$,

$$\partial_\Lambda \Gamma_\Lambda^{(2)}(\boldsymbol{k}) = \frac{\beta}{2N} \sum_{\boldsymbol{q}} \frac{V_{\boldsymbol{q}} \Gamma_\Lambda^{(4)}(-\boldsymbol{q}, \boldsymbol{q}, -\boldsymbol{k}, \boldsymbol{k})}{\left[\Gamma_\Lambda^{(2)}(\boldsymbol{q}) + \beta R_\Lambda(\boldsymbol{q})\right]^2}. \tag{3.58}$$

T_c/T_{c0} for $S = 1/2$			
D	vertex expansion	benchmark	rel. error / %
1	0	0	0
2	0	0.57	-
3	0.744	0.752	1
4	0.839	0.835	0.5
5	0.880	0.878	0.3
6	0.904	0.903	0.2
7	0.920	0.919	0.1

Table 3.1: Critical temperature T_c in units of the mean-field result T_{c0} for the spin-1/2 Ising model on a D-dimensional hypercubic lattice with nearest-neighbour interaction. The second column refers to our results from the vertex expansion which have been computed by numerically solving the flow equations (3.54) and (3.55), while the third column shows the accepted results [108–111].

T_c/T_{c0} for $D = 3$			
S	vertex expansion	benchmark	rel. error / %
1/2	0.744	0.752	1
1	0.805	0.799	1
3/2	0.823	0.814	1
2	0.830	0.820	1
3	0.837	0.826	1
∞	0.843	0.832	1

Table 3.2: Critical temperature T_c in units of the mean-field result T_{c0} for the spin-S Ising model on a cubic lattice. Analogous to Table 3.1, the second column refers to our results from the vertex expansion, while the third column shows the accepted results [109, 112].

To leading order in $1/D$ we can replace both $\Gamma_\Lambda^{(2)}$ and $\Gamma_\Lambda^{(4)}$ on the right-hand side of Eq. (3.58) by their initial condition, so that

$$\partial_\Lambda \Gamma_\Lambda^{(2)}(\boldsymbol{k}) = \frac{\beta \Gamma_0^{(4)}}{2N} \sum_{\boldsymbol{q}} \frac{V_{\boldsymbol{q}}}{\left[\frac{1}{b'} - \beta \Lambda V_{\boldsymbol{q}}\right]^2} + O(D^{-2}). \tag{3.59}$$

Since it is easy to see that for any integer $n \geq 0$ we have

$$\sum_{\boldsymbol{q}} (\gamma_{\boldsymbol{q}})^{2n} = \sum_{\boldsymbol{q}} \left[\frac{1}{D}\sum_{i=1}^{D} \cos(k_i a)\right]^{2n} = O(D^{-n}), \tag{3.60}$$

$$\sum_{\boldsymbol{q}} (\gamma_{\boldsymbol{q}})^{2n+1} = 0, \tag{3.61}$$

we can expand the denominator as

$$\begin{aligned}\partial_\Lambda \Gamma_\Lambda^{(2)}(\boldsymbol{k}) &= \frac{\beta (b')^2 \Gamma_0^{(4)}}{2N} \sum_{\boldsymbol{q}} V_{\boldsymbol{q}} \left(1 + 2\beta\Lambda b' V_{\boldsymbol{q}}\right) + O(D^{-2}) \\ &= -\frac{\Lambda b''' g^2}{2(b')^3 D} + O(D^{-2}),\end{aligned} \tag{3.62}$$

where we have introduced the dimensionless parameter

$$g = \beta b' V_0 = \frac{T_{c0}}{T} \mathrm{sgn}(V_0). \tag{3.63}$$

Eq. (3.62) is then easily integrated to

$$\Gamma_{\Lambda=1}^{(2)}(\boldsymbol{k}) = \frac{1}{b'}\left[1 - \gamma_{\boldsymbol{k}} g - \frac{b''' g^2}{4(b')^2 D} + O(D^{-2})\right]. \tag{3.64}$$

Since this function is of quadratic order in g, it is trivial to calculate its roots and we can immediately write down the resulting expression for the critical temperature,

$$\frac{T_c}{T_{c0}} = \frac{1}{2}\left[1 + \sqrt{1 - \frac{|b'''|}{(b')^2 D}}\right]. \tag{3.65}$$

As can be seen from Table 3.3, Eq. (3.65) is quite accurate in higher dimensions, but it also yields qualitatively correct results for lower dimensions, especially for $D = 2$ where it predicts a finite T_c. Our result (3.65) works equally well for arbitrary spin S, as can be seen from the comparison in Table 3.4.

It is straightforward to extend our $1/D$ expansion of the irreducible two-point vertex beyond the first-order result (3.64); the explicit calculations can

D	T_c/T_{c0} for $S = 1/2$				rel. error / %		
	$O(D^{-1})$	$O(D^{-2})$	$O(D^{-3})$	benchmark	$O(D^{-1})$	$O(D^{-2})$	$O(D^{-3})$
1	-	-	-	0	-	-	-
2	0.50	-	-	0.57	12	-	-
3	0.79	0.740	-	0.752	5	2	-
4	0.85	0.839	0.832	0.835	2	0.5	0.4
5	0.89	0.880	0.8782	0.8778	1	0.3	0.04
6	0.908	0.9041	0.9032	0.9029	0.6	0.1	0.03
7	0.923	0.9198	0.9193	0.9192	0.4	0.06	0.01
8	0.933	0.9310	0.9308	0.9307	0.3	0.04	0.01
9	0.941	0.9395	0.93931	0.93926	0.2	0.02	0.005
10	0.9472	0.9461	0.94595	0.94593	0.1	0.01	0.002

Table 3.3: Critical temperature T_c in units of the mean-field result T_{c0} for the spin-1/2 Ising model on a D-dimensional hypercubic lattice. The second column refers to the leading-order result (3.65) from the $1/D$ expansion, while the third and fourth columns refer to the higher-order truncations of the irreducible two-point vertex in Eqs. (3.66) and (3.67), respectively. The accepted results are shown in the fifth column as a comparison [108–111].

S	T_c/T_{c0} for $D=3$			rel. error / %	
	$O(D^{-1})$	$O(D^{-2})$	benchmark	$O(D^{-1})$	$O(D^{-2})$
1/2	0.79	0.740	0.752	5	2
1	0.85	0.806	0.799	7	1
3/2	0.87	0.826	0.814	7	2
2	0.88	0.834	0.820	7	2
3	0.88	0.842	0.826	7	2
∞	0.89	0.849	0.832	7	2

Table 3.4: Critical temperature T_c in units of the mean-field result T_{c0} for the spin-S Ising model on a cubic lattice. Analogous to Table 3.3, the second column refers to the leading-order result (3.65) from the $1/D$ expansion, while the third column refers to the next-to-leading-order truncation (3.66). The fourth column shows the accepted results [109, 112].

be found in Appendix B.1. To next-to-leading order we find a momentum-dependent contribution of the order g^3 and a momentum-independent term of the order g^4,

$$b'\Gamma^{(2)}_{\Lambda=1}(\boldsymbol{k}) =1 - \gamma_{\boldsymbol{k}} g - \frac{b''' g^2}{4(b')^2 D} - \frac{(b''')^2 \gamma_{\boldsymbol{k}} g^3}{24(b')^4 D^2} - \frac{(b^{(5)} + 12 b' b''') g^4}{32 (b')^3 D^2} + O(D^{-3}). \tag{3.66}$$

Setting $\Gamma^{(2)}_{\Lambda=1}(\boldsymbol{k}) = 0$ and solving for g, we find that an instability first occurs for $\gamma_{\boldsymbol{k}} = \mathrm{sgn}(V_0)$. This signals a phase transition to a ferromagnetic or to a Néel state, respectively, where T_c is the same for both cases as it should be. Since Eq. (3.66) is of quartic order in g, it is still possible to express T_c analytically; the results for various value of D and S are shown in Table 3.3 and Table 3.4. Finally, expanding $\Gamma^{(2)}_{\Lambda=1}(0)$ to third order in $1/D$ yields

$$\begin{aligned} b'\Gamma^{(2)}_{\Lambda=1}(0) = 1 - g + \frac{C_1 g^2}{D} - \frac{C_2 g^3}{D^2} + \frac{C_3 g^4}{D^2} - \frac{C_4 g^4}{D^3} - \frac{C_5 g^5}{D^3} + \frac{C_6 g^6}{D^3} \\ + O(D^{-4}), \end{aligned} \tag{3.67}$$

where we have assumed $V_0 > 0$ since this does not affect the critical temperature. The spin dependence is encoded in the coefficients C_i, which take on positive values of order unity and are explicitly given by

$$C_1 = -\frac{b'''}{4(b')^2}, \tag{3.68a}$$

$$C_2 = \frac{(b''')^2}{24(b')^4}, \tag{3.68b}$$

$$C_3 = -\frac{b^{(5)} + 12b'b'''}{32(b')^3}, \tag{3.68c}$$

$$C_4 = \frac{b'''b^{(5)} - 36(b')^3 b'''}{192(b')^5}, \tag{3.68d}$$

$$C_5 = \frac{b'b'''b^{(5)} - (b''')^3 + 9(b')^2(b''')^2}{48(b')^6}, \tag{3.68e}$$

$$C_6 = -\frac{b'b^{(7)} + 3b'''b^{(5)} + 36(b')^2 b^{(5)} + 80b'(b''')^2 + 360(b')^3 b'''}{384(b')^5}. \tag{3.68f}$$

For example, setting $S = 1/2$ results in

$$\frac{1}{4}\Gamma^{(2)}_{\Lambda=1}(0) = 1 - g + \frac{g^2}{2D} - \frac{g^3}{6D^2} + \frac{g^4}{4D^2} - \frac{5g^4}{24D^3} - \frac{g^5}{4D^3} + \frac{g^6}{2D^3} + O(D^{-4}). \tag{3.69}$$

For a given choice of D and S it is then trivial to find T_c by calculating the roots of Eq. (3.67) numerically. The resulting T_c for $S = 1/2$ and various values of D, which corresponds to the lowest positive root of Eq. (3.69), is shown in Table 3.3.

Comparing the behaviour of the different truncations in Table 3.3 for small D, it seems plausible that our expansion of the irreducible two-point vertex is asymptotic; to nth order in $1/D$, the prediction for T_c seems to be reliable as long as $D > n$. Note that, despite its formal appearance, our approach is not identical to a high-temperature expansion of $\Gamma^{(2)}_{\Lambda=1}$; truncating the $1/D$ expansion after the nth order with $n > 1$, we find that the coefficients of the terms up to g^{n+1} coincide with the high-temperature expansion, while the higher-order terms up to g^{2n} have a different coefficient. This seems to result in nicer analytic properties: comparing with the work by Butera and Pernici who have computed T_c for the spin-1/2 Ising model by expanding the spin susceptibility in a high-temperature series up to the 20th order and subsequently applying a generalization of the Padé approximant method [111], we find that our result for T_c, which follows simply from calculating the roots of the sixth-order polynomial in Eq. (3.69), lies just outside their error bars for $D = 10$.

3.2.5 Choice of the initial condition for quantum spin systems

Isolated spins

Let us now come back to the more general SFRG formalism for quantum spin systems. An important point that we have not touched upon so far concerns the existence of the Taylor expansion of the average effective action $\Gamma_\Lambda[\boldsymbol{M}]$ around its minimum. Since $\Gamma_\Lambda[\boldsymbol{M}]$ is defined as the subtracted Legendre transform of the generating functional of the connected spin correlators $\mathcal{G}_\Lambda[\boldsymbol{h}]$, we have to express the source fields $\boldsymbol{h}_i(\tau)$ as a functional of the local magnetization $\boldsymbol{M}_i(\tau)$ by inverting relation (3.14). According to the implicit function theorem, this requires that we can invert the spin-propagator matrix $\mathbf{G}_\Lambda[\boldsymbol{h}]$ defined in Eq. (3.17). For practical calculations, however, we also require that the Taylor expansion of $\Gamma_\Lambda[\boldsymbol{M}]$ around its minimum at $\boldsymbol{M}_i(\tau) = \bar{\boldsymbol{M}}_\Lambda$ is well defined. Together with Eq. (3.15), this leads to the stronger condition that the spin-propagator matrix $\mathbf{G}_\Lambda \equiv \mathbf{G}_\Lambda[\bar{\boldsymbol{h}}_\Lambda = V_0 \bar{\boldsymbol{M}}_\Lambda]$ is invertible. To show that this condition may be violated, let us consider a deformation scheme where we start with isolated spins, $V_{ij}^{\Lambda=0} = 0$, so that

$$\mathcal{G}_0[\boldsymbol{h}] = \ln \mathrm{Tr} \left[e^{-\beta H_0} \mathcal{T} e^{\int_0^\beta d\tau \sum_i \boldsymbol{h}_i(\tau)\cdot \boldsymbol{S}_i(\tau)} \right], \tag{3.70}$$

where

$$H_0 = -h_0 \sum_i S_i^z \tag{3.71}$$

is the free part of the Hamiltonian. Due to the rotational symmetry around the z axis, the spin-propagator matrix has the form

$$[\mathbf{G}_\Lambda]_{i\tau, j\tau'} \to \begin{pmatrix} G^{xx}_{\Lambda,ij}(\tau,\tau') & G^{xy}_{\Lambda,ij}(\tau,\tau') & 0 \\ G^{yx}_{\Lambda,ij}(\tau,\tau') & G^{yy}_{\Lambda,ij}(\tau,\tau') & 0 \\ 0 & 0 & G^{zz}_{\Lambda,ij}(\tau,\tau') \end{pmatrix}. \tag{3.72}$$

However, since S_i^z commutes with H_0,

$$[S_i^z, H_0] = 0, \tag{3.73}$$

it is obvious from Eqs. (3.4) and (3.6) that the longitudinal part of the propagator is initially time independent, $G^{zz}_{0,ij}(\tau,\tau') = G^{zz}_{0,ij}$, which implies that the determinant of $\mathbf{G}_0$ vanishes. To get a better understanding of this point, we introduce the spin ladder operators

$$S_i^\pm = \frac{1}{\sqrt{2}}(S_i^x \pm i S_i^y) \tag{3.74}$$

as well as the notation

$$G_{\Lambda}^{\alpha\alpha'}(K,K') = \delta(K+K')G_{\Lambda}^{\alpha\alpha'}(K), \tag{3.75}$$

where $K = (\boldsymbol{k}, i\omega)$ is a collective label for momentum and Matsubara frequency, $\delta(K) = \beta N \delta_{\boldsymbol{k},0}\delta_{\omega,0}$, and

$$G_{\Lambda}^{\alpha\alpha'}(K,-K) = \int_0^{\beta} d\tau \int_0^{\beta} d\tau' \sum_{ij} e^{-i\boldsymbol{k}\cdot(\boldsymbol{r}_i - \boldsymbol{r}_j) + i\omega(\tau-\tau')} G_{\Lambda,ij}^{\alpha\alpha'}(\tau,\tau') \tag{3.76}$$

is the Fourier transform of the spin propagator. We can then write

$$\mathbf{G}_{\Lambda}(K) \to \begin{pmatrix} G_{\Lambda}^{+-}(K) & 0 & 0 \\ 0 & G_{\Lambda}^{-+}(K) & 0 \\ 0 & 0 & G_{\Lambda}^{zz}(K) \end{pmatrix}, \tag{3.77}$$

where obviously

$$G_{\Lambda}^{+-}(K) = G_{\Lambda}^{-+}(-K). \tag{3.78}$$

In the local limit of isolated spins, the transversal and the longitudinal part of the spin correlator are given by

$$G_0^{+-}(K) = \frac{b(\beta h)}{h - i\omega}, \quad G_0^{zz}(K) = \delta(\omega) b'(\beta h), \tag{3.79}$$

where $h = h_0 + \bar{h}_0$ and $\delta(\omega) = \beta\delta_{\omega,0}$. While $G_0^{+-}(K)$ has a non-trivial dynamics due to the external magnetic field which breaks the rotational invariance, $G_0^{zz}(K)$ vanishes for finite frequencies so that its inverse diverges. As a result, we cannot use the local limit of isolated spins as an initial condition for the pure SFRG formalism developed above. In the following, we will therefore discuss several other initial conditions that do result in well-defined irreducible vertices. Note that in Sec. 3.3 we will derive an alternative formulation of the SFRG based on a Hubbard-Stratonovich decoupling of the exchange interaction; this will allow us to define a generating functional of irreducible vertices which is still well defined in the local limit of isolated spins.

High-temperature expansion

While we cannot turn off the exchange interaction completely within the pure SFRG formalism, we can instead tune it to a very small but finite value. We can do this in a systematic way by expanding the connected spin correlators of the full Heisenberg Hamiltonian (3.2) in a high-temperature series. One possibility to generate this series is to choose the deformation scheme $V_{ij}^{\Lambda} = \Lambda V_{ij}$ and to solve the infinite hierarchy of flow equations in Eq. (3.11) iteratively.[3] Introducing the notation

$$\Gamma_{\Lambda}^{\alpha\alpha'}(K, K') = \delta(K + K')\Gamma_{\Lambda}^{\alpha\alpha'}(K') \tag{3.80}$$

for the Fourier transform of $\Gamma_{\Lambda,ij}^{\alpha\alpha'}(\tau, \tau'; \bar{\boldsymbol{M}}_{\Lambda})$, setting $h_0 = 0$ so that

$$\Gamma_{\Lambda}^{\alpha\alpha'}(K) = \delta_{\alpha,\alpha'}\Gamma_{\Lambda}(K), \tag{3.81}$$

and assuming a nearest-neighbor interaction on a D-dimensional hypercubic lattice, we find that the irreducible two-point vertex is to leading order given by

$$\Gamma_{\Lambda=1}(K) + V_{\boldsymbol{k}} \approx \frac{\delta_{\omega,0}}{\beta b'}\left[1 + \frac{g^2}{24D}\left(\frac{10|b'''|}{(b')^2} + \frac{\gamma_{\boldsymbol{k}}}{b'}\right)\right] + \frac{1 - \delta_{\omega,0}}{\beta}\frac{\beta^2\omega^2 D}{(1 - \gamma_{\boldsymbol{k}})g^2}, \tag{3.82}$$

where we have again used $g = \beta b' V_0$. Taking the limit $g \to 0$ in Eq. (3.82), we recover the local limit of isolated spins where the finite-frequency part of the irreducible two-point vertex diverges. Analogous to $\Gamma_{\Lambda}(K)$, we can also expand higher-order irreducible vertices in a high-temperature series. For example, the leading behaviour of the irreducible three-point vertex with $S = 1/2$ is given by

$$\begin{aligned}\Gamma_{\Lambda=1}^{\alpha_1\alpha_2\alpha_3}(K_1, K_2, K_3) \approx \delta(K_1 + K_2 + K_3)&\frac{\epsilon_{\alpha_1\alpha_2\alpha_3}\beta^2 D^2}{2g^4(1 - \gamma_{\boldsymbol{k}_1})(1 - \gamma_{\boldsymbol{k}_2})(1 - \gamma_{\boldsymbol{k}_3})} \\ &\times \Big[(\omega_1 - \omega_2)(\omega_2 - \omega_3)(\omega_3 - \omega_1) + \gamma_{\boldsymbol{k}_1}\omega_2\omega_3(\omega_2 - \omega_3) \\ &+ \gamma_{\boldsymbol{k}_2}\omega_1\omega_3(\omega_3 - \omega_1) + \gamma_{\boldsymbol{k}_3}\omega_1\omega_2(\omega_1 - \omega_2)\Big],\end{aligned} \tag{3.83}$$

where $\epsilon_{\alpha_1\alpha_2\alpha_3}$ is the three-dimensional Levi-Civita symbol with $\epsilon_{xyz} = 1$. We can then use Eqs. (3.82) and (3.83) as an initial condition for the pure SFRG as developed in Sec. 3.2.1.

Note that both $\Gamma_{\Lambda=1}(K)$ and $\Gamma_{\Lambda=1}^{\alpha_1\alpha_2\alpha_3}(K_1, K_2, K_3)$ as given above diverge for vanishing momentum and finite frequency, since the definition (3.57) of the structure factor implies $\gamma_{\boldsymbol{k}=0} = 1$. This is not an artifact of our truncation, but rather a property of the quantum Heisenberg model, which results from the fact that the total magnetization in z direction is conserved,

$$\left[\sum_i S_i^z, H\right] = 0. \tag{3.84}$$

[3] In practice, it is more efficient to employ the Hubbard-Stratonovich SFRG formalism and calculate the irreducible vertices introduced in Sec. 3.3 in a high-temperature series, which we can then use to derive the high-temperature series of the connected spin correlators.

As a consequence,

$$\sum_{ij} G^{zz}_{ij}(\tau, \tau') = \langle \mathcal{T}[\sum_i S^z_i(\tau) \sum_j S^z_j(\tau')] \rangle - \langle S^z_i(\tau) \rangle \langle S^z_j(\tau') \rangle \tag{3.85}$$

is time independent, so that

$$G^{zz}(\boldsymbol{k} = 0, i\omega) = \frac{1}{\beta N} \int_0^\beta d\tau \int_0^\beta d\tau' \sum_{ij} e^{i\omega(\tau - \tau')} G^{zz}_{ij}(\tau, \tau') \tag{3.86}$$

vanishes for $\omega \neq 0$. We thus conclude that, strictly speaking, the Taylor expansion of the average effective action $\Gamma[\boldsymbol{M}]$ around its minimum at $\boldsymbol{M}_i(\tau) = \bar{\boldsymbol{M}}_\Lambda$ does not exist in the quantum Heisenberg model. However, since the point $\boldsymbol{k} = 0$ has Lebesgue measure zero in the thermodynamic limit, this should not lead to any problems in practical calculations.

Spin dimers

Another possibility to obtain a non-trivial dynamics for the longitudinal part of the spin correlator consists in coupling each spin $\boldsymbol{S}_i$ in the Heisenberg model to an auxiliary spin $\boldsymbol{T}_i$,

$$H = -\frac{1}{2} \sum_{ij} V_{ij} \boldsymbol{S}_i \cdot \boldsymbol{S}_j + J \sum_i \boldsymbol{S}_i \cdot \boldsymbol{T}_i - h_0 \sum_i S^z_i, \tag{3.87}$$

while coupling the source field $\boldsymbol{h}$ only to the $\boldsymbol{S}_i$ spins,

$$\mathcal{G}_\Lambda[\boldsymbol{h}] = \ln \mathrm{Tr} \left[e^{-\beta H_0} \mathcal{T} e^{\int_0^\beta d\tau \left[\sum_i \boldsymbol{h}_i(\tau) \cdot \boldsymbol{S}_i(\tau) - \mathcal{V}_\Lambda(\tau) \right]} \right], \tag{3.88}$$

where the free part of the Hamiltonian is now given by

$$H_0 = J \sum_i \boldsymbol{S}_i \cdot \boldsymbol{T}_i - h_0 \sum_i S^z_i. \tag{3.89}$$

We can then use a deformation scheme V^Λ_{ij} where the exchange interaction between the $\boldsymbol{S}_i$ is initially turned off completely,

$$\mathcal{V}_{\Lambda=0}(\tau) = -\frac{1}{2} \sum_{ij} V^{\Lambda=0}_{ij} \boldsymbol{S}_i(\tau) \cdot \boldsymbol{S}_j(\tau) = 0, \tag{3.90}$$

so that the system decouples into N isolated spin dimers which can be treated analytically. In the simplest case we set $h_0 = 0$ and $S = T = 1/2$, so that the spin propagator reads

$$G_0(K) = \frac{\delta(\omega) J^2 + (e^{\beta J} - 1) J}{2(e^{\beta J} + 3)(J^2 + \omega^2)}, \tag{3.91}$$

where we have used the notation

$$G_\Lambda^{\alpha\alpha'}(K) = \delta_{\alpha,\alpha'} G_\Lambda(K) \tag{3.92}$$

for rotationally invariant systems. It is easy to invert this result, which yields the irreducible two-point vertex

$$\Gamma_0(K) + V_{\boldsymbol{k}} = \frac{2(e^{\beta J}+3)(J^2+\omega^2)}{\delta(\omega)J^2 + (e^{\beta J}-1)J}. \tag{3.93}$$

Note that it is important that we have not coupled the source field $\boldsymbol{h}$ to the $\boldsymbol{T}_i$ spins in Eq. (3.88). The reason for this is that the determinant of the full spin-propagator matrix including both $\boldsymbol{S}_i$ and $\boldsymbol{T}_i$ vanishes due to the conservation of the total spin length,

$$\left[(\boldsymbol{S}_i + \boldsymbol{T}_i)^2, H_0\right] = 0, \tag{3.94}$$

so that the corresponding irreducible vertices, containing information about the correlations of both the $\boldsymbol{S}_i$ and the $\boldsymbol{T}_i$ spins, would not be well defined. The existence of the irreducible two-point vertex (3.93) thus depends on the fact that $\boldsymbol{S_i}$ on its own does not commute with H_0.

It is straightforward to compute also higher-order irreducible vertices which appear in the flow equation of $\Gamma_\Lambda(K)$. For example, the connected three-point spin correlator is given by

$$\begin{aligned} G_0^{\alpha_1\alpha_2\alpha_3}(K_1,K_2,K_3) &= \epsilon_{\alpha_1\alpha_2\alpha_3}\delta(K_1+K_2+K_3)(1-\delta_{\omega_1,0}\delta_{\omega_2,0}\delta_{\omega_3,0}) \\ &\times \Bigg[-\frac{(e^{\beta J}-1)J(\omega_1-\omega_2)(\omega_2-\omega_3)(\omega_3-\omega_1)}{4(e^{\beta J}+3)(J^2+\omega_1^2)(J^2+\omega_2^2)(J^2+\omega_3^2)} \\ &\quad + \sum_{l=1}^{3}\delta(\omega_{l+1})\frac{J^2+2\omega_l^2}{4(e^{\beta J}+3)\omega_l(J^2+\omega_l^2)}\Bigg], \end{aligned} \tag{3.95}$$

where the delta functions in front take priority and we identify $\omega_4 \equiv \omega_1$. Due to $h_0 = 0$, we can then express the irreducible three-point vertex via the exact relation

$$\Gamma_0^{\alpha_1\alpha_2\alpha_3}(K_1,K_2,K_3) = \frac{G_0^{\alpha_1\alpha_2\alpha_3}(-K_1,-K_2,-K_3)}{G_0(-K_1)G_0(-K_2)G_0(-K_3)} \tag{3.96}$$

as

$$\begin{aligned} \Gamma_0^{\alpha_1\alpha_2\alpha_3}(K_1,K_2,K_3) &= \epsilon_{\alpha_1\alpha_2\alpha_3}\delta(K_1+K_2+K_3)(1-\delta_{\omega_1,0}\delta_{\omega_2,0}\delta_{\omega_3,0}) \\ &\times \Bigg[\frac{2(e^{\beta J}+3)^2(\omega_1-\omega_2)(\omega_2-\omega_3)(\omega_3-\omega_1)}{(e^{\beta J}-1)^2J^2} \\ &\quad + \sum_{l=1}^{3}\delta(\omega_{l-1})\frac{2(e^{\beta J}+3)^2J(J^2+3\omega_l^2)}{(e^{\beta J}-1)^2(e^{\beta J}-1+\beta J)\omega_l}\Bigg]. \end{aligned} \tag{3.97}$$

Note that for $\beta J \ll 1$, Eq. (3.97) resembles the high-temperature result (3.83) with $D = 1$ if we neglect its momentum dependence and identify $V_0 = \sqrt{2}J$. In this limit of a weak intra-dimer coupling, the spin-dimer approach thus results in simpler initial conditions for the irreducible vertices than the high-temperature expansion discussed above. However, the added complexity in the high-temperature expansion might be beneficial in some situations, because the momentum dependence of the irreducible vertices is generated by the physical exchange coupling. Furthermore, it is conceptually trivial to generalize the high-temperature expansion to arbitrary spin S by using the generalized Wick theorem [1, 3]; in contrast, calculating the irreducible vertices for a spin dimer while keeping one of its spins general is conceptually more demanding.

Coupling the spins to a bath

The spin-dimer approach relies on the fact that the coupling of an isolated spin $\boldsymbol{S}_i$ to an auxiliary spin $\boldsymbol{T}_i$ results in a non-trivial dynamics of the spin $\boldsymbol{S}_i$, which leads to well-defined irreducible vertices. More generally, we can couple the isolated spins to any system which results in an invertible spin-propagator matrix of the $\boldsymbol{S}_i$. A well-known toy model for such a configuration is the spin-boson model, where a single spin is coupled to a bosonic bath [113, 114]. Another famous example is the Kondo model, where a single magnetic impurity is coupled to a fermionic bath of conduction electrons [31, 115]. It is then natural to insert a momentum-dependent regulator in the fermionic propagator and to generalize the SFRG to include fermionic degrees of freedom. A recent application of this approach is given by our work in Ref. [98], where we derive a generalized Wetterich equation for the Kondo model within the SFRG, which we then solve in a simple approximation to recover the one-loop “poor man’s scaling” equations for an arbitrary impurity spin [31].

XY model

As discussed in the beginning of Sec. 3.2.5, we cannot invert the spin-propagator matrix of an isolated spin in an external magnetic field. From Eq. (3.79) we see that the transversal part has a non-trivial dynamics due to the external field, while the longitudinal part of the spin propagator is time independent so that $\det \mathbf{G}_0 = 0$. We can avoid this problem by coupling the source field $\boldsymbol{h}$ only to the transversal part of the spins,

$$\mathcal{G}_\Lambda[h^x, h^y] = \ln \mathrm{Tr}\left[e^{-\beta H_0} \mathcal{T} e^{\int_0^\beta d\tau \left[\sum_i h_i^x(\tau) S_i^x(\tau) + \sum_i h_i^y(\tau) S_i^y(\tau) - \mathcal{V}_\Lambda(\tau)\right]} \right], \tag{3.98}$$

where the free part of the Hamiltonian is still given by

$$H_0 = -h_0 \sum_i S_i^z. \tag{3.99}$$

However, since our SFRG formalism requires that the right-hand side of the flow equation of $\mathcal{G}_\Lambda[h^x, h^y]$ can be expressed in terms of derivatives of this generating functional, $\mathcal{V}_\Lambda(\tau)$ now has to be independent of the longitudinal part S_i^z of the spins. This condition is naturally fulfilled in the quantum XY model

$$H = -\frac{1}{2} \sum_{ij} V_{ij} \left[S_i^x S_j^x + S_i^y S_j^y \right] - h_0 \sum_i S_i^z, \tag{3.100}$$

where

$$\mathcal{V}_\Lambda(\tau) = -\frac{1}{2} \sum_{ij} V_{ij}^\Lambda \left[S_i^x(\tau) S_j^x(\tau) + S_i^y(\tau) S_j^y(\tau) \right]. \tag{3.101}$$

Since the spin-propagator matrix now has the form

$$\mathbf{G}_\Lambda(K) \to \begin{pmatrix} G_\Lambda^{+-}(K) & 0 \\ 0 & G_\Lambda^{-+}(K) \end{pmatrix}, \tag{3.102}$$

it is still invertible if we turn off the exchange interaction completely as long as $h_0 \neq 0$, which can be seen from the initial condition

$$G_0^{+-}(K) = G_0^{-+}(-K) = \frac{b(\beta h)}{h - i\omega}. \tag{3.103}$$

Only at the end of the calculation one may then take the limit $h_0 \to 0$. This approach has been employed by Rançon to describe the spin-1/2 quantum XY model in two and three dimensions [106]; while that work relies on the mapping of spin-1/2 operators to hardcore bosons, it should be straightforward to generalize it to arbitrary spins by using our SFRG formalism.

3.2.6 Overview and future applications

Let us at this point summarize the main points of the present section on the pure SFRG. In Sec. 3.2.1 we have shown that the Legendre transform of the generating functional of the connected spin correlators obeys an exact flow equation that is formally identical to the Wetterich equation for bosonic degrees of freedom. Our derivation of this flow equation is formulated directly in terms of spin operators, without any mapping to bosonic or fermionic fields. The non-trivial $\mathfrak{su}(2)$ algebra is fully taken into account via the initial conditions of the RG flow.

As a demonstration of our method, we have then applied the pure SFRG formalism to the spin-S Ising model on a D-dimensional hypercubic lattice, which allowed us to derive quantitatively accurate estimates for the critical temperature. Due to the more complicated initial conditions for quantum spin systems as discussed in Sec. 3.2.5, a generalization of this procedure to quantum spin systems is cumbersome within the pure SFRG; in the next section, we will present an alternative formulation of the SFRG to deal more efficiently with this problem.

A first application of the pure SFRG to a non-trivial quantum system is given by our recent work on the Kondo model in Ref. [98], where we derive a generalized Wetterich equation that describes the conduction electrons as well as the impurity spin. Using a standard Litim cutoff in momentum space, we show how to derive the one-loop scaling equations for the anisotropic Kondo model within a simple truncation of the infinite hierarchy of flow equations. In contrast to the unconventional T-matrix renormalization in Anderson's "poor man's scaling" approach, we use the language of the modern FRG which allows for a significantly simpler derivation. Moreover, it is straightforward to generalize our SFRG approach to keep track of the electronic self-energy, which contains information about the spatial distribution of the charge density in the vicinity of the impurity spin. Within a cutoff scheme where the electronic bandwidth initially vanishes, the SFRG can also be used to study the strong coupling regime.

Another interesting problem is the application of the SFRG to frustrated spin systems. For the specific example of the Γ-Heisenberg-Kitaev model, a possible line of attack within the pure SFRG is to start with decoupled dimers, since in this case the initial conditions of the irreducible vertices are well defined as shown recently by Arnold [116]. The interdimer interaction can then be turned on continuously during the flow. While this approach seems promising, we have not worked out a concrete implementation yet.

3.3 Hubbard-Stratonovich SFRG

3.3.1 General formalism

In this section we will develop an alternative SFRG formalism, which conceptually relies on a Hubbard-Stratonovich transformation that decouples the exchange interaction between the spins. Working with the generating functional of the connected correlation functions of the Hubbard-Stratonovich field, we will find that its Legendre transform is well defined even in the local limit of isolated spins. Moreover, the corresponding irreducible vertices have a direct relation to the spin-diagrammatic approach of Vaks, Larkin, and Pikin (VLP) [1–3]. This allows us to recover their results within our SFRG formalism with its comparably simple diagrammatics, while at the same time making it straightforward to improve on their work.

Amputated connected spin correlators

We start by defining the generating functional of the amputated connected spin correlators $\mathcal{F}_\Lambda[\boldsymbol{M}]$ as [33]

$$e^{\mathcal{F}_\Lambda[\boldsymbol{M}]} = \mathrm{Tr}\left[e^{-\beta\mathcal{H}_0}\mathcal{T}e^{\frac{1}{2}\int_0^\beta d\tau \sum_{ij} V_{ij}^\Lambda[\boldsymbol{M}_i(\tau)+\boldsymbol{S}_i(\tau)]\cdot[\boldsymbol{M}_j(\tau)+\boldsymbol{S}_j(\tau)]}\right], \tag{3.104}$$

where

$$H_0 = -h_0 \sum_i S_i^z. \tag{3.105}$$

From Eq. (3.104) we immediately see that $\mathcal{F}_\Lambda[\boldsymbol{M}]$ is related to the generating functional of the connected spin correlators by

$$\mathcal{F}_\Lambda[\boldsymbol{M}] = \frac{1}{2}\int_0^\beta d\tau \sum_{ij} V_{ij}^\Lambda \boldsymbol{M}_i(\tau)\cdot\boldsymbol{M}_j(\tau) + \mathcal{G}_\Lambda\Big[\sum_j V_{ij}^\Lambda \boldsymbol{M}_j(\tau)\Big], \tag{3.106}$$

which allows us to express the amputated connected spin correlators

$$F_{\Lambda,i_1\ldots i_n}^{\alpha_1\ldots\alpha_n}(\tau_1,\ldots,\tau_n) = \left.\frac{\delta^n \mathcal{F}_\Lambda[\boldsymbol{M}]}{\delta M_{i_1}^{\alpha_1}(\tau_1)\ldots\delta M_{i_n}^{\alpha_n}(\tau_n)}\right|_{\boldsymbol{M}=\bar{\boldsymbol{M}}_\Lambda} \tag{3.107}$$

in terms of the more fundamental connected spin correlators. Here we have expanded $\mathcal{F}_\Lambda[\boldsymbol{M}]$ around the scale-dependent uniform field configuration [cf. Eqs. (3.118) and (3.122)]

$$\bar{\boldsymbol{M}}_\Lambda = \left[\frac{1}{V_\Lambda(\boldsymbol{k}=0)} - \frac{1}{V_{\Lambda=1}(\boldsymbol{k}=0)}\right]\bar{\boldsymbol{h}}_\Lambda, \tag{3.108}$$

where $\bar{\boldsymbol{h}}_\Lambda$ is the flowing minimum of the Legendre transform of $\mathcal{F}_\Lambda[\boldsymbol{M}]$ which we will define in Eq. (3.115).[4] To derive the flow equation of $\mathcal{F}_\Lambda[\boldsymbol{M}]$ and

[4]Note that the definition of $\bar{\boldsymbol{M}}_\Lambda$ and $\bar{\boldsymbol{h}}_\Lambda$ in Sec. 3.2.1 is not compatible with the definition in the present section; e.g., Eq. (3.108) implies that $\bar{\boldsymbol{M}}_\Lambda$ vanishes for $\Lambda = 1$, while in the pure SFRG it flows to the physical magnetization. However, since one either works within the pure or the Hubbard-Stratonovich formalism, this should not lead to any confusion.

to get a better intuition for the amputated connected spin correlators, it is helpful to decouple the exchange interaction V_{ij}^{Λ} via a Hubbard-Stratonovich transformation,

$$e^{\mathcal{F}_{\Lambda}[\boldsymbol{M}]} = \frac{\int \mathcal{D}[\boldsymbol{\phi}]\, e^{-\frac{1}{2}\sum_{\tilde{\alpha}\tilde{\alpha}'}\left[\mathbf{V}_{\Lambda}^{-1}\right]_{\tilde{\alpha}\tilde{\alpha}'}\phi_{\tilde{\alpha}}\phi_{\tilde{\alpha}'}+\sum_{\tilde{\alpha}} M_{\tilde{\alpha}}\phi_{\tilde{\alpha}}}\, \mathrm{Tr}\left[e^{-\beta\mathcal{H}_0}\mathcal{T}e^{\sum_{\tilde{\alpha}}\phi_{\tilde{\alpha}}S_{\tilde{\alpha}}}\right]}{\int \mathcal{D}[\boldsymbol{\phi}]\, e^{-\frac{1}{2}\sum_{\tilde{\alpha}\tilde{\alpha}'}\left[\mathbf{V}_{\Lambda}^{-1}\right]_{\tilde{\alpha}\tilde{\alpha}'}\phi_{\tilde{\alpha}}\phi_{\tilde{\alpha}'}}}. \tag{3.109}$$

Here $\mathbf{V}_{\Lambda}^{-1}$ is the matrix inverse of the exchange-interaction matrix

$$[\mathbf{V}_{\Lambda}]_{\tilde{\alpha}\tilde{\alpha}'} = [\mathbf{V}_{\Lambda}]_{\alpha i\tau,\alpha' j\tau'} = \delta_{\alpha,\alpha'}\delta(\tau-\tau')V_{ij}^{\Lambda} \tag{3.110}$$

and we have introduced the superindex $\tilde{\alpha} = \{\alpha, i, \tau\}$ with

$$\sum_{\tilde{\alpha}} = \int_0^{\beta} d\tau \sum_{i,\alpha}. \tag{3.111}$$

We can thus interpret the amputated connected spin correlators as the connected correlators of the Hubbard-Stratonovich field $\phi_{\tilde{\alpha}} = \phi_i^{\alpha}(\tau)$, which mediates the exchange interaction between the spins. As a consequence, the amputated connected two-point spin correlator plays the role of an effective interaction,

$$F_{\Lambda}^{zz}(K) = V_{\Lambda}(\boldsymbol{k}) + V_{\Lambda}(\boldsymbol{k})G_{\Lambda}^{zz}(K)V_{\Lambda}(\boldsymbol{k}), \tag{3.112a}$$

$$F_{\Lambda}^{+-}(K) = V_{\Lambda}(\boldsymbol{k}) + V_{\Lambda}(\boldsymbol{k})G_{\Lambda}^{+-}(K)V_{\Lambda}(\boldsymbol{k}), \tag{3.112b}$$

where again $S_i^{\pm} = \frac{1}{\sqrt{2}}(S_i^x \pm iS_i^y)$ and we have used the notation

$$F_{\Lambda}^{\alpha\alpha'}(K,K') = \delta(K+K')F_{\Lambda}^{\alpha\alpha'}(K') \tag{3.113}$$

for the Fourier transform of $F_{\Lambda,ij}^{\alpha\alpha'}(\tau,\tau')$. In the limit $\Lambda \to 1$, we can identify the relations (3.112a) and (3.112b) with Eqs. (16a) and (16b) of Ref. [1], so that $F_{\Lambda=1}^{zz}(K)$ and $F_{\Lambda=1}^{+-}(K)$ are indeed identical to the effective interaction in the spin-diagrammatic approach of VLP. To compute the flow of the amputated connected spin correlators, we need the flow equation of $\mathcal{F}_{\Lambda}[\boldsymbol{M}]$. We therefore differentiate Eq. (3.109) with respect to Λ to obtain the Polchinkski equation [24]

$$\begin{aligned}\partial_{\Lambda}\mathcal{F}_{\Lambda}[\boldsymbol{M}] = &-\frac{1}{2}\sum_{\tilde{\alpha}\tilde{\alpha}'}\left[\partial_{\Lambda}\mathbf{V}_{\Lambda}^{-1}\right]_{\tilde{\alpha}\tilde{\alpha}'}\left[\frac{\delta^2\mathcal{F}_{\Lambda}[\boldsymbol{M}]}{\delta M_{\tilde{\alpha}}\delta M_{\tilde{\alpha}'}} + \frac{\delta\mathcal{F}_{\Lambda}[\boldsymbol{M}]}{\delta M_{\tilde{\alpha}}}\frac{\delta\mathcal{F}_{\Lambda}[\boldsymbol{M}]}{\delta M_{\tilde{\alpha}'}}\right]\\ &+\frac{1}{2}\mathrm{Tr}\left[\mathbf{V}_{\Lambda}\partial_{\Lambda}\mathbf{V}_{\Lambda}^{-1}\right].\end{aligned} \tag{3.114}$$

Irreducible vertices

Analogous to the construction of the pure SFRG in Sec. 3.2.1, we now introduce the subtracted Legendre transform $\Phi_\Lambda[\boldsymbol{h}]$ of the generating functional of the amputated connected spin correlators,

$$\Phi_\Lambda[\boldsymbol{h}] = \sum_{\tilde{\alpha}} M_{\tilde{\alpha}} h_{\tilde{\alpha}} - \mathcal{F}_\Lambda[\boldsymbol{M}[\boldsymbol{h}]] - \frac{1}{2} \sum_{\tilde{\alpha}\tilde{\alpha}'} \left[\tilde{\mathbf{R}}_\Lambda\right]_{\tilde{\alpha}\tilde{\alpha}'} h_{\tilde{\alpha}} h_{\tilde{\alpha}'}, \tag{3.115}$$

where the local magnetization $M_{\tilde{\alpha}} = M_i^\alpha(\tau)$ is to be understood as a functional of the source fields $h_{\tilde{\alpha}} = h_i^\alpha(\tau)$ by inverting the relation

$$h_{\tilde{\alpha}} = \frac{\delta \mathcal{F}_\Lambda[\boldsymbol{M}]}{\delta M_{\tilde{\alpha}}}, \tag{3.116}$$

and the regulator matrix $\tilde{\mathbf{R}}_\Lambda$ is defined as

$$\tilde{\mathbf{R}}_\Lambda = \mathbf{V}_\Lambda^{-1} - \mathbf{V}^{-1}, \tag{3.117}$$

where $\mathbf{V} = \mathbf{V}_{\Lambda=1}$ is the bare exchange-interaction matrix. On a technical level, $\Phi_\Lambda[\boldsymbol{h}]$ is the generating functional of the vertices which are irreducible with respect to the cutting of a single (effective) interaction line. This is to be contrasted with $\Gamma_\Lambda[\boldsymbol{M}]$ as defined in Eq. (3.12), which generates the vertices that are irreducible with respect to the cutting of a single propagator line. To derive the flow equation of $\Phi_\Lambda[\boldsymbol{h}]$, let us consider its first few derivatives. In full analogy to Eqs. (3.15) and (3.16), the first derivative reads

$$\frac{\delta \Phi_\Lambda[\boldsymbol{h}]}{\delta h_{\tilde{\alpha}}} = M_{\tilde{\alpha}} - \sum_{\tilde{\alpha}'} \left[\tilde{\mathbf{R}}_\Lambda\right]_{\tilde{\alpha}\tilde{\alpha}'} h_{\tilde{\alpha}'}, \tag{3.118}$$

whereas the Hessian matrix $\boldsymbol{\Phi}''_\Lambda[\boldsymbol{h}]$ is given by

$$[\boldsymbol{\Phi}''_\Lambda[\boldsymbol{h}]]_{\tilde{\alpha}\tilde{\alpha}'} = \frac{\delta^2 \Phi_\Lambda[\boldsymbol{h}]}{\delta h_{\tilde{\alpha}} \delta h_{\tilde{\alpha}'}} = \left[\mathbf{F}_\Lambda^{-1}[\boldsymbol{M}] - \tilde{\mathbf{R}}_\Lambda\right]_{\tilde{\alpha}\tilde{\alpha}'}, \tag{3.119}$$

where $\mathbf{F}_\Lambda^{-1}[\boldsymbol{M}]$ is the matrix inverse of

$$[\mathbf{F}_\Lambda[\boldsymbol{M}]]_{\tilde{\alpha}\tilde{\alpha}'} = \frac{\delta^2 \mathcal{F}_\Lambda[\boldsymbol{M}]}{\delta M_{\tilde{\alpha}} \delta M_{\tilde{\alpha}'}}. \tag{3.120}$$

Differentiating Eq. (3.114) with respect to Λ, we then find that $\Phi_\Lambda[\boldsymbol{h}]$ obeys the Wetterich equation [34]

$$\begin{aligned} \partial_\Lambda \Phi_\Lambda[\boldsymbol{h}] &= \frac{1}{2} \mathrm{Tr} \left[\left(\boldsymbol{\Phi}''_\Lambda[\boldsymbol{h}] + \tilde{\mathbf{R}}_\Lambda \right)^{-1} \partial_\Lambda \tilde{\mathbf{R}}_\Lambda \right] - \frac{1}{2} \mathrm{Tr} \left[\mathbf{V}_\Lambda \partial_\Lambda \mathbf{V}_\Lambda^{-1} \right] \\ &= \frac{1}{2} \mathrm{Tr} \left\{ \left[\left(\boldsymbol{\Phi}''_\Lambda[\boldsymbol{h}] + \tilde{\mathbf{R}}_\Lambda \right)^{-1} - \mathbf{V}_\Lambda \right] \partial_\Lambda \tilde{\mathbf{R}}_\Lambda \right\}, \end{aligned} \tag{3.121}$$

where in the second line we have used $\partial_\Lambda \mathbf{V}_\Lambda^{-1} = \partial_\Lambda \tilde{\mathbf{R}}_\Lambda$. Note that $\Phi_\Lambda[\boldsymbol{h}]$ has a minimum at the scale-dependent uniform field configuration $h_{\tilde{\alpha}} = \bar{h}_{\Lambda,\tilde{\alpha}} = \bar{h}_\Lambda^\alpha$ which is defined via

$$\left.\frac{\delta \Phi_\Lambda[\boldsymbol{h}]}{\delta h_{\tilde{\alpha}}}\right|_{\boldsymbol{h}=\bar{\boldsymbol{h}}_\Lambda} = 0, \tag{3.122}$$

where $\bar{\boldsymbol{h}}_\Lambda$ will be non-zero for a finite external magnetic field h_0 or in the presence of a finite spontaneous magnetization. This can be seen from

$$\bar{\boldsymbol{h}}_\Lambda = V_0 \left\langle \boldsymbol{S}_i(\tau) \right\rangle_{\Lambda, \left[1-\frac{V_\Lambda(\boldsymbol{k}=0)}{V_{\Lambda=1}(\boldsymbol{k}=0)}\right]\bar{\boldsymbol{h}}_\Lambda}, \tag{3.123}$$

where $V_\Lambda(\boldsymbol{k})$ is the Fourier transform of the deformed exchange interaction V_{ij}^Λ and

$$\left\langle S_{\tilde{\alpha}} \right\rangle_{\Lambda,\boldsymbol{h}} = \frac{\delta \mathcal{G}_\Lambda[\boldsymbol{h}]}{\delta h_{\tilde{\alpha}}}. \tag{3.124}$$

In the limit $\Lambda = 1$ this simplifies to

$$\bar{\boldsymbol{h}}_{\Lambda=1} = V_0 \left\langle \boldsymbol{S}_i(\tau) \right\rangle, \tag{3.125}$$

which relates $\bar{\boldsymbol{h}}_{\Lambda=1}$ to the physical magnetization of the system. Note that Eq. (3.123) follows from Eqs. (3.118) and (3.122) together with the general relation

$$\sum_{\tilde{\alpha}'} \left[\mathbf{V}_\Lambda^{-1}\right]_{\tilde{\alpha}\tilde{\alpha}'} h_{\tilde{\alpha}'} = M_{\tilde{\alpha}} + \left\langle S_{\tilde{\alpha}} \right\rangle_{\Lambda, \sum_{\tilde{\alpha}''}[\mathbf{V}_\Lambda]_{\tilde{\alpha}'\tilde{\alpha}''} M_{\tilde{\alpha}''}}, \tag{3.126}$$

which in turn follows directly from Eqs. (3.106) and (3.116). Physically, we can interpret $\bar{\boldsymbol{h}}_\Lambda$ as the scale-dependent exchange correction to the external magnetic field h_0. We should therefore shift the fluctuating exchange field $\boldsymbol{h}_i(\tau) = \bar{\boldsymbol{h}}_\Lambda + \boldsymbol{\eta}_i(\tau)$ and consider the generating functional

$$\tilde{\Phi}_\Lambda[\boldsymbol{\eta}] = \Phi_\Lambda[\bar{\boldsymbol{h}}_\Lambda + \boldsymbol{\eta}], \tag{3.127}$$

which obeys the flow equation

$$\begin{aligned}\partial_\Lambda \tilde{\Phi}_\Lambda[\boldsymbol{\eta}] &= \partial_\Lambda \Phi_\Lambda[\boldsymbol{h}]\big|_{\boldsymbol{h}\to\bar{\boldsymbol{h}}_\Lambda+\boldsymbol{\eta}} + \sum_{\tilde{\alpha}} \frac{\delta \tilde{\Phi}_\Lambda[\boldsymbol{\eta}]}{\delta \eta_{\tilde{\alpha}}} \partial_\Lambda \bar{h}_{\Lambda,\tilde{\alpha}} \\ &= \frac{1}{2}\mathrm{Tr}\left\{\left[\left(\tilde{\mathbf{\Phi}}''_\Lambda[\boldsymbol{\eta}] + \tilde{\mathbf{R}}_\Lambda\right)^{-1} - \mathbf{V}_\Lambda\right]\partial_\Lambda \tilde{\mathbf{R}}_\Lambda\right\} + \sum_{\tilde{\alpha}} \frac{\delta \tilde{\Phi}_\Lambda[\boldsymbol{\eta}]}{\delta \eta_{\tilde{\alpha}}} \partial_\Lambda \bar{h}_{\Lambda,\tilde{\alpha}}.\end{aligned} \tag{3.128}$$

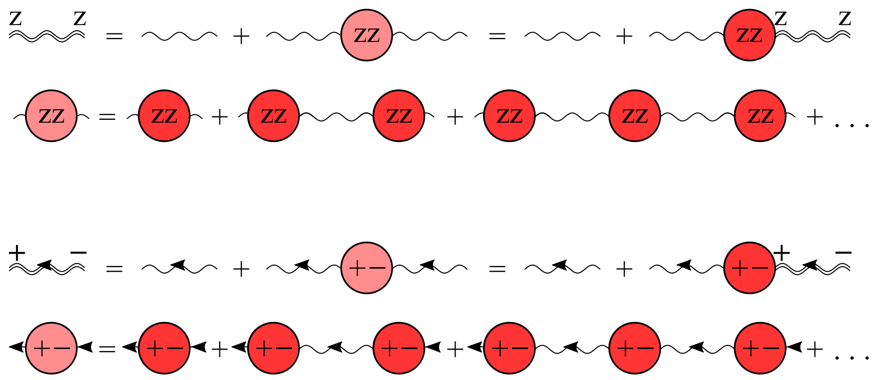

Figure 3.3: Graphical representation of the relations between the longitudinal two-point functions $F^{zz}_\Lambda(K)$, $\Pi^{zz}_\Lambda(K)$, and $G^{zz}_\Lambda(K)$ as given in Eqs. (3.112a), (3.132a), and (3.134a) (upper half) and the corresponding relations between the transverse two-point functions $F^{+-}_\Lambda(K)$, $\Pi^{+-}_\Lambda(K)$, and $G^{+-}_\Lambda(K)$ as given in Eqs. (3.112b), (3.132b), and (3.134b) (lower half). The connected two-point spin correlators $G^{\alpha\alpha'}_\Lambda(K)$ are denoted by light-colored circles, while the polarization functions $\Pi^{\alpha\alpha'}_\Lambda(K)$ are denoted by dark-colored circles. Double wavy lines represent the amputated connected two-point spin correlators $F^{\alpha\alpha'}_\Lambda(K)$, while single wavy lines represent the deformed exchange interaction $V_\Lambda(\boldsymbol{k})$. (Figure reproduced from Ref. [99])

Polarization functions

Below Eqs. (3.112a) and (3.112b) we have already pointed out that for $\Lambda \to 1$, we can identify the amputated connected two-point spin correlators $F^{zz}_\Lambda(K)$ and $F^{+-}_\Lambda(K)$ with the effective interaction of VLP. Introducing the notation

$$\tilde{\Phi}^{\alpha\alpha'}_\Lambda(K, K') = \delta(K + K')\tilde{\Phi}^{\alpha\alpha'}_\Lambda(K) \tag{3.129}$$

for the Fourier transform of the irreducible two-point vertex

$$\left[\tilde{\boldsymbol{\Phi}}''_\Lambda\right]_{\tilde{\alpha}\tilde{\alpha}'} = \tilde{\Phi}^{\alpha\alpha'}_{\Lambda,ij}(\tau, \tau') = \left.\frac{\delta^2\tilde{\Phi}_\Lambda[\boldsymbol{\eta}]}{\delta\eta^\alpha_i(\tau)\delta\eta^{\alpha'}_j(\tau')}\right|_{\boldsymbol{\eta}=0}, \tag{3.130}$$

we will now show that in the same limit $\Lambda \to 1$, we can identify the polarization functions

$$\Pi^{zz}_\Lambda(K) = V^{-1}_{\boldsymbol{k}} - \tilde{\Phi}^{zz}_\Lambda(K), \tag{3.131a}$$

$$\Pi^{+-}_\Lambda(K) = V^{-1}_{\boldsymbol{k}} - \tilde{\Phi}^{+-}_\Lambda(K), \tag{3.131b}$$

with the irreducible vertices $\Sigma^{zz}(K)$ and $\Sigma^{+-}(K)$ of VLP. From Eq. (3.119) we see that the definitions (3.131a) and (3.131b) imply

$$F_\Lambda^{zz}(K) = \frac{1}{\tilde{\Phi}_\Lambda^{zz}(K) + \tilde{R}_\Lambda(\boldsymbol{k})} = \frac{V_\Lambda(\boldsymbol{k})}{1 - V_\Lambda(\boldsymbol{k})\Pi_\Lambda^{zz}(K)}, \tag{3.132a}$$

$$F_\Lambda^{+-}(K) = \frac{1}{\tilde{\Phi}_\Lambda^{+-}(K) + \tilde{R}_\Lambda(\boldsymbol{k})} = \frac{V_\Lambda(\boldsymbol{k})}{1 - V_\Lambda(\boldsymbol{k})\Pi_\Lambda^{+-}(K)}, \tag{3.132b}$$

where $\tilde{R}_\Lambda(\boldsymbol{k})$ is the non-trivial part of the Fourier transform of $\left[\tilde{\mathbf{R}}_\Lambda\right]_{\alpha i\tau,\alpha' j\tau'}$,

$$\tilde{R}_\Lambda^{\alpha\alpha'}(K, K') = \delta_{\alpha,\alpha'}\delta(K + K')\tilde{R}_\Lambda(\boldsymbol{k}). \tag{3.133}$$

As a result, we can express the spin propagators in terms of the polarization functions,

$$G_\Lambda^{zz}(K) = \frac{\Pi_\Lambda^{zz}(K)}{1 - V_\Lambda(\boldsymbol{k})\Pi_\Lambda^{zz}(K)}, \tag{3.134a}$$

$$G_\Lambda^{+-}(K) = \frac{\Pi_\Lambda^{+-}(K)}{1 - V_\Lambda(\boldsymbol{k})\Pi_\Lambda^{+-}(K)}. \tag{3.134b}$$

These expressions are identical to Eq. (13) of Ref. [1] in the limit $\Lambda = 1$, which shows that $\Pi_{\Lambda=1}^{zz}(K)$ and $\Pi_{\Lambda=1}^{+-}(K)$ are indeed the irreducible vertices of VLP. See Fig. 3.3 for a graphical representation of the relations between $F_\Lambda^{\alpha\alpha'}(K)$, $\Pi_\Lambda^{\alpha\alpha'}(K)$, and $G_\Lambda^{\alpha\alpha'}(K)$. Finally, we note that we can express the polarization functions $\Pi_\Lambda^{zz}(K)$ and $\Pi_\Lambda^{+-}(K)$ in terms of the irreducible two-point vertices $\Gamma_\Lambda^{zz}(K)$ and $\Gamma_\Lambda^{+-}(K)$ from Sec. 3.2 via the exact relations

$$\Pi_\Lambda^{zz}(K) = \frac{1}{\Gamma_\Lambda^{zz}(K) + V_{\boldsymbol{k}}}, \tag{3.135a}$$

$$\Pi_\Lambda^{+-}(K) = \frac{1}{\Gamma_\Lambda^{+-}(K) + V_{\boldsymbol{k}}}, \tag{3.135b}$$

which follow directly from Eqs. (3.16), (3.134a) and (3.134b). In Sec. 3.3.4, these relations will allow us to generalize our $1/D$ expansion for the Ising model to the quantum Heisenberg model, where we first expand $\Pi_\Lambda^{zz}(K)$ in powers of $1/D$ and only afterwards use Eq. (3.135a) to convert our result into an expansion of $\Gamma_\Lambda^{zz}(K)$.

3.3.2 Initial condition of isolated spins

As we have discussed in Sec. 3.2.5, the irreducible vertices generated by the average effective action $\Gamma_\Lambda[\boldsymbol{M}]$ do not exist in the limit of a vanishing exchange interaction, which excludes the simple initial condition of isolated spins. However, we will show in the following that this is not the case for the irreducible vertices that are generated by $\tilde{\Phi}_\Lambda[\boldsymbol{\eta}]$. Assuming a deformation scheme where $V_{ij}^{\Lambda=0} = 0$, it follows from Eqs. (3.106), (3.115), and (3.126) that the initial functional $\Phi_0[\boldsymbol{h}]$ is for a uniform source field $\bar{\boldsymbol{h}} = \bar{h}\boldsymbol{e}_z$ given by

$$\Phi_0[\bar{\boldsymbol{h}}] = N\left\{\frac{\beta\bar{h}^2}{2V_0} - B\left[\beta(h_0 + \bar{h})\right]\right\}, \tag{3.136}$$

where $B(y)$ is the primitive integral of the Brillouin function $b(y)$ as defined in Eq. (3.35). It is thus obvious that the minimum $\bar{h}_\Lambda$ of the functional $\Phi_\Lambda[\boldsymbol{h}]$ initially fulfills the self-consistency equation

$$\bar{h}_0 = V_0 b(\beta(h_0 + \bar{h}_0)), \tag{3.137}$$

which is consistent with the more general relation (3.123). As a consequence, all correlation functions at $\Lambda = 0$ depend on the total magnetic field

$$h = h_0 + \bar{h}_0. \tag{3.138}$$

Writing $\bar{h}_0 = V_0\bar{M}_0$, we note that Eq. (3.137) is equivalent to the familiar result for the magnetization within self-consistent mean-field theory,

$$\bar{M}_0 = b(\beta(h_0 + V_0\bar{M}_0)). \tag{3.139}$$

Considering the irreducible two-point vertex, it is obvious from Eqs. (3.134a) and (3.134b) that the polarization functions are initially given by the connected two-point spin correlators of an isolated spin subject to the magnetic field h,

$$\Pi_0^{zz}(K) = G_0^{zz}(K), \tag{3.140a}$$

$$\Pi_0^{+-}(K) = G_0^{+-}(K). \tag{3.140b}$$

To derive the initial condition of higher-order irreducible vertices, it is instructive to first look at the irreducible three-point vertex for arbitrary Λ,

$$\left[\tilde{\boldsymbol{\Phi}}_\Lambda'''\right]_{\tilde{\alpha}_1\tilde{\alpha}_2\tilde{\alpha}_3} = \tilde{\Phi}^{\alpha_1\alpha_2\alpha_3}_{\Lambda,i_1i_2i_3}(\tau_1,\tau_2,\tau_3) = \left.\frac{\delta^3\tilde{\Phi}_\Lambda[\boldsymbol{\eta}]}{\delta\eta_{i_1}^{\alpha_1}(\tau_1)\delta\eta_{i_2}^{\alpha_2}(\tau_2)\delta\eta_{i_3}^{\alpha_3}(\tau_3)}\right|_{\boldsymbol{\eta}=0}. \tag{3.141}$$

From Eqs. (3.106) and (3.119) we then find an exact relation between $\tilde{\boldsymbol{\Phi}}_\Lambda'''$ and the connected spin correlators,

$$\left[\tilde{\boldsymbol{\Phi}}_\Lambda'''\right]_{\tilde{\alpha}_1\tilde{\alpha}_2\tilde{\alpha}_3} = -\sum_{\tilde{\beta}_1\tilde{\beta}_2\tilde{\beta}_3}\prod_{i=1}^{3}\left[(\mathbb{1} + \mathbf{G}_\Lambda\mathbf{V}_\Lambda)^{-1}\right]_{\tilde{\alpha}_i\tilde{\beta}_i}\left[\mathbf{G}_\Lambda'''\right]_{\tilde{\beta}_1\tilde{\beta}_2\tilde{\beta}_3}, \tag{3.142}$$

where $\mathbf{G}'''_\Lambda$ is given by

$$[\mathbf{G}'''_\Lambda]_{\tilde{\alpha}_1\tilde{\alpha}_2\tilde{\alpha}_3} = G^{\alpha_1\alpha_2\alpha_3}_{\Lambda,i_1i_2i_3}(\tau_1,\tau_2,\tau_3) = \left.\frac{\delta^3\mathcal{G}_\Lambda[\boldsymbol{h}]}{\delta h^{\alpha_1}_{i_1}(\tau_1)\delta h^{\alpha_2}_{i_2}(\tau_2)\delta h^{\alpha_3}_{i_3}(\tau_3)}\right|_{\boldsymbol{h}=V_\Lambda(\boldsymbol{k}=0)\bar{\boldsymbol{M}}_\Lambda}. \tag{3.143}$$

Since we are interested in the initial condition $\mathbf{V}_{\Lambda=0} = 0$, it follows from Eq. (3.142) that in Fourier space

$$\tilde{\Phi}^{\alpha_1\alpha_2\alpha_3}_0(K_1,K_2,K_3) = -G^{\alpha_1\alpha_2\alpha_3}_0(K_1,K_2,K_3). \tag{3.144}$$

Analogously, the irreducible four-point vertex $\tilde{\boldsymbol{\Phi}}^{(4)}_\Lambda$ can be expressed as

$$\begin{aligned}\left[\tilde{\boldsymbol{\Phi}}^{(4)}_\Lambda\right]_{\tilde{\alpha}_1\tilde{\alpha}_2\tilde{\alpha}_3\tilde{\alpha}_4} &= -\sum_{\tilde{\beta}_1\tilde{\beta}_2\tilde{\beta}_3\tilde{\beta}_4}\prod_{i=1}^{4}\left[(\mathbb{1}+\mathbf{G}_\Lambda\mathbf{V}_\Lambda)^{-1}\right]_{\tilde{\alpha}_i\tilde{\beta}_i}\left[\mathbf{G}^{(4)}_\Lambda\right]_{\tilde{\beta}_1\tilde{\beta}_2\tilde{\beta}_3\tilde{\beta}_4}\\ &\quad+\frac{1}{2}\mathcal{S}_{\tilde{\alpha}_1,\tilde{\alpha}_2;\tilde{\alpha}_3,\tilde{\alpha}_4}\sum_{\tilde{\beta}_1\tilde{\beta}_2}\left[\tilde{\boldsymbol{\Phi}}'''_\Lambda\right]_{\tilde{\alpha}_1\tilde{\alpha}_2\tilde{\beta}_1}[\mathbf{V}_\Lambda+\mathbf{V}_\Lambda\mathbf{G}_\Lambda\mathbf{V}_\Lambda]_{\tilde{\beta}_1\tilde{\beta}_2}\left[\tilde{\boldsymbol{\Phi}}'''_\Lambda\right]_{\tilde{\beta}_2\tilde{\alpha}_3\tilde{\alpha}_4},\end{aligned} \tag{3.145}$$

where the symmetrization operator $\mathcal{S}_{\tilde{\alpha}_1,\tilde{\alpha}_2;\tilde{\alpha}_3,\tilde{\alpha}_4}$ symmetrizes the expression to its right with respect to the exchange of all labels [33]. Since the second line of Eq. (3.145) is proportional to $\mathbf{V}_\Lambda$, we find that the irreducible four-point vertex is initially given by

$$\tilde{\Phi}^{\alpha_1\alpha_2\alpha_3\alpha_4}_0(K_1,K_2,K_3,K_4) = -G^{\alpha_1\alpha_2\alpha_3\alpha_4}_0(K_1,K_2,K_3,K_4). \tag{3.146}$$

This procedure is easily generalized to higher orders, so that the irreducible n-point vertex with $n \geq 3$ has the initial condition

$$\tilde{\Phi}^{\alpha_1\ldots\alpha_n}_0(K_1\ldots,K_n) = -G^{\alpha_1\ldots\alpha_n}_0(K_1,\ldots,K_n). \tag{3.147}$$

In the spin-diagrammatic formalism of VLP, the connected spin correlators $G^{\alpha_1\ldots\alpha_n}_0(K_1,\ldots,K_n)$ of an isolated spin in an external magnetic field are known as blocks (or as generalized blocks in Ref. [3]). Since they can be calculated systematically via the generalized Wick theorem for spin operators [1, 3], it is straightforward to compute the initial condition of the irreducible vertices $\tilde{\boldsymbol{\Phi}}^{(n)}_\Lambda$ in a deformation scheme where $V^{\Lambda=0}_{ij} = 0$.

3.3.3 Expansion in the inverse interaction range

Free energy

In the previous section, we have shown that the Hubbard-Stratonovich SFRG is closely related to the spin-diagrammatic approach of VLP [1–3]. It should therefore be possible to recover the their expansion of both the free energy and the polarization functions of the ferromagnetic Heisenberg model in powers of the inverse interaction range $1/r_0$ [1, 2]. To show how this comes about, let us first consider the deformed free energy in units of temperature, $\tilde{\Phi}_\Lambda \equiv \tilde{\Phi}_\Lambda[0]$. Using Eq. (3.128) and noting that the irreducible one-point vertex $\tilde{\Phi}^\alpha_\Lambda$ vanishes by construction, we find that the exact flow equation of $\tilde{\Phi}_\Lambda$ reads

$$\partial_\Lambda \tilde{\Phi}_\Lambda = \frac{1}{2}\mathrm{Tr}\left\{\left[\left(\tilde{\mathbf{\Phi}}''_\Lambda + \tilde{\mathbf{R}}_\Lambda\right)^{-1} - \mathbf{V}_\Lambda\right]\partial_\Lambda \tilde{\mathbf{R}}_\Lambda\right\}. \tag{3.148}$$

To make contact with the calculations of VLP, we choose the deformation scheme $V^\Lambda_{ij} = \Lambda V_{ij}$. The flow equation of the free energy can then be written as

$$\partial_\Lambda \tilde{\Phi}_\Lambda[0] = -\frac{1}{2}\sum_{\boldsymbol{k},\omega}\frac{V_{\boldsymbol{k}}\Pi^{zz}_\Lambda(K)}{1-\Lambda V_{\boldsymbol{k}}\Pi^{zz}_\Lambda(K)} - \sum_{\boldsymbol{k},\omega}\frac{V_{\boldsymbol{k}}\Pi^{+-}_\Lambda(K)}{1-\Lambda V_{\boldsymbol{k}}\Pi^{+-}_\Lambda(K)}, \tag{3.149}$$

where we have used $\Pi_0^{-+}(K) = \Pi_0^{+-}(-K)$. Since the expansion in powers of $1/r_0$ amounts to an expansion in the number of momentum integrals, we can recover the leading correction to the free energy by replacing the polarization functions Π^{zz}_Λ and Π^{+-}_Λ on the right-hand side of Eq. (3.149) by their initial condition. Integrating over Λ and inserting

$$\begin{aligned}\Pi^{zz}_0(K) &= \delta(\omega)b'(\beta h),\\ \Pi^{+-}_0(K) &= \frac{b(\beta h)}{h-i\omega},\end{aligned} \tag{3.150}$$

results in the leading correction

$$\begin{aligned}\tilde{\Phi}_{\Lambda=1}[0] - \tilde{\Phi}_0[0] &\approx \frac{1}{2}\sum_{\boldsymbol{k},\omega}\ln\left[1 - V_{\boldsymbol{k}}\Pi^{zz}_0(K)\right] + \sum_{\boldsymbol{k},\omega}\ln\left[1 - V_{\boldsymbol{k}}\Pi^{+-}_0(K)\right]\\ &= \frac{1}{2}\sum_{\boldsymbol{k}}\ln\left[1-\beta V_{\boldsymbol{k}}b'(\beta h)\right] + \sum_{\boldsymbol{k},\omega}\ln\left[1 - \frac{V_{\boldsymbol{k}}b(\beta h)}{h-i\omega}\right].\end{aligned} \tag{3.151}$$

The fact that the Matsubara sum in the transversal part is ill-defined can be traced back to the ambiguity of $S^\pm_i(\tau)S^\mp_i(\tau)$ under the time-ordering symbol as discussed at the end of Sec. 3.2.1. We therefore modify the time dependence of the regulator matrix $\tilde{\mathbf{R}}_{\boldsymbol{\Lambda}}$ accordingly,

$$\delta(\tau-\tau') \to \delta(\tau-\tau'-0^\pm), \tag{3.152}$$

so that its Fourier transform now reads

$$\tilde{R}^{\alpha\alpha'}_\Lambda(K,K') = \delta_{\alpha,\alpha'}\delta(K+K')\tilde{R}_\Lambda(\boldsymbol{k})e^{i\omega 0^\pm}. \tag{3.153}$$

Since we have combined the transversal terms in Eq. (3.149) via $\Pi_0^{-+}(K) = \Pi_0^{+-}(-K)$, we have to use the average of both regularization factors,

$$\frac{1}{2}\left(e^{i\omega 0^+} + e^{i\omega 0^-}\right) = \cos(\omega 0^+). \tag{3.154}$$

We can incorporate this choice by replacing the Matsubara sum over an arbitrary function by a contour integral in the following way:

$$\frac{1}{\beta}\sum_{\omega} f(i\omega) = -\frac{1}{2}\frac{(-1)}{2\pi i}\int_{\mathcal{C}} dz \coth\left(\frac{\beta z}{2}\right) f(z), \tag{3.155}$$

where the contour $\mathcal{C}$ encircles all Matsubara frequencies in a counterclockwise manner [3, 41]. This allows us to perform the Matsubara sum in Eq. (3.151) so that the leading correction to the free energy reads

$$\tilde{\Phi}_{\Lambda=1}[0] - \tilde{\Phi}_0[0] \approx \frac{1}{2}\sum_{\boldsymbol{k}} \ln\left[1 - \beta V_{\boldsymbol{k}} b'(\beta h)\right] + \sum_{\boldsymbol{k}} \ln\left[\frac{\sinh\left(\frac{\beta h - \beta V_{\boldsymbol{k}} b(\beta h)}{2}\right)}{\sinh\left(\frac{\beta h}{2}\right)}\right], \tag{3.156}$$

which is manifestly invariant under the transformation $h \to -h$. For vanishing on-site interaction, our expression (3.156) is identical to the result of VLP as given in Eq. (17) of Ref. [1].

Longitudinal polarization function

The same approach can be used to compute higher-order irreducible vertices. As a specific example, we will compute the leading correction to the longitudinal polarization function $\Pi_0^{zz}(K)$. For this, we first need the exact flow equation of the irreducible two-point vertex which follows from the vertex expansion [33] of the Wetterich equation (3.128),

$$\begin{aligned}\partial_\Lambda \left[\tilde{\boldsymbol{\Phi}}''_\Lambda\right]_{\tilde{\alpha}_1\tilde{\alpha}_2} &= \frac{1}{2}\mathrm{Tr}\left[\dot{\mathbf{F}}_\Lambda \tilde{\boldsymbol{\Phi}}^{(4)}_{\Lambda,\tilde{\alpha}_1\tilde{\alpha}_2}\right] - \frac{1}{2}\mathcal{S}_{\tilde{\alpha}_1;\tilde{\alpha}_2}\,\mathrm{Tr}\left[\dot{\mathbf{F}}_\Lambda \tilde{\boldsymbol{\Phi}}'''_{\Lambda,\tilde{\alpha}_1}\mathbf{F}_\Lambda \tilde{\boldsymbol{\Phi}}'''_{\Lambda,\tilde{\alpha}_2}\right] \\ &\quad + \sum_{\tilde{\beta}} \left[\tilde{\boldsymbol{\Phi}}'''_\Lambda\right]_{\tilde{\alpha}_1\tilde{\alpha}_2\tilde{\beta}} \partial_\Lambda \bar{h}_{\Lambda,\tilde{\beta}}.\end{aligned} \tag{3.157}$$

Here the quadratic matrices $\tilde{\boldsymbol{\Phi}}^{(n)}_{\Lambda,\tilde{\alpha}_1\ldots\tilde{\alpha}_{n-2}}$ which appear in the trace are defined as

$$\left[\tilde{\boldsymbol{\Phi}}^{(n)}_{\Lambda,\tilde{\alpha}_1\ldots\tilde{\alpha}_{n-2}}\right]_{\tilde{\alpha}_{n-1}\tilde{\alpha}_n} = \left[\tilde{\boldsymbol{\Phi}}^{(n)}_\Lambda\right]_{\tilde{\alpha}_1\ldots\tilde{\alpha}_n} = \left.\frac{\delta^n \tilde{\Phi}_\Lambda[\boldsymbol{\eta}]}{\delta\eta_{\tilde{\alpha}_1}\ldots\delta\eta_{\tilde{\alpha}_n}}\right|_{\boldsymbol{\eta}=0} \tag{3.158}$$

and we have introduced the single-scale propagator matrix

$$\dot{\mathbf{F}}_\Lambda = -\mathbf{F}_\Lambda \left(\partial_\Lambda \tilde{\mathbf{R}}_\Lambda \right) \mathbf{F}_\Lambda . \tag{3.159}$$

More explicitly, the exact flow equation of $\Pi_\Lambda^{zz}(K)$ can be written as

$$\begin{aligned}
\partial_\Lambda \Pi_\Lambda^{zz}(K) = & -\frac{1}{2} \int_Q \dot{F}_\Lambda^{zz}(Q) \tilde{\Phi}_\Lambda^{zzzz}(Q,-Q,K) - \int_Q \dot{F}_\Lambda^{+-}(Q) \tilde{\Phi}_\Lambda^{+-zz}(Q,-Q,K) \\
& + \int_Q \dot{F}_\Lambda^{zz}(Q) F_\Lambda^{zz}(Q+K) \tilde{\Phi}_\Lambda^{zzz}(Q,-Q-K) \tilde{\Phi}_\Lambda^{zzz}(Q+K,-Q) \\
& + \int_Q \left[\dot{F}_\Lambda^{+-}(Q) F_\Lambda^{+-}(Q+K) + F_\Lambda^{+-}(Q) \dot{F}_\Lambda^{+-}(Q+K) \right] \\
& \quad \times \tilde{\Phi}_\Lambda^{+-z}(Q,-Q-K) \tilde{\Phi}_\Lambda^{+-z}(Q+K,-Q) - \tilde{\Phi}_\Lambda^{zzz}(K,-K) \partial_\Lambda h_\Lambda .
\end{aligned} \tag{3.160}$$

Here we have introduced the notation $\int_K = \frac{1}{\beta N} \sum_{\boldsymbol{k},\omega}$ and

$$\tilde{\Phi}_\Lambda^{\alpha_1 \ldots \alpha_n}(K_1, \ldots, K_n) = \delta(K_1 + \ldots + K_n) \tilde{\Phi}_\Lambda^{\alpha_1 \ldots \alpha_n}(K_1, \ldots, K_{n-1}) \tag{3.161}$$

as well as the renormalized effective magnetic field $h_\Lambda = h_0 + \bar{h}_\Lambda$, while the functions

$$\dot{F}_\Lambda^{zz}(K) = - \left[F_\Lambda^{zz}(K) \right]^2 \partial_\Lambda \tilde{R}_\Lambda(\boldsymbol{k}) = \frac{\partial_\Lambda V_\Lambda(\boldsymbol{k})}{\left[1 - V_\Lambda(\boldsymbol{k}) \Pi_\Lambda^{zz}(K) \right]^2}, \tag{3.162a}$$

$$\dot{F}_\Lambda^{+-}(K) = - \left[F_\Lambda^{+-}(K) \right]^2 \partial_\Lambda \tilde{R}_\Lambda(\boldsymbol{k}) = \frac{\partial_\Lambda V_\Lambda(\boldsymbol{k})}{\left[1 - V_\Lambda(\boldsymbol{k}) \Pi_\Lambda^{+-}(K) \right]^2}, \tag{3.162b}$$

are related to the Fourier-space components of the single-scale propagator by

$$\dot{F}_\Lambda^{zz}(K, K') = \delta(K + K') \dot{F}_\Lambda^{zz}(K'), \tag{3.163a}$$

$$\dot{F}_\Lambda^{+-}(K, K') = \delta(K + K') \dot{F}_\Lambda^{+-}(K'). \tag{3.163b}$$

A graphical representation of the exact flow equation (3.160) is shown in Fig. 3.4. We also need the flow equation of h_Λ,

$$\tilde{\Phi}_\Lambda^{zz}(0) \partial_\Lambda h_\Lambda = -\frac{1}{2} \int_Q \dot{F}_\Lambda^{zz}(Q) \tilde{\Phi}_\Lambda^{zzz}(Q,-Q) - \int_Q \dot{F}_\Lambda^{+-}(Q) \tilde{\Phi}_\Lambda^{+-z}(Q,-Q), \tag{3.164}$$

which can be obtained from the condition that the irreducible one-point vertex $\tilde{\Phi}_\Lambda^{\alpha}$ vanishes. To derive the leading correction to the longitudinal polarization function, we now approximate the polarization functions and the higher-order irreducible vertices on the right-hand side of Eq. (3.160) and in Eq. (3.164)

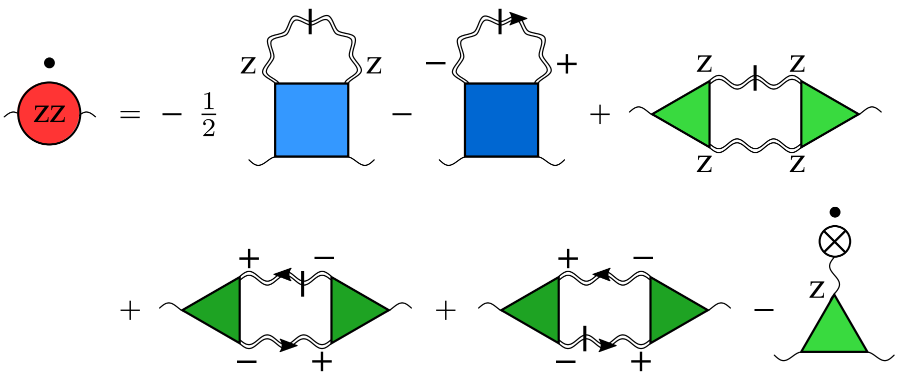

Figure 3.4: Graphical representation of the exact flow equation (3.160) of the longitudinal polarization function Π^{zz}_{Λ}. In our notation, a dot over a diagram represents the derivative ∂_Λ, a slashed double wavy line denotes the corresponding single-scale propagator, and the renormalized effective magnetic field h_Λ is symbolized by a crossed circle. Except for the last term which is considered separately by VLP, the diagrams on the right-hand side of the above flow equation correspond to the diagrams in Fig. (3a) of Ref. [2] if we set $V_\Lambda(\boldsymbol{k}) = \Lambda V_{\boldsymbol{k}}$, approximate the polarization functions as well as the higher-order irreducible vertices by their initial value, and integrate over Λ. (Figure reproduced with modifications from Ref. [99])

by their initial condition. Choosing the deformation scheme $V_\Lambda(\boldsymbol{k}) = \Lambda V_{\boldsymbol{k}}$, we can then perform all Matsubara sums as well as the integrals over Λ analytically. Postponing the evaluation of the last diagram in Fig. 3.4 for a moment, we show in Appendix B.2 that

$$\int_0^1 d\Lambda \left[\partial_\Lambda \Pi^{zz}_\Lambda(K) + \tilde{\Phi}^{zzz}_\Lambda(K,-K)\partial_\Lambda h_\Lambda\right] \approx \int_{\boldsymbol{q}} \frac{n_{\boldsymbol{q}} - n_{\boldsymbol{q}+\boldsymbol{k}}}{\epsilon_{\boldsymbol{q}+\boldsymbol{k}} - \epsilon_{\boldsymbol{q}} - i\omega} + \delta(\omega)\int_{\boldsymbol{q}} \Bigg\{ n'_y + \beta V_{\boldsymbol{q}} \left[\frac{b'''}{2} L_{\boldsymbol{q}} + \frac{(b'')^2}{2}\beta V_{\boldsymbol{q}+\boldsymbol{k}} L_{\boldsymbol{q}} L_{\boldsymbol{q}+\boldsymbol{k}} + b'' n_{\boldsymbol{q}} + \frac{\beta (b')^2 V_{\boldsymbol{q}+\boldsymbol{k}} - 2b'}{\beta(\epsilon_{\boldsymbol{q}+\boldsymbol{k}} - \epsilon_{\boldsymbol{q}})}(n_{\boldsymbol{q}} - n_{\boldsymbol{q}+\boldsymbol{k}}) \right] \Bigg\}, \tag{3.165}$$

where we have followed VLP in assuming a vanishing on-site interaction, $\sum_{\boldsymbol{k}} V_{\boldsymbol{k}} = 0$, as well as in defining

$$y = \beta h, \quad \epsilon_{\boldsymbol{k}} = h - bV_{\boldsymbol{k}}, \quad n_{\boldsymbol{k}} = \frac{1}{e^{\beta\epsilon_{\boldsymbol{k}}} - 1}, \quad n_y = \frac{1}{e^y - 1}, \quad L_{\boldsymbol{k}} = \frac{1}{1 - \beta b' V_{\boldsymbol{k}}}. \tag{3.166}$$

Our result (3.165) agrees exactly with Eq. (36) of Ref. [2], which corresponds to the first-order correction to the longitudinal polarization function without taking the renormalization of the effective magnetic field into account. To compute this missing contribution within the formalism of VLP, we first determine the correction $\Delta y = \beta \Delta h$ to the dimensionless magnetic field from the minimum of the free energy up to first order in the inverse interaction range,

$$\Delta y = \frac{\beta V_0}{1 - \beta b' V_0} \left[\frac{b''}{2} \int_{\boldsymbol{q}} \beta V_{\boldsymbol{q}} L_{\boldsymbol{q}} - \int_{\boldsymbol{q}} (n_{\boldsymbol{q}} \left[1 - \beta b' V_{\boldsymbol{q}}\right] - n_y) \right], \tag{3.167}$$

see Eqs. (17) and (18) of Ref. [1]. Inserting this correction into the initial condition $\Pi_0^{zz}(K) = \delta(\omega) b'(y)$ of the longitudinal polarization function then yields

$$\delta(\omega) b'(y + \Delta y) - \delta(\omega) b'(y) \approx \delta(\omega) b''(y) \Delta y. \tag{3.168}$$

In Appendix B.2.5 we show that this is exactly the leading-order contribution of the last diagram in Fig. 3.4,

$$\begin{aligned} & - \tilde{\Phi}_0^{zzz}(K, -K) \int_0^1 d\Lambda \, \partial_\Lambda h_\Lambda \\ \approx & \delta(\omega) b'' \frac{\beta V_0}{1 - \beta b' V_0} \left[\frac{b''}{2} \int_{\boldsymbol{q}} \beta V_{\boldsymbol{q}} L_{\boldsymbol{q}} - \int_{\boldsymbol{q}} (n_{\boldsymbol{q}} \left[1 - \beta b' V_{\boldsymbol{q}}\right] - n_y) \right]. \end{aligned} \tag{3.169}$$

We thus see that our SFRG exactly reproduces VLP's result for the leading correction to the longitudinal polarization function.

Together with our previous result (3.156) for the free energy, this suggest that we can generate the expansion in the inverse interaction range $1/r_0$ within our SFRG by expanding the exact flow equations of the irreducible vertices iteratively in the number of momentum integrals. Compared to the spin-diagrammatic formalism of VLP, this is a significant simplification. Note that in the context of the three-dimensional Heisenberg ferromagnet, the expansion in powers of $1/r_0$ is known to yield an accurate description of the thermodynamics for arbitrary spin, magnetic field, and temperature except for a narrow region around the critical point [1]; moreover, for $T < T_c$ it enables us to study the transversal and longitudinal spin correlations [2]. While we have seen that it is possible to derive these results in a simpler way within the SFRG, it also allows us to go beyond the $1/r_0$ expansion: as we will discuss in Sec. 3.5, an interesting problem that we currently investigate is the fate of spin waves above the critical temperature. Furthermore, in contrast to the perturbative approach of VLP, our SFRG is still valid close to T_c, which gives us access to the critical regime.

3.3.4 Applying the $1/D$ expansion to the quantum Heisenberg model

While we have shown in Sec. 3.3.3 that our Hubbard-Stratonovich SFRG enables us to recover VLP's expansion in $1/r_0$ in a simple way, it also allows us to employ new approximation schemes. An obvious application is the generalization of our $1/D$ expansion for the Ising model in Sec. 3.2.4 to quantum systems. Since the irreducible vertices of a quantum spin model have well-defined initial conditions for vanishing interaction within the Hubbard-Stratonovich SFRG, it is straightforward to generalize our calculation for the Ising model in Appendix B.1 to the quantum Heisenberg model. Again assuming a D-dimensional hypercubic lattice with nearest-neighbour interaction, we show in Appendix B.3.1 that the critical temperature of the spin-S quantum Heisenberg model is to leading order in $1/D$ determined by the quadratic equation

$$1 - g\gamma_{\boldsymbol{k}} - \frac{g^2}{24D}\left(\frac{10b'''}{(b')^2} - \frac{\gamma_{\boldsymbol{k}}}{b'}\right) = 0, \tag{3.170}$$

where $g = \beta b' V_0$. This equation is readily solved by

$$\frac{T_c}{T_{c0}} = \frac{1}{2}\left[1 + \sqrt{1 - \frac{1}{D}\left[\frac{5}{3}\frac{|b'''|}{(b')^2} \pm \frac{1}{6b'}\right]}\right], \tag{3.171}$$

where $T_{c0} = b'|V_0|$ is the mean-field result. We note that the last term in the inner brackets is directly related to the quantumness of the model, since it breaks the symmetry between a ferromagnetic (upper sign) and an antiferromagnetic (lower sign) exchange interaction; this symmetry is only restored in the classical limit $S \to \infty$ where $1/b' \to 0$. This behaviour is seen explicitly in Fig. 3.5, where we compare our first-order result (3.171) for the critical temperature in three dimensions to the predictions of Cuccoli et al. [117] as well as to quantum Monte Carlo data [118, 119]. We find good agreement (with a relative error below ten percent) for arbitrary spin S in the antiferromagnetic case and for $S > 1/2$ in the ferromagnetic case. While we assume that for $D > 3$ our leading-order expression (3.171) yields accurate results over the full range of S for arbitrary sign of V_0, it seems difficult to find good benchmarks.

It is conceptually simple to extend our first-order calculation in Appendix B.3.1 to higher orders in $1/D$. However, since we have not yet evaluated the five- and six-point correlators of an isolated quantum spin for arbitrary S, we focus on the limiting cases $S = 1/2$ and $S \to \infty$. The quantum limit is considered in Appendix B.3.2, where we show that the

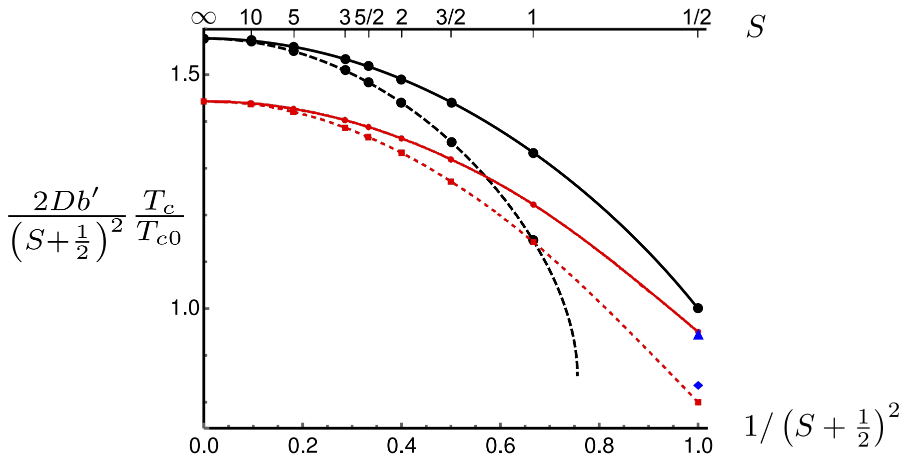

Figure 3.5: Critical temperature of the spin-S quantum Heisenberg model on a cubic lattice for a ferromagnetic (dashed) or an antiferromagnetic (solid) nearest-neighbour interaction. The upper (black) lines correspond to our first-order result (3.171), while the lower (red) lines refer to the predictions of Cuccoli et al. [117] which are calibrated to Monte Carlo results [120] for $S \to \infty$. The blue diamond and triangle refer to quantum Monte Carlo results [118, 119] for the spin-1/2 ferromagnetic and antiferromagnetic quantum Heisenberg model, respectively.

critical temperature is to second order in $1/D$ determined by the quartic equation

$$1 - g\gamma_{\boldsymbol{k}} + \frac{g^2(5+\gamma_{\boldsymbol{k}})}{6D} - \frac{g^3(1+\gamma_{\boldsymbol{k}})}{3D^2} + \frac{g^4}{18D^2}(1-\gamma_{\boldsymbol{k}}) = 0. \tag{3.172}$$

For the ferromagnetic Heisenberg model on a cubic lattice we now do find a phase transition at $2Db'T_c/T_{c0} = 1$, which qualitatively improves on the first-order result, while for an antiferromagnetic interaction in $D = 3$ our second-order result yields no phase transition. Similar to our first-order result, we find that Eq. (3.172) predicts a finite T_c for $D > 3$ regardless of the sign of V_0.

Finally, in Appendix B.3.3 we derive the second-order correction for $S \to \infty$, which results in[5]

$$1 - g\gamma_{\boldsymbol{k}} + \frac{g^2}{2D} - \frac{g^3\gamma_{\boldsymbol{k}}}{10D^2} + \frac{g^4}{4D^2} = 0. \tag{3.173}$$

[5]We note that Eq. (3.173) is invariant under the transformation $\{g, \gamma_{\boldsymbol{k}}\} \to \{-g, -\gamma_{\boldsymbol{k}}\}$, which is in agreement with the fact that thermodynamic properties of the zero-field classical Heisenberg model on a bipartite lattice do not depend on the sign of the exchange interaction.

Solving this equation for $D = 3$ yields $2T_c/T_{c0} \approx 1.42$, which is rather close to $2T_c^{MC}/T_{c0} \approx 1.44$ obtained from Monte Carlo simulations [120].

3.4 Hybrid SFRG

3.4.1 General formalism

Motivation

So far we have considered two different formulations of the spin FRG: on the one hand, the pure SFRG developed in Sec. 3.2.1 deals directly with the connected spin correlators and the corresponding irreducible vertices, which are irreducible with respect to the cutting of a single propagator line. While this formulation is very close to the usual FRG approach for bosonic and fermionic systems, it has the disadvantage that the irreducible vertices do not exist for the initial condition of isolated spins. This artifact is cured in the Hubbard-Stratonovich SFRG, which is formulated in terms of the amputated connected spin correlators and where irreducibility is defined with respect to the cutting of a single (effective) interaction line. While this allows us to use the comparably simple initial condition of isolated spins, it implies by construction that we do not work with the usual irreducible vertices. On the level of the irreducible two-point vertices, e.g., this means that we work with the inverse of the usual self-energy $\Gamma_\Lambda^{\alpha\alpha'}(K)$ [cf. Eqs. (3.135a) and (3.135b)], which might render some common approximation schemes less useful.

For magnetically ordered systems, it can therefore be useful to combine the pure SFRG and the Hubbard-Stratonovich SFRG. In this hybrid SFRG, we describe transversal fluctuations in a way similar to the pure SFRG formalism which allows us to work directly with the usual irreducible vertices [e.g., with the self-energy $\Gamma_\Lambda^{+-}(K)$], while the longitudinal fluctuations are treated analogously to the Hubbard-Stratonovich SFRG so that the corresponding irreducible vertices are well defined even in the local limit of isolated spins.

Auxiliary generating functional

On a technical level, we first define the auxiliary generating functional $\mathcal{A}_\Lambda[\boldsymbol{h}^\perp, M^z]$ via [cf. Eqs. (3.3) and (3.104)]

$$e^{\mathcal{A}_\Lambda[\boldsymbol{h}^\perp, M^z]}$$
$$= \mathrm{Tr}\left[e^{-\beta\mathcal{H}_0} \mathcal{T} e^{\int_0^\beta d\tau \left\{ \sum_i \boldsymbol{h}_i^\perp(\tau)\cdot \boldsymbol{S}_i^\perp(\tau) + \frac{1}{2}\sum_{ij} V_{ij}^\Lambda \left[M_i^z(\tau)+S_i^z(\tau)\right]\left[M_j^z(\tau)+S_j^z(\tau)\right] - \mathcal{H}_\Lambda^\perp(\tau) \right\}} \right], \tag{3.174}$$

where $\boldsymbol{h}_i^\perp = (h_i^x, h_i^y, 0)^{\mathrm{T}}$, $\boldsymbol{S}_i^\perp = (S_i^x, S_i^y, 0)^{\mathrm{T}}$, and $\mathcal{H}_\Lambda^\perp$ denotes the transversal part of the deformed Hamiltonian,

$$\mathcal{H}_\Lambda^\perp = -\frac{1}{2}\sum_{ij} V_{ij}^\Lambda \boldsymbol{S}_i^\perp \cdot \boldsymbol{S}_j^\perp = -\frac{1}{2}\sum_{ij} V_{ij}^\Lambda \left(S_i^+ S_j^- + S_i^- S_j^+\right). \tag{3.175}$$

Similar to Eq. (3.106), we can also express $\mathcal{A}_\Lambda[\boldsymbol{h}^\perp, M^z]$ in terms of the generating functional of the connected spin correlators (3.3),

$$\mathcal{A}_\Lambda[\boldsymbol{h}^\perp, M^z] = \frac{1}{2}\int_0^\beta d\tau \sum_{ij} V_{ij}^\Lambda M_i^z(\tau) M_j^z(\tau) + \mathcal{G}_\Lambda\Big[\boldsymbol{h}_i^\perp(\tau), \sum_j V_{ij}^\Lambda M_j^z(\tau)\Big], \tag{3.176}$$

which will be useful later on. Conceptually, it is helpful to express Eq. (3.174) in yet another way by decoupling the deformed exchange interaction via a Hubbard-Stratonovich transformation in the longitudinal channel only,

$$\begin{aligned} &e^{\mathcal{A}_\Lambda[\boldsymbol{h}^\perp, M^z]} \\ =&\frac{\int \mathcal{D}[\phi^z]\, e^{-\frac{1}{2}\sum_{\tilde{\alpha}\tilde{\alpha}'}\left[\mathbf{V}_\Lambda^{-1}\right]_{\tilde{\alpha}\tilde{\alpha}'}\phi^z_{\tilde{\alpha}}\phi^z_{\tilde{\alpha}'}}\, \mathrm{Tr}\left[e^{-\beta\mathcal{H}_0}\mathcal{T} e^{\sum_{\tilde{\alpha}}\left[\left(M^z_{\tilde{\alpha}}+S^z_{\tilde{\alpha}}\right)\phi^z_{\tilde{\alpha}} + h^\perp_{\tilde{\alpha}} S^\perp_{\tilde{\alpha}}\right] - \int_0^\beta d\tau\, \mathcal{H}_\Lambda^\perp(\tau)}\right]}{\int \mathcal{D}[\phi^z]\, e^{-\frac{1}{2}\sum_{\tilde{\alpha}\tilde{\alpha}'}\left[\mathbf{V}_\Lambda^{-1}\right]_{\tilde{\alpha}\tilde{\alpha}'}\phi^z_{\tilde{\alpha}}\phi^z_{\tilde{\alpha}'}}}, \end{aligned} \tag{3.177}$$

so that the derivatives of $\mathcal{A}_\Lambda[\boldsymbol{h}^\perp, M^z]$ with respect to $M_i^z(\tau)$ can be interpreted as the connected correlators of the Hubbard-Stratonovich field $\phi_i^z(\tau)$. The inverse deformed exchange-interaction matrix $\mathbf{V}_\Lambda^{-1}$ and the superindex notation have already been introduced in Eq. (3.109); here we have also defined $\phi^z_{\tilde{\alpha}} = \delta_{\alpha,z}\phi_i^z(\tau)$, $M^z_{\tilde{\alpha}} = \delta_{\alpha,z} M_i^z(\tau)$ and $h^\perp_{\tilde{\alpha}} = \boldsymbol{h}_i^\perp(\tau)\cdot \boldsymbol{e}_\alpha$, where $\boldsymbol{e}_\alpha$ is the unit vector along the α axis. Differentiating Eq. (3.177) on both sides with respect to Λ, we directly see that our auxiliary generating functional $\mathcal{A}_\Lambda[\boldsymbol{h}^\perp, M^z]$ obeys the exact flow equation

$$\begin{aligned} &\partial_\Lambda \mathcal{A}_\Lambda[\boldsymbol{h}^\perp, M^z] \\ =&\frac{1}{2}\sum_{\tilde{\alpha}\tilde{\alpha}'}\left[\partial_\Lambda \mathbf{V}_\Lambda^\perp\right]_{\tilde{\alpha}\tilde{\alpha}'}\left[\frac{\delta^2\mathcal{A}_\Lambda[\boldsymbol{h}^\perp, M^z]}{\delta h^\perp_{\tilde{\alpha}}\delta h^\perp_{\tilde{\alpha}'}} + \frac{\delta\mathcal{A}_\Lambda[\boldsymbol{h}^\perp, M^z]}{\delta h^\perp_{\tilde{\alpha}}}\frac{\delta\mathcal{A}_\Lambda[\boldsymbol{h}^\perp, M^z]}{\delta h^\perp_{\tilde{\alpha}'}}\right] \\ -&\frac{1}{2}\sum_{\tilde{\alpha}\tilde{\alpha}'}\left[\partial_\Lambda\left(\mathbf{V}_\Lambda^z\right)^{-1}\right]_{\tilde{\alpha}\tilde{\alpha}'}\left[\frac{\delta^2\mathcal{A}_\Lambda[\boldsymbol{h}^\perp, M^z]}{\delta M^z_{\tilde{\alpha}}\delta M^z_{\tilde{\alpha}'}} + \frac{\delta\mathcal{A}_\Lambda[\boldsymbol{h}^\perp, M^z]}{\delta M^z_{\tilde{\alpha}}}\frac{\delta\mathcal{A}_\Lambda[\boldsymbol{h}^\perp, M^z]}{\delta M^z_{\tilde{\alpha}'}}\right] \\ &+\frac{1}{2}\mathrm{Tr}\left[\mathbf{V}_\Lambda^z\partial_\Lambda\left(\mathbf{V}_\Lambda^z\right)^{-1}\right], \end{aligned} \tag{3.178}$$

where $\mathbf{V}_\Lambda^\perp$ and $\mathbf{V}_\Lambda^z$ refer to the transversal and to the longitudinal part of the deformed exchange-interaction matrix, respectively, so that $\mathbf{V}_\Lambda = \mathbf{V}_\Lambda^\perp + \mathbf{V}_\Lambda^z$.

We can write this flow equation more efficiently by introducing the superfield $\boldsymbol{J}_i = (h_i^x, h_i^y, M_i^z)^{\mathrm{T}}$ and the partially inverted exchange-interaction matrix $\mathbf{U}_\Lambda = \mathbf{V}_\Lambda^\perp - (\mathbf{V}_\Lambda^z)^{-1}$, so that

$$\begin{aligned}\partial_\Lambda \mathcal{A}_\Lambda[\boldsymbol{J}] = \frac{1}{2} \sum_{\tilde{\alpha}\tilde{\alpha}'} [\partial_\Lambda \mathbf{U}_\Lambda]_{\tilde{\alpha}\tilde{\alpha}'} \left[\frac{\delta^2 \mathcal{A}_\Lambda[\boldsymbol{J}]}{\delta J_{\tilde{\alpha}} \delta J_{\tilde{\alpha}'}} + \frac{\delta \mathcal{A}_\Lambda[\boldsymbol{J}]}{\delta J_{\tilde{\alpha}}} \frac{\delta \mathcal{A}_\Lambda[\boldsymbol{J}]}{\delta J_{\tilde{\alpha}'}} \right] \\ + \frac{1}{2} \mathrm{Tr} \left[\mathbf{V}_\Lambda^z \partial_\Lambda \left(\mathbf{V}_\Lambda^z \right)^{-1} \right]. \end{aligned} \tag{3.179}$$

Irreducible vertices

Similar to the pure and the Hubbard-Stratonovich SFRG, we now define the subtracted Legendre transform $\Psi_\Lambda[\boldsymbol{j}]$ of our auxiliary generating functional $\mathcal{A}_\Lambda[\boldsymbol{J}] = \mathcal{A}_\Lambda[\boldsymbol{h}^\perp, M^z]$ as

$$\Psi_\Lambda[\boldsymbol{j}] = \sum_{\tilde{\alpha}} J_{\tilde{\alpha}} j_{\tilde{\alpha}} - \mathcal{A}_\Lambda[\boldsymbol{J}[\boldsymbol{j}]] - \frac{1}{2} \sum_{\tilde{\alpha}\tilde{\alpha}'} \left[\bar{\mathbf{R}}_\Lambda \right]_{\tilde{\alpha}\tilde{\alpha}'} j_{\tilde{\alpha}} j_{\tilde{\alpha}'}, \tag{3.180}$$

where $\boldsymbol{J}_i = (h_i^x, h_i^y, M_i^z)^{\mathrm{T}}$ is to be understood as a functional of the superfield $\boldsymbol{j}_i = (M_i^x, M_i^y, h_i^z)^{\mathrm{T}}$ by inverting the relation

$$j_{\tilde{\alpha}} = \frac{\delta \mathcal{A}_\Lambda[\boldsymbol{J}]}{\delta J_{\tilde{\alpha}}}. \tag{3.181}$$

The hybrid regulator matrix $\bar{\mathbf{R}}_\Lambda$ is given by

$$\bar{\mathbf{R}}_\Lambda = \mathbf{R}_\Lambda^\perp + \mathbf{R}_\Lambda^z, \tag{3.182}$$

where $\mathbf{R}_\Lambda^\perp$ and $\mathbf{R}_\Lambda^z$ are in turn defined as

$$\begin{aligned} \mathbf{R}_\Lambda^\perp &= \mathbf{V}^\perp - \mathbf{V}_\Lambda^\perp, \\ \mathbf{R}_\Lambda^z &= \left(\mathbf{V}_\Lambda^z\right)^{-1} - \left(\mathbf{V}^z\right)^{-1}, \end{aligned} \tag{3.183}$$

which implies

$$\partial_\Lambda \bar{\mathbf{R}}_\Lambda = -\partial_\Lambda \mathbf{U}_\Lambda. \tag{3.184}$$

Due to its hybrid nature, $\Psi_\Lambda[\boldsymbol{j}]$ is the generating functional of the vertices which are irreducible with respect to the cutting of either a single transversal propagator line or a single longitudinal (effective) interaction line. Due to our superfield notation, the derivatives of $\Psi_\Lambda[\boldsymbol{j}]$ have the usual form: while its first derivative reads

$$\frac{\delta \Psi_\Lambda[\boldsymbol{j}]}{\delta j_{\tilde{\alpha}}} = J_{\tilde{\alpha}} - \sum_{\tilde{\alpha}'} \left[\bar{\mathbf{R}}_\Lambda \right]_{\tilde{\alpha}\tilde{\alpha}'} j_{\tilde{\alpha}'}, \tag{3.185}$$

the Hessian matrix $\mathbf{\Psi}''_\Lambda[\boldsymbol{j}]$ is

$$[\mathbf{\Psi}''_\Lambda[\boldsymbol{j}]]_{\tilde{\alpha}\tilde{\alpha}'} = \frac{\delta^2 \Psi_\Lambda[\boldsymbol{j}]}{\delta j_{\tilde{\alpha}} \delta j_{\tilde{\alpha}'}} = \left[\mathbf{A}_\Lambda^{-1}[\boldsymbol{J}] - \bar{\mathbf{R}}_\Lambda\right]_{\tilde{\alpha}\tilde{\alpha}'}, \tag{3.186}$$

where $\mathbf{A}_\Lambda^{-1}[\boldsymbol{J}]$ is the matrix inverse of

$$[\mathbf{A}_\Lambda[\boldsymbol{J}]]_{\tilde{\alpha}\tilde{\alpha}'} = \frac{\delta^2 \mathcal{A}_\Lambda[\boldsymbol{J}]}{\delta J_{\tilde{\alpha}} \delta J_{\tilde{\alpha}'}}. \tag{3.187}$$

This allows us to write the exact flow equation of $\Psi_\Lambda[\boldsymbol{j}]$ as

$$\begin{aligned} \partial_\Lambda \Psi_\Lambda[\boldsymbol{j}] &= \frac{1}{2} \operatorname{Tr}\left[\left(\mathbf{\Psi}''_\Lambda[\boldsymbol{j}] + \bar{\mathbf{R}}_\Lambda\right)^{-1} \partial_\Lambda \bar{\mathbf{R}}_\Lambda\right] - \frac{1}{2}\operatorname{Tr}\left[\mathbf{V}_\Lambda^z \partial_\Lambda \left(\mathbf{V}_\Lambda^z\right)^{-1}\right] \\ &= \frac{1}{2} \operatorname{Tr}\left\{\left[\left(\mathbf{\Psi}''_\Lambda[\boldsymbol{j}] + \bar{\mathbf{R}}_\Lambda\right)^{-1} - \mathbf{V}_\Lambda^z\right] \partial_\Lambda \bar{\mathbf{R}}_\Lambda\right\}, \end{aligned} \tag{3.188}$$

where in the second line we have used that $\mathbf{V}_\Lambda^z$ and $\mathbf{V}_\Lambda^\perp$ are defined by projecting $\mathbf{V}_\Lambda$ onto orthogonal subspaces. In general, $\Psi_\Lambda[\boldsymbol{j}]$ will have a minimum at the scale-dependent uniform superfield configuration $j_{\tilde{\alpha}} = \bar{j}_{\Lambda,\tilde{\alpha}} = \bar{h}_{\Lambda,\tilde{\alpha}} = \delta_{\alpha,z} \bar{h}_\Lambda$ that fulfills

$$\left.\frac{\delta \Psi_\Lambda[\boldsymbol{j}]}{\delta j_{\tilde{\alpha}}}\right|_{\boldsymbol{j}=\bar{\boldsymbol{h}}_\Lambda} = 0, \tag{3.189}$$

where the scale-dependent exchange correction to the external magnetic field $\bar{\boldsymbol{h}}_\Lambda = \bar{h}_\Lambda \boldsymbol{e}_z$ will be non-zero if the $O(3)$ symmetry of the quantum Heisenberg model is either explicitly or spontaneously broken. We therefore introduce the shifted generating functional

$$\tilde{\Psi}_\Lambda[\boldsymbol{\eta}] = \Psi_\Lambda[\bar{\boldsymbol{h}}_\Lambda + \boldsymbol{\eta}], \tag{3.190}$$

where the superfield $\boldsymbol{\eta}_i(\tau) = \boldsymbol{j}_i(\tau) - \bar{\boldsymbol{h}}_\Lambda$ measures the distance to the minimum of $\Psi_\Lambda[\boldsymbol{j}]$. The Wetterich equation [34] for $\tilde{\Psi}_\Lambda[\boldsymbol{\eta}]$ thus reads [cf. Eq. (3.128)]

$$\begin{aligned} \partial_\Lambda \tilde{\Psi}_\Lambda[\boldsymbol{\eta}] &= \partial_\Lambda \Psi_\Lambda[\boldsymbol{j}]|_{\boldsymbol{j}\to\bar{\boldsymbol{h}}_\Lambda+\boldsymbol{\eta}} + \sum_{\tilde{\alpha}} \frac{\delta \tilde{\Psi}_\Lambda[\boldsymbol{\eta}]}{\delta \eta_{\tilde{\alpha}}} \partial_\Lambda \bar{h}_{\Lambda,\tilde{\alpha}} \\ &= \frac{1}{2} \operatorname{Tr}\left\{\left[\left(\tilde{\mathbf{\Psi}}''_\Lambda[\boldsymbol{\eta}] + \bar{\mathbf{R}}_\Lambda\right)^{-1} - \mathbf{V}_\Lambda^z\right] \partial_\Lambda \bar{\mathbf{R}}_\Lambda\right\} + \sum_{\tilde{\alpha}} \frac{\delta \tilde{\Psi}_\Lambda[\boldsymbol{\eta}]}{\delta \eta_{\tilde{\alpha}}} \partial_\Lambda \bar{h}_{\Lambda,\tilde{\alpha}}. \end{aligned} \tag{3.191}$$

3.4.2 Initial condition of isolated spins

Exchange correction to the external magnetic field

As mentioned in the beginning of Sec. 3.4.1, one motivation for the hybrid SFRG is the fact that the corresponding irreducible vertices exist even in the local limit of isolated spins as long as there is a finite (effective) magnetic field during the flow ($\bar{\boldsymbol{h}}_\Lambda \neq 0$ for $\Lambda < 1$). In the following, we will show explicitly how this comes about by deriving the irreducible n-point vertices of an isolated spin for $n \leq 4$. We start with the generating functional itself: assuming a uniform source field $\bar{\boldsymbol{h}} = \bar{h}\boldsymbol{e}_z$ and a deformation scheme where $V_{ij}^{\Lambda=0} = 0$, we find that $\Psi_\Lambda[\bar{\boldsymbol{h}}]$ is initially given by

$$\Psi_0[\bar{\boldsymbol{h}}] = N \left\{ \frac{\beta \bar{h}^2}{2V_0} - B\left[\beta(h_0 + \bar{h})\right] \right\}; \tag{3.192}$$

the derivation of this expression is completely analogous to the derivation of Eq. (3.136). Minimizing $\Psi_0[\bar{\boldsymbol{h}}]$ then yields a self-consistency equation for the initial value of $\bar{h}_\Lambda$,

$$\bar{h}_0 = V_0 b(\beta(h_0 + \bar{h}_0)). \tag{3.193}$$

This self-consistent mean-field result is identical to our initial condition (3.137) in the Hubbard-Stratonovich SFRG, which is to be expected since the hybrid SFRG treats longitudinal fluctuations in the same way.

Irreducible two-point vertices

To derive the initial condition of the irreducible two-point vertices, we first note that Eq. (3.176) implies the general relations

$$A_\Lambda^{zz}(K) = V_\Lambda(\boldsymbol{k}) + V_\Lambda(\boldsymbol{k}) G_\Lambda^{zz}(K) V_\Lambda(\boldsymbol{k}), \tag{3.194a}$$

$$A_\Lambda^{+-}(K) = G_\Lambda^{+-}(K). \tag{3.194b}$$

Here we have used the notation

$$A_\Lambda^{zz}(K, K') = \delta(K + K') A_\Lambda^{zz}(K'), \tag{3.195a}$$

$$A_\Lambda^{+-}(K, K') = \delta(K + K') A_\Lambda^{+-}(K), \tag{3.195b}$$

for the components of $\mathbf{A}_\Lambda[\bar{\boldsymbol{J}}_\Lambda]$ in Fourier space, where the scale-dependent uniform superfield configuration $\bar{\boldsymbol{J}}_\Lambda = \bar{M}_\Lambda \boldsymbol{e}_z$ is defined via [see Eqs. (3.185) and (3.189)]

$$\bar{M}_\Lambda = \left[\frac{1}{V_\Lambda(\boldsymbol{k} = 0)} - \frac{1}{V_{\Lambda=1}(\boldsymbol{k} = 0)} \right] \bar{h}_\Lambda. \tag{3.196}$$

It then follows directly from Eq. (3.186) that the irreducible two-point vertices can be related to the connected spin correlators by

$$\Pi_\Lambda(K) = \frac{G^{zz}_\Lambda(K)}{1 + V_\Lambda(\boldsymbol{k}) G^{zz}_\Lambda(K)}, \tag{3.197a}$$

$$\Sigma_\Lambda(K) = \frac{1 + V_\Lambda(\boldsymbol{k}) G^{+-}_\Lambda(K)}{G^{+-}_\Lambda(K)} = \frac{1}{G^{+-}_\Lambda(K)} + V_\Lambda(\boldsymbol{k}), \tag{3.197b}$$

where we have parametrized the Fourier-space representation of $\tilde{\boldsymbol{\Psi}}''_\Lambda[0] = \boldsymbol{\Psi}''_\Lambda[\bar{\boldsymbol{h}}_\Lambda]$ as

$$\tilde{\Psi}^{zz}_\Lambda(K, K') = \delta(K + K') \tilde{\Psi}^{zz}_\Lambda(K) = \delta(K + K') \left[V^{-1}_{\boldsymbol{k}} - \Pi_\Lambda(K) \right], \tag{3.198a}$$

$$\tilde{\Psi}^{+-}_\Lambda(K, K') = \delta(K + K') \tilde{\Psi}^{+-}_\Lambda(K') = \delta(K + K') \Big[\Sigma_\Lambda(K') - V_{\boldsymbol{k}'} \Big]. \tag{3.198b}$$

In a deformation scheme where we start the flow in the local limit of isolated spins [i.e., $V_{\Lambda=0}(\boldsymbol{k}) = 0$], we then find that $\Pi_\Lambda(K)$ and $\Sigma_\Lambda(K)$ are initially given by

$$\Pi_0(K) = G^{zz}_0(K) = \delta(\omega) b', \tag{3.199a}$$

$$b\Sigma_0(K) = \frac{b}{G^{+-}_0(K)} = h - i\omega, \tag{3.199b}$$

where the Brillouin function $b = b(\beta h)$ and its derivative $b' = b'(\beta h)$ depend on the total magnetic field $h = h_0 + \bar{h}_0$. Finally, it may be useful to define

$$\tilde{\Pi}_\Lambda(K) = \Pi_\Lambda(K) - \Pi_0(K), \tag{3.200a}$$

$$\tilde{\Sigma}_\Lambda(K) = b\Sigma_\Lambda(K) - b\Sigma_0(K), \tag{3.200b}$$

so that the irreducible two-point vertices can be written as

$$\tilde{\Psi}^{zz}_\Lambda(K) = V^{-1}_{\boldsymbol{k}} - \delta(\omega) b' - \tilde{\Pi}_\Lambda(K), \tag{3.201a}$$

$$b\tilde{\Psi}^{+-}_\Lambda(K) = \epsilon_{\boldsymbol{k}} - i\omega + \tilde{\Sigma}_\Lambda(K), \tag{3.201b}$$

where the spin-wave dispersion $\epsilon_{\boldsymbol{k}} = h - bV_{\boldsymbol{k}}$ was already introduced in Eq. (3.166). Most strikingly, the transversal part of the spin propagator is then given by

$$G^{+-}_\Lambda(K) = \frac{b}{\epsilon_{\boldsymbol{k}} - i\omega + \tilde{\Sigma}_\Lambda(K) + bR_\Lambda(\boldsymbol{k})}; \tag{3.202}$$

this strongly resembles the usual form of a bosonic or fermionic propagator in the presence of an additive cutoff $bR_\Lambda(\boldsymbol{k}) = bV_{\boldsymbol{k}} - bV_\Lambda(\boldsymbol{k})$, where $\tilde{\Sigma}_\Lambda(K)$ plays the role of a self-energy [33].

Irreducible three-point vertices

In the next step we consider the third derivative of the hybrid generating functional $\tilde{\Psi}_\Lambda[\boldsymbol{\eta}]$,

$$\left[\tilde{\mathbf{\Psi}}_\Lambda'''[\boldsymbol{\eta}]\right]_{\tilde{\alpha}_1\tilde{\alpha}_2\tilde{\alpha}_3} = \frac{\delta^3 \tilde{\Psi}_\Lambda[\boldsymbol{\eta}]}{\delta\eta_{\tilde{\alpha}_1}\delta\eta_{\tilde{\alpha}_2}\delta\eta_{\tilde{\alpha}_3}}. \tag{3.203}$$

Differentiating the Hessian matrix $\tilde{\mathbf{\Psi}}_\Lambda''[\boldsymbol{\eta}] = \mathbf{\Psi}_\Lambda''[\bar{\boldsymbol{h}}_\Lambda + \boldsymbol{\eta}]$ with respect to the superfield $\boldsymbol{\eta}_i = \left(M_i^x, M_i^y, h_i^z - \bar{h}_\Lambda\right)^{\mathrm{T}}$, we find according to Eq. (3.186)

$$\left[\tilde{\mathbf{\Psi}}_\Lambda'''[\boldsymbol{\eta}]\right]_{\tilde{\alpha}_1\tilde{\alpha}_2\tilde{\alpha}_3} = -\sum_{\tilde{\alpha}_1\tilde{\alpha}_2\tilde{\alpha}_3}\prod_{i=1}^{3}\left[\mathbf{A}_\Lambda^{-1}[\boldsymbol{J}]\right]_{\tilde{\alpha}_i\tilde{\beta}_i}\left[\mathbf{A}_\Lambda'''[\boldsymbol{J}]\right]_{\tilde{\beta}_1\tilde{\beta}_2\tilde{\beta}_3}, \tag{3.204}$$

where we have defined

$$\left[\mathbf{A}_\Lambda'''[\boldsymbol{J}]\right]_{\tilde{\alpha}_1\tilde{\alpha}_2\tilde{\alpha}_3} = \frac{\delta^3 \mathcal{A}_\Lambda[\boldsymbol{J}]}{\delta J_{\tilde{\alpha}_1}\delta J_{\tilde{\alpha}_2}\delta J_{\tilde{\alpha}_3}}. \tag{3.205}$$

With Eq. (3.176) we can show that the Fourier-space components of $\tilde{\mathbf{\Psi}}_\Lambda'''[0]$ are given by

$$\tilde{\Psi}_\Lambda^{zzz}(K_1,K_2,K_3) = -\prod_{i=1}^{3}\left[1 + V_\Lambda(\boldsymbol{k}_i)G_\Lambda^{zz}(K_i)\right]^{-1} G_\Lambda^{zzz}(K_1,K_2,K_3), \tag{3.206a}$$

$$\tilde{\Psi}_\Lambda^{+-z}(K_1,K_2,K_3) = -\frac{G_\Lambda^{+-z}(-K_1,-K_2,K_3)}{G_\Lambda^{+-}(-K_1)G_\Lambda^{+-}(K_2)\left[1 + V_\Lambda(\boldsymbol{k}_3)G_\Lambda^{zz}(K_3)\right]}, \tag{3.206b}$$

which relates the irreducible three-point vertices to the connected spin correlators. For the initial condition of isolated spins it is then straightforward to evaluate these expression explicitly,

$$\tilde{\Psi}_0^{zzz}(K_1,K_2) = -\delta(K_1)\delta(K_2)b'', \tag{3.207a}$$

$$b\tilde{\Psi}_0^{+-z}(K_1,K_2) = 1 - \delta(K_1+K_2)\frac{b'}{b}(h - i\omega_2), \tag{3.207b}$$

where we have parametrized

$$\tilde{\Psi}_\Lambda^{zzz}(K_1,K_2,K_3) = \delta(K_1+K_2+K_3)\tilde{\Psi}_\Lambda^{zzz}(K_1,K_2), \tag{3.208a}$$

$$\tilde{\Psi}_\Lambda^{+-z}(K_1,K_2,K_3) = \delta(K_1+K_2-K_3)\tilde{\Psi}_\Lambda^{+-z}(K_1,K_2). \tag{3.208b}$$

Irreducible four-point vertices

The last case that we will explicitly consider concerns the fourth derivative of the hybrid generating functional,

$$\left[\tilde{\mathbf{\Psi}}^{(4)}_{\Lambda}[\boldsymbol{\eta}]\right]_{\tilde{\alpha}_1\tilde{\alpha}_2\tilde{\alpha}_3\tilde{\alpha}_4} = \frac{\delta^4 \tilde{\Psi}_{\Lambda}[\boldsymbol{\eta}]}{\delta\eta_{\tilde{\alpha}_1}\delta\eta_{\tilde{\alpha}_2}\delta\eta_{\tilde{\alpha}_3}\delta\eta_{\tilde{\alpha}_4}}. \tag{3.209}$$

From Eq. (3.204) it directly follows that

$$\begin{aligned}\left[\tilde{\mathbf{\Psi}}^{(4)}_{\Lambda}[\boldsymbol{\eta}]\right]_{\tilde{\alpha}_1\tilde{\alpha}_2\tilde{\alpha}_3\tilde{\alpha}_4} =& - \sum_{\tilde{\alpha}_1\tilde{\alpha}_2\tilde{\alpha}_3\tilde{\alpha}_4} \prod_{i=1}^{4} \left[\mathbf{A}^{-1}_{\Lambda}[\boldsymbol{J}]\right]_{\tilde{\alpha}_i\tilde{\beta}_i} \left[\mathbf{A}^{(4)}_{\Lambda}[\boldsymbol{J}]\right]_{\tilde{\beta}_1\tilde{\beta}_2\tilde{\beta}_3\tilde{\beta}_4} \\ &+ \frac{1}{2}\,\mathcal{S}_{\tilde{\alpha}_1\tilde{\alpha}_2;\tilde{\alpha}_3\tilde{\alpha}_4} \sum_{\tilde{\beta}_1\tilde{\beta}_2} \left[\tilde{\mathbf{\Psi}}'''_{\Lambda}[\boldsymbol{\eta}]\right]_{\tilde{\alpha}_1\tilde{\alpha}_2\tilde{\beta}_1} \left[\mathbf{A}_{\Lambda}[\boldsymbol{J}]\right]_{\tilde{\beta}_1\tilde{\beta}_2} \left[\tilde{\mathbf{\Psi}}'''_{\Lambda}[\boldsymbol{\eta}]\right]_{\tilde{\beta}_2\tilde{\alpha}_3\tilde{\alpha}_4},\end{aligned} \tag{3.210}$$

where

$$\left[\mathbf{A}^{(4)}_{\Lambda}[\boldsymbol{J}]\right]_{\tilde{\alpha}_1\tilde{\alpha}_2\tilde{\alpha}_3\tilde{\alpha}_4} = \frac{\delta^4 \mathcal{A}_{\Lambda}[\boldsymbol{J}]}{\delta J_{\tilde{\alpha}_1}\delta J_{\tilde{\alpha}_2}\delta J_{\tilde{\alpha}_3}\delta J_{\tilde{\alpha}_4}}. \tag{3.211}$$

Setting $\boldsymbol{\eta} = 0$ and transforming into Fourier space, we find that the fully longitudinal irreducible four-point vertex is given by

$$\tilde{\Psi}^{zzzz}_{\Lambda}(K_1,K_2,K_3,K_4) = -\prod_{i=1}^{4}\left[1+V_{\Lambda}(\boldsymbol{k}_i)G^{zz}_{\Lambda}(K_i)\right]^{-1} G^{zzzz}_{\Lambda}(K_1,K_2,K_3,K_4), \tag{3.212}$$

the mixed irreducible four-point vertex reads

$$\begin{aligned}&\tilde{\Psi}^{+-zz}_{\Lambda}(K_1,K_2,K_3,K_4) \\ &= -\frac{G^{+-zz}_{\Lambda}(-K_1,-K_2,K_3,K_4)}{G^{+-}_{\Lambda}(-K_1)G^{+-}_{\Lambda}(K_2)\left[1+V_{\Lambda}(\boldsymbol{k}_3)G^{zz}_{\Lambda}(K_3)\right]\left[1+V_{\Lambda}(\boldsymbol{k}_4)G^{zz}_{\Lambda}(K_4)\right]} \\ &+\delta(K_1+K_2-K_3-K_4) \\ &\times\Big[\,\mathcal{S}_{K_3;K_4}\,G^{+-}_{\Lambda}(-K_1+K_3)\tilde{\Psi}^{+-z}_{\Lambda}(K_1,-K_1+K_3)\tilde{\Psi}^{+-z}_{\Lambda}(K_1-K_3,K_2) \\ &+V_{\boldsymbol{k}_1+\boldsymbol{k}_2}\left[1+V_{\boldsymbol{k}_1+\boldsymbol{k}_2}G^{zz}_{\Lambda}(K_1+K_2)\right]\tilde{\Psi}^{+-z}_{\Lambda}(K_1,K_2)\tilde{\Psi}^{zzz}_{\Lambda}(K_3,K_4)\Big],\end{aligned} \tag{3.213}$$

and the fully transversal irreducible four-point vertex can be expressed as

$$\begin{aligned}&\tilde{\Psi}^{+-+-}_{\Lambda}(K_1,K_2,K_3,K_4) \\ &= -\frac{G^{+-+-}_{\Lambda}(-K_1,-K_2,-K_3,-K_4)}{G^{+-}_{\Lambda}(-K_1)G^{+-}_{\Lambda}(K_2)G^{+-}_{\Lambda}(-K_3)G^{+-}_{\Lambda}(K_4)} \\ &+\mathcal{S}_{K_1;K_3}\,\delta(K_1+K_2+K_3+K_4)V_{\Lambda}(\boldsymbol{k}_1+\boldsymbol{k}_2)\left[1+V_{\Lambda}(\boldsymbol{k}_1+\boldsymbol{k}_2)G^{zz}_{\Lambda}(K_1+K_2)\right] \\ &\times\tilde{\Psi}^{+-z}_{\Lambda}(K_1,K_2)\tilde{\Psi}^{+-z}_{\Lambda}(K_3,K_4).\end{aligned} \tag{3.214}$$

For vanishing exchange interaction, these objects simplify to

$$\tilde{\Psi}_{\Lambda}^{zzzz}(K_1, K_2, K_3) = -\delta(\omega_1)\delta(\omega_2)\delta(\omega_3)b''', \tag{3.215a}$$

$$\begin{aligned} b\tilde{\Psi}_{\Lambda}^{+-zz}(K_1, K_2, K_3) = &- [\delta(\omega_3) + \delta(\omega_1 + \omega_2 - \omega_3)] \frac{b'}{b} \\ &+ \delta(\omega_3)\delta(\omega_1 + \omega_2 - \omega_3)\frac{2(b')^2 - bb''}{b^2}(h - i\omega_2), \end{aligned} \tag{3.215b}$$

$$\begin{aligned} b^2\tilde{\Psi}_{\Lambda}^{+-+-}(K_1, K_2, K_3) = &\frac{1}{b}(2h + i\omega_1 + i\omega_3) \\ &- [\delta(\omega_1 + \omega_2) + \delta(\omega_3 + \omega_2)] \frac{b'}{b^2}(h + i\omega_1)(h + i\omega_3), \end{aligned} \tag{3.215c}$$

where we have defined

$$\tilde{\Psi}_{\Lambda}^{zzzz}(K_1, K_2, K_3, K_4) = \delta(K_1 + K_2 + K_3 + K_4)\tilde{\Psi}_{\Lambda}^{zzzz}(K_1, K_2, K_3), \tag{3.216a}$$

$$\tilde{\Psi}_{\Lambda}^{+-zz}(K_1, K_2, K_3, K_4) = \delta(K_1 + K_2 - K_3 - K_4)\tilde{\Psi}_{\Lambda}^{+-zz}(K_1, K_2, K_3), \tag{3.216b}$$

$$\tilde{\Psi}_{\Lambda}^{+-+-}(K_1, K_2, K_3, K_4) = \delta(K_1 + K_2 + K_3 + K_4)\tilde{\Psi}_{\Lambda}^{+-+-}(K_1, K_2, K_3). \tag{3.216c}$$

Although the initial conditions of the irreducible vertices have a non-trivial structure, we note that they all consist of polynomials in the frequencies. This is a direct consequence of the fact that we have performed a Hubbard-Stratonovich transformation only in the longitudinal channel, which initially does not exhibit any dynamics.

3.4.3 Exact flow equations

Exact flow equation of the free energy

To conclude our presentation of the hybrid SFRG approach, we will in the following derive exact flow equations which connect the initial conditions in Sec. 3.4.2 to the corresponding quantities of the fully interacting system. Our starting point is the Wetterich equation for the hybrid generating functional $\tilde{\Psi}_{\Lambda}[\boldsymbol{\eta}]$,

$$\partial_{\Lambda}\tilde{\Psi}_{\Lambda}[\boldsymbol{\eta}] = \frac{1}{2}\operatorname{Tr}\left\{\left[\left(\tilde{\boldsymbol{\Psi}}''_{\Lambda}[\boldsymbol{\eta}] + \bar{\mathbf{R}}_{\Lambda}\right)^{-1} - \mathbf{V}^{z}_{\Lambda}\right]\partial_{\Lambda}\bar{\mathbf{R}}_{\Lambda}\right\} + \sum_{\tilde{\alpha}}\frac{\delta\tilde{\Psi}_{\Lambda}[\boldsymbol{\eta}]}{\delta\eta_{\tilde{\alpha}}}\partial_{\Lambda}\bar{h}_{\Lambda,\tilde{\alpha}}. \tag{3.217}$$

The exact flow equation of the deformed free energy in units of temperature, $\tilde{\Psi}_\Lambda \equiv \tilde{\Psi}_\Lambda[0]$, is obtained by simply setting $\boldsymbol{\eta} = 0$ in Eq. (3.217),

$$\begin{aligned}\partial_\Lambda \tilde{\Psi}_\Lambda &= \frac{1}{2}\,\mathrm{Tr}\left\{\left[\left(\boldsymbol{\Psi}''_\Lambda[0] + \bar{\mathbf{R}}_\Lambda\right)^{-1} - \mathbf{V}^z_\Lambda\right]\partial_\Lambda \bar{\mathbf{R}}_\Lambda\right\} \\ &= -\frac{1}{2}\sum_{\boldsymbol{k},\omega}\left[\partial_\Lambda V_\Lambda(\boldsymbol{k})\right]\frac{\Pi_\Lambda(K)}{1 - V_\Lambda(\boldsymbol{k})\Pi_\Lambda(K)} - \sum_{\boldsymbol{k},\omega}\frac{\partial_\Lambda V_\Lambda(\boldsymbol{k})}{\Sigma_\Lambda(K) - V_\Lambda(\boldsymbol{k})}. \end{aligned} \tag{3.218}$$

Using the deformation scheme $V_\Lambda(\boldsymbol{k}) = \Lambda V_{\boldsymbol{k}}$ and replacing both $\Sigma_\Lambda(K)$ and $\Pi_\Lambda(K)$ by their initial value, we would of course arrive at the same result (3.156) as in the Hubbard-Stratonovich SFRG.

Exact flow equation of the effective magnetic field

To derive the flow equation of the renormalized effective magnetic field $h_\Lambda = h_0 + \bar{h}_\Lambda$, we need to go one level higher in the hierarchy of the irreducible vertices. Using the fact that the irreducible one-point vertex vanishes by construction, we arrive at

$$0 = \frac{1}{2}\,\mathrm{Tr}\left[\dot{\mathbf{A}}_\Lambda \tilde{\boldsymbol{\Psi}}'''_{\Lambda,\tilde{\alpha}}\right] + \sum_{\tilde{\beta}}\left[\tilde{\boldsymbol{\Psi}}''_\Lambda\right]_{\tilde{\alpha}\tilde{\beta}}\partial_\Lambda h_{\Lambda,\tilde{\beta}}, \tag{3.219}$$

where we have introduced the single-scale propagator

$$\dot{\mathbf{A}}_\Lambda = -\mathbf{A}_\Lambda\left(\partial_\Lambda \bar{\mathbf{R}}_\Lambda\right)\mathbf{A}_\Lambda \tag{3.220}$$

as well as the notation

$$\left[\tilde{\boldsymbol{\Psi}}^{(n)}_{\Lambda,\tilde{\alpha}_1\ldots\tilde{\alpha}_{n-2}}\right]_{\tilde{\alpha}_{n-1}\tilde{\alpha}_n} = \left[\tilde{\boldsymbol{\Psi}}^{(n)}_\Lambda\right]_{\tilde{\alpha}_1\ldots\tilde{\alpha}_n} = \left.\frac{\delta^n \tilde{\Psi}_\Lambda[\boldsymbol{\eta}]}{\delta\eta_{\tilde{\alpha}_1}\ldots\delta\eta_{\tilde{\alpha}_n}}\right|_{\boldsymbol{\eta}=0}. \tag{3.221}$$

More explicitly, we find

$$\tilde{\Psi}^{zz}_\Lambda(0)\partial_\Lambda h_\Lambda = -\frac{1}{2}\int_Q \dot{A}^{zz}_\Lambda(Q)\tilde{\Psi}^{zzz}_\Lambda(Q,-Q) - \int_Q \dot{A}^{+-}_\Lambda(Q)\tilde{\Psi}^{+-z}_\Lambda(-Q,Q), \tag{3.222}$$

where the functions

$$\dot{A}^{zz}_\Lambda(K) = \frac{\partial_\Lambda V_\Lambda(\boldsymbol{k})}{\left[1 - V_\Lambda(\boldsymbol{k})\Pi_\Lambda(K)\right]^2}, \tag{3.223}$$

$$\dot{A}^{+-}_\Lambda(K) = \frac{\partial_\Lambda V_\Lambda(\boldsymbol{k})}{\left[\Sigma_\Lambda(\boldsymbol{k}) - V_\Lambda(\boldsymbol{k})\right]^2}, \tag{3.224}$$

are related to the single-scale propagator in Fourier space by

$$\dot{A}^{zz}_\Lambda(K,K') = \delta(K+K')\dot{A}^{zz}_\Lambda(K'), \tag{3.225}$$

$$\dot{A}^{+-}_\Lambda(K,K') = \delta(K+K')\dot{A}^{+-}_\Lambda(K). \tag{3.226}$$

Exact flow equation of the irreducible two-point vertices

Finally, let us derive the exact flow equations of $\Pi_\Lambda(K)$ and $\Sigma_\Lambda(K)$. Differentiating Eq. (3.217) twice with respect to $\boldsymbol{\eta}$ and setting $\boldsymbol{\eta} = 0$ afterwards yields the general relation

$$\partial_\Lambda \left[\tilde{\boldsymbol{\Psi}}''_\Lambda\right]_{\tilde{\alpha}_1\tilde{\alpha}_2} = \frac{1}{2}\operatorname{Tr}\left[\dot{\mathbf{A}}_\Lambda \tilde{\boldsymbol{\Psi}}^{(4)}_{\Lambda,\tilde{\alpha}_1\tilde{\alpha}_2}\right] - \frac{1}{2}\mathcal{S}_{\tilde{\alpha}_1;\tilde{\alpha}_2}\operatorname{Tr}\left[\dot{\mathbf{A}}_\Lambda \tilde{\boldsymbol{\Psi}}'''_{\Lambda,\tilde{\alpha}_1}\mathbf{A}_\Lambda \tilde{\boldsymbol{\Psi}}'''_{\Lambda,\tilde{\alpha}_2}\right] + \sum_{\tilde{\beta}}\left[\tilde{\boldsymbol{\Psi}}'''_\Lambda\right]_{\tilde{\alpha}_1\tilde{\alpha}_2\tilde{\beta}}\partial_\Lambda h_{\Lambda,\tilde{\beta}}, \tag{3.227}$$

whose longitudinal part corresponds to

$$\begin{aligned}\partial_\Lambda \Pi_\Lambda(K) = &-\frac{1}{2}\int_Q \dot{A}^{zz}_\Lambda(Q)\tilde{\Psi}^{zzzz}_\Lambda(Q,-Q,K) - \int_Q \dot{A}^{+-}_\Lambda(Q)\tilde{\Psi}^{+-zz}_\Lambda(-Q,Q,K)\\ &+\int_Q \dot{A}^{zz}_\Lambda(Q)A^{zz}_\Lambda(Q+K)\tilde{\Psi}^{zzz}_\Lambda(Q,-Q-K)\tilde{\Psi}^{zzz}_\Lambda(Q+K,-Q)\\ &+\int_Q\left[\dot{A}^{+-}_\Lambda(Q)A^{+-}_\Lambda(Q+K)+A^{+-}_\Lambda(Q)\dot{A}^{+-}_\Lambda(Q+K)\right]\\ &\qquad\times\tilde{\Psi}^{+-z}_\Lambda(-Q,Q+K)\tilde{\Psi}^{+-z}_\Lambda(-Q-K,Q)\\ &-\tilde{\Psi}^{zzz}_\Lambda(K,-K)\partial_\Lambda h_\Lambda,\end{aligned} \tag{3.228}$$

while the transversal part yields

$$\begin{aligned}\partial_\Lambda \Sigma_\Lambda(K) = &\frac{1}{2}\int_Q \dot{A}^{zz}_\Lambda(Q)\tilde{\Psi}^{+-zz}_\Lambda(-K,K,Q) + \int_Q \dot{A}^{+-}_\Lambda(Q)\tilde{\Psi}^{+-+-}_\Lambda(-K,K,-Q)\\ &-\int_Q\left[\dot{A}^{zz}_\Lambda(Q)A^{+-}_\Lambda(K+Q)+A^{zz}_\Lambda(Q)\dot{A}^{+-}_\Lambda(K+Q)\right]\\ &\qquad\times\tilde{\Psi}^{+-z}_\Lambda(-K,K+Q)\tilde{\Psi}^{+-z}_\Lambda(-K-Q,K)\\ &+\tilde{\Psi}^{+-z}_\Lambda(-K,K)\partial_\Lambda h_\Lambda.\end{aligned} \tag{3.229}$$

A graphical representation of these exact flow equations is shown in the upper and the lower half of Fig. 3.6, respectively.

3.5 Summary and outlook

Before we conclude the present chapter, let us give a short overview on the current status of the SFRG. We have developed three different formulations of our method, which each have their own strengths and shortcomings. The pure SFRG is conceptually very close to the usual formulation of the FRG for bosons and fermions, since it is formulated in terms of connected spin correlators and the corresponding irreducible vertices. With respect to approximation

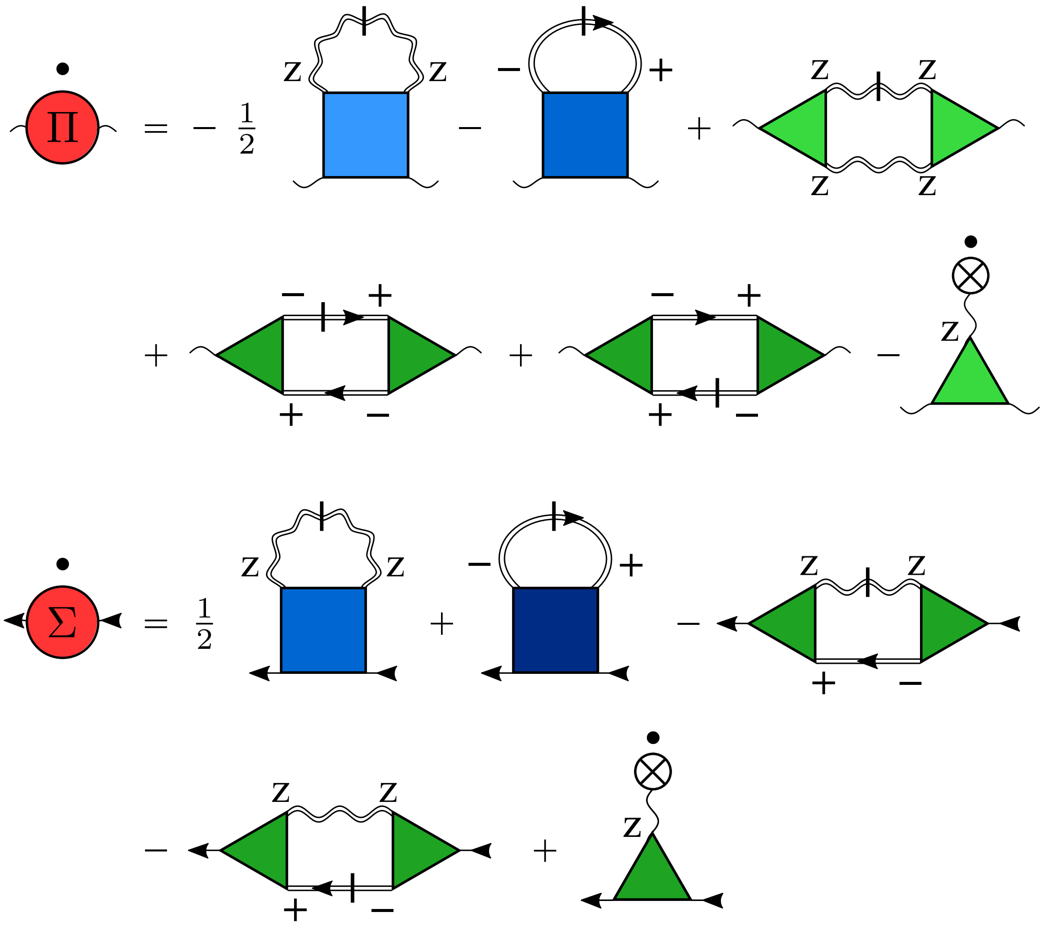

Figure 3.6: Graphical representation of the exact flow equations (3.228) and (3.229) of $\Pi_\Lambda(K)$ and $\Sigma_\Lambda(K)$, respectively. Here $A^{zz}_\Lambda(K)$ is denoted by a double wavy line, while a double solid line refers to $A^{+-}_\Lambda(K)$. A slashed double line of either kind represents the corresponding single-scale propagator, the dot over the diagrams denotes the derivative ∂_Λ, and the renormalized effective magnetic field h_Λ is symbolized by a crossed circle.

strategies, this should allow us to transfer the intuition gained from previous FRG works on bosonic or fermionic fields. An example of this is our application of the pure SFRG to the spin-S Ising model in Sec. 3.2.3, where we have used a simple truncation of the vertex expansion to get quantitatively good results for the critical temperature. When it comes to quantum spin systems, however, a drawback of the pure SFRG are the complicated initial conditions: since the irreducible vertices $\tilde{\mathbf{\Gamma}}^{(n)}_\Lambda$ do not exist in the local limit of isolated spins as discussed in Sec. 3.2.5, we are forced to consider a more complex initial configuration.

This shortcoming is cured in the Hubbard-Stratonovich SFRG, where the irreducible vertices $\tilde{\mathbf{\Phi}}^{(n)}_\Lambda$ are well defined even in the limit of a single spin without an external magnetic field. While the internal structure of the $\mathfrak{su}(2)$ algebra enforces a certain amount of complexity, the initial conditions of the $\tilde{\mathbf{\Phi}}^{(n)}_\Lambda$ can thus be chosen to be comparatively simple. This has enabled us, e.g., to apply the $1/D$ expansion to the spin-S quantum Heisenberg model (see Sec. 3.3.4). Another advantage of the Hubbard-Stratonovich SFRG is its conceptual closeness to the spin-diagrammatic formalism of Vaks, Larkin, and Pikin, which allows us to formulate their ideas in a more powerful yet simpler way. As we have shown in Sec. 3.3.3, it is straightforward to recover their expansion in the inverse interaction within our formalism, while at the same time avoiding the complicated diagrammatic rules of their spin-diagrammatic formalism. A possible disadvantage of the Hubbard-Stratonovich SFRG is that the $\tilde{\mathbf{\Phi}}^{(n)}_\Lambda$ are by construction irreducible with respect to the cutting of a single (effective) interaction line instead of a single propagator line. It might therefore be more difficult to translate common approximation schemes that are known to work within the usual FRG formalism to the Hubbard-Stratonovich SFRG. This is already seen in the $1/D$ expansion of the quantum Heisenberg model mentioned above, where the calculation of the polarization function $\Pi^{zz}_\Lambda(K)$ is only a means to generate the Taylor series of the self-energy $\Gamma^{zz}_\Lambda(K)$; while it would be possible to determine T_c directly from $\Pi^{zz}_\Lambda(K)$, the results turn out to be inferior.

Finally, the hybrid SFRG developed in Sec. 3.4 naturally shares features with both the pure and the Hubbard-Stratonovich SFRG. In terms of complexity of the initial conditions it occupies an intermediate position: while the irreducible vertices $\tilde{\mathbf{\Psi}}^{(n)}_\Lambda$ can still be well defined for isolated spins, this is only possible if the $O(3)$ symmetry of the Heisenberg model is either explicitly or spontaneously broken. While in the present thesis we have not shown a practical application of the hybrid SFRG, preliminary calculations suggest that in the presence of a finite magnetization it might be preferable to the Hubbard-Stratonovich SFRG.

As already discussed in Sec. 3.2.6, promising future applications of the pure SFRG include an extension of our recent work on the Kondo model in Ref. [98] to the strong coupling regime and the study of frustrated spin systems. On the other hand, a specific problem that can be studied within the Hubbard-Stratonovich and the hybrid SFRG is the question about the fate of spin waves in a quantum Heisenberg ferromagnet above the critical temperature. While the total magnetization averaged over the full system vanishes in this regime, this is not the case if we only consider subregions that are small compared to the correlation length ξ. As a consequence, the concept of spin waves should still be meaningful above T_c as long as their wavevector k is much larger than $1/\xi$. Since the initial condition for the magnetization is in our SFRG given by self-consistent mean-field theory, the scale-dependent magnetization $\bar{M}_\Lambda$ can be finite during the flow even in two dimensions. Using a regulator in momentum space to separate short-distance and long-distance fluctuations, we can then study how the properties of spin waves change when we increase the length scale.

Appendix A

Technical details regarding the BKT transition

A.1 Flow equations of the marginal couplings to leading order in $\tilde{y}_l$

As we have shown in Sec. 2.4.3, the flow equation of the marginal couplings $c_\Lambda^{(2n)}$ is for $n = 2, 3, 4$ given by [cf. Eq. (2.121)]

$$\partial_l c_\Lambda^{(2n)} = \frac{c_\Lambda^{(2n+2)}}{4\pi\tau_l} + (-1)^n (4\pi)^{2n-3} \tilde{y}_l^2 + O(\tilde{y}_l^3). \tag{A.1}$$

In the following we will show that this flow equation indeed holds for all $n \geq 2$ by considering the general flow equation of the irreducible $2n$-point vertex. Only retaining terms up to second order in $\tilde{y}_l$, we can parametrize it as

$$\partial_\Lambda \Gamma_\Lambda^{(2n)}(\boldsymbol{k}) = \dot{\Gamma}_\Lambda^{(2n,1)}(\boldsymbol{k}) + \dot{\Gamma}_\Lambda^{(2n,2)}(\boldsymbol{k}), \tag{A.2}$$

where the $\dot{\Gamma}_\Lambda^{(2n,m)}(\boldsymbol{k})$ are defined as containing only terms with exactly m irreducible vertices. This is possible since all $\Gamma_\Lambda^{(2n)}$ for $n \geq 2$ are at least of the order of $\tilde{y}_l$. For $m = 1$ we find [33]

$$\begin{aligned} \dot{\Gamma}_\Lambda^{(2n,1)}(\boldsymbol{k}) &= \frac{1}{2N} \sum_{\boldsymbol{q}} \dot{G}_\Lambda(\boldsymbol{q}) \Gamma_\Lambda^{(2n+2)}(\boldsymbol{q}, -\boldsymbol{q}, \boldsymbol{k}, -\boldsymbol{k}, 0, \ldots, 0) \\ &\approx \frac{A_\Lambda}{2} \Gamma_\Lambda^{(2n+2)}(\boldsymbol{k}), \end{aligned} \tag{A.3}$$

where the coefficient A_Λ was defined in Eq. (2.96) and we have neglected the dependence of the internal vertex $\Gamma_\Lambda^{(2n+2)}$ on the loop momentum $\boldsymbol{q}$, as it would either involve irrelevant couplings or terms of higher order in $\tilde{y}_l$. The second contribution $\dot{\Gamma}_\Lambda^{(2n,2)}(\boldsymbol{k})$ is more complicated; it consists of terms of the form [33]

$$\frac{1}{N}\sum_{\boldsymbol{pq}} \dot{G}_\Lambda(\boldsymbol{q})G_\Lambda(\boldsymbol{p})\Gamma_\Lambda^{(n_1+2)}(\boldsymbol{q},-\boldsymbol{p},\boldsymbol{k}_1,\ldots,\boldsymbol{k}_{n_1})\Gamma_\Lambda^{(n_2+2)}(\boldsymbol{p},-\boldsymbol{q},\boldsymbol{k}_{n_1+1},\ldots,\boldsymbol{k}_{2n}), \tag{A.4}$$

where n_1 and n_2 are positive even integers with $n_1+n_2=n$ and the set of momenta $\{\boldsymbol{k}_1,\ldots,\boldsymbol{k}_{2n}\}$ is a permutation of $\{\boldsymbol{k},-\boldsymbol{k},0,\ldots,0\}$. We can neglect all terms where $\boldsymbol{k}$ and $-\boldsymbol{k}$ belong to the same internal vertex, as they contribute at least to order $\tilde{y}_l^3$ to the flow of $c_\Lambda^{(2n)}$. Approximating the internal vertices in the remaining terms by their momentum-independent parts and taking account of the proper combinatorial factors then gives

$$\dot{\Gamma}_\Lambda^{(2n,2)}(\boldsymbol{k}) \approx -\frac{1}{2}\sum_{n_1=1}^{\infty}\sum_{n_2=1}^{\infty}\delta_{n_1+n_2,2n}\frac{2n_1n_2(2n-2)!}{n_1!n_2!}u_\Lambda^{(n_1+2)}u_\Lambda^{(n_2+2)}B_\Lambda(k), \tag{A.5}$$

where B_Λ was defined in Eq. (2.112). The combinatorial factors in the numerator correspond to the symmetry $\boldsymbol{k}\leftrightarrow-\boldsymbol{k}$, to the n_1 (n_2) possibilities to assign $\boldsymbol{k}$ or $-\boldsymbol{k}$ to the first (second) internal vertex, and to the $(2n-2)!$ possibilities of distributing the remaining vanishing momenta, while the denominator results from the $n_1!$ ($n_2!$) different permutations of the indices of the first (second) internal vertex. Since the relevant couplings $u_\Lambda^{(n)}$ vanish for odd n in our model, we can rewrite this expression using binomial coefficients as

$$\dot{\Gamma}_\Lambda^{(2n,2)}(\boldsymbol{k}) \approx -\sum_{i=1}^{n-1}\binom{2n-2}{2i-1}u_\Lambda^{(2i+2)}u_\Lambda^{(2n-2i+2)}B_\Lambda(k). \tag{A.6}$$

According to Eqs. (2.102) and (2.105) we have

$$u_\Lambda^{(2i+2)}u_\Lambda^{(2n-2i+2)} = (-1)^n c_\Lambda^2\Lambda^4(2\pi)^{2n-2}\tilde{y}_l^2, \tag{A.7}$$

which is clearly independent of the summation index i. The sum can thus be performed analytically, so that

$$\dot{\Gamma}_\Lambda^{(2n,2)}(\boldsymbol{k}) \approx -2^{2n-3}u_\Lambda^{(4)}u_\Lambda^{(2n)}B_\Lambda(k) \tag{A.8}$$

and hence

$$\partial_\Lambda\Gamma_\Lambda^{(2n)}(\boldsymbol{k}) \approx \frac{A_\Lambda}{2}\Gamma_\Lambda^{(2n+2)}(\boldsymbol{k}) - 2^{2n-3}u_\Lambda^{(4)}u_\Lambda^{(2n)}B_\Lambda(k). \tag{A.9}$$

The flow equation of $c_\Lambda^{(2n)}$ is given by the second-order term of a Taylor expansion in k of this expression. Replacing $\partial_\Lambda = -\Lambda^{-1}\partial_l$ and inserting our leading-order results for A_Λ and B_Λ we then recover Eq. (A.1).

A.2 Next-to-leading-order correction to the flow equation of $\tilde{y}_l$

A.2.1 Flow equations of the relevant couplings to next-to-leading order

As we have mentioned at the end of Sec. 2.4.3, we also need to consider the $\tilde{y}_l^2$ correction at $\tau = \pi/2$ to the flow of $\tilde{y}_l$. To this end, we will in the following derive the subleading $\tilde{y}_l^2$ correction to the flow equation of the relevant couplings $u_\Lambda^{(2n)}$, which to leading order is given by [cf. Eq. (2.98)]

$$\partial_l u_\Lambda^{(2n)} = \frac{u_\Lambda^{(2n+2)}}{4\pi\tau_l} + O(y_\Lambda^2), \quad n \in \mathbb{Z}^+. \tag{A.10}$$

We need to compute

$$\partial_\Lambda \Gamma_\Lambda^{(2n)}(0) = \dot{\Gamma}_\Lambda^{(2n,1)}(0) + \dot{\Gamma}_\Lambda^{(2n,2)}(0), \tag{A.11}$$

where we use the same notation as in Eq. (A.2). The first term is in general given by [33]

$$\dot{\Gamma}_\Lambda^{(2n,1)}(0) = \frac{1}{2N}\sum_{\boldsymbol{q}} \dot{G}_\Lambda(\boldsymbol{q})\Gamma_\Lambda^{(2n+2)}(\boldsymbol{q}). \tag{A.12}$$

With the long-wavelength expansion (2.84) this becomes

$$\dot{\Gamma}_\Lambda^{(2n,1)}(0) = \frac{A_\Lambda}{2} u_\Lambda^{(2n+2)} + \frac{A_\Lambda^{(2)}}{4} a^2 c_\Lambda^{(2n+2)}, \tag{A.13}$$

where we have dropped all irrelevant couplings and have defined

$$A_\Lambda^{(2)} = \frac{1}{N}\sum_{\boldsymbol{q}} \dot{G}_\Lambda(\boldsymbol{q}) q^2 = -\frac{\Lambda}{4\pi\tau_l} + O(y_\Lambda). \tag{A.14}$$

Since $c_\Lambda^{(2n+2)}$ is already of second order in y_Λ, it is sufficient to consider only the leading contribution to $A_\Lambda^{(2)}$, while for A_Λ as defined in Eq. (2.96) we also need the first-order correction,

$$A_\Lambda = -\frac{1}{2\pi\tau_\Lambda\Lambda} + \frac{u_\Lambda^{(2)}}{\pi\tau_\Lambda c_\Lambda \Lambda^3} + O(y_\Lambda^2). \tag{A.15}$$

We thus arrive at

$$-\Lambda\dot{\Gamma}_\Lambda^{(2n,1)}(0) = \frac{u_\Lambda^{(2n+2)}}{4\pi\tau_l} - \frac{u_\Lambda^{(2)} u_\Lambda^{(2n+2)}}{2\pi\tau_l c_\Lambda \Lambda^2} + \frac{a^2\Lambda^2 c_\Lambda^{(2n+2)}}{16\pi\tau_l} + O(y_\Lambda^3). \tag{A.16}$$

In the next step we consider the second contribution $\dot{\Gamma}_{\Lambda}^{(2n,2)}(0)$, which we can write as [33]

$$\dot{\Gamma}_{\Lambda}^{(2n,2)}(0) = -\frac{1}{2N}\sum_{n_1,n_2=1}^{\infty}\delta_{2n,n_1+n_2}\frac{(2n)!}{n_1!n_2!}\sum_{\boldsymbol{q}}\dot{G}_{\Lambda}(\boldsymbol{q})G_{\Lambda}(\boldsymbol{q})\Gamma_{\Lambda}^{(n_1+2)}(\boldsymbol{q})\Gamma_{\Lambda}^{(n_2+2)}(\boldsymbol{q}). \tag{A.17}$$

Here the combinatorial factors are due to the $(2n)!$ possibilities of distributing the $2n$ vanishing external momenta on the internal vertices and due to the $n_1!(n_2!)$ different permutations of the indices of the first (second) internal vertex. Since the internal vertices are at least of order y_{Λ}, we can neglect their dependence on the loop-momentum $\boldsymbol{q}$, which results in the simpler expression

$$\dot{\Gamma}_{\Lambda}^{(2n,2)}(0) = -\frac{B_{\Lambda}(0)}{2}\sum_{i=1}^{n-1}\binom{2n}{2i}u_{\Lambda}^{(2i+2)}u_{\Lambda}^{(2n-2i+2)}, \tag{A.18}$$

where we have used the definition (2.112) of $B_{\Lambda}(\boldsymbol{k})$ as well as the fact that vertices with an odd number of legs vanish. With our leading-order result for $B_{\Lambda}(0)$ we can write this as

$$-\Lambda\dot{\Gamma}_{\Lambda}^{(2n,2)}(0) = -\sum_{i=1}^{n-1}\binom{2n}{2i}\frac{u_{\Lambda}^{(2i+2)}u_{\Lambda}^{(2n-2i+2)}}{4\pi\tau_l c_{\Lambda}\Lambda^2}, \tag{A.19}$$

so that in total

$$\partial_l u_{\Lambda}^{(2n)} = \frac{u_{\Lambda}^{(2n+2)}}{4\pi\tau_l} + \frac{a^2\Lambda^2 c_{\Lambda}^{(2n+2)}}{16\pi\tau_l} - \sum_{i=0}^{n}\binom{2n}{2i}\frac{u_{\Lambda}^{(2i+2)}u_{\Lambda}^{(2n-2i+2)}}{4\pi\tau_l c_{\Lambda}\Lambda^2} + O(y_{\Lambda}^3). \tag{A.20}$$

Since we know from Eq. (A.7) that $u_{\Lambda}^{(2i+2)}u_{\Lambda}^{(2n-2i+2)}$ is to second order in y_{Λ} independent of the summation index i, we can explicitly perform the sum to arrive at

$$\partial_l u_{\Lambda}^{(2n)} = \frac{u_{\Lambda}^{(2n+2)}}{4\pi\tau_l} + \frac{a^2\Lambda^2 c_{\Lambda}^{(2n+2)}}{16\pi\tau_l} - \frac{(-1)^n a^2\Lambda^2(4\pi)^{2n-2}\tilde{y}_l^2}{2\pi} + O(y_{\Lambda}^3). \tag{A.21}$$

Inserting our parametrization (2.125) for $c_{\Lambda}^{(2n)}$ then yields

$$\partial_l u_{\Lambda}^{(2n)} = \frac{u_{\Lambda}^{(2n+2)}}{4\pi\tau_l} + (-1)^{n+1}a^2\Lambda^2(4\pi)^{2n-2}\tilde{y}_l^2\left[\frac{\tilde{c}_l}{4\tau_l} + \frac{1}{2\pi}\right] + O(y_{\Lambda}^3), \quad n \in \mathbb{Z}^+. \tag{A.22}$$

A.2.2 Next-to-leading-order correction to $\Gamma_{\Lambda_0}[\bar{m}]$

In order to solve the flow equation (A.22) for the relevant couplings, it is helpful to first consider the y_0^2 correction to the initial value of $\Gamma_\Lambda[\bar{m}]$. We start by expanding $\mathcal{G}_{\Lambda_0}$ up to second order in y_0 [cf. Eq. (2.71)],

$$\mathcal{G}_{\Lambda_0}[\bar{m}] = \sum_i \left[\frac{h_i^2}{2\lambda_0} + \ln\sqrt{\frac{2\pi}{\lambda_0}} + 2y_0\cos\left(\frac{2\pi h_i}{\lambda_0}\right) - 2y_0^2\cos^2\left(\frac{2\pi h_i}{\lambda_0}\right) + O(y_0^3)\right], \tag{A.23}$$

which results in the field-dependent propagator

$$G_{\Lambda_0,\boldsymbol{k}}[h] = \frac{1}{\lambda_0} - \frac{1}{N}\sum_i\left[\frac{8\pi^2 y_0}{\lambda_0^2}\cos\left(\frac{2\pi h_i}{\lambda_0}\right) - \frac{16\pi^2 y_0^2}{\lambda_0^2}\cos\left(\frac{4\pi h_i}{\lambda_0}\right) + O(y_0^3)\right]. \tag{A.24}$$

This allows us to compute $\Gamma^{(2)}_{\Lambda_0,\boldsymbol{k}}[\bar{m}]$ via the relation

$$\Gamma^{(2)}_{\Lambda_0,\boldsymbol{k}}[\bar{m}] = (G_{\Lambda_0,\boldsymbol{k}}[h_{\Lambda_0}[\bar{m}]])^{-1} - R_{\Lambda_0}(\boldsymbol{k}) = (G_{\Lambda_0,\boldsymbol{k}}[h_{\Lambda_0}[\bar{m}]])^{-1} - \lambda_0 + \omega_{\boldsymbol{k}}, \tag{A.25}$$

yielding

$$\begin{aligned}\Gamma^{(2)}_{\Lambda_0,\boldsymbol{k}}[\bar{m}] &= \omega_{\boldsymbol{k}} + \frac{8\pi^2 y_0}{N}\sum_i\cos\left(\frac{2\pi h_{\Lambda_0,i}[\bar{m}]}{\lambda_0}\right)\\ &\quad + \frac{16\pi^2 y_0^2}{N}\sum_i\left[\frac{4\pi^2}{\lambda_0}\cos^2(2\pi\bar{m}_i) - \cos(4\pi\bar{m}_i)\right] + O(y_0^3),\end{aligned} \tag{A.26}$$

where in the second-order term we have already used our first-order result (2.75) for $h_{\Lambda_0,i}[\bar{m}]$,

$$h_{\Lambda_0,i}[\bar{m}] = \lambda_0\bar{m}_i + 4\pi y_0\sin(2\pi\bar{m}_i) + O(y_0^2). \tag{A.27}$$

Also expressing $h_{\Lambda_0,i}[\bar{m}]$ in terms of $\bar{m}_i$ in the first-order term, we find that the momentum-independent part of $\Gamma^{(2)}_{\Lambda,\boldsymbol{k}}[\bar{m}]$ is initially given by

$$\Gamma^{(2)}_{\Lambda_0,\boldsymbol{k}=0}[\bar{m}] = \frac{1}{N}\sum_i\left[8\pi^2 y_0\cos(2\pi\bar{m}_i) + 8\pi^2 y_0^2\frac{\pi^2-2\tau}{\tau}\cos(4\pi\bar{m}_i) + O(y_0^3)\right], \tag{A.28}$$

where we have also used that $\lambda_0 = 8\tau$. The initial value of the relevant couplings $u_\Lambda^{(2n)}$ then results from a simple Taylor expansion of the cosine terms,

$$u_{\Lambda_0}^{(2n)} = (-1)^{n+1}(2\pi)^{2n}2y_0\left[1 + \frac{\pi^2-2\tau}{\tau}4^{n-1}y_0\right] + O(y_0^3). \tag{A.29}$$

For $n = 1$ this becomes

$$u_{\Lambda_0}^{(2)} = (2\pi)^2 2y_0 \left[1 + \frac{\pi^2 - 2\tau}{\tau} y_0\right] + O(y_0^3), \tag{A.30}$$

so that according to the definition (2.89) of the flowing vortex fugacity y_Λ its initial value reads

$$y_{\Lambda_0} = y_0 \left[1 + \frac{\pi^2 - 2\tau}{\tau} y_0\right] + O(y_0^3). \tag{A.31}$$

Since y_Λ is the quantity we actually work with, we finally express y_0 through y_{Λ_0} in Eq. (A.29) to get

$$u_{\Lambda_0}^{(2n)} = (-1)^{n+1}(2\pi)^{2n} 2y_{\Lambda_0} \left[1 + \frac{\pi^2 - 2\tau}{\tau}(4^{n-1} - 1) y_{\Lambda_0}\right] + O(y_{\Lambda_0}^3). \tag{A.32}$$

A.2.3 Evaluation of the $\tilde{y}_l^2$ correction to $\partial_l \tilde{y}_l$

With our results (A.22) and (A.32) we are now in a position to evaluate the $\tilde{y}_l^2$ correction to the flow equation of $\tilde{y}_l$. We first parametrize the flowing relevant couplings $u_\Lambda^{(2n)}$ as

$$u_\Lambda^{(2n)} = (-1)^{n+1}(2\pi)^{2n-3}\tau_l a^2 \Lambda^2 \tilde{y}_l \left[1 + (4^{n-1} - 1) v_l^{(2n)} \tilde{y}_l\right], \quad n \geq 2, \tag{A.33}$$

so that all $v_l^{(2n)}$ have the same initial condition,

$$v_0^{(2n)} = \frac{(\pi^2 - 2\tau)}{2\pi^3}, \tag{A.34}$$

which will be useful in the following. Inserting our ansatz (A.33) into the flow equation (A.22) with $n = 1$ yields

$$\frac{\partial_l \tilde{y}_l}{\tilde{y}_l} = 2 - \frac{\pi}{\tau_l} + \left(\frac{\tilde{c}_l}{2\tau_l} + \frac{1}{\pi} - 3v_l^{(4)}\right)\frac{\pi}{\tau_l}\tilde{y}_l + O(\tilde{y}_l^2). \tag{A.35}$$

On the other hand, for $n \geq 2$ our ansatz gives to leading order in $\tilde{y}_l$

$$\begin{aligned} \partial_l u_\Lambda^{(2n)} = (-1)^{n+1}(2\pi)^{2n-3}\tau_l a^2 \Lambda^2 \tilde{y}_l \Bigg\{ &\left[\frac{\tilde{y}_l}{\tilde{y}_l} - 2\right]\left[1 + \left(4^{n-1} - 1\right) v_l^{(2n)} \tilde{y}_l\right] \\ &+ \left(4^{n-1} - 1\right) \tilde{y}_l \left[\left(2 - \frac{\pi}{\tau_l}\right) v_l^{(2n)} + \partial_l v_l^{(2n)}\right] \Bigg\}, \end{aligned} \tag{A.36}$$

which together with the flow equations (A.22) and (A.35) yields

$$\partial_l \upsilon_l^{(2n)} = 2\left(\frac{\pi}{\tau_l} - 1\right)\upsilon_l^{(2n)} + \frac{\pi}{\tau_l}\left(\frac{\tilde{c}_l}{2\tau_l} + \frac{1}{\pi}\right) - \frac{4\pi\left[(4^n-1)\upsilon_l^{(2n+2)} - 3\upsilon_l^{(4)}\right]}{\tau_l(4^n-4)}. \tag{A.37}$$

This infinite hierarchy of coupled flow equations is solved by the obvious ansatz

$$\upsilon_l^{(2n)} = \upsilon_l^{(4)}, \tag{A.38}$$

which results in the n-independent flow equation

$$\partial_l \upsilon_l^{(4)} = -2\left(1 + \frac{\pi}{\tau_l}\right)\upsilon_l^{(4)} + \frac{\pi}{\tau_l}\left(\frac{\tilde{c}_l}{2\tau_l} + \frac{1}{\pi}\right) + O(\tilde{y}_l). \tag{A.39}$$

We thus arrive at the following set of coupled flow equations,

$$\partial_l \tilde{y}_l = \left(2 - \frac{\pi}{\tau_l}\right)\tilde{y}_l + \left(\frac{\tilde{c}_l}{2\tau_l} + \frac{1}{\pi} - 3\upsilon_l^{(4)}\right)\frac{\pi}{\tau_l}\tilde{y}_l^2, \tag{A.40a}$$

$$\partial_l \tau_l = \frac{\tilde{c}_l \tilde{y}_l^2}{2\tau_l}, \tag{A.40b}$$

$$\partial_l \tilde{c}_l = 1 - \tilde{c}_l\left(4 + \frac{2\pi}{\tau_l}\right), \tag{A.40c}$$

$$\partial_l \upsilon_l^{(4)} = \frac{\pi}{\tau_l}\left(\frac{\tilde{c}_l}{2\tau_l} + \frac{1}{\pi}\right) - 2\left(1 + \frac{\pi}{\tau_l}\right)\upsilon_l^{(4)}. \tag{A.40d}$$

Close to the line of Gaussian fixed points at $\tilde{y}_l = 0$ and $\tau_l \leq \pi/2$ we find that $\tilde{c}_l$ and $\upsilon_l^{(4)}$ rapidly converge to

$$\tilde{c}_l = \frac{1}{4 + \frac{2\pi}{\tau_l}}, \tag{A.41}$$

$$\upsilon_l^{(4)} = \frac{8\tau_l + 5\pi}{8\left(\tau_l + \pi\right)\left(2\tau_l + \pi\right)}, \tag{A.42}$$

which finally allows us to write the flow equation of $\tilde{y}_l$ as

$$\partial_l \tilde{y}_l = \left(2 - \frac{\pi}{\tau_l}\right)\tilde{y}_l + \frac{8\tau_l + 5\pi}{8\left(\tau_l + \pi\right)\left(2\tau_l + \pi\right)}\left(2 - \frac{\pi}{\tau_l}\right)\tilde{y}_l^2 + O(\tilde{y}_l^3). \tag{A.43}$$

A.3 Flow of the additional coupling $\tilde{g}_l$ due to amplitude fluctuations

A.3.1 Derivation of the flow equation of $\tilde{g}_l$

In this section we will derive the flow equation of the quartic coupling g_Λ, which according to Sec. 2.6 has a non-zero initial value in the $O(2)$ model due to amplitude fluctuations. In addition to approximating the irreducible vertices by their long-wavelength expansion as was done for the XY model [cf. Eq. (2.84)],

$$\Gamma_\Lambda^{(2n)}(\boldsymbol{k}, -\boldsymbol{k}, 0, \ldots, 0) = u_\Lambda^{(2n)} + \frac{1}{2} c_\Lambda^{(2n)} a^2 k^2 + O(\boldsymbol{k}^4), \tag{A.44}$$

we therefore also include a higher-order momentum dependence of the four-point vertex via the term

$$-\frac{g_\Lambda}{4!N} \sum_{\boldsymbol{k}_1\boldsymbol{k}_2\boldsymbol{k}_3\boldsymbol{k}_4} \delta_{\boldsymbol{k}_1+\boldsymbol{k}_2+\boldsymbol{k}_3+\boldsymbol{k}_4,0} V_{\boldsymbol{k}_1,\boldsymbol{k}_2,\boldsymbol{k}_3,\boldsymbol{k}_4} \bar{m}_{\boldsymbol{k}_1} \bar{m}_{\boldsymbol{k}_2} \bar{m}_{\boldsymbol{k}_3} \bar{m}_{\boldsymbol{k}_4}, \tag{A.45}$$

where $V_{\boldsymbol{k}_1,\boldsymbol{k}_2,\boldsymbol{k}_3,\boldsymbol{k}_4}$ was defined in Eqs. (2.212) and (2.213). Since

$$V_{\boldsymbol{k},\boldsymbol{k},-\boldsymbol{k},-\boldsymbol{k}} \approx a^4 k^4 \tag{A.46}$$

in the long-wavelength limit, we find that the flow equation of g_Λ is given by

$$\begin{aligned} \partial_\Lambda g_\Lambda &= -\frac{1}{4!a^4} \lim_{k\to 0} \partial_k^4 \partial_\Lambda \Gamma^{(4)}_{\Lambda,\boldsymbol{k},\boldsymbol{k},-\boldsymbol{k},-\boldsymbol{k}} \\ &= \frac{1}{4!a^4 N} \sum_{\boldsymbol{p}} \dot{G}_\Lambda(\boldsymbol{p}) \lim_{k\to 0} \partial_k^4 \Bigg[2G_\Lambda(\boldsymbol{p}) \left(\Gamma^{(4)}_{\Lambda,\boldsymbol{p},-\boldsymbol{p},\boldsymbol{k},-\boldsymbol{k}}\right)^2 \\ &\qquad + G_\Lambda(\boldsymbol{p}+2\boldsymbol{k}) \left(\Gamma^{(4)}_{\Lambda,\boldsymbol{p},-\boldsymbol{p}-2\boldsymbol{k},\boldsymbol{k},\boldsymbol{k}}\right)^2 \Bigg]. \end{aligned} \tag{A.47}$$

Up to second order in y_Λ and g_Λ, we can write this more explicitly as

$$\begin{aligned} \partial_\Lambda g_\Lambda = {} & \frac{1}{4!a^4 N} \sum_{\boldsymbol{p}} \dot{G}_\Lambda(\boldsymbol{p}) \\ & \times \lim_{k\to 0} \Bigg[\left(u_\Lambda^{(4)}\right)^2 \partial_k^4 G_\Lambda(\boldsymbol{p}+2\boldsymbol{k}) - 12 u_\Lambda^{(4)} g_\Lambda \left(\partial_k^2 G_\Lambda(\boldsymbol{p}+2\boldsymbol{k})\right) \partial_k^2 V_{\boldsymbol{p},-\boldsymbol{p}-2\boldsymbol{k},\boldsymbol{k},\boldsymbol{k}} \\ & \qquad + 18 g_\Lambda^2 G_\Lambda(\boldsymbol{p}) \left(\partial_k^2 V_{\boldsymbol{p},-\boldsymbol{p},\boldsymbol{k},-\boldsymbol{k}}\right)^2 \Bigg]. \end{aligned} \tag{A.48}$$

For the second and third term we need the long-wavelength expansion

$$V_{\boldsymbol{p},-\boldsymbol{p},\boldsymbol{k},-\boldsymbol{k}} \approx -V_{\boldsymbol{p},-\boldsymbol{p}-2\boldsymbol{k},\boldsymbol{k},\boldsymbol{k}} \approx \frac{a^4 p^2 k^2}{3} \left(1 + 2\cos^2\varphi_p\right), \tag{A.49}$$

and in turn

$$\frac{1}{N} \sum_{\boldsymbol{p}} p^2 \left(1 + 2\cos^2\varphi_p\right) \dot{G}_\Lambda(\boldsymbol{p}) \lim_{k\to 0} \partial_k^2 G_\Lambda(\boldsymbol{p}+2\boldsymbol{k}) = \frac{5}{\pi \tau_\Lambda^2 a^2 \Lambda^3} + O(\tilde{y}_l). \tag{A.50}$$

The first term involving the fourth derivative of the propagator is more complicated; a rather tedious calculation yields

$$\frac{1}{4!a^4N}\sum_{\boldsymbol{p}}\dot{G}_\Lambda(\boldsymbol{p})\lim_{k\to 0}\partial_k^4 G_\Lambda(\boldsymbol{p}+2\boldsymbol{k}) = \frac{2}{\pi\tau_\Lambda^2 a^6\Lambda^7} + O(\tilde{y}_l), \tag{A.51}$$

so that in total the flow equation of g_Λ becomes

$$\partial_l g_\Lambda = -\frac{8\pi\tilde{y}_l^2}{a^2\Lambda^2} + \frac{10\tilde{y}_l g_\Lambda}{3\tau_l} + \frac{a^2\Lambda^2 g_\Lambda^2}{4\pi\tau_\Lambda^2} + O(\tilde{y}_l^3, \tilde{y}_l^2 g_\Lambda, \tilde{y}_l g_\Lambda^2, g_\Lambda^3). \tag{A.52}$$

In terms of the rescaled coupling

$$\tilde{g}_l = \frac{c_\Lambda\Lambda^2}{2\pi} g_\Lambda, \tag{A.53}$$

this flow equation simplifies to

$$\partial_l\tilde{g}_l = \left(-2 + \frac{10\tilde{y}_l}{3\tau_l} + \frac{\tilde{g}_l}{2\tau_l^3}\right)\tilde{g}_l - 4\tau_l\tilde{y}_l^2 \approx -2\tilde{g}_l - 4\tau_l\tilde{y}_l^2. \tag{A.54}$$

As mentioned in Sec. 2.6.2, for $\tau_l \approx \pi/2$ and $\tilde{y}_l \ll 1$ this results in the asymptotic behaviour

$$\tilde{g}_l \underset{l\to\infty}{\sim} -2\tau_l\tilde{y}_l^2, \tag{A.55}$$

which justifies neglecting the second and third term in Eq. (A.54).

A.3.2 Effect of $\tilde{g}_l$ on the flow equation of τ_l

We are now in a position to evaluate the effect of a finite $\tilde{g}_l$ on the flowing dimensionless temperature τ_l, which obeys the exact flow equation

$$\partial_\Lambda\tau_l = \frac{1}{4a^2N}\sum_{\boldsymbol{q}}\dot{G}_\Lambda(\boldsymbol{q})\lim_{k\to 0}\partial_k^2\Gamma_\Lambda^{(4)}(\boldsymbol{k},-\boldsymbol{k},\boldsymbol{q},-\boldsymbol{q}). \tag{A.56}$$

Inserting our result (2.129) for $\partial_l\tau_l$ from the XY model and using the long-wavelength expansion (A.49) as well as

$$\frac{1}{N}\sum_{\boldsymbol{q}}\dot{G}_\Lambda(\boldsymbol{q})q^2\left(1+2\cos^2\varphi_q\right) = -\frac{\Lambda}{2\pi\tau_\Lambda} + O\left(\tilde{y}_\Lambda\right), \tag{A.57}$$

we find to leading order

$$\partial_l\tau_\Lambda = \frac{\tilde{y}_l^2}{8\tau_l+4\pi} + \frac{g_\Lambda\Lambda}{4a^2N}\sum_{\boldsymbol{q}}\dot{G}_\Lambda(\boldsymbol{q})\lim_{k\to 0}\partial_k^2 V_{\boldsymbol{k},-\boldsymbol{k},\boldsymbol{q},-\boldsymbol{q}} = \frac{\tilde{y}_l^2}{8\tau_l+4\pi} - \frac{g_\Lambda a^2\Lambda^2}{12\pi\tau_\Lambda}. \tag{A.58}$$

In terms of the rescaled coupling $\tilde{g}_l$ this becomes

$$\partial_l \tau_l = \frac{\tilde{y}_l^2}{8\tau_l + 4\pi} - \frac{\tilde{g}_l}{6\tau_l^2}. \tag{A.59}$$

Finally, in the regime close to the BKT transition we may approximate $\tau_l \approx \pi/2$ and insert our result (A.55) for the asymptotic behaviour of $\tilde{g}_l$, so that

$$\partial_l \tau_l = \frac{\tilde{y}_l^2}{8\pi}\left(1 + \frac{16}{3}\right). \tag{A.60}$$

Appendix B

Technical details regarding the spin FRG

B.1 $1/D$ expansion of $\Gamma_\Lambda^{(2)}$ in the spin-S Ising model

B.1.1 Alternative derivation of the leading correction to $\Gamma_0^{(2)}$

In Sec. 3.2.4 we have used the pure SFRG formalism to derive the leading correction in $1/D$ to the irreducible two-point vertex $\Gamma_0^{(2)}(\boldsymbol{k})$ within the spin-S Ising model,

$$\Gamma_{\Lambda=1}^{(2)}(\boldsymbol{k}) = \frac{1}{b'}\left[1 - \gamma_{\boldsymbol{k}} g - \frac{b''' g^2}{4(b')^2 D} + O(D^{-2})\right], \tag{B.1}$$

where we have assumed a nearest-neighbor interaction on a D-dimensional hypercubic lattice. While it is straightforward to extend this calculation to higher orders in $1/D$, we will in the following choose a slightly different way: instead of working within the pure SFRG formalism, we employ the Hubbard-Stratonovich SFRG developed in Sec. 3.3. This has the advantage that our procedure can be directly generalized to the spin-S quantum Heisenberg model, which would not be possible within the pure SFRG. While in Sec. 3.3 we have derived the Hubbard-Stratonovich SFRG for the Heisenberg model, it is easy to apply our formalism to the Ising model. We therefore restrict ourselves to purely longitudinal correlators, which are now time independent since all operators in the zero-field Ising model commute with each other.

To demonstrate the procedure, we start by rederiving the leading-order result (B.1). Adapting Eq. (3.160) to the Ising model, we see that the exact flow equation of the polarization function $\Pi_\Lambda^{zz}(K) = \delta(\omega)\Pi_\Lambda(\boldsymbol{k})$ is for $h_\Lambda = 0$ given by

$$\partial_\Lambda \Pi_\Lambda(\boldsymbol{k}) = -\frac{1}{2}\int_{\boldsymbol{q}} \dot{F}_\Lambda(\boldsymbol{q})\tilde{\Phi}_\Lambda^{(4)}(\boldsymbol{q}, -\boldsymbol{q}, \boldsymbol{k}), \tag{B.2}$$

where $\int_{\boldsymbol{q}} = \frac{1}{N}\sum_{\boldsymbol{q}}$ and we have introduced the notation

$$\tilde{\Phi}_\Lambda^{zzzz}(K_1, K_2, K_3) = \delta(\omega_1)\delta(\omega_2)\delta(\omega_3)\tilde{\Phi}_\Lambda^{(4)}(\boldsymbol{k}_1, \boldsymbol{k}_2, \boldsymbol{k}_3). \tag{B.3}$$

Again using the deformation scheme $V_\Lambda(\boldsymbol{k}) = \Lambda V_{\boldsymbol{k}}$, we find that the single-scale propagator $\dot{F}_\Lambda(\boldsymbol{k})$ reads

$$\dot{F}_\Lambda(\boldsymbol{k}) = \beta \dot{F}_\Lambda^{zz}(K) = \frac{\beta V_{\boldsymbol{k}}}{[1 - \Lambda\beta V_{\boldsymbol{k}}\Pi_\Lambda(\boldsymbol{k})]^2}, \tag{B.4}$$

so that the exact flow equation of $\Pi_\Lambda(\boldsymbol{k})$ becomes

$$\partial_\Lambda \Pi_\Lambda(\boldsymbol{k}) = -\frac{1}{2}\int_{\boldsymbol{q}} \frac{\beta V_{\boldsymbol{q}}\tilde{\Phi}_\Lambda^{(4)}(\boldsymbol{q}, -\boldsymbol{q}, \boldsymbol{k})}{[1 - \Lambda\beta V_{\boldsymbol{q}}\Pi_\Lambda(\boldsymbol{q})]^2}. \tag{B.5}$$

To leading order in $1/D$, we can replace Π_Λ and $\tilde{\Phi}_\Lambda^{(4)}$ on the right-hand side of Eq. (B.5) by their initial conditions $\Pi_0 = b'$ and $\tilde{\Phi}_0^{(4)} = -b'''$, respectively, and expand the denominator to first order in $V_{\boldsymbol{q}}$,

$$\partial_\Lambda \Pi_\Lambda(\boldsymbol{k}) = \frac{1}{2}\int_{\boldsymbol{q}} \beta V_{\boldsymbol{q}} b''' \left[1 + 2\Lambda\beta V_{\boldsymbol{q}} b'\right] = \frac{\Lambda b''' g^2}{2b' D}, \tag{B.6}$$

where we have again used the notation

$$V_{\boldsymbol{k}} = V_0\gamma_{\boldsymbol{k}} \quad \text{with} \quad \gamma_{\boldsymbol{k}} = \frac{1}{D}\sum_{i=1}^{D}\cos(k_i a) \tag{B.7}$$

and $g = \beta b' V_0$. Integrating Eq. (B.6) then yields the polarization function to leading order in $1/D$,

$$\Pi_\Lambda(\boldsymbol{k}) = b'\left[1 + \frac{\Lambda^2 b''' g^2}{4(b')^2 D} + O(D^{-2})\right]. \tag{B.8}$$

To make contact with our previous calculation in Sec. 3.2.4, we use the exact relation (3.135a) between $\Pi_\Lambda^{zz}(K)$ and $\Gamma_\Lambda^{zz}(K)$, which in the Ising model can be written as

$$\Gamma_\Lambda^{(2)}(\boldsymbol{k}) = \frac{1}{\Pi_\Lambda(\boldsymbol{k})} - \beta V_{\boldsymbol{k}}. \tag{B.9}$$

Inserting our leading-order result (B.8) for $\Lambda = 1$ and expanding the denominator to first order in $1/D$, we recover our earlier result (B.1).

B.1.2 Next-to-leading-order correction

First-order correction to the irreducible four-point vertex

In order to calculate the second-order correction in $1/D$, we need the leading correction to the irreducible four-point vertex. Its exact flow equation reads

$$\partial_\Lambda \tilde{\Phi}^{(4)}_{\Lambda,1234} = \frac{1}{2}\,\mathrm{Tr}\left[\dot{F}_\Lambda \tilde{\Phi}^{(6)}_{\Lambda,1234}\right] - \frac{1}{2}\mathcal{S}_{12;34}\,\mathrm{Tr}\left[\dot{F}_\Lambda \tilde{\Phi}^{(4)}_{\Lambda,12} F_\Lambda \tilde{\Phi}^{(4)}_{\Lambda,34}\right], \tag{B.10}$$

where the objects inside the trace are to be understood as matrices in momentum space in the obvious way and we have defined

$$\tilde{\Phi}^{(n)}_{\Lambda,1\ldots n} = \delta_{\boldsymbol{k}_1+\ldots+\boldsymbol{k}_n,0}\tilde{\Phi}^{(n)}_\Lambda(\boldsymbol{k}_1,\ldots,\boldsymbol{k}_{n-1}) \tag{B.11}$$

as well as

$$\mathcal{S}_{12;34} = \mathcal{S}_{\boldsymbol{k}_1,\boldsymbol{k}_2;\boldsymbol{k}_3,\boldsymbol{k}_4} \tag{B.12}$$

to simplify the notation. The first term is more explicitly given by

$$\frac{1}{2}\,\mathrm{Tr}\left[\dot{F}_\Lambda \tilde{\Phi}^{(6)}_{\Lambda,1234}\right] = \frac{1}{2}\int_{\boldsymbol{q}} \frac{\beta V_{\boldsymbol{q}} \tilde{\Phi}^{(6)}_{\Lambda,1234,\boldsymbol{q},-\boldsymbol{q}}}{[1-\Lambda\beta V_{\boldsymbol{q}}\Pi_{\Lambda,\boldsymbol{q}}]^2}, \tag{B.13}$$

where

$$\tilde{\Phi}^{(6)}_{\Lambda,1234,\boldsymbol{q},-\boldsymbol{q}} = \tilde{\Phi}^{(6)}_\Lambda(\boldsymbol{k}_1,\ldots,\boldsymbol{k}_4,\boldsymbol{q},-\boldsymbol{q}) \tag{B.14}$$

and

$$\Pi_{\Lambda,\boldsymbol{q}} = \Pi_\Lambda(\boldsymbol{q}). \tag{B.15}$$

Similar to the calculation in the previous section, we approximate $\Pi_{\Lambda,\boldsymbol{q}} \approx \Pi_{0,\boldsymbol{q}} = b'$ as well as $\tilde{\Phi}^{(6)}_{\Lambda,1234,\boldsymbol{q},-\boldsymbol{q}} \approx \tilde{\Phi}^{(6)}_{0,1234,\boldsymbol{q},-\boldsymbol{q}} = -b^{(5)}$ and expand the denominator to first order in the exchange interaction. We then find

$$\frac{1}{2}\,\mathrm{Tr}\left[\dot{F}_\Lambda \tilde{\Phi}^{(6)}_{\Lambda,1234}\right] \approx -\frac{1}{2}\int_{\boldsymbol{q}} \beta V_{\boldsymbol{q}} b^{(5)}\left[1+2\Lambda\beta V_{\boldsymbol{q}} b'\right] = -\frac{\Lambda b^{(5)} g^2}{2b'D}. \tag{B.16}$$

For the second term in Eq. (B.10) we have to consider

$$\begin{aligned}\frac{1}{2}\,\mathrm{Tr}\left[\dot{F}_\Lambda \tilde{\Phi}^{(4)}_{\Lambda,12} F_\Lambda \tilde{\Phi}^{(4)}_{\Lambda,34}\right] &= \frac{1}{2}\int_{\boldsymbol{q}} \frac{\Lambda\beta^2 V_{\boldsymbol{q}} V_{\boldsymbol{q}+1+2} \tilde{\Phi}^{(4)}_{\Lambda,12,\boldsymbol{q},-\boldsymbol{q}-1-2} \tilde{\Phi}^{(4)}_{\Lambda,34,-\boldsymbol{q},\boldsymbol{q}+1+2}}{[1-\Lambda\beta V_{\boldsymbol{q}}\Pi_{\Lambda,\boldsymbol{q}}]^2\,[1-\Lambda\beta V_{\boldsymbol{q}+1+2}\Pi_{\Lambda,\boldsymbol{q}+1+2}]} \\ &\approx \frac{\Lambda(b''')^2 g^2}{2(b')^2}\int_{\boldsymbol{q}} \gamma_{\boldsymbol{q}}\gamma_{\boldsymbol{q}+1+2} = \frac{\Lambda(b''')^2 g^2 \gamma_{1+2}}{4(b')^2 D},\end{aligned} \tag{B.17}$$

where we have used

$$\int_{\boldsymbol{q}} \gamma_{\boldsymbol{q}} \gamma_{\boldsymbol{q}+\boldsymbol{k}} = \frac{\gamma_{\boldsymbol{k}}}{2D}. \tag{B.18}$$

We thus find

$$\partial_\Lambda \tilde{\Phi}^{(4)}_{\Lambda,1234} = -\frac{\Lambda b^{(5)} g^2}{2b' D} - \frac{\Lambda (b''')^2 g^2}{4(b')^2 D} \mathcal{S}_{12;34}\, \gamma_{1+2}, \tag{B.19}$$

which integrates to

$$\tilde{\Phi}^{(4)}_{\Lambda,1234} = -b''' - \frac{\Lambda^2 b^{(5)} g^2}{4b' D} - \frac{\Lambda^2 (b''')^2 g^2}{8(b')^2 D} \mathcal{S}_{12;34}\, \gamma_{1+2}. \tag{B.20}$$

More explicitly, the last part is given by

$$\mathcal{S}_{12;34}\, \gamma_{1+2} = \gamma_{\boldsymbol{k}_1+\boldsymbol{k}_2} + \gamma_{\boldsymbol{k}_1+\boldsymbol{k}_3} + \gamma_{\boldsymbol{k}_1+\boldsymbol{k}_4} + \gamma_{\boldsymbol{k}_2+\boldsymbol{k}_3} + \gamma_{\boldsymbol{k}_2+\boldsymbol{k}_4} + \gamma_{\boldsymbol{k}_3+\boldsymbol{k}_4}, \tag{B.21}$$

which for $\{\boldsymbol{k}_1, \boldsymbol{k}_2, \boldsymbol{k}_3, \boldsymbol{k}_4\} = \{\boldsymbol{q}, -\boldsymbol{q}, \boldsymbol{k}, -\boldsymbol{k}\}$ simplifies to

$$\mathcal{S}_{12;34}\, \gamma_{1+2} = 2 + 2(\gamma_{\boldsymbol{k}+\boldsymbol{q}} + \gamma_{\boldsymbol{k}-\boldsymbol{q}}), \tag{B.22}$$

so that to leading order

$$\tilde{\Phi}^{(4)}_{\Lambda}(\boldsymbol{q}, -\boldsymbol{q}, \boldsymbol{k}) = -b''' - \frac{\Lambda^2 \left[b' b^{(5)} + (b''')^2 \right] g^2}{4(b')^2 D} - \frac{\Lambda^2 (b''')^2 g^2 (\gamma_{\boldsymbol{k}+\boldsymbol{q}} + \gamma_{\boldsymbol{k}-\boldsymbol{q}})}{4(b')^2 D}. \tag{B.23}$$

Second-order correction to the irreducible two-point vertex

We can now insert our results (B.8) and (B.23) in the exact flow equation (B.5) of $\Pi_\Lambda(\boldsymbol{k})$ to compute its next-to-leading-order correction. We start with the $\boldsymbol{q}$-independent part of $\tilde{\Phi}^{(4)}_{\Lambda}$. Since the resulting calculation is basically identical to the one leading to Eq. (B.6), we can just replace

$$\frac{\Lambda g^2}{2b' D} b''' \to \frac{\Lambda g^2}{2b' D} \frac{\Lambda^2 \left[b' b^{(5)} + (b''')^2 \right] g^2}{4(b')^2 D} = \frac{\Lambda^3 \left[b' b^{(5)} + (b''')^2 \right] g^4}{8(b')^3 D^2} \tag{B.24}$$

to find its second-order contribution. On the other hand, the $\boldsymbol{q}$-dependent part of $\tilde{\Phi}^{(4)}_{\Lambda}$ results in

$$\begin{aligned} \frac{\Lambda^2 (b''')^2 g^3}{8(b')^3 D} \int_{\boldsymbol{q}} \frac{\gamma_{\boldsymbol{q}} (\gamma_{\boldsymbol{k}+\boldsymbol{q}} + \gamma_{\boldsymbol{k}-\boldsymbol{q}})}{[1 - \Lambda \beta V_{\boldsymbol{q}} \Pi_{\Lambda,\boldsymbol{q}}]^2} &\approx \frac{\Lambda^2 (b''')^2 g^3}{8(b')^3 D} \int_{\boldsymbol{q}} \gamma_{\boldsymbol{q}} (\gamma_{\boldsymbol{k}+\boldsymbol{q}} + \gamma_{\boldsymbol{k}-\boldsymbol{q}}) \\ &= \frac{\Lambda^2 (b''')^2 g^3 \gamma_{\boldsymbol{k}}}{8(b')^3 D^2}. \end{aligned} \tag{B.25}$$

The last second-order contribution comes from the denominator in Eq. (B.5),

$$\begin{aligned}
&\frac{b'''g}{2b'}\int_{\boldsymbol{q}}\frac{\gamma_{\boldsymbol{q}}}{[1-\Lambda\beta V_{\boldsymbol{q}}\Pi_{\Lambda,\boldsymbol{q}}]^2}\\
\approx&\frac{b'''g}{2b'}\int_{\boldsymbol{q}}\gamma_{\boldsymbol{q}}\left[1+2\Lambda\beta V_{\boldsymbol{q}}\Pi_{\Lambda,\boldsymbol{q}}+3\left(\Lambda\beta V_{\boldsymbol{q}}\Pi_{0,\boldsymbol{q}}\right)^2+4\left(\Lambda\beta V_{\boldsymbol{q}}\Pi_{0,\boldsymbol{q}}\right)^3\right]\\
=&\frac{b'''g}{2b'}\int_{\boldsymbol{q}}\gamma_{\boldsymbol{q}}\left[2\Lambda\beta V_{\boldsymbol{q}}\Pi_{\Lambda,\boldsymbol{q}}+4\left(\Lambda g\gamma_{\boldsymbol{q}}\right)^3\right]. \qquad \text{(B.26)}
\end{aligned}$$

Inserting our leading-order result (B.8) for $\Pi_\Lambda(\boldsymbol{k})$ then yields the second-order contribution

$$\frac{\Lambda b'''g^2}{b'}\int_{\boldsymbol{q}}\gamma_{\boldsymbol{q}}^2\left[\frac{\Lambda^2 b'''g^2}{4(b')^2D}+2\Lambda^2g^2\gamma_{\boldsymbol{q}}^2\right]\approx\frac{\Lambda^3\left[(b''')^2+12(b')^2b'''\right]g^4}{8(b')^3D^2}, \qquad \text{(B.27)}$$

where we have used

$$\int_{\boldsymbol{q}}\gamma_{\boldsymbol{q}}^4=\frac{3}{4D^2}-\frac{3}{8D^3}. \qquad \text{(B.28)}$$

Combining our results (B.24), (B.25), and (B.27) we find to second order

$$\partial_\Lambda\Pi_\Lambda(\boldsymbol{k})=\frac{\Lambda b'''g^2}{2b'D}+\frac{\Lambda^2(b''')^2g^3\gamma_{\boldsymbol{k}}}{8(b')^3D^2}+\frac{\Lambda^3\left[b'b^{(5)}+2(b''')^2+12(b')^2b'''\right]g^4}{8(b')^3D^2}, \qquad \text{(B.29)}$$

which integrates to

$$\Pi_\Lambda(\boldsymbol{k})=b'+\frac{\Lambda^2b'''g^2}{4b'D}+\frac{\Lambda^3(b''')^2g^3\gamma_{\boldsymbol{k}}}{24(b')^3D^2}+\frac{\Lambda^4\left[b'b^{(5)}+2(b''')^2+12(b')^2b'''\right]g^4}{32(b')^3D^2}. \qquad \text{(B.30)}$$

B.1.3 Third-order correction

First-order correction to the irreducible six-point vertex

In analogy to the second-order calculation where we had to consider the irreducible four-point vertex to leading order in $1/D$, we now need the irreducible six-point vertex, which obeys the exact flow equation

$$\begin{aligned}
\partial_\Lambda\tilde{\Phi}^{(6)}_{\Lambda,123456}=&\frac{1}{2}\,\mathrm{Tr}\left[\dot{F}_\Lambda\tilde{\Phi}^{(8)}_{\Lambda,123456}\right]-\frac{1}{2}\,\mathcal{S}_{12;3456}\,\mathrm{Tr}\left[\dot{F}_\Lambda\tilde{\Phi}^{(4)}_{\Lambda,12}F_\Lambda\tilde{\Phi}^{(6)}_{\Lambda,3456}\right]\\
&-\frac{1}{2}\,\mathcal{S}_{1234;56}\,\mathrm{Tr}\left[\dot{F}_\Lambda\tilde{\Phi}^{(6)}_{\Lambda,1234}F_\Lambda\tilde{\Phi}^{(4)}_{\Lambda,56}\right]+\frac{1}{2}\,\mathcal{S}_{12;34;56}\,\mathrm{Tr}\left[\dot{F}_\Lambda\tilde{\Phi}^{(4)}_{\Lambda,12}F_\Lambda\tilde{\Phi}^{(4)}_{\Lambda,34}F_\Lambda\tilde{\Phi}^{(4)}_{\Lambda,56}\right]. \qquad \text{(B.31)}
\end{aligned}$$

We already observe that the last term involves two F_Λ propagators in addition to the single-scale propagator $\dot{F}_\Lambda$. As a consequence, it only contributes to subleading order in $1/D$ and can therefore be neglected in the present calculation, leaving us with the first three terms. The contribution which involves the irreducible eight-point vertex can be evaluated in complete analogy to Eq. (B.16), so that

$$\frac{1}{2}\operatorname{Tr}\left[\dot{F}_\Lambda \tilde{\Phi}^{(8)}_{\Lambda,123456}\right] \approx -\frac{\Lambda b^{(7)} g^2}{2b' D}. \tag{B.32}$$

For the second term in Eq. (B.31) we first consider

$$\begin{aligned}\frac{1}{2}\operatorname{Tr}\left[\dot{F}_\Lambda \tilde{\Phi}^{(4)}_{\Lambda,12} F_\Lambda \tilde{\Phi}^{(6)}_{\Lambda,3456}\right] &\approx \frac{1}{2}\int_{\boldsymbol{q}} \frac{\Lambda\beta^2 V_{\boldsymbol{q}} V_{\boldsymbol{q}+1+2} b''' b^{(5)}}{\left[1-\Lambda\beta V_{\boldsymbol{q}}\Pi_{\Lambda,\boldsymbol{q}}\right]^2 \left[1-\Lambda\beta V_{\boldsymbol{q}+1+2}\Pi_{\Lambda,\boldsymbol{q}+1+2}\right]} \\ &\approx \frac{\Lambda b''' b^{(5)} g^2}{2(b')^2}\int_{\boldsymbol{q}} \gamma_{\boldsymbol{q}}\gamma_{\boldsymbol{q}+1+2} = \frac{\Lambda b''' b^{(5)} g^2 \gamma_{1+2}}{4(b')^2 D}.\end{aligned} \tag{B.33}$$

In the same way we find

$$\frac{1}{2}\operatorname{Tr}\left[\dot{F}_\Lambda \tilde{\Phi}^{(6)}_{\Lambda,1234} F_\Lambda \tilde{\Phi}^{(4)}_{\Lambda,56}\right] \approx \frac{\Lambda b''' b^{(5)} g^2 \gamma_{5+6}}{4(b')^2 D}. \tag{B.34}$$

For the specific choice $\{\boldsymbol{k}_1, \boldsymbol{k}_2, \boldsymbol{k}_3, \boldsymbol{k}_4, \boldsymbol{k}_5, \boldsymbol{k}_6\} = \{\boldsymbol{k}, -\boldsymbol{k}, \boldsymbol{p}, -\boldsymbol{p}, \boldsymbol{q}, -\boldsymbol{q}\}$ we may therefore evaluate the symmetrization operators in Eq. (B.31) as

$$\begin{aligned}\mathcal{S}_{12;3456}\,\gamma_{1+2} &= \mathcal{S}_{1234;56}\,\gamma_{5+6} \\ &= 3 + 2(\gamma_{\boldsymbol{k}+\boldsymbol{p}} + \gamma_{\boldsymbol{k}-\boldsymbol{p}} + \gamma_{\boldsymbol{k}+\boldsymbol{q}} + \gamma_{\boldsymbol{k}-\boldsymbol{q}} + \gamma_{\boldsymbol{p}+\boldsymbol{q}} + \gamma_{\boldsymbol{p}-\boldsymbol{q}}).\end{aligned} \tag{B.35}$$

Combining these results yields the flow equation

$$\begin{aligned}\partial_\Lambda \tilde{\Phi}^{(6)}_\Lambda(\boldsymbol{k}, -\boldsymbol{k}, \boldsymbol{p}, -\boldsymbol{p}, \boldsymbol{q}) = &-\frac{\Lambda\left[b' b^{(7)} + 3 b''' b^{(5)}\right] g^2}{2(b')^2 D} \\ &- \frac{\Lambda b''' b^{(5)} g^2}{(b')^2 D}(\gamma_{\boldsymbol{k}+\boldsymbol{p}} + \gamma_{\boldsymbol{k}-\boldsymbol{p}} + \gamma_{\boldsymbol{k}+\boldsymbol{q}} + \gamma_{\boldsymbol{k}-\boldsymbol{q}} + \gamma_{\boldsymbol{p}+\boldsymbol{q}} + \gamma_{\boldsymbol{p}-\boldsymbol{q}}),\end{aligned} \tag{B.36}$$

which is easily solved as

$$\begin{aligned}\tilde{\Phi}^{(6)}_\Lambda(\boldsymbol{k}, -\boldsymbol{k}, \boldsymbol{p}, -\boldsymbol{p}, \boldsymbol{q}) = &-b^{(5)} - \frac{\Lambda^2\left[b' b^{(7)} + 3 b''' b^{(5)}\right] g^2}{4(b')^2 D} \\ &- \frac{\Lambda^2 b''' b^{(5)} g^2}{2(b')^2 D}(\gamma_{\boldsymbol{k}+\boldsymbol{p}} + \gamma_{\boldsymbol{k}-\boldsymbol{p}} + \gamma_{\boldsymbol{k}+\boldsymbol{q}} + \gamma_{\boldsymbol{k}-\boldsymbol{q}} + \gamma_{\boldsymbol{p}+\boldsymbol{q}} + \gamma_{\boldsymbol{p}-\boldsymbol{q}}).\end{aligned} \tag{B.37}$$

Second-order correction to the irreducible four-point vertex

We can now use our leading-order result (B.37) for $\tilde{\Phi}_\Lambda^{(6)}$ to derive the next-to-leading-order correction to the irreducible four-point vertex. According to its exact flow equation

$$\partial_\Lambda \tilde{\Phi}^{(4)}_{\Lambda,1234} = \frac{1}{2}\operatorname{Tr}\left[\dot{F}_\Lambda \tilde{\Phi}^{(6)}_{\Lambda,1234}\right] - \frac{1}{2}\mathcal{S}_{12;34}\operatorname{Tr}\left[\dot{F}_\Lambda \tilde{\Phi}^{(4)}_{\Lambda,12} F_\Lambda \tilde{\Phi}^{(4)}_{\Lambda,34}\right], \tag{B.38}$$

we have to consider two terms, which themselves consist of several contributions. The first term has the form

$$\frac{1}{2}\operatorname{Tr}\left[\dot{F}_\Lambda \tilde{\Phi}^{(6)}_{\Lambda,1234}\right] = \frac{1}{2}\int_{\boldsymbol{q}} \frac{\beta V_{\boldsymbol{q}} \tilde{\Phi}^{(6)}_{\Lambda,1234,\boldsymbol{q},-\boldsymbol{q}}}{\left[1-\Lambda\beta V_{\boldsymbol{q}}\Pi_{\Lambda,\boldsymbol{q}}\right]^2}, \tag{B.39}$$

which we have previously only evaluated to leading order in $1/D$. For $\{\boldsymbol{k}_1,\boldsymbol{k}_2,\boldsymbol{k}_3,\boldsymbol{k}_4\} = \{\boldsymbol{k},-\boldsymbol{k},\boldsymbol{p},-\boldsymbol{p}\}$, we find that the $\boldsymbol{q}$-independent terms of $\tilde{\Phi}_\Lambda^{(6)}$ trivially result in the second-order correction

$$-\frac{\Lambda^3\left[b'b^{(7)}+3b'''b^{(5)}\right]g^4}{8(b')^3D^2} - \frac{\Lambda^3 b''' b^{(5)} g^4}{4(b')^3D^2}(\gamma_{\boldsymbol{k}+\boldsymbol{p}}+\gamma_{\boldsymbol{k}-\boldsymbol{p}}), \tag{B.40}$$

while the $\boldsymbol{q}$-dependent terms of $\tilde{\Phi}_\Lambda^{(6)}$ yield

$$-\frac{\Lambda^2 b''' b^{(5)} g^3}{4(b')^3 D}\int_{\boldsymbol{q}} \frac{\gamma_{\boldsymbol{q}}(\gamma_{\boldsymbol{k}+\boldsymbol{q}}+\gamma_{\boldsymbol{k}-\boldsymbol{q}}+\gamma_{\boldsymbol{p}+\boldsymbol{q}}+\gamma_{\boldsymbol{p}-\boldsymbol{q}})}{\left[1-\Lambda\beta V_{\boldsymbol{q}}\Pi_{\Lambda,\boldsymbol{q}}\right]^2} \approx -\frac{\Lambda^2 b''' b^{(5)} g^3}{4(b')^3D^2}(\gamma_{\boldsymbol{k}}+\gamma_{\boldsymbol{p}}). \tag{B.41}$$

The last second-order contribution to the first term (B.39) comes from the expansion of the denominator,

$$\begin{aligned}
&-\frac{b^{(5)}}{2}\int_{\boldsymbol{q}} \frac{\beta V_{\boldsymbol{q}}}{\left[1-\Lambda\beta V_{\boldsymbol{q}}\Pi_{\Lambda,\boldsymbol{q}}\right]^2} \\
&\approx -\frac{b^{(5)}}{2}\int_{\boldsymbol{q}} \beta V_{\boldsymbol{q}}\left[1+2\Lambda\beta V_{\boldsymbol{q}}\Pi_{\Lambda,\boldsymbol{q}}+3\left(\Lambda\beta V_{\boldsymbol{q}}\Pi_{0,\boldsymbol{q}}\right)^2+4\left(\Lambda\beta V_{\boldsymbol{q}}\Pi_{0,\boldsymbol{q}}\right)^3\right] \\
&= -\frac{b^{(5)}g}{2b'}\int_{\boldsymbol{q}} \gamma_{\boldsymbol{q}}\left[2\Lambda\beta V_{\boldsymbol{q}}\Pi_{\Lambda,\boldsymbol{q}}+4\left(\Lambda g\gamma_{\boldsymbol{q}}\right)^3\right].
\end{aligned} \tag{B.42}$$

With our leading-order result (B.8) for $\Pi_\Lambda(\boldsymbol{k})$ we then find the second-order contribution

$$-\frac{\Lambda b^{(5)} g^2}{2b'}\int_{\boldsymbol{q}} \gamma_{\boldsymbol{q}}^2\left[\frac{\Lambda^2 b''' g^2}{2(b')^2 D}+4\Lambda^2 g^2\gamma_{\boldsymbol{q}}^2\right] \approx -\frac{\Lambda^3\left[b'''b^{(5)}+12(b')^2b^{(5)}\right]g^4}{8(b')^3D^2}. \tag{B.43}$$

The first term in Eq. (B.38) is therefore up to second order in $1/D$ given by

$$\frac{1}{2}\,\mathrm{Tr}\left[\dot{F}_\Lambda \tilde{\Phi}^{(6)}_{\Lambda,1234}\right] = -\frac{\Lambda b^{(5)} g^2}{2b' D} - \frac{\Lambda^3\left[b' b^{(7)} + 4b''' b^{(5)} + 12(b')^2 b^{(5)}\right] g^4}{8(b')^3 D^2}$$
$$- \frac{\Lambda^3 b''' b^{(5)} g^4}{4(b')^3 D^2}(\gamma_{\boldsymbol{k}+\boldsymbol{p}} + \gamma_{\boldsymbol{k}-\boldsymbol{p}}) - \frac{\Lambda^2 b''' b^{(5)} g^3}{4(b')^3 D^2}(\gamma_{\boldsymbol{k}} + \gamma_{\boldsymbol{p}}). \tag{B.44}$$

Since it is sufficient for the calculation of T_c to consider the special case $\boldsymbol{k} = 0$, we can further simplify this expression as

$$\frac{1}{2}\,\mathrm{Tr}\left[\dot{F}_\Lambda \tilde{\Phi}^{(6)}_{\Lambda,1234}\right] = -\frac{\Lambda b^{(5)} g^2}{2b' D} - \frac{\Lambda^3\left[b' b^{(7)} + 4b''' b^{(5)} + 12(b')^2 b^{(5)}\right] g^4}{8(b')^3 D^2}$$
$$- \frac{\Lambda^3 b''' b^{(5)} g^4 \gamma_{\boldsymbol{p}}}{2(b')^3 D^2} - \frac{\Lambda^2 b''' b^{(5)} g^3}{4(b')^3 D^2}(1 + \gamma_{\boldsymbol{p}}). \tag{B.45}$$

Let us now turn our attention to the second term in the flow equation of $\tilde{\Phi}^{(4)}_\Lambda$, where we need to evaluate

$$\frac{1}{2}\,\mathrm{Tr}\left[\dot{F}_\Lambda \tilde{\Phi}^{(4)}_{\Lambda,12} F_\Lambda \tilde{\Phi}^{(4)}_{\Lambda,34}\right] = \frac{1}{2}\int_{\boldsymbol{q}} \frac{\Lambda\beta^2 V_{\boldsymbol{q}} V_{\boldsymbol{q}+1+2} \tilde{\Phi}^{(4)}_{\Lambda,12,\boldsymbol{q},-\boldsymbol{q}-1-2} \tilde{\Phi}^{(4)}_{\Lambda,34,-\boldsymbol{q},\boldsymbol{q}+1+2}}{\left[1 - \Lambda\beta V_{\boldsymbol{q}} \Pi_{\Lambda,\boldsymbol{q}}\right]^2 \left[1 - \Lambda\beta V_{\boldsymbol{q}+1+2} \Pi_{\Lambda,\boldsymbol{q}+1+2}\right]}. \tag{B.46}$$

With our earlier result (B.20) for $\tilde{\Phi}^{(4)}_\Lambda$,

$$\tilde{\Phi}^{(4)}_{\Lambda,1234} = -b''' - \frac{\Lambda^2 b^{(5)} g^2}{4b' D} - \frac{\Lambda^2 (b''')^2 g^2}{8(b')^2 D}\,\mathcal{S}_{12;34}\,\gamma_{1+2}, \tag{B.47}$$

we find that

$$\tilde{\Phi}^{(4)}_{\Lambda,12,\boldsymbol{q},-\boldsymbol{q}-1-2} \tilde{\Phi}^{(4)}_{\Lambda,34,-\boldsymbol{q},\boldsymbol{q}+1+2}$$
$$\approx (b''')^2 + \frac{\Lambda^2 b''' b^{(5)} g^2}{2b' D} + \frac{\Lambda^2 (b''')^3 g^2}{4(b')^2 D}(2\gamma_{1+2} + \gamma_{\boldsymbol{q}+1} + \gamma_{\boldsymbol{q}+2} + \gamma_{\boldsymbol{q}-3} + \gamma_{\boldsymbol{q}-4}). \tag{B.48}$$

Here we have used

$$\mathcal{S}_{12;\boldsymbol{q},-\boldsymbol{q}-1-2}\,\gamma_{1+2} = 2(\gamma_{1+2} + \gamma_{\boldsymbol{q}+1} + \gamma_{\boldsymbol{q}+2}), \tag{B.49a}$$
$$\mathcal{S}_{34;-\boldsymbol{q},\boldsymbol{q}+1+2}\,\gamma_{3+4} = 2(\gamma_{1+2} + \gamma_{\boldsymbol{q}-3} + \gamma_{\boldsymbol{q}-4}), \tag{B.49b}$$

which in turn follows from $\gamma_{3+4} = \gamma_{-1-2} = \gamma_{1+2}$. While the $\boldsymbol{q}$-dependent terms in Eq. (B.48) only contribute to third order in $1/D$ to the flow of $\tilde{\Phi}^{(4)}_\Lambda$, inserting the $\boldsymbol{q}$-independent terms from Eq. (B.48) into Eq. (B.46) yields the second-order correction

$$\begin{aligned}
&\frac{1}{2}\int_{\boldsymbol{q}} \frac{\Lambda\beta^2 V_{\boldsymbol{q}} V_{\boldsymbol{q}+1+2}\left[\frac{\Lambda^2 b''' b^{(5)} g^2}{2b' D} + \frac{\Lambda^2 (b''')^3 g^2 \gamma_{1+2}}{2(b')^2 D}\right]}{\left[1-\Lambda\beta V_{\boldsymbol{q}}\Pi_{\Lambda,\boldsymbol{q}}\right]^2\left[1-\Lambda\beta V_{\boldsymbol{q}+1+2}\Pi_{\Lambda,\boldsymbol{q}+1+2}\right]} \\
\approx&\frac{\Lambda^3 g^4}{4(b')^4 D}\left[b' b''' b^{(5)} + (b''')^3\gamma_{1+2}\right]\int_{\boldsymbol{q}}\gamma_{\boldsymbol{q}}\gamma_{\boldsymbol{q}+1+2} \\
=&\frac{\Lambda^3 b''' b^{(5)} g^4 \gamma_{1+2}}{8(b')^3 D^2} + \frac{\Lambda^3 (b''')^3 g^4 \gamma_{1+2}^2}{8(b')^4 D^2}.
\end{aligned} \tag{B.50}$$

The last contribution we have to evaluate comes from the denominator of Eq. (B.46),

$$\begin{aligned}
&\frac{1}{2}\int_{\boldsymbol{q}} \frac{\Lambda\beta^2 V_{\boldsymbol{q}} V_{\boldsymbol{q}+1+2}(b''')^2}{\left[1-\Lambda\beta V_{\boldsymbol{q}}\Pi_{\Lambda,\boldsymbol{q}}\right]^2\left[1-\Lambda\beta V_{\boldsymbol{q}+1+2}\Pi_{\Lambda,\boldsymbol{q}+1+2}\right]} \\
\approx&\frac{\Lambda(b''')^2 g^2}{2(b')^2}\int_{\boldsymbol{q}}\frac{\gamma_{\boldsymbol{q}}\gamma_{\boldsymbol{q}+1+2}}{\left[1-\Lambda g\gamma_{\boldsymbol{q}}\right]^2\left[1-\Lambda g\gamma_{\boldsymbol{q}+1+2}\right]}.
\end{aligned} \tag{B.51}$$

Subtracting the first-order term, we find that the momentum integral results in

$$\begin{aligned}
&\int_{\boldsymbol{q}}\frac{\gamma_{\boldsymbol{q}}\gamma_{\boldsymbol{q}+1+2}}{\left[1-\Lambda g\gamma_{\boldsymbol{q}}\right]^2\left[1-\Lambda g\gamma_{\boldsymbol{q}+1+2}\right]} - \int_{\boldsymbol{q}}\gamma_{\boldsymbol{q}}\gamma_{\boldsymbol{q}+1+2} \\
\approx&\int_{\boldsymbol{q}}\gamma_{\boldsymbol{q}}\gamma_{\boldsymbol{q}+1+2}\left\{\left[1+2\Lambda g\gamma_{\boldsymbol{q}} + 3\left(\Lambda g\gamma_{\boldsymbol{q}}\right)^2\right]\left[1+\Lambda g\gamma_{\boldsymbol{q}+1+2} + \left(\Lambda g\gamma_{\boldsymbol{q}+1+2}\right)^2\right] - 1\right\} \\
\approx&\Lambda^2 g^2\int_{\boldsymbol{q}}\left(3\gamma_{\boldsymbol{q}}^3\gamma_{\boldsymbol{q}+1+2} + 2\gamma_{\boldsymbol{q}}^2\gamma_{\boldsymbol{q}+1+2}^2 + \gamma_{\boldsymbol{q}}\gamma_{\boldsymbol{q}+1+2}^3\right) \approx \frac{\Lambda^2 g^2}{2D^2}\left(1+6\gamma_{1+2}+2\gamma_{1+2}^2\right),
\end{aligned} \tag{B.52}$$

where we have used

$$\int_{\boldsymbol{q}}\gamma_{\boldsymbol{q}}^3\gamma_{\boldsymbol{q}+\boldsymbol{k}} = \int_{\boldsymbol{q}}\gamma_{\boldsymbol{q}}\gamma_{\boldsymbol{q}+\boldsymbol{k}}^3 = \frac{3\gamma_{\boldsymbol{k}}}{4D^2} - \frac{3\gamma_{\boldsymbol{k}}}{8D^3}, \tag{B.53a}$$

$$\int_{\boldsymbol{q}}\gamma_{\boldsymbol{q}}^2\gamma_{\boldsymbol{q}+\boldsymbol{k}}^2 = \frac{1+2\gamma_{\boldsymbol{k}}^2}{4D^2} - \frac{2+\gamma_{2\boldsymbol{k}}}{8D^3}. \tag{B.53b}$$

Together with our result (B.50) we thus get

$$\begin{aligned}
\frac{1}{2}\,\mathrm{Tr}\left[\dot{F}_\Lambda\tilde{\Phi}_{\Lambda,12}^{(4)} F_\Lambda\tilde{\Phi}_{\Lambda,34}^{(4)}\right] =& \frac{\Lambda(b''')^2 g^2\gamma_{1+2}}{4(b')^2 D} + \frac{\Lambda^3(b''')^2 g^4}{4(b')^2 D^2}\left(1+6\gamma_{1+2}+2\gamma_{1+2}^2\right) \\
&+ \frac{\Lambda^3 b''' b^{(5)} g^4\gamma_{1+2}}{8(b')^3 D^2} + \frac{\Lambda^3(b''')^3 g^4\gamma_{1+2}^2}{8(b')^4 D^2},
\end{aligned} \tag{B.54}$$

which for $\{\boldsymbol{k}_1, \boldsymbol{k}_2, \boldsymbol{k}_3, \boldsymbol{k}_4\} = \{0, 0, \boldsymbol{p}, -\boldsymbol{p}\}$ yields

$$\begin{aligned}
&\frac{1}{2}\mathcal{S}_{12;34}\,\mathrm{Tr}\left[\dot{F}_\Lambda \tilde{\Phi}^{(4)}_{\Lambda,12} F_\Lambda \tilde{\Phi}^{(4)}_{\Lambda,34}\right] \\
=&\frac{\Lambda(b''')^2 g^2(1+2\gamma_{\boldsymbol{p}})}{2(b')^2 D} + \frac{\Lambda^3\left[b'b'''b^{(5)} + (b''')^3 + 22(b')^2(b''')^2\right] g^4}{4(b')^4 D^2} \\
+&\frac{\Lambda^3\left[b'''b^{(5)} + 12b'(b''')^2\right] g^4\gamma_{\boldsymbol{p}}}{2(b')^3 D^2} + \frac{\Lambda^3\left[(b''')^3 + 4(b')^2(b''')^2\right] g^4\gamma_{\boldsymbol{p}}^2}{2(b')^4 D^2}.
\end{aligned} \tag{B.55}$$

Integrating Eqs. (B.45) and (B.55) with respect to Λ and replacing $\boldsymbol{p} \to \boldsymbol{q}$, we thus find that the irreducible four-point vertex is to second order in $1/D$ given by

$$\begin{aligned}
&\tilde{\Phi}^{(4)}_\Lambda(\boldsymbol{q}, -\boldsymbol{q}, 0) \\
=&-b''' - \frac{\Lambda^2\left[b'b^{(5)} + (b''')^2\right] g^2}{4(b')^2 D} - \frac{\Lambda^2(b''')^2 g^2\gamma_{\boldsymbol{q}}}{2(b')^2 D} - \frac{\Lambda^3 b''' b^{(5)} g^3(1+\gamma_{\boldsymbol{q}})}{12(b')^3 D^2} \\
-&\frac{\Lambda^4\left[(b')^2 b^{(7)} + 6b'b'''b^{(5)} + 12(b')^3 b^{(5)} + 2(b''')^3 + 44(b')^2(b''')^2\right] g^4}{32(b')^4 D^2} \\
-&\frac{\Lambda^4\left[b'''b^{(5)} + 6b'(b''')^2\right] g^4\gamma_{\boldsymbol{q}}}{4(b')^3 D^2} - \frac{\Lambda^4\left[(b''')^3 + 4(b')^2(b''')^2\right] g^4\gamma_{\boldsymbol{q}}^2}{8(b')^4 D^2}.
\end{aligned} \tag{B.56}$$

Third-order correction to the irreducible two-point vertex

With our next-to-leading-order result (B.56) for $\tilde{\Phi}^{(4)}_\Lambda$, we can evaluate the flow equation of the irreducible two-point vertex with vanishing external momentum,

$$\partial_\Lambda \Pi_\Lambda(0) = -\frac{1}{2}\int_{\boldsymbol{q}} \frac{\beta V_{\boldsymbol{q}} \tilde{\Phi}^{(4)}_\Lambda(\boldsymbol{q}, -\boldsymbol{q}, 0)}{\left[1 - \Lambda\beta V_{\boldsymbol{q}}\Pi_{\Lambda,\boldsymbol{q}}\right]^2}, \tag{B.57}$$

to third order in $1/D$. Let us first consider the contribution from the $\boldsymbol{q}$-independent second-order terms in Eq. (B.56), which is in analogy to Eq. (B.24) given by

$$\begin{aligned}
\frac{\Lambda b''' g^2}{2b' D} \to &\frac{\Lambda^4 b''' b^{(5)} g^5}{24(b')^4 D^3} \\
&+ \frac{\Lambda^5\left[(b')^2 b^{(7)} + 6b'b'''b^{(5)} + 12(b')^3 b^{(5)} + 2(b''')^3 + 44(b')^2(b''')^2\right] g^6}{64(b')^5 D^3}.
\end{aligned} \tag{B.58}$$

The situation is equally simple for the $\boldsymbol{q}$-dependent second-order terms in Eq. (B.56); while the $\gamma_{\boldsymbol{q}}^2$ term only contributes to fourth order in $1/D$, the linear-in-$\gamma_{\boldsymbol{q}}$ terms result in

$$-\frac{1}{2}\int_{\boldsymbol{q}} \frac{\beta V_{\boldsymbol{q}}\left[-\frac{\Lambda^3 b''' b^{(5)} g^3 \gamma_{\boldsymbol{q}}}{12(b')^3 D^2} - \frac{\Lambda^4\left[b''' b^{(5)} + 6b'(b''')^2\right] g^4 \gamma_{\boldsymbol{q}}}{4(b')^3 D^2}\right]}{\left[1-\Lambda\beta V_{\boldsymbol{q}}\Pi_{\Lambda,\boldsymbol{q}}\right]^2}$$
$$\approx \frac{\Lambda^3 b''' b^{(5)} g^4}{48(b')^4 D^3} + \frac{\Lambda^4\left[b''' b^{(5)} + 6b'(b''')^2\right] g^5}{16(b')^4 D^3}. \tag{B.59}$$

Now we take the first-order terms in Eq. (B.56) into account. For the part that is linear in $\gamma_{\boldsymbol{q}}$ we get

$$-\frac{1}{2}\int_{\boldsymbol{q}} \frac{\beta V_{\boldsymbol{q}}\left[-\frac{\Lambda^2 (b''')^2 g^2 \gamma_{\boldsymbol{q}}}{2(b')^2 D}\right]}{\left[1-\Lambda\beta V_{\boldsymbol{q}}\Pi_{\Lambda,\boldsymbol{q}}\right]^2} \approx \frac{\Lambda^2 (b''')^2 g^3}{4(b')^3 D}\int_{\boldsymbol{q}} \gamma_{\boldsymbol{q}}^2\left[1 + 2\Lambda\beta V_{\boldsymbol{q}}\Pi_{\Lambda,\boldsymbol{q}} + 3\left(\Lambda g \gamma_{\boldsymbol{q}}\right)^2\right]. \tag{B.60}$$

Only the last term in the square brackets leads to a third-order contribution, which reads

$$\frac{3\Lambda^4 (b''')^2 g^5}{4(b')^3 D}\int_{\boldsymbol{q}} \gamma_{\boldsymbol{q}}^4 \approx \frac{9\Lambda^4 (b''')^2 g^5}{16(b')^3 D^3}. \tag{B.61}$$

The first-order, momentum-independent part of Eq. (B.56) leads to a slightly more complicated calculation,

$$\frac{1}{2}\int_{\boldsymbol{q}} \frac{\beta V_{\boldsymbol{q}} \frac{\Lambda^2\left[b' b^{(5)} + (b''')^2\right] g^2}{4(b')^2 D}}{\left[1-\Lambda\beta V_{\boldsymbol{q}}\Pi_{\Lambda,\boldsymbol{q}}\right]^2}$$
$$\approx \frac{\Lambda^2\left[b' b^{(5)} + (b''')^2\right] g^3}{8(b')^3 D}\int_{\boldsymbol{q}} \gamma_{\boldsymbol{q}}\left[1 + 2\Lambda\beta V_{\boldsymbol{q}}\Pi_{\Lambda,\boldsymbol{q}} + 3\left(\Lambda\beta V_{\boldsymbol{q}}\Pi_{\Lambda,\boldsymbol{q}}\right)^2 + 4\left(\Lambda g \gamma_{\boldsymbol{q}}\right)^3\right]$$
$$\approx \frac{\Lambda^2\left[b' b^{(5)} + (b''')^2\right] g^3}{8(b')^3 D}\int_{\boldsymbol{q}} \gamma_{\boldsymbol{q}}\left[2\Lambda\beta V_{\boldsymbol{q}}\Pi_{\Lambda,\boldsymbol{q}} + 4\left(\Lambda g \gamma_{\boldsymbol{q}}\right)^3\right]. \tag{B.62}$$

Inserting our leading-order result (B.8) for the irreducible two-point vertex then yields the third-order correction

$$\frac{\Lambda^2\left[b' b^{(5)} + (b''')^2\right] g^3}{8(b')^3 D}\int_{\boldsymbol{q}}\left[\frac{\Lambda^3 b''' g^3}{2(b')^2 D}\gamma_{\boldsymbol{q}}^2 + 4\Lambda^3 g^3 \gamma_{\boldsymbol{q}}^4\right]$$
$$\approx \frac{\Lambda^5\left[b' b^{(5)} + (b''')^2\right]\left[b''' + 12(b')^2\right] g^6}{32(b')^5 D^3}. \tag{B.63}$$

The last contribution that we have to evaluate comes from the initial value of the irreducible four-point vertex,

$$\begin{aligned}\frac{1}{2}\int_{\boldsymbol{q}}\frac{\beta V_{\boldsymbol{q}}b'''}{\left[1-\Lambda\beta V_{\boldsymbol{q}}\Pi_{\Lambda,\boldsymbol{q}}\right]^2} &\approx \frac{b'''g}{2b'}\int_{\boldsymbol{q}}\gamma_{\boldsymbol{q}}\Big[1+2\Lambda\beta V_{\boldsymbol{q}}\Pi_{\Lambda,\boldsymbol{q}}+3\left(\Lambda\beta V_{\boldsymbol{q}}\Pi_{\Lambda,\boldsymbol{q}}\right)^2 \\ &\qquad +4\left(\Lambda\beta V_{\boldsymbol{q}}\Pi_{\Lambda,\boldsymbol{q}}\right)^3+5\left(\Lambda\beta V_{\boldsymbol{q}}\Pi_{\Lambda,\boldsymbol{q}}\right)^4+6\left(\Lambda g\gamma_{\boldsymbol{q}}\right)^5\Big] \\ &\approx \frac{b'''g}{2b'}\int_{\boldsymbol{q}}\gamma_{\boldsymbol{q}}\left[2\Lambda\beta V_{\boldsymbol{q}}\Pi_{\Lambda,\boldsymbol{q}}+4\left(\Lambda\beta V_{\boldsymbol{q}}\Pi_{\Lambda,\boldsymbol{q}}\right)^3+6\left(\Lambda g\gamma_{\boldsymbol{q}}\right)^5\right].\end{aligned} \tag{B.64}$$

Here we need $\Pi_{\Lambda,\boldsymbol{k}}$ up to second order in $1/D$, which according to Eq. (B.30) reads

$$\frac{\Pi_\Lambda(\boldsymbol{k})}{b'}=1+\frac{\Lambda^2b'''g^2}{4(b')^2D}+\frac{\Lambda^3(b''')^2g^3\gamma_{\boldsymbol{k}}}{24(b')^4D^2}+\frac{\Lambda^4\left[b'b^{(5)}+2(b''')^2+12(b')^2b'''\right]g^4}{32(b')^4D^2}. \tag{B.65}$$

With

$$\left[\frac{\Pi_\Lambda(\boldsymbol{q})}{b'}\right]^3\approx\left[1+\frac{\Lambda^2b'''g^2}{4(b')^2D}\right]^3\approx 1+\frac{3\Lambda^2b'''g^2}{4(b')^2D} \tag{B.66}$$

and

$$\int_{\boldsymbol{q}}\gamma_{\boldsymbol{q}}^4=\frac{3}{4D^2}-\frac{3}{8D^3} \tag{B.67}$$

we then arrive at the third-order contribution

$$\begin{aligned}&-\frac{3\Lambda^3b'''g^4}{4b'D^3}+\frac{\Lambda^5b'''g^6}{2b'}\int_{\boldsymbol{q}}\left[\frac{b'b^{(5)}+2(b''')^2+12(b')^2b'''}{16(b')^4D^2}\gamma_{\boldsymbol{q}}^2+\frac{3b'''}{(b')^2D}\gamma_{\boldsymbol{q}}^4+6\gamma_{\boldsymbol{q}}^6\right] \\ \approx &-\frac{3\Lambda^3b'''g^4}{4b'D^3}+\frac{\Lambda^5\left[b'b'''b^{(5)}+2(b''')^3+84(b')^2(b''')^2+360(b')^4b'''\right]g^6}{64(b')^5D^3},\end{aligned} \tag{B.68}$$

where we have also used

$$\int_{\boldsymbol{q}}\gamma_{\boldsymbol{q}}^6=\frac{15}{8D^3}-\frac{45}{16D^4}+\frac{5}{4D^5}. \tag{B.69}$$

Integrating the third-order contributions to Π_Λ from Eqs. (B.58), (B.59), (B.61), (B.63), and (B.68) with respect to Λ and combining them with our previous result (B.65), we arrive at

$$\Pi_{\Lambda=1}(0) = b' + \frac{b'''g^2}{4b'D} + \frac{(b''')^2 g^3}{24(b')^3 D^2} + \frac{\left[b'b^{(5)} + 2(b''')^2 + 12(b')^2 b'''\right] g^4}{32(b')^3 D^2}$$
$$+ \frac{b''' \left[b^{(5)} - 36(b')^3\right] g^4}{192(b')^4 D^3} + \frac{\left[b'''b^{(5)} + 9b'(b''')^2\right] g^5}{48(b')^4 D^3}$$
$$+ \frac{\left[(b')^2 b^{(7)} + 9b'b'''b^{(5)} + 36(b')^3 b^{(5)} + 6(b''')^3 + 152(b')^2(b''')^2 + 360(b')^4 b'''\right] g^6}{384(b')^5 D^3}. \tag{B.70}$$

Finally, expanding the inverse of this expression in powers of $1/D$ and using the exact relation

$$\Gamma_\Lambda^{(2)}(\boldsymbol{k}) = \frac{1}{\Pi_\Lambda(\boldsymbol{k})} - \beta V_{\boldsymbol{k}} \tag{B.71}$$

then results in Eq. (3.67) of the main text,

$$b'\Gamma_{\Lambda=1}^{(2)}(0) = 1 - g + \frac{C_1 g^2}{D} - \frac{C_2 g^3}{D^2} + \frac{C_3 g^4}{D^2} - \frac{C_4 g^4}{D^3} - \frac{C_5 g^5}{D^3} + \frac{C_6 g^6}{D^3}$$
$$+ O(D^{-4}), \tag{B.72}$$

where the spin-dependent coefficients C_i are given in Eqs. (3.68a)–(3.68f).

B.2 $1/r_0$ expansion of Π_Λ^{zz} in the Heisenberg model

In Sec. 3.3 we have developed the Hubbard-Stratonovich SFRG formalism, which has the advantage that the corresponding irreducible vertices are still well defined in the local limit of isolated spins. Furthermore, these irreducible vertices are closely related to the irreducible vertices of VLP, which allows us to recover their expansion in powers of the inverse interaction range $1/r_0$ [1, 2] within a simple truncation of our flow equations with the deformation scheme $V_{ij}^\Lambda = \Lambda V_{ij}$. While we have already derived the first-order correction to the free energy in Sec. 3.3.3, we will in the following calculate the leading correction to the longitudinal polarization function $\Pi_\Lambda^{zz}(K)$, which obeys the exact flow equation

$$\begin{aligned}\partial_\Lambda \Pi^{zz}_\Lambda(K) = &-\frac{1}{2}\int_Q \dot{F}^{zz}_\Lambda(Q)\tilde{\Phi}^{zzzz}_\Lambda(Q,-Q,K) - \int_Q \dot{F}^{+-}_\Lambda(Q)\tilde{\Phi}^{+-zz}_\Lambda(Q,-Q,K)\\ &+\int_Q \dot{F}^{zz}_\Lambda(Q)F^{zz}_\Lambda(Q+K)\tilde{\Phi}^{zzz}_\Lambda(Q,-Q-K)\tilde{\Phi}^{zzz}_\Lambda(Q+K,-Q)\\ &+\int_Q \left[\dot{F}^{+-}_\Lambda(Q)F^{+-}_\Lambda(Q+K)+F^{+-}_\Lambda(Q)\dot{F}^{+-}_\Lambda(Q+K)\right]\\ &\quad\times \tilde{\Phi}^{+-z}_\Lambda(Q,-Q-K)\tilde{\Phi}^{+-z}_\Lambda(Q+K,-Q) - \tilde{\Phi}^{zzz}_\Lambda(K,-K)\partial_\Lambda h_\Lambda.\end{aligned} \tag{B.73}$$

A graphical representation of this flow equation is shown in Fig. 3.4. To leading order in the inverse interaction range, we can replace the polarization functions and the higher-order irreducible vertices on the right-hand side of Eq. (B.73) by their initial values, which will allow us to perform all Matsubara sums and Λ integrals analytically. To simplify the comparison with the results of VLP, we will in the following assume that the on-site interaction vanishes.

B.2.1 Contribution from $\tilde{\Phi}^{zzzz}_\Lambda$

We start with the contribution of the first term in Eq. (B.73), which we can write as

$$-\frac{1}{2}\int_\Lambda\int_Q \dot{F}^{zz}_\Lambda(Q)\tilde{\Phi}^{zzzz}_\Lambda(Q,-Q,K) = -\frac{1}{2}\int_\Lambda\int_Q \frac{V_{\boldsymbol{q}}\tilde{\Phi}^{zzzz}_\Lambda(Q,-Q,K)}{\left[1-\Lambda V_{\boldsymbol{q}}\Pi^{zz}_\Lambda(Q)\right]^2}, \tag{B.74}$$

where we have introduced the notation $\int_\Lambda = \int_0^1 d\Lambda$. We now approximate Π^{zz}_Λ and $\tilde{\Phi}^{zzzz}_\Lambda$ by their initial conditions

$$\Pi^{zz}_0(K) = \delta(\omega)b', \tag{B.75}$$

$$\tilde{\Phi}^{zzzz}_0(Q,-Q,K) = -\delta(\nu)\delta(-\nu)\delta(\omega)b'''. \tag{B.76}$$

Note that we here use the abbreviations $b' = b'(\beta h)$ and $b''' = b'''(\beta h)$ to denote the derivatives of the Brillouin function at finite field. We then find

$$\delta(\omega)\frac{b'''}{2}\int_\Lambda\int_{\boldsymbol{q}}\frac{\beta V_{\boldsymbol{q}}}{(1-\Lambda\beta b' V_{\boldsymbol{q}})^2} = \delta(\omega)\frac{b'''}{2}\int_{\boldsymbol{q}}\frac{\beta V_{\boldsymbol{q}}}{1-\beta b' V_{\boldsymbol{q}}} = \delta(\omega)\frac{b'''}{2}\int_{\boldsymbol{q}}\beta V_{\boldsymbol{q}} L_{\boldsymbol{q}}, \tag{B.77}$$

where we have adopted VLP's notation

$$L_{\boldsymbol{k}} = \frac{1}{1-\beta b' V_{\boldsymbol{k}}}. \tag{B.78}$$

B.2.2 Contribution from $\tilde{\Phi}^{+-zz}_\Lambda$

The contribution from the mixed irreducible four-point vertex $\tilde{\Phi}^{+-zz}_\Lambda$ is more complicated due to its initial condition [1, 3]

$$\begin{aligned}\tilde{\Phi}^{+-zz}_0(Q,-Q,K) = &-\frac{b}{(h-i\nu)^2}\left[\frac{1}{h-i(\nu+\omega)}+\frac{1}{h-i(\nu-\omega)}\right]\\ &+\delta(\omega)\left[\frac{2b'}{(h-i\nu)^2}-\frac{\beta b''}{h-i\nu}\right].\end{aligned} \tag{B.79}$$

Together with the initial condition of the transversal polarization function,

$$\Pi^{+-}_0(K) = \frac{b}{h-i\omega}, \tag{B.80}$$

we find

$$\begin{aligned}-\int_\Lambda\int_Q \dot{F}^{+-}_\Lambda(Q)\tilde{\Phi}^{+-zz}_\Lambda(Q,-Q,K) &\approx -\int_\Lambda\int_Q \frac{V_{\boldsymbol{q}}\tilde{\Phi}^{+-zz}_0(Q,-Q,K)}{\left(1-\Lambda\frac{bV_{\boldsymbol{q}}}{h-i\nu}\right)^2}\\ &= -\int_Q \frac{V_{\boldsymbol{q}}(h-i\nu)\tilde{\Phi}^{+-zz}_0(Q,-Q,K)}{h-i\nu-bV_{\boldsymbol{q}}}.\end{aligned} \tag{B.81}$$

Let us first consider the general case $\omega \neq 0$, for which the irreducible four-point vertex can be written as

$$\tilde{\Phi}^{+-zz}_0(Q,-Q,K) = -\frac{2b}{(h-i\nu)(h-i\nu-i\omega)(h-i\nu+i\omega)}. \tag{B.82}$$

We now insert this expression into Eq. (B.81) and replace the Matsubara sum by a contour integral,

$$\frac{1}{\beta}\sum_\nu f(i\nu) = \frac{(-1)}{2\pi i}\int_{\mathcal{C}} \frac{dz}{1-e^{\beta z}} f(z). \tag{B.83}$$

In contrast to the more general expression (3.155), we here follow VLP in assuming a vanishing on-site interaction to facilitate the comparison with their results. As discussed at the end of Sec. 3.2.1, this allows us to choose any regularization scheme for equal-time expressions. We thus arrive at the finite-frequency contribution

$$
\begin{aligned}
&-\int_Q \frac{2bV_{\boldsymbol{q}}}{(i\nu - h + bV_{\boldsymbol{q}})(i\nu - h + i\omega)(i\nu - h - i\omega)} \\
=&\frac{(-1)}{2\pi i}\int_{\boldsymbol{q}}\int_C \frac{dz}{e^{\beta z}-1}\frac{2bV_{\boldsymbol{q}}}{(z-h+bV_{\boldsymbol{q}})(z-h+i\omega)(z-h-i\omega)} \\
=&2b\int_{\boldsymbol{q}} V_{\boldsymbol{q}}\left[\frac{n_{\boldsymbol{q}}}{(i\omega - bV_{\boldsymbol{q}})(-i\omega - bV_{\boldsymbol{q}})} + \frac{n_y}{2i\omega}\left(\frac{1}{bV_{\boldsymbol{q}}+i\omega} - \frac{1}{bV_{\boldsymbol{q}}-i\omega}\right)\right] \\
=&2b\int_{\boldsymbol{q}} V_{\boldsymbol{q}}\frac{n_{\boldsymbol{q}} - n_y}{(bV_{\boldsymbol{q}})^2+\omega^2}.
\end{aligned}
\tag{B.84}
$$

Here we have used the notation of VLP [2],

$$
n_{\boldsymbol{k}} = \frac{1}{e^{\beta\epsilon_{\boldsymbol{k}}}-1}, \quad n_y = \frac{1}{e^y - 1}, \tag{B.85}
$$

where in turn

$$
\epsilon_{\boldsymbol{k}} = h - bV_{\boldsymbol{k}}, \quad y = \beta h. \tag{B.86}
$$

On the other hand, for the static case $\omega = 0$ we find

$$
\begin{aligned}
&\int_Q \frac{V_{\boldsymbol{q}}}{h - i\nu - bV_{\boldsymbol{q}}}\left[\frac{2b}{(h-i\nu)^2} - \frac{2\beta b'}{h-i\nu} + \beta^2 b''\right] \\
=&\frac{(-1)}{2\pi i}\int_{\boldsymbol{q}} V_{\boldsymbol{q}}\int_C \frac{dz}{(e^{\beta z}-1)(z-h+bV_{\boldsymbol{q}})}\left[\frac{2b}{(z-h)^2} + \frac{2\beta b'}{z-h} + \beta^2 b''\right] \\
=&2\beta n_y' + \int_{\boldsymbol{q}}\frac{2(n_{\boldsymbol{q}} - n_y)}{bV_{\boldsymbol{q}}} + \frac{2\beta b'}{b}\int_{\boldsymbol{q}}(n_y - n_{\boldsymbol{q}}) + \beta^2 b''\int_{\boldsymbol{q}} V_{\boldsymbol{q}} n_{\boldsymbol{q}},
\end{aligned}
\tag{B.87}
$$

where we have defined $n_y' = \partial_y n_y$. To leading order in the inverse interaction range, the total contribution from $\tilde{\Phi}_\Lambda^{+-zz}$ thus reads

$$
\begin{aligned}
&-\int_\Lambda\int_Q \frac{V_{\boldsymbol{q}}\tilde{\Phi}_0^{+-zz}(Q,-Q,K)}{\left(1-\Lambda V_{\boldsymbol{q}}\Pi_0^{+-}(Q)\right)^2} \\
=&2b\int_{\boldsymbol{q}}\frac{V_{\boldsymbol{q}}(n_{\boldsymbol{q}} - n_y)}{(bV_{\boldsymbol{q}})^2+\omega^2} + \delta(\omega)\int_{\boldsymbol{q}}\left[2n_y' + \frac{2b'}{b}(n_y - n_{\boldsymbol{q}}) + b''\beta V_{\boldsymbol{q}} n_{\boldsymbol{q}}\right].
\end{aligned}
\tag{B.88}
$$

B.2.3 Contribution from $\left(\tilde{\Phi}_\Lambda^{zzz}\right)^2$

We continue with the purely longitudinal part involving the irreducible three-point vertex $\tilde{\Phi}_\Lambda^{zzz}$, which has the initial condition

$$
\tilde{\Phi}_0^{zzz}(Q,-Q-K) = -\delta(\nu)\delta(\nu-\omega)b''. \tag{B.89}
$$

To leading order we then find

$$\begin{aligned}
&\int_\Lambda \int_Q \dot{F}_\Lambda^{zz}(Q) F_\Lambda^{zz}(Q+K) \tilde{\Phi}_\Lambda^{zzz}(Q,-Q-K) \tilde{\Phi}_\Lambda^{zzz}(Q+K,-Q) \\
\approx& \delta(\omega)(b'')^2 \int_\Lambda \int_{\boldsymbol{q}} \frac{\Lambda \beta^2 V_{\boldsymbol{q}} V_{\boldsymbol{q}+\boldsymbol{k}}}{\left(1-\Lambda\beta b' V_{\boldsymbol{q}}\right)^2 \left(1-\Lambda\beta b' V_{\boldsymbol{q}+\boldsymbol{k}}\right)} \\
=& \delta(\omega)(b'')^2 \int_\Lambda \int_{\boldsymbol{q}} \frac{\Lambda \beta^2 V_{\boldsymbol{q}} V_{\boldsymbol{q}+\boldsymbol{k}} \left[2-\Lambda\beta b' \left(V_{\boldsymbol{q}}+V_{\boldsymbol{q}+\boldsymbol{k}}\right)\right]}{2\left(1-\Lambda\beta b' V_{\boldsymbol{q}}\right)^2 \left(1-\Lambda\beta b' V_{\boldsymbol{q}+\boldsymbol{k}}\right)^2} \\
=& \delta(\omega)(b'')^2 \int_{\boldsymbol{q}} \frac{\beta V_{\boldsymbol{q}} \beta V_{\boldsymbol{q}+\boldsymbol{k}}}{2\left(1-\beta b' V_{\boldsymbol{q}}\right)\left(1-\beta b' V_{\boldsymbol{q}+\boldsymbol{k}}\right)} = \delta(\omega) \frac{(b'')^2}{2} \int_{\boldsymbol{q}} \beta^2 V_{\boldsymbol{q}} V_{\boldsymbol{q}+\boldsymbol{k}} L_{\boldsymbol{q}} L_{\boldsymbol{q}+\boldsymbol{k}},
\end{aligned} \tag{B.90}$$

where in the third line we have used the transformation $\boldsymbol{q} \to -\boldsymbol{q}-\boldsymbol{k}$ to render the expression more symmetric.

B.2.4 Contribution from $\left(\tilde{\Phi}_\Lambda^{+-z}\right)^2$

The contribution involving the mixed irreducible three-point vertex $\tilde{\Phi}_\Lambda^{+-z}$ is again more difficult to evaluate. The first part, which corresponds to the fourth diagram in Fig. 3.4, can be written as

$$\begin{aligned}
&\int_\Lambda \int_Q \dot{F}_\Lambda^{+-}(Q) F_\Lambda^{+-}(Q+K) \tilde{\Phi}_\Lambda^{+-z}(Q,-Q-K) \tilde{\Phi}_\Lambda^{+-z}(Q+K,-Q) \\
\approx& \int_\Lambda \int_Q \frac{\Lambda V_{\boldsymbol{q}} V_{\boldsymbol{q}+\boldsymbol{k}} \tilde{\Phi}_0^{+-z}(Q,-Q-K) \tilde{\Phi}_0^{+-z}(Q+K,-Q)}{\left[1-\Lambda V_{\boldsymbol{q}} \Pi_0^{+-}(Q)\right]^2 \left[1-\Lambda V_{\boldsymbol{q}+\boldsymbol{k}} \Pi_0^{+-}(Q+K)\right]} \\
=& \int_\Lambda \int_Q \frac{\Lambda V_{\boldsymbol{q}} V_{\boldsymbol{q}+\boldsymbol{k}} \tilde{\Phi}_0^{+-z}(Q,-Q+K) \tilde{\Phi}_0^{+-z}(Q-K,-Q)}{\left[1-\Lambda V_{\boldsymbol{q}} \Pi_0^{+-}(Q)\right] \left[1-\Lambda V_{\boldsymbol{q}+\boldsymbol{k}} \Pi_0^{+-}(Q-K)\right]^2},
\end{aligned} \tag{B.91}$$

where in the last line we have used the transformations $\boldsymbol{q} \to -\boldsymbol{q}-\boldsymbol{k}$ and $\nu \to \nu-\omega$. Together with the contribution from the fifth diagram in Fig. 3.4, which can be obtained by replacing $K \to -K$ in Eq. (B.91), we arrive at the more symmetric expression

$$\begin{aligned}
&\int_\Lambda \int_Q \frac{\Lambda V_{\boldsymbol{q}} V_{\boldsymbol{q}+\boldsymbol{k}} \left[2 - \Lambda V_{\boldsymbol{q}} \Pi_0^{+-}(Q) - \Lambda V_{\boldsymbol{q}+\boldsymbol{k}} \Pi_0^{+-}(Q+K)\right]}{\left[1 - \Lambda V_{\boldsymbol{q}} \Pi_0^{+-}(Q)\right]^2 \left[1 - \Lambda V_{\boldsymbol{q}+\boldsymbol{k}} \Pi_0^{+-}(Q+K)\right]^2} \\
&\qquad \times \tilde{\Phi}_0^{+-z}(Q, -Q-K) \tilde{\Phi}_0^{+-z}(Q+K, -Q) \\
&= \int_Q \frac{V_{\boldsymbol{q}} V_{\boldsymbol{q}+\boldsymbol{k}} \tilde{\Phi}_0^{+-z}(Q, -Q-K) \tilde{\Phi}_0^{+-z}(Q+K, -Q)}{\left[1 - V_{\boldsymbol{q}} \Pi_0^{+-}(Q)\right] \left[1 - V_{\boldsymbol{q}+\boldsymbol{k}} \Pi_0^{+-}(Q+K)\right]} \\
&= \int_Q \frac{V_{\boldsymbol{q}} V_{\boldsymbol{q}+\boldsymbol{k}}}{(i\nu - h + bV_{\boldsymbol{q}})(i\nu - h + i\omega + bV_{\boldsymbol{q}+\boldsymbol{k}})} \\
&\qquad \times \left[\frac{b^2}{(i\nu - h)(i\nu - h + i\omega)} + \delta(\omega)\left(\frac{2bb'}{i\nu - h} + \beta (b')^2\right)\right], \qquad \text{(B.92)}
\end{aligned}$$

where we have used the initial condition of the mixed irreducible three-point vertex [1, 3],

$$\tilde{\Phi}_0^{+-z}(K_1, K_2) = \frac{b}{(h - i\omega_1)(h + i\omega_2)} - \delta(\omega_3) \frac{b'}{h - i\omega_1}. \qquad \text{(B.93)}$$

For the general case of $\omega \neq 0$ we then find

$$\begin{aligned}
&b^2 \frac{(-1)}{2\pi i} \int_{\boldsymbol{q}} \int_C \frac{dz}{1 - e^{\beta z}} \frac{V_{\boldsymbol{q}} V_{\boldsymbol{q}+\boldsymbol{k}}}{(z - h + bV_{\boldsymbol{q}})(z - h + i\omega + bV_{\boldsymbol{q}+\boldsymbol{k}})(z - h)(z - h + i\omega)} \\
&= \int_{\boldsymbol{q}} 2bV_{\boldsymbol{q}+\boldsymbol{k}} n_{\boldsymbol{q}} \frac{(bV_{\boldsymbol{q}})^2 - bV_{\boldsymbol{q}} bV_{\boldsymbol{q}+\boldsymbol{k}} - \omega^2}{[(bV_{\boldsymbol{q}})^2 + \omega^2]\,[(bV_{\boldsymbol{q}} - bV_{\boldsymbol{q}+\boldsymbol{k}})^2 + \omega^2]} + \int_{\boldsymbol{q}} \frac{2bV_{\boldsymbol{q}} n_y}{(bV_{\boldsymbol{q}})^2 + \omega^2} \\
&= \int_{\boldsymbol{q}} \frac{n_{\boldsymbol{q}} - n_{\boldsymbol{q}+\boldsymbol{k}}}{\epsilon_{\boldsymbol{q}+\boldsymbol{k}} - \epsilon_{\boldsymbol{q}} - i\omega} - 2b \int_{\boldsymbol{q}} \frac{V_{\boldsymbol{q}}(n_{\boldsymbol{q}} - n_y)}{(bV_{\boldsymbol{q}})^2 + \omega^2}. \qquad \text{(B.94)}
\end{aligned}$$

On the other hand, the static case $\omega = 0$ results in the three contributions

$$\begin{aligned}
\int_Q \frac{b^2 V_{\boldsymbol{q}} V_{\boldsymbol{q}+\boldsymbol{k}}}{(i\nu - h + bV_{\boldsymbol{q}})(i\nu - h + bV_{\boldsymbol{q}+\boldsymbol{k}})(i\nu - h)^2} &= \int_{\boldsymbol{q}} \frac{2V_{\boldsymbol{q}+\boldsymbol{k}} n_{\boldsymbol{q}}}{bV_{\boldsymbol{q}}(V_{\boldsymbol{q}} - V_{\boldsymbol{q}+\boldsymbol{k}})} + \int_{\boldsymbol{q}} \frac{2n_y}{bV_{\boldsymbol{q}}} \\
&\quad - \beta n_y', \qquad \text{(B.95a)} \\
\int_Q \frac{2\beta bb' V_{\boldsymbol{q}} V_{\boldsymbol{q}+\boldsymbol{k}}}{(i\nu - h + bV_{\boldsymbol{q}})(i\nu - h + bV_{\boldsymbol{q}+\boldsymbol{k}})(i\nu - h)} &= -2\beta b' \int_{\boldsymbol{q}} V_{\boldsymbol{q}} \frac{n_{\boldsymbol{q}} - n_{\boldsymbol{q}+\boldsymbol{k}}}{\epsilon_{\boldsymbol{q}+\boldsymbol{k}} - \epsilon_{\boldsymbol{q}}} \\
&\quad + \frac{2\beta b'}{b} \int_{\boldsymbol{q}} (n_{\boldsymbol{q}} - n_y), \qquad \text{(B.95b)} \\
\int_Q \frac{\beta^2 (b')^2 V_{\boldsymbol{q}} V_{\boldsymbol{q}+\boldsymbol{k}}}{(i\nu - h + bV_{\boldsymbol{q}})(i\nu - h + bV_{\boldsymbol{q}+\boldsymbol{k}})} &= \beta^2 (b')^2 \int_{\boldsymbol{q}} V_{\boldsymbol{q}} V_{\boldsymbol{q}+\boldsymbol{k}} \frac{n_{\boldsymbol{q}} - n_{\boldsymbol{q}+\boldsymbol{k}}}{\epsilon_{\boldsymbol{q}+\boldsymbol{k}} - \epsilon_{\boldsymbol{q}}}. \qquad \text{(B.95c)}
\end{aligned}$$

The total contribution from the mixed three-point vertices can thus be written as

$$\begin{aligned}
&\int_\Lambda \int_Q \frac{\Lambda V_{\boldsymbol{q}} V_{\boldsymbol{q}+\boldsymbol{k}} \tilde{\Phi}_0^{+-z}(Q,-Q+K)\tilde{\Phi}_0^{+-z}(Q-K,-Q)}{\left[1-\Lambda V_{\boldsymbol{q}}\Pi_0^{+-}(Q)\right]\left[1-\Lambda V_{\boldsymbol{q}+\boldsymbol{k}}\Pi_0^{+-}(Q-K)\right]^2} + (K\leftrightarrow -K) \\
&= \int_{\boldsymbol{q}} \frac{n_{\boldsymbol{q}}-n_{\boldsymbol{q}+\boldsymbol{k}}}{\epsilon_{\boldsymbol{q}+\boldsymbol{k}}-\epsilon_{\boldsymbol{q}}-i\omega} - 2b\int_{\boldsymbol{q}} \frac{V_{\boldsymbol{q}}(n_{\boldsymbol{q}}-n_y)}{(bV_{\boldsymbol{q}})^2+\omega^2} + \delta(\omega)\Bigg[-n_y' - 2b'\int_{\boldsymbol{q}} V_{\boldsymbol{q}} \frac{n_{\boldsymbol{q}}-n_{\boldsymbol{q}+\boldsymbol{k}}}{\epsilon_{\boldsymbol{q}+\boldsymbol{k}}-\epsilon_{\boldsymbol{q}}} \\
&\qquad + \frac{2b'}{b}\int_{\boldsymbol{q}}(n_{\boldsymbol{q}}-n_y) + \beta(b')^2\int_{\boldsymbol{q}} V_{\boldsymbol{q}}V_{\boldsymbol{q}+\boldsymbol{k}} \frac{n_{\boldsymbol{q}}-n_{\boldsymbol{q}+\boldsymbol{k}}}{\epsilon_{\boldsymbol{q}+\boldsymbol{k}}-\epsilon_{\boldsymbol{q}}}\Bigg]. \qquad \text{(B.96)}
\end{aligned}$$

B.2.5 Contribution from $\partial_\Lambda h_\Lambda$

The final contribution that we have to evaluate stems from the Λ dependence of the renormalized effective magnetic field h_Λ,

$$-\int_\Lambda \tilde{\Phi}^{zzz}_\Lambda(K,-K)\partial_\Lambda h_\Lambda \approx -\tilde{\Phi}^{zzz}_0(K,-K)\int_\Lambda \partial_\Lambda h_\Lambda. \qquad \text{(B.97)}$$

From the flow equation (3.164) of h_Λ we find

$$\begin{aligned}
\tilde{\Phi}^{zz}_0(0)\int_\Lambda \partial_\Lambda h_\Lambda &\approx -\frac{1}{2}\int_\Lambda\int_Q \frac{V_{\boldsymbol{q}}\tilde{\Phi}^{zzz}_0(Q,-Q)}{[1-\Lambda V_{\boldsymbol{q}}\Pi^{zz}_0(Q)]^2} - \int_\Lambda\int_Q \frac{V_{\boldsymbol{q}}\tilde{\Phi}^{+-z}_0(Q,-Q)}{\left[1-\Lambda V_{\boldsymbol{q}}\Pi^{+-}_0(Q)\right]^2} \\
&= \frac{b''}{2}\int_{\boldsymbol{q}} \frac{\beta V_{\boldsymbol{q}}}{1-\beta b' V_{\boldsymbol{q}}} - \int_Q \frac{V_{\boldsymbol{q}}}{i\nu - h + bV_{\boldsymbol{q}}}\left[\frac{b}{i\nu-h}+\beta b'\right] \\
&= \frac{b''}{2}\int_{\boldsymbol{q}} \beta V_{\boldsymbol{q}} L_{\boldsymbol{q}} + \int_{\boldsymbol{q}}(n_y-n_{\boldsymbol{q}}) + b'\int_{\boldsymbol{q}}\beta V_{\boldsymbol{q}} n_{\boldsymbol{q}}, \qquad \text{(B.98)}
\end{aligned}$$

so that

$$\begin{aligned}
&-\tilde{\Phi}^{zzz}_0(K,-K)\int_\Lambda \partial_\Lambda h_\Lambda \\
&\approx \delta(\omega) b'' \frac{\beta V_0}{1-\beta b' V_0}\left[\frac{b''}{2}\int_{\boldsymbol{q}}\beta V_{\boldsymbol{q}} L_{\boldsymbol{q}} - \int_{\boldsymbol{q}}(n_{\boldsymbol{q}}\left[1-\beta b' V_{\boldsymbol{q}}\right]-n_y)\right]. \qquad \text{(B.99)}
\end{aligned}$$

B.3 $1/D$ expansion of Γ^{zz}_Λ in the quantum Heisenberg model

B.3.1 Leading correction to Γ^{zz}_Λ

In order to determine the critical temperature of the spin-S Heisenberg model on a D-dimensional hypercubic lattice with nearest-neighbor interaction to leading order in $1/D$, we need the exact flow equation

$$\partial_\Lambda \left[\tilde{\mathbf{\Phi}}''_\Lambda\right]_{\tilde{\alpha}_1\tilde{\alpha}_2} = \frac{1}{2}\mathrm{Tr}\left[\dot{\mathbf{F}}_\Lambda \tilde{\mathbf{\Phi}}^{(4)}_{\Lambda,\tilde{\alpha}_1\tilde{\alpha}_2}\right] - \frac{1}{2}\mathcal{S}_{\tilde{\alpha}_1;\tilde{\alpha}_2}\,\mathrm{Tr}\left[\dot{\mathbf{F}}_\Lambda \tilde{\mathbf{\Phi}}'''_{\Lambda,\tilde{\alpha}_1}\mathbf{F}_\Lambda \tilde{\mathbf{\Phi}}'''_{\Lambda,\tilde{\alpha}_2}\right], \tag{B.100}$$

which follows from Eq. (3.157) by assuming $h_\Lambda = 0$. Since this assumption also implies that the $O(3)$ symmetry of the quantum Heisenberg model is intact,

$$\Pi^{\alpha\alpha'}_\Lambda(K) = \delta_{\alpha,\alpha'}\Pi^{zz}_\Lambda(K), \tag{B.101}$$

it is sufficient to consider Π^{zz}_Λ. Within the deformation scheme $V_\Lambda(\boldsymbol{k}) = \Lambda V_{\boldsymbol{k}}$ we thus get

$$\begin{aligned}\partial_\Lambda \Pi^{zz}_\Lambda(K) = &-\frac{1}{2}\sum_\alpha \int_Q \frac{V_{\boldsymbol{q}}\tilde{\Phi}^{\alpha\alpha zz}_\Lambda(Q,-Q,K)}{\left[1-\Lambda V_{\boldsymbol{q}}\Pi^{\alpha\alpha}_\Lambda(Q)\right]^2} \\ &+\frac{\Lambda}{2}\mathcal{S}_{K;-K}\sum_{\alpha\gamma}\int_Q \frac{V_{\boldsymbol{q}}V_{\boldsymbol{q}+\boldsymbol{k}}\tilde{\Phi}^{\alpha\gamma z}_\Lambda(Q,-Q-K)\tilde{\Phi}^{\gamma\alpha z}_\Lambda(Q+K,-Q)}{\left[1-\Lambda V_{\boldsymbol{q}}\Pi^{\alpha\alpha}_\Lambda(Q)\right]^2\left[1-\Lambda V_{\boldsymbol{q}+\boldsymbol{k}}\Pi^{\gamma\gamma}_\Lambda(Q+K)\right]}.\end{aligned} \tag{B.102}$$

To first order in $1/D$, we can further restrict ourselves to the evaluation of

$$\begin{aligned}\partial_\Lambda \Pi^{zz}_\Lambda(\boldsymbol{k}) = &-\frac{1}{2}\sum_\alpha \int_Q \frac{V_{\boldsymbol{q}}\tilde{\Phi}^{\alpha\alpha zz}_\Lambda(Q,-Q,\boldsymbol{k})}{\left[1-\Lambda V_{\boldsymbol{q}}\Pi^{\alpha\alpha}_\Lambda(Q)\right]^2} \\ &+\Lambda\sum_{\alpha\gamma}\int_Q \frac{V_{\boldsymbol{q}}V_{\boldsymbol{q}+\boldsymbol{k}}\tilde{\Phi}^{\alpha\gamma z}_\Lambda(Q,-Q-\boldsymbol{k})\tilde{\Phi}^{\gamma\alpha z}_\Lambda(Q+\boldsymbol{k},-Q)}{\left[1-\Lambda V_{\boldsymbol{q}}\Pi^{\alpha\alpha}_\Lambda(Q)\right]^2\left[1-\Lambda V_{\boldsymbol{q}+\boldsymbol{k}}\Pi^{\gamma\gamma}_\Lambda(Q+\boldsymbol{k})\right]},\end{aligned} \tag{B.103}$$

where $\boldsymbol{k}$ appearing as an argument to a polarization function or to an irreducible vertex is a shorthand for $(\boldsymbol{k}, i\omega = 0)$; e.g.,

$$\Pi^{zz}_\Lambda(\boldsymbol{k}) \equiv \Pi^{zz}_\Lambda\Big((\boldsymbol{k}, i\omega = 0)\Big). \tag{B.104}$$

Approximating the polarization functions and the irreducible vertices by their initial values, we find that the first term on the right-hand side of Eq. (B.103) becomes

$$\begin{aligned}&-\frac{1}{2}\sum_\alpha\int_Q \frac{V_{\boldsymbol{q}}\tilde{\Phi}^{\alpha\alpha zz}_0(Q,-Q,\boldsymbol{k})}{(1-\Lambda V_{\boldsymbol{q}}b'\delta(\nu))^2} = -\frac{1}{2\beta}\sum_\alpha\int_{\boldsymbol{q}}\frac{V_{\boldsymbol{q}}\tilde{\Phi}^{\alpha\alpha zz}_0(0,0,0)}{(1-\Lambda\beta b' V_{\boldsymbol{q}})^2} \\ \approx &-\frac{1}{2\beta}\sum_\alpha \tilde{\Phi}^{\alpha\alpha zz}_0(0,0,0)\int_{\boldsymbol{q}} V_{\boldsymbol{q}}(1+2\Lambda\beta b' V_{\boldsymbol{q}}) = -\frac{\Lambda g^2}{2\beta^2 b' D}\sum_\alpha \tilde{\Phi}^{\alpha\alpha zz}_0(0,0,0) \\ = &\ \frac{5\Lambda\beta b''' g^2}{6b'D},\end{aligned} \tag{B.105}$$

where we have used the zero-field limit of Eqs. (B.76) and (B.79),

$$\tilde{\Phi}_0^{zzzz}(Q,-Q,K) = -\beta b'''\delta(\nu)\delta(\omega), \tag{B.106}$$

$$\tilde{\Phi}_0^{xxzz}(Q,-Q,K) = \tilde{\Phi}_0^{yyzz}(Q,-Q,K) = \beta \begin{cases} -\beta^2 b'''/3, & \nu=\omega=0, \\ -2b'/(\omega^2), & \nu=0,\omega\neq 0, \\ -2b'/(\nu^2), & \nu\neq 0,\omega=0 \\ b'/(\omega^2), & |\nu|=|\omega|\neq 0 \\ 0, & \text{else}, \end{cases} \tag{B.107}$$

and we have again introduced the dimensionless parameter $g = \beta b' V_0$. The second term results in

$$\begin{aligned} &\Lambda \sum_{\alpha\gamma} \int_Q \frac{V_{\boldsymbol{q}} V_{\boldsymbol{q}+\boldsymbol{k}} \tilde{\Phi}_0^{\alpha\gamma z}(Q,-Q-\boldsymbol{k}) \tilde{\Phi}_0^{\gamma\alpha z}(Q+\boldsymbol{k},-Q)}{\left[1-\Lambda V_{\boldsymbol{q}} \Pi_0^{\alpha\alpha}(Q)\right]^2 \left[1-\Lambda V_{\boldsymbol{q}+\boldsymbol{k}} \Pi_0^{\gamma\gamma}(Q+\boldsymbol{k})\right]} \\ \approx &-\Lambda \sum_{\alpha\gamma} \int_Q V_{\boldsymbol{q}} V_{\boldsymbol{q}+\boldsymbol{k}} \left[\tilde{\Phi}_0^{\alpha\gamma z}(\nu,-\nu)\right]^2 = -\frac{\Lambda\beta g^2 \gamma_{\boldsymbol{k}}}{12D}, \end{aligned} \tag{B.108}$$

where ν appearing as an argument to an irreducible vertex is a shorthand for $(0, i\nu)$, i.e.,

$$\tilde{\Phi}_0^{\alpha\gamma z}(\nu,-\nu) \equiv \tilde{\Phi}_0^{\alpha\gamma z}\Big((\boldsymbol{q}=0,i\nu),(\boldsymbol{q}=0,-i\nu)\Big), \tag{B.109}$$

and we have inserted the zero-field limit of Eqs. (B.89) and (B.93),

$$\tilde{\Phi}_0^{\alpha\gamma z}(K_1,K_2) = \epsilon_{\alpha\gamma z} b' \left(1-\delta_{\omega_1,0}\delta_{\omega_2,0}\right) \left(\frac{\delta(\omega_1)}{\omega_2} + \frac{\delta(\omega_2)}{\omega_3} + \frac{\delta(\omega_3)}{\omega_1}\right), \tag{B.110}$$

where $\epsilon_{\alpha\gamma z}$ is the Levi-Civita symbol. In total we therefore find

$$\partial_\Lambda \Pi_\Lambda^{zz}(\boldsymbol{k}) = \frac{\Lambda\beta g^2}{12b'D}\left(10b''' - b'\gamma_{\boldsymbol{k}}\right), \tag{B.111}$$

so that to leading order in $1/D$

$$\Pi_\Lambda^{zz}(\boldsymbol{k}) = \beta b' \left[1 + \frac{\Lambda^2 g^2}{24D}\left(\frac{10b'''}{(b')^2} - \frac{\gamma_{\boldsymbol{k}}}{b'}\right)\right]. \tag{B.112}$$

Inserting this result into Eq. (3.135a) we arrive at

$$\Gamma_\Lambda^{zz}(\boldsymbol{k}) + V_{\boldsymbol{k}} = \frac{1}{\beta b'}\left[1 - \frac{\Lambda^2 g^2}{24D}\left(\frac{10b'''}{(b')^2} - \frac{\gamma_{\boldsymbol{k}}}{b'}\right)\right]. \tag{B.113}$$

Together with the condition $\Gamma^{zz}_{\Lambda=1}(\boldsymbol{k}) = 0$ for the critical temperature, this leads to the quadratic equation

$$1 - g\gamma_{\boldsymbol{k}} - \frac{g^2}{24D}\left(\frac{10b'''}{(b')^2} - \frac{\gamma_{\boldsymbol{k}}}{b'}\right) = 0, \tag{B.114}$$

which is trivially solved by

$$\frac{T_c}{T_{c0}} = \frac{1}{2}\left[1 + \sqrt{1 - \frac{1}{D}\left[\frac{5}{3}\frac{|b'''|}{(b')^2} \pm \frac{1}{6b'}\right]}\right], \tag{B.115}$$

where $T_{c0} = b'|V_0|$ is the mean-field result for the critical temperature.

B.3.2 Second-order correction to Γ^{zz}_{Λ} for $S = 1/2$

First-order correction to the irreducible four-point vertex

It is straightforward to extend our result (B.113) for $\Pi^{zz}_{\Lambda}(\boldsymbol{k})$ to second order in $1/D$. Since the flow equation of the polarization function depends on the irreducible four-point vertex $\tilde{\Phi}^{\alpha\alpha zz}_{\Lambda}(Q, -Q, \boldsymbol{k})$, we need to solve its exact flow equation to first order in $1/D$. While the full expression for the exact flow equation is quite lengthy (see Ref. [33] for a diagrammatic representation), we can neglect several terms to leading order in $1/D$ so that

$$\begin{aligned}\partial_\Lambda \left[\tilde{\mathbf{\Phi}}^{(4)}_{\Lambda}\right]_{\tilde{\alpha}_1\tilde{\alpha}_2\tilde{\alpha}_3\tilde{\alpha}_4} \approx\; & \frac{1}{2}\mathrm{Tr}\left[\dot{\mathbf{F}}_\Lambda \tilde{\mathbf{\Phi}}^{(6)}_{\Lambda,\tilde{\alpha}_1\tilde{\alpha}_2\tilde{\alpha}_3\tilde{\alpha}_4}\right] \\ & - \frac{1}{2}\mathcal{S}_{\tilde{\alpha}_1\tilde{\alpha}_2;\tilde{\alpha}_3\tilde{\alpha}_4}\,\mathrm{Tr}\left[\dot{\mathbf{F}}_\Lambda \tilde{\mathbf{\Phi}}^{(4)}_{\Lambda,\tilde{\alpha}_1\tilde{\alpha}_2}\mathbf{F}_\Lambda \tilde{\mathbf{\Phi}}^{(4)}_{\Lambda,\tilde{\alpha}_3\tilde{\alpha}_4}\right] \\ & - \mathcal{S}_{\tilde{\alpha}_1;\tilde{\alpha}_2\tilde{\alpha}_3\tilde{\alpha}_4}\,\mathrm{Tr}\left[\dot{\mathbf{F}}_\Lambda \tilde{\mathbf{\Phi}}^{(3)}_{\Lambda,\tilde{\alpha}_1}\mathbf{F}_\Lambda \tilde{\mathbf{\Phi}}^{(5)}_{\Lambda,\tilde{\alpha}_2\tilde{\alpha}_3\tilde{\alpha}_4}\right].\end{aligned} \tag{B.116}$$

To better organize the following calculations, we rewrite this flow equation as

$$\begin{aligned}\partial_\Lambda \left[\tilde{\mathbf{\Phi}}^{(4)}_{\Lambda}\right]_{\tilde{\alpha}_1\tilde{\alpha}_2\tilde{\alpha}_3\tilde{\alpha}_4} \approx\; & \left[\mathbf{\Delta}^{(6)}_{\Lambda}\right]_{\tilde{\alpha}_1\tilde{\alpha}_2\tilde{\alpha}_3\tilde{\alpha}_4} - \mathcal{S}_{\tilde{\alpha}_1\tilde{\alpha}_2;\tilde{\alpha}_3\tilde{\alpha}_4}\left[\mathbf{\Delta}^{(4,4)}_{\Lambda}\right]_{\tilde{\alpha}_1\tilde{\alpha}_2\tilde{\alpha}_3\tilde{\alpha}_4} \\ & - \mathcal{S}_{\tilde{\alpha}_1;\tilde{\alpha}_2\tilde{\alpha}_3\tilde{\alpha}_4}\left[\mathbf{\Delta}^{(3,5)}_{\Lambda}\right]_{\tilde{\alpha}_1\tilde{\alpha}_2\tilde{\alpha}_3\tilde{\alpha}_4},\end{aligned} \tag{B.117}$$

where the tensors $\mathbf{\Delta}^{(6)}_{\Lambda}$, $\mathbf{\Delta}^{(4,4)}_{\Lambda}$, and $\mathbf{\Delta}^{(3,5)}_{\Lambda}$ are defined as

$$\left[\mathbf{\Delta}^{(6)}_{\Lambda}\right]_{\tilde{\alpha}_1\tilde{\alpha}_2\tilde{\alpha}_3\tilde{\alpha}_4} \equiv \frac{1}{2}\mathrm{Tr}\left[\dot{\mathbf{F}}_\Lambda \tilde{\mathbf{\Phi}}^{(6)}_{\Lambda,\tilde{\alpha}_1\tilde{\alpha}_2\tilde{\alpha}_3\tilde{\alpha}_4}\right], \tag{B.118}$$

$$\left[\mathbf{\Delta}^{(4,4)}_{\Lambda}\right]_{\tilde{\alpha}_1\tilde{\alpha}_2\tilde{\alpha}_3\tilde{\alpha}_4} \equiv \frac{1}{2}\mathrm{Tr}\left[\dot{\mathbf{F}}_\Lambda \tilde{\mathbf{\Phi}}^{(4)}_{\Lambda,\tilde{\alpha}_1\tilde{\alpha}_2}\mathbf{F}_\Lambda \tilde{\mathbf{\Phi}}^{(4)}_{\Lambda,\tilde{\alpha}_3\tilde{\alpha}_4}\right], \tag{B.119}$$

$$\left[\mathbf{\Delta}^{(3,5)}_{\Lambda}\right]_{\tilde{\alpha}_1\tilde{\alpha}_2\tilde{\alpha}_3\tilde{\alpha}_4} \equiv \mathrm{Tr}\left[\dot{\mathbf{F}}_\Lambda \tilde{\mathbf{\Phi}}^{(3)}_{\Lambda,\tilde{\alpha}_1}\mathbf{F}_\Lambda \tilde{\mathbf{\Phi}}^{(5)}_{\Lambda,\tilde{\alpha}_2\tilde{\alpha}_3\tilde{\alpha}_4}\right]. \tag{B.120}$$

We also introduce the following notation for their components in Fourier space:

$$\left[\boldsymbol{\Delta}^{(x)}_\Lambda\right]_{\tilde{\alpha}_1\tilde{\alpha}_2\tilde{\alpha}_3\tilde{\alpha}_4} \to \delta(K_1+K_2+K_3+K_4)\Delta^{(x),\alpha_1\alpha_2\alpha_3\alpha_4}_\Lambda(K_1,K_2,K_3). \quad (B.121)$$

Note that the calculation of these tensors to leading order involves the initial conditions of the irreducible five- and six-point vertices. While it is straightforward to derive them for general spin S via the generalized Wick theorem [1, 3], we have so far only evaluated them for the special cases of $S = 1/2$ and $S \to \infty$. In the present section we therefore consider the spin-1/2 Heisenberg model, while in Appendix B.3.3 we will cover the classical Heisenberg model. We also note that, according to the exact flow equation (B.103) of $\Pi^{zz}_\Lambda(\boldsymbol{k})$, the first-order correction to the irreducible four-point vertex only appears in the expression

$$\begin{aligned}
&-\frac{1}{2}\sum_\alpha\int_Q \frac{V_{\boldsymbol{q}}\tilde{\Phi}^{\alpha\alpha zz}_\Lambda(Q,-Q,\boldsymbol{k})}{\left[1-\Lambda V_{\boldsymbol{q}}\Pi^{\alpha\alpha}_\Lambda(Q)\right]^2} \approx -\frac{1}{2}\sum_\alpha\int_Q \frac{V_{\boldsymbol{q}}\tilde{\Phi}^{\alpha\alpha zz}_\Lambda(Q,-Q,\boldsymbol{k})}{\left[1-\Lambda V_{\boldsymbol{q}} b'\delta(\nu)\right]^2} \\
&\approx -\frac{1}{2\beta}\sum_\alpha\int_{\boldsymbol{q}} V_{\boldsymbol{q}}\tilde{\Phi}^{\alpha\alpha zz}_\Lambda(\boldsymbol{q},-\boldsymbol{q},\boldsymbol{k}) - \Lambda b'\sum_\alpha\int_{\boldsymbol{q}} V^2_{\boldsymbol{q}}\tilde{\Phi}^{\alpha\alpha zz}_\Lambda(\boldsymbol{q},-\boldsymbol{q},\boldsymbol{k}) \\
&\quad -\frac{1}{2\beta}\sum_\alpha\int_{\boldsymbol{q}}\sum_{\nu\neq 0} V_{\boldsymbol{q}}\tilde{\Phi}^{\alpha\alpha zz}_\Lambda(Q,-Q,\boldsymbol{k}). \qquad (B.122)
\end{aligned}$$

Together with Eq. (3.61), this implies that for $\nu \neq 0$ we can neglect the $\boldsymbol{q}$-independent part of the first-order correction to $\tilde{\Phi}^{\alpha\alpha zz}_\Lambda(Q,-Q,\boldsymbol{k})$, which will simplify the following calculations.

Contribution from $\boldsymbol{\Delta}^{(6)}_\Lambda$ We start with the term involving the irreducible six-point vertex, which to leading order reads

$$\begin{aligned}
\Delta^{(6),\alpha\alpha zz}_\Lambda(Q,-Q,\boldsymbol{k}) &\approx \frac{1}{2}\sum_\gamma\int_P \frac{V_{\boldsymbol{p}}\tilde{\Phi}^{\gamma\gamma\alpha\alpha zz}_0(P,-P,Q,-Q,\boldsymbol{k})}{\left[1-\Lambda V_{\boldsymbol{p}} b'\delta(\rho)\right]^2} \\
&= \frac{1}{2\beta}\sum_\gamma \tilde{\Phi}^{\gamma\gamma\alpha\alpha zz}_0(0,0,\nu,-\nu,0)\int_{\boldsymbol{p}}\frac{V_{\boldsymbol{p}}}{\left[1-\Lambda\beta b' V_{\boldsymbol{p}}\right]^2} \\
&\approx \frac{\Lambda g^2}{2\beta^2 b' D}\sum_\gamma \tilde{\Phi}^{\gamma\gamma\alpha\alpha zz}_0(0,0,\nu,-\nu,0). \qquad (B.123)
\end{aligned}$$

Since this result is always independent of $\boldsymbol{q}$, we only need to consider the special case where $\nu = 0$. For $S = 1/2$ we find

$$\sum_{\alpha\gamma}\tilde{\Phi}^{\gamma\gamma\alpha\alpha zz}_0(0,0,0,0,0) = -\frac{7}{12}\beta^5, \qquad (B.124)$$

so that

$$\sum_{\alpha} \Delta_{\Lambda}^{(6),\alpha\alpha zz}(\boldsymbol{q},-\boldsymbol{q},\boldsymbol{k}) \approx -\frac{7\Lambda\beta^3 g^2}{6D}. \tag{B.125}$$

Contribution from $\boldsymbol{\Delta}_{\Lambda}^{(4,4)}$ Next we consider the tensor $\boldsymbol{\Delta}_{\Lambda}^{(4,4)}$, whose components in Fourier space are in general described by

$$\begin{aligned}
&\Delta_{\Lambda}^{(4,4),\alpha_1\alpha_2\alpha_3\alpha_4}(K_1,K_2,K_3)\\
=&\frac{1}{2}\sum_{\gamma\delta}\int_P \dot{F}_{\Lambda}^{\gamma\gamma}(P)\tilde{\Phi}_{\Lambda}^{\gamma\delta\alpha_1\alpha_2}(P,-P-K_1-K_2,K_1)F_{\Lambda}^{\delta\delta}(P+K_1+K_2)\\
&\qquad\times\tilde{\Phi}_{\Lambda}^{\delta\gamma\alpha_3\alpha_4}(P+K_1+K_2,-P,K_3)\\
\approx&\frac{\Lambda}{2\beta}\sum_{\gamma\delta}\sum_{\rho}\tilde{\Phi}_{0}^{\gamma\delta\alpha_1\alpha_2}(\rho,-\rho-\omega_1-\omega_2,\omega_1)\tilde{\Phi}_{0}^{\delta\gamma\alpha_3\alpha_4}(\rho+\omega_1+\omega_2,-\rho,\omega_3)\\
&\times\int_{\boldsymbol{p}}\frac{V_{\boldsymbol{p}}V_{\boldsymbol{p}+\boldsymbol{k}_1+\boldsymbol{k}_2}}{\left[1-\Lambda V_{\boldsymbol{p}}b'\delta(\rho)\right]^2\left[1-\Lambda V_{\boldsymbol{p}+\boldsymbol{k}_1+\boldsymbol{k}_2}b'\delta(\rho+\omega_1+\omega_2)\right]}\\
\approx&\frac{\Lambda g^2\gamma_{\boldsymbol{k}_1+\boldsymbol{k}_2}}{4\beta^3(b')^2D}\sum_{\gamma\delta}\sum_{\rho}\tilde{\Phi}_{0}^{\gamma\delta\alpha_1\alpha_2}(\rho,-\rho-\omega_1-\omega_2,\omega_1)\tilde{\Phi}_{0}^{\delta\gamma\alpha_3\alpha_4}(\rho+\omega_1+\omega_2,-\rho,\omega_3).
\end{aligned} \tag{B.126}$$

For our purpose, we specifically need

$$\Delta_{\Lambda}^{(4,4),\alpha_1\alpha_2\alpha_3\alpha_4}(K_1,K_2,K_3) = \Delta_{\Lambda}^{(4,4),\alpha\alpha zz}(Q,-Q,\boldsymbol{k}), \tag{B.127}$$

so that for $\nu = 0$ and $S = 1/2$ we get

$$\begin{aligned}
&\sum_{\alpha}\mathcal{S}_{\tilde{\alpha}_1\tilde{\alpha}_2;\tilde{\alpha}_3\tilde{\alpha}_4}\,\Delta_{\Lambda}^{(4,4),\alpha\alpha zz}(Q,-Q,\boldsymbol{k})\\
\approx&\frac{\Lambda g^2}{2\beta^3(b')^2D}\sum_{\alpha\gamma\delta}\sum_{\rho}\Big[(\gamma_{\boldsymbol{q}+\boldsymbol{k}}+\gamma_{\boldsymbol{q}-\boldsymbol{k}})\tilde{\Phi}_{0}^{\gamma\delta\alpha z}(\rho,-\rho,0)\tilde{\Phi}_{0}^{\delta\gamma\alpha z}(\rho,-\rho,0)\\
&\qquad+\tilde{\Phi}_{0}^{\gamma\delta\alpha\alpha}(\rho,-\rho,0)\tilde{\Phi}_{0}^{\delta\gamma zz}(\rho,-\rho,0)\Big]\\
=&\frac{\Lambda\beta^3 g^2}{2D}\sum_{\rho}\begin{cases}(\gamma_{\boldsymbol{q}+\boldsymbol{k}}+\gamma_{\boldsymbol{q}-\boldsymbol{k}})5/12+25/36, & \rho=0,\\ (\gamma_{\boldsymbol{q}+\boldsymbol{k}}+\gamma_{\boldsymbol{q}-\boldsymbol{k}})12/(\beta\rho)^4+16/(\beta\rho)^4, & \rho\neq 0\end{cases}\\
=&\frac{\Lambda\beta^3 g^2}{120D}\left[43+26(\gamma_{\boldsymbol{q}+\boldsymbol{k}}+\gamma_{\boldsymbol{q}-\boldsymbol{k}})\right],
\end{aligned} \tag{B.128}$$

where, with a slight abuse of notation, the symmetrization operator now symmetrizes the function to its right with respect to the function's variables in Fourier space. On the other hand, for finite ν and $S = 1/2$ we find

$$
\begin{aligned}
&\frac{1}{\beta}\sum_{\nu\neq 0}\sum_{\alpha}\mathcal{S}_{\tilde{\alpha}_1\tilde{\alpha}_2;\tilde{\alpha}_3\tilde{\alpha}_4}\,\Delta_\Lambda^{(4,4),\alpha\alpha zz}(Q,-Q,\boldsymbol{k})\\
\approx&\frac{\Lambda g^2}{2\beta^4(b')^2 D}\sum_{\alpha\gamma\delta}\sum_{\nu\neq 0}\sum_{\rho}\Big[(\gamma_{\boldsymbol{q}+\boldsymbol{k}}+\gamma_{\boldsymbol{q}-\boldsymbol{k}})\tilde{\Phi}_0^{\gamma\delta\alpha z}(\rho,-\rho-\nu,\nu)\tilde{\Phi}_0^{\delta\gamma\alpha z}(\rho+\nu,-\rho,-\nu)\\
&\qquad\qquad\qquad\qquad+\tilde{\Phi}_0^{\gamma\delta\alpha\alpha}(\rho,-\rho,\nu)\tilde{\Phi}_0^{\delta\gamma zz}(\rho,-\rho,0)\Big]\\
=&\frac{\Lambda g^2}{2\beta^2 D}\sum_{\nu\neq 0}\sum_{\rho}\Bigg\{(\gamma_{\boldsymbol{q}+\boldsymbol{k}}+\gamma_{\boldsymbol{q}-\boldsymbol{k}})\Bigg[(\delta_{\rho,0}+\delta_{\rho,-\nu})\frac{12}{\nu^4}+(1-\delta_{\rho,0})(1-\delta_{\rho,-\nu})\\
&\qquad\times\left(\frac{2}{\nu^2\rho^2}+\frac{2}{\nu^2(\nu+\rho)^2}+\frac{2}{\rho^2(\nu+\rho)^2}\right)\Bigg]-\delta_{\rho,0}\frac{10\beta^2}{3\nu^2}-(\delta_{\nu,\rho}+\delta_{\nu,-\rho})\frac{8}{\nu^4}\Bigg\}\\
=&\frac{\Lambda\beta^2 g^2}{30D}\left[-\frac{9}{2}+\gamma_{\boldsymbol{q}+\boldsymbol{k}}+\gamma_{\boldsymbol{q}-\boldsymbol{k}}\right],
\end{aligned}
\tag{B.129}
$$

which implies

$$
\int_{\boldsymbol{q}}V_{\boldsymbol{q}}\frac{1}{\beta}\sum_{\nu\neq 0}\sum_{\alpha}\mathcal{S}_{\tilde{\alpha}_1\tilde{\alpha}_2;\tilde{\alpha}_3\tilde{\alpha}_4}\,\Delta_\Lambda^{(4,4),\alpha\alpha zz}(Q,-Q,\boldsymbol{k})=\frac{2\Lambda\beta g^3\gamma_{\boldsymbol{k}}}{15D^2}. \tag{B.130}
$$

Contribution from $\boldsymbol{\Delta}_\Lambda^{(3,5)}$ The final contribution that we have to evaluate comes from $\boldsymbol{\Delta}_\Lambda^{(3,5)}$, which in general yields

$$
\begin{aligned}
&\Delta_\Lambda^{(3,5),\alpha_1\alpha_2\alpha_3\alpha_4}(K_1,K_2,K_3)\\
=&\sum_{\gamma\delta}\int_P \dot{F}_\Lambda^{\gamma\gamma}(P)\tilde{\Phi}_\Lambda^{\gamma\delta\alpha_1}(P,-P-K_1)F_\Lambda^{\delta\delta}(P+K_1)\\
&\quad\times\tilde{\Phi}_\Lambda^{\delta\gamma\alpha_2\alpha_3\alpha_4}(P+K_1,-P,K_2,K_3)\\
\approx&\frac{\Lambda g^2\gamma_{\boldsymbol{k}_1}}{2\beta^3(b')^2 D}\sum_{\gamma\delta}\sum_{\rho}\tilde{\Phi}_0^{\gamma\delta\alpha_1}(\rho,-\rho-\omega_1)\tilde{\Phi}_0^{\delta\gamma\alpha_2\alpha_3\alpha_4}(\rho+\omega_1,-\rho,\omega_2,\omega_3).
\end{aligned}
\tag{B.131}
$$

Choosing

$$
\Delta_\Lambda^{(3,5),\alpha_1\alpha_2\alpha_3\alpha_4}(K_1,K_2,K_3)=\Delta_\Lambda^{(3,5),\alpha\alpha zz}(Q,-Q,\boldsymbol{k}) \tag{B.132}
$$

and assuming $\nu = 0$ as well as $S = 1/2$, we arrive at

$$\begin{aligned}
&\sum_{\alpha} \mathcal{S}_{\tilde{\alpha}_1;\tilde{\alpha}_2\tilde{\alpha}_3\tilde{\alpha}_4}\, \Delta_{\Lambda}^{(3,5),\alpha\alpha zz}(Q,-Q,\boldsymbol{k}) \\
\approx &\frac{\Lambda g^2}{\beta^3 (b')^2 D} \sum_{\alpha\gamma\delta} \sum_{\rho} \Big[\gamma_{\boldsymbol{q}} \tilde{\Phi}_0^{\gamma\delta\alpha}(\rho,-\rho) \tilde{\Phi}_0^{\delta\gamma\alpha zz}(\rho,-\rho,0,0) \\
&\qquad\qquad + \gamma_{\boldsymbol{k}} \tilde{\Phi}_0^{\gamma\delta z}(\rho,-\rho) \tilde{\Phi}_0^{\delta\gamma\alpha\alpha z}(\rho,-\rho,0,0) \Big] \\
= &\frac{5\Lambda g^2 (\gamma_{\boldsymbol{q}} + \gamma_{\boldsymbol{k}})}{3\beta D} \sum_{\rho\neq 0} \frac{12 + \beta^2\rho^2}{\rho^4} = \frac{\Lambda \beta^3 g^2 (\gamma_{\boldsymbol{q}} + \gamma_{\boldsymbol{k}})}{6D}.
\end{aligned} \tag{B.133}$$

For $\nu \neq 0$ we are only interested in the $\boldsymbol{q}$-dependent terms, so that it is in this case sufficient to consider

$$\begin{aligned}
&\int_{\boldsymbol{q}} V_{\boldsymbol{q}} \frac{1}{\beta} \sum_{\nu\neq 0} \sum_{\alpha} \Big[\Delta_{\Lambda}^{(3,5),\alpha\alpha zz}(Q,-Q,\boldsymbol{k}) + \Delta_{\Lambda}^{(3,5),\alpha\alpha zz}(-Q,Q,\boldsymbol{k}) \Big] \\
\approx &\int_{\boldsymbol{q}} V_{\boldsymbol{q}} \frac{\Lambda g^2 \gamma_{\boldsymbol{q}}}{\beta^4 (b')^2 D} \sum_{\alpha\gamma\delta} \sum_{\nu\neq 0} \sum_{\rho} \tilde{\Phi}_0^{\gamma\delta\alpha}(\rho,-\rho-\nu) \tilde{\Phi}_0^{\delta\gamma\alpha zz}(\rho+\nu,-\rho,-\nu,0) \\
= &\frac{10\Lambda g^3}{3\beta^3 D^2} \sum_{\nu\neq 0} \sum_{\rho} (\delta_{\rho,0} + \delta_{\rho,-\nu}) \frac{12 + \beta^2 \nu^2}{\nu^4} = \frac{2\Lambda\beta g^3}{3D^2}.
\end{aligned} \tag{B.134}$$

Second-order contribution to the flow of Π_{Λ}^{zz} from the leading correction to $\tilde{\boldsymbol{\Phi}}_{\Lambda}^{(4)}$ Collecting all relevant terms, we find in the static case

$$\begin{aligned}
\partial_{\Lambda} \sum_{\alpha} \tilde{\Phi}_{\Lambda}^{\alpha\alpha zz}(\boldsymbol{q},-\boldsymbol{q},\boldsymbol{k}) \approx &-\frac{7\Lambda\beta^3 g^2}{6D} - \frac{\Lambda\beta^3 g^2}{120D} \left[43 + 26(\gamma_{\boldsymbol{q}+\boldsymbol{k}} + \gamma_{\boldsymbol{q}-\boldsymbol{k}})\right] \\
&- \frac{\Lambda\beta^3 g^2 (\gamma_{\boldsymbol{q}} + \gamma_{\boldsymbol{k}})}{6D} \\
= &-\frac{\Lambda\beta^3 g^2}{6D} \left[\frac{183}{20} + \frac{13}{10}(\gamma_{\boldsymbol{q}+\boldsymbol{k}} + \gamma_{\boldsymbol{q}-\boldsymbol{k}}) + \gamma_{\boldsymbol{q}} + \gamma_{\boldsymbol{k}} \right],
\end{aligned} \tag{B.135}$$

so that

$$-\frac{1}{2\beta} \sum_{\alpha} \int_{\boldsymbol{q}} V_{\boldsymbol{q}} \tilde{\Phi}_{\Lambda}^{\alpha\alpha zz}(\boldsymbol{q},-\boldsymbol{q},\boldsymbol{k}) \approx \frac{\Lambda^2 \beta g^3}{12D^2} \left(1 + \frac{13}{5}\gamma_{\boldsymbol{k}}\right), \tag{B.136}$$

$$-\Lambda b' \sum_{\alpha} \int_{\boldsymbol{q}} V_{\boldsymbol{q}}^2 \left[\tilde{\Phi}_{\Lambda}^{\alpha\alpha zz}(\boldsymbol{q},-\boldsymbol{q},\boldsymbol{k}) - \tilde{\Phi}_0^{\alpha\alpha zz}(0,0,0) \right] \approx \frac{\Lambda^3 \beta g^4}{6D^2} \left(\frac{183}{20} + \gamma_{\boldsymbol{k}} \right), \tag{B.137}$$

while for $\nu \neq 0$ we have

$$-\frac{1}{2\beta}\sum_\alpha \int_{\boldsymbol{q}} \sum_{\nu\neq 0} V_{\boldsymbol{q}} \tilde{\Phi}_\Lambda^{\alpha\alpha zz}(Q,-Q,\boldsymbol{k}) \approx \frac{\Lambda^2\beta g^3}{30D^2}\left(5+\gamma_{\boldsymbol{k}}\right). \tag{B.138}$$

The total second-order contribution to the flow of $\Pi_\Lambda^{zz}(\boldsymbol{k})$ from the first-order correction to the irreducible four-point vertex thus reads

$$\begin{aligned}
&\frac{\Lambda^2\beta g^3}{12D^2}\left(1+\frac{13}{5}\gamma_{\boldsymbol{k}}\right)+\frac{\Lambda^3\beta g^4}{6D^2}\left(\frac{183}{20}+\gamma_{\boldsymbol{k}}\right)+\frac{\Lambda^2\beta g^3}{30D^2}\left(5+\gamma_{\boldsymbol{k}}\right)\\
=&\frac{\Lambda^2\beta g^3}{4D^2}\left(1+\gamma_{\boldsymbol{k}}\right)+\frac{\Lambda^3\beta g^4}{6D^2}\left(\frac{183}{20}+\gamma_{\boldsymbol{k}}\right).
\end{aligned} \tag{B.139}$$

First-order correction to the irreducible three-point vertex

Analogous to the previous calculation, we also have to derive the first-order correction to the irreducible three-point vertex. To leading order in $1/D$, this vertex obeys the flow equation

$$\begin{aligned}
\partial_\Lambda \left[\tilde{\boldsymbol{\Phi}}_\Lambda^{(3)}\right]_{\tilde{\alpha}_1\tilde{\alpha}_2\tilde{\alpha}_3} &\approx \frac{1}{2}\mathrm{Tr}\left[\dot{\mathbf{F}}_\Lambda \tilde{\boldsymbol{\Phi}}^{(5)}_{\Lambda,\tilde{\alpha}_1\tilde{\alpha}_2\tilde{\alpha}_3}\right] - \mathcal{S}_{\tilde{\alpha}_1;\tilde{\alpha}_2\tilde{\alpha}_3}\,\mathrm{Tr}\left[\dot{\mathbf{F}}_\Lambda \tilde{\boldsymbol{\Phi}}^{(3)}_{\Lambda,\tilde{\alpha}_1}\mathbf{F}_\Lambda \tilde{\boldsymbol{\Phi}}^{(4)}_{\Lambda,\tilde{\alpha}_2\tilde{\alpha}_3}\right]\\
&= \left[\boldsymbol{\Delta}_\Lambda^{(5)}\right]_{\tilde{\alpha}_1\tilde{\alpha}_2\tilde{\alpha}_3} - \mathcal{S}_{\tilde{\alpha}_1;\tilde{\alpha}_2\tilde{\alpha}_3}\left[\boldsymbol{\Delta}_\Lambda^{(3,4)}\right]_{\tilde{\alpha}_1\tilde{\alpha}_2\tilde{\alpha}_3},
\end{aligned} \tag{B.140}$$

where the tensors $\boldsymbol{\Delta}_\Lambda^{(5)}$ and $\boldsymbol{\Delta}_\Lambda^{(3,4)}$ are defined as

$$\left[\boldsymbol{\Delta}_\Lambda^{(5)}\right]_{\tilde{\alpha}_1\tilde{\alpha}_2\tilde{\alpha}_3} \equiv \frac{1}{2}\mathrm{Tr}\left[\dot{\mathbf{F}}_\Lambda \tilde{\boldsymbol{\Phi}}^{(5)}_{\Lambda,\tilde{\alpha}_1\tilde{\alpha}_2\tilde{\alpha}_3}\right], \tag{B.141}$$

$$\left[\boldsymbol{\Delta}_\Lambda^{(3,4)}\right]_{\tilde{\alpha}_1\tilde{\alpha}_2\tilde{\alpha}_3} \equiv \mathrm{Tr}\left[\dot{\mathbf{F}}_\Lambda \tilde{\boldsymbol{\Phi}}^{(3)}_{\Lambda,\tilde{\alpha}_1}\mathbf{F}_\Lambda \tilde{\boldsymbol{\Phi}}^{(4)}_{\Lambda,\tilde{\alpha}_2\tilde{\alpha}_3}\right], \tag{B.142}$$

and we again use the notation

$$\left[\boldsymbol{\Delta}_\Lambda^{(x)}\right]_{\tilde{\alpha}_1\tilde{\alpha}_2\tilde{\alpha}_3} \to \delta(K_1+K_2+K_3)\Delta_\Lambda^{(x),\alpha_1\alpha_2\alpha_3}(K_1,K_2) \tag{B.143}$$

for their components in Fourier space. According to the exact flow equation (B.103) of $\Pi_\Lambda^{zz}(\boldsymbol{k})$, the first-order correction to the irreducible three-point vertex only appears in the expression

$$\begin{aligned}
&\Lambda\sum_{\alpha\gamma}\int_Q \frac{V_{\boldsymbol{q}}V_{\boldsymbol{q}+\boldsymbol{k}}\tilde{\Phi}_\Lambda^{\alpha\gamma z}(Q,-Q-\boldsymbol{k})\tilde{\Phi}_\Lambda^{\gamma\alpha z}(Q+\boldsymbol{k},-Q)}{\left[1-\Lambda V_{\boldsymbol{q}}\Pi_\Lambda^{\alpha\alpha}(Q)\right]^2\left[1-\Lambda V_{\boldsymbol{q}+\boldsymbol{k}}\Pi_\Lambda^{\gamma\gamma}(Q+\boldsymbol{k})\right]}\\
\approx&\Lambda\sum_{\alpha\gamma}\int_Q V_{\boldsymbol{q}}V_{\boldsymbol{q}+\boldsymbol{k}}\tilde{\Phi}_\Lambda^{\alpha\gamma z}(Q,-Q-\boldsymbol{k})\tilde{\Phi}_\Lambda^{\gamma\alpha z}(Q+\boldsymbol{k},-Q)\\
=&2\Lambda\int_Q V_{\boldsymbol{q}}V_{\boldsymbol{q}+\boldsymbol{k}}\tilde{\Phi}_\Lambda^{xyz}(Q,-Q-\boldsymbol{k})\tilde{\Phi}_\Lambda^{xyz}(-Q,Q+\boldsymbol{k}).
\end{aligned} \tag{B.144}$$

It is therefore sufficient to focus on the flow equation of $\tilde{\Phi}_\Lambda^{xyz}(Q, -Q - \boldsymbol{k})$. Together with Eq. (3.61) it is also clear that, to leading order in $1/D$, we can neglect all $\boldsymbol{q}$-dependent terms in the first-order correction to the irreducible three-point vertex.

Contribution from $\boldsymbol{\Delta}_\Lambda^{(5)}$ The first contribution to the flow of the irreducible three-point vertex is given by

$$\begin{aligned}
\Delta_\Lambda^{(5),xyz}(Q, -Q - \boldsymbol{k}) &\approx \frac{1}{2} \sum_\gamma \int_P \frac{V_{\boldsymbol{p}} \tilde{\Phi}_0^{\gamma\gamma xyz}(P, -P, Q, -Q - \boldsymbol{k})}{[1 - \Lambda V_{\boldsymbol{p}} b' \delta(\rho)]^2} \\
&= \frac{1}{2\beta} \sum_\gamma \tilde{\Phi}_0^{\gamma\gamma xyz}(0, 0, \nu, -\nu) \int_{\boldsymbol{p}} \frac{V_{\boldsymbol{p}}}{[1 - \Lambda \beta b' V_{\boldsymbol{p}}]^2} \\
&\approx \frac{\Lambda g^2}{2\beta^2 b' D} \sum_\gamma \tilde{\Phi}_0^{\gamma\gamma xyz}(0, 0, \nu, -\nu) \\
&= -(1 - \delta_{\nu,0}) \frac{5(12 + \beta^2\nu^2)\Lambda g^2}{12\beta\nu^3 D},
\end{aligned} \tag{B.145}$$

where in the last line we have set $S = 1/2$.

Contribution from $\boldsymbol{\Delta}_\Lambda^{(3,4)}$ For the second contribution we first consider the general relation

$$\begin{aligned}
&\Delta_\Lambda^{(3,4),\alpha_1\alpha_2\alpha_3}(K_1, K_2) \\
=&\sum_{\gamma\delta} \int_P \dot{F}_\Lambda^{\gamma\gamma}(P) \tilde{\Phi}_\Lambda^{\gamma\delta\alpha_1}(P, -P - K_1) F_\Lambda^{\delta\delta}(P + K_1) \tilde{\Phi}_\Lambda^{\delta\gamma\alpha_2\alpha_3}(P + K_1, -P, K_2) \\
\approx&\frac{\Lambda g^2 \gamma_{\boldsymbol{k}_1}}{2\beta^3 (b')^2 D} \sum_{\gamma\delta} \sum_\rho \tilde{\Phi}_0^{\gamma\delta\alpha_1}(\rho, -\rho - \omega_1) \tilde{\Phi}_0^{\delta\gamma\alpha_2\alpha_3}(\rho + \omega_1, -\rho, \omega_2).
\end{aligned} \tag{B.146}$$

While the full contribution to the flow of $\tilde{\Phi}_\Lambda^{xyz}(Q, -Q - \boldsymbol{k})$ is given by

$$\begin{aligned}
&\mathcal{S}_{\tilde{\alpha}_1;\tilde{\alpha}_2\tilde{\alpha}_3} \Delta_\Lambda^{(3,4),xyz}(Q, -Q - \boldsymbol{k}) \\
=&\Delta_\Lambda^{(3,4),xyz}(Q, -Q - \boldsymbol{k}) + \Delta_\Lambda^{(3,4),yzx}(-Q - \boldsymbol{k}, \boldsymbol{k}) + \Delta_\Lambda^{(3,4),zxy}(\boldsymbol{k}, Q),
\end{aligned} \tag{B.147}$$

only the last term is independent of $\boldsymbol{q}$,

$$\begin{aligned}
\Delta_\Lambda^{(3,4),zxy}(\boldsymbol{k}, Q) &= \frac{\Lambda g^2 \gamma_{\boldsymbol{k}}}{2\beta^3 (b')^2 D} \sum_{\gamma\delta} \sum_\rho \tilde{\Phi}_0^{\gamma\delta z}(\rho, -\rho) \tilde{\Phi}_0^{\delta\gamma xy}(\rho, -\rho, \nu) \\
&= (1 - \delta_{\nu,0}) \frac{\Lambda g^2 \gamma_{\boldsymbol{k}}}{2\beta D} \sum_{\rho \neq 0} \left[\frac{\delta_{\rho,\nu} + \delta_{\rho,-\nu}}{\nu^3} + \frac{2}{\nu\rho^2} \right] \\
&= (1 - \delta_{\nu,0}) \frac{(12 + \beta^2\nu^2)\Lambda g^2 \gamma_{\boldsymbol{k}}}{12\beta\nu^3 D},
\end{aligned} \tag{B.148}$$

where we have again set $S = 1/2$.

Second-order contribution to the flow of Π_Λ^{zz} from the leading correction to $\tilde{\mathbf{\Phi}}_\Lambda^{(3)}$ We thus arrive at

$$\int_{\boldsymbol{q}} \partial_\Lambda \tilde{\Phi}_\Lambda^{xyz}(Q, -Q-\boldsymbol{k}) \approx -(1-\delta_{\nu,0}) \frac{(12+\beta^2\nu^2)(5+\gamma_{\boldsymbol{k}})\Lambda g^2}{12\beta\nu^3 D}, \tag{B.149}$$

where the momentum integral removes the irrelevant $\boldsymbol{q}$-dependent terms. Integrating up the flow then leads to

$$\int_{\boldsymbol{q}} \tilde{\Phi}_\Lambda^{xyz}(Q, -Q-\boldsymbol{k}) \approx (1-\delta_{\nu,0}) \frac{\beta}{4\nu} \left[1 - \frac{(12+\beta^2\nu^2)(5+\gamma_{\boldsymbol{k}})\Lambda^2 g^2}{6\beta^2\nu^2 D} \right], \tag{B.150}$$

so that the total second-order contribution to the flow equation of $\Pi_\Lambda^{zz}(\boldsymbol{k})$ from the first-order correction to the irreducible three-point vertex reads

$$\begin{aligned}
&2\Lambda \int_Q V_{\boldsymbol{q}} V_{\boldsymbol{q}+\boldsymbol{k}} \left[\tilde{\Phi}_\Lambda^{xyz}(Q, -Q-\boldsymbol{k}) \tilde{\Phi}_\Lambda^{xyz}(-Q, Q+\boldsymbol{k}) - \tilde{\Phi}_0^{xyz}(\nu, -\nu) \tilde{\Phi}_0^{xyz}(-\nu, \nu) \right] \\
&\approx 2\Lambda \int_Q V_{\boldsymbol{q}} V_{\boldsymbol{q}+\boldsymbol{k}} (1-\delta_{\nu,0}) \frac{\beta^2}{16\nu(-\nu)} (-2) \frac{(12+\beta^2\nu^2)(5+\gamma_{\boldsymbol{k}})\Lambda^2 g^2}{6\beta^2\nu^2 D} \\
&= \frac{\gamma_{\boldsymbol{k}}(5+\gamma_{\boldsymbol{k}})\beta\Lambda^3 g^4}{3D^2} \sum_{\nu \neq 0} \frac{12+\beta^2\nu^2}{\beta^4\nu^4} = \frac{\gamma_{\boldsymbol{k}}(5+\gamma_{\boldsymbol{k}})\beta\Lambda^3 g^4}{30D^2}.
\end{aligned} \tag{B.151}$$

First-order correction to $\Pi_\Lambda^{zz}(K)$ for $\omega \neq 0$

Since the polarization function $\Pi_\Lambda^{zz}(K)$ itself appears on the right-hand side of its flow equation (B.103), we also have to evaluate its first-order correction in $1/D$ for finite frequencies. Assuming $\omega \neq 0$, the term involving the irreducible four-point vertex is to leading order given by

$$-\frac{1}{2} \sum_\alpha \int_Q \frac{V_{\boldsymbol{q}} \tilde{\Phi}_0^{\alpha\alpha zz}(\nu, -\nu, \omega)}{\left[1 - \Lambda V_{\boldsymbol{q}} b' \delta(\nu)\right]^2} \approx -\frac{\Lambda g^2}{2\beta^2 b' D} \sum_\alpha \tilde{\Phi}_0^{\alpha\alpha zz}(0, 0, \omega) = \frac{2\Lambda g^2}{\beta\omega^2 D}, \tag{B.152}$$

while the term involving the irreducible three-point vertex yields

$$\begin{aligned}
&\Lambda \sum_{\alpha\gamma} \int_Q V_{\boldsymbol{q}} V_{\boldsymbol{q}+\boldsymbol{k}} \tilde{\Phi}_0^{\alpha\gamma z}(\nu, -\nu-\omega) \tilde{\Phi}_0^{\gamma\alpha z}(\nu+\omega, -\nu) \\
&= -\frac{\Lambda g^2 \gamma_{\boldsymbol{k}}}{\beta^3 (b')^2 D} \sum_\nu \left[\tilde{\Phi}_0^{xyz}(\nu, -\nu-\omega) \right]^2 = -\frac{2\Lambda g^2 \gamma_{\boldsymbol{k}}}{\beta\omega^2 D}.
\end{aligned} \tag{B.153}$$

We thus find

$$\partial_\Lambda \Pi_\Lambda^{zz}\big((\boldsymbol{k}, i\omega \neq 0)\big) = \frac{2\Lambda g^2(1-\gamma_{\boldsymbol{k}})}{\beta\omega^2 D}, \tag{B.154}$$

which together with our earlier result (B.112) for the static case leads to

$$\Pi_\Lambda^{zz}(K) = \delta(\omega) b' \left[1 + \frac{\Lambda^2 g^2}{24D}\left(\frac{10b'''}{(b')^2} - \frac{\gamma_{\boldsymbol{k}}}{b'}\right)\right] + (1-\delta_{\omega,0})\frac{\Lambda^2 g^2 (1-\gamma_{\boldsymbol{k}})}{\beta\omega^2 D}. \tag{B.155}$$

Second-order contributions from the denominators

We are now in a position to evaluate the final contribution to the flow of $\Pi_\Lambda^{zz}(\boldsymbol{k})$, which comes from the denominators in

$$\begin{aligned} \partial_\Lambda \Pi_\Lambda^{zz}(\boldsymbol{k}) = &-\frac{1}{2}\sum_\alpha \int_Q \frac{V_{\boldsymbol{q}} \tilde{\Phi}_\Lambda^{\alpha\alpha zz}(Q, -Q, \boldsymbol{k})}{[1 - \Lambda V_{\boldsymbol{q}} \Pi_\Lambda^{\alpha\alpha}(Q)]^2} \\ &+ \Lambda \sum_{\alpha\gamma} \int_Q \frac{V_{\boldsymbol{q}} V_{\boldsymbol{q}+\boldsymbol{k}} \tilde{\Phi}_\Lambda^{\alpha\gamma z}(Q, -Q-\boldsymbol{k}) \tilde{\Phi}_\Lambda^{\gamma\alpha z}(Q+\boldsymbol{k}, -Q)}{[1 - \Lambda V_{\boldsymbol{q}} \Pi_\Lambda^{\alpha\alpha}(Q)]^2 \, [1 - \Lambda V_{\boldsymbol{q}+\boldsymbol{k}} \Pi_\Lambda^{\gamma\gamma}(Q+\boldsymbol{k})]}. \end{aligned} \tag{B.156}$$

Since the denominator of the second term only contributes to third order in $1/D$, we are left with

$$\begin{aligned} &-\frac{1}{2}\sum_\alpha \int_Q \frac{V_{\boldsymbol{q}} \tilde{\Phi}_0^{\alpha\alpha zz}(\nu, -\nu, 0)}{[1 - \Lambda V_{\boldsymbol{q}} \Pi_\Lambda^{\alpha\alpha}(Q)]^2} \\ \approx &-\frac{1}{2\beta}\sum_\alpha \sum_\nu \tilde{\Phi}_0^{\alpha\alpha zz}(\nu, -\nu, 0) \int_{\boldsymbol{q}} V_{\boldsymbol{q}} \left[2\Lambda V_{\boldsymbol{q}} \Pi_\Lambda^{\alpha\alpha}(Q) + \delta_{\nu,0} 4(\Lambda\beta b' V_{\boldsymbol{q}})^3\right]. \end{aligned} \tag{B.157}$$

Subtracting the trivial leading correction, the first term in this expression is easily evaluated as

$$\begin{aligned} &-\frac{\Lambda}{\beta}\sum_\alpha \sum_\nu \tilde{\Phi}_0^{\alpha\alpha zz}(\nu, -\nu, 0) \int_{\boldsymbol{q}} V_{\boldsymbol{q}}^2 \left[\Pi_\Lambda^{\alpha\alpha}(Q) - \Pi_0^{\alpha\alpha}(Q)\right] \\ \approx &-\frac{5b'''\Lambda^3 g^2}{12b'D}\sum_\alpha \tilde{\Phi}_0^{\alpha\alpha zz}(0,0,0)\int_{\boldsymbol{q}} V_{\boldsymbol{q}}^2 - \frac{\Lambda^3 g^2}{D}\sum_\alpha \sum_{\nu\neq 0} \tilde{\Phi}_0^{\alpha\alpha zz}(\nu, -\nu, 0)\int_{\boldsymbol{q}} \frac{V_{\boldsymbol{q}}^2}{\beta^2\nu^2} \\ = &\frac{25\beta\Lambda^3 g^4}{72D^2} + \frac{8\beta\Lambda^3 g^4}{D^2}\sum_{\nu\neq 0}\frac{1}{\beta^4\nu^4} = \frac{43\beta\Lambda^3 g^4}{120D^2}, \end{aligned} \tag{B.158}$$

where in the last line we have set $S = 1/2$. For the second term we find

$$-2\Lambda^3\beta^2(b')^3 \sum_\alpha \tilde{\Phi}_0^{\alpha\alpha zz}(0,0,0)\int_{\boldsymbol{q}} V_{\boldsymbol{q}}^4 = -\frac{5\beta\Lambda^3 g^4}{12b'}\int_{\boldsymbol{q}} \gamma_{\boldsymbol{q}}^4 \approx -\frac{5\beta\Lambda^3 g^4}{4D^2}, \tag{B.159}$$

where we have used Eq. (B.67). The total second-order contribution to the flow of $\Pi^{zz}_{\Lambda}(\boldsymbol{k})$ from the denominators is thus

$$\frac{43\beta\Lambda^3 g^4}{120D^2} - \frac{5\beta\Lambda^3 g^4}{4D^2} = -\frac{107\beta\Lambda^3 g^4}{120D^2}. \tag{B.160}$$

Total second-order contribution to the flow of $\Pi^{zz}_{\Lambda}(\boldsymbol{k})$

Collecting all intermediate second-order results (B.139), (B.151), and (B.160) yields

$$\begin{aligned}&\frac{\beta\Lambda^2 g^3}{4D^2}(1+\gamma_{\boldsymbol{k}}) + \frac{\beta\Lambda^3 g^4}{6D^2}\left(\frac{183}{20}+\gamma_{\boldsymbol{k}}\right) + \frac{\gamma_{\boldsymbol{k}}(5+\gamma_{\boldsymbol{k}})\beta\Lambda^3 g^4}{30D^2} - \frac{107\beta\Lambda^3 g^4}{120D^2}\\ =&\frac{\beta\Lambda^2 g^3}{4D^2}(1+\gamma_{\boldsymbol{k}}) + \frac{\beta\Lambda^3 g^4}{30D^2}(19+10\gamma_{\boldsymbol{k}}+\gamma_{\boldsymbol{k}}^2).\end{aligned} \tag{B.161}$$

Integrating this expression over Λ and combining it with our first-order result (B.112), we arrive at the static, zero-field polarization function for $S = 1/2$ to second order in $1/D$,

$$\frac{1}{\beta b'}\Pi^{zz}_{\Lambda=1}(\boldsymbol{k}) = 1 - \frac{g^2(5+\gamma_{\boldsymbol{k}})}{6D} + \frac{g^3(1+\gamma_{\boldsymbol{k}})}{3D^2} + \frac{g^4}{3D^2}\left(\frac{19}{10}+\gamma_{\boldsymbol{k}}+\frac{\gamma_{\boldsymbol{k}}^2}{10}\right). \tag{B.162}$$

Finally, via Eq. (3.135a) we can use this result to derive the $1/D$ expansion of $\Gamma^{zz}_{\Lambda=1}(\boldsymbol{k})$ to second order,

$$\beta b'\Gamma^{zz}_{\Lambda}(\boldsymbol{k}) = 1 - g\gamma_{\boldsymbol{k}} + \frac{g^2(5+\gamma_{\boldsymbol{k}})}{6D} - \frac{g^3(1+\gamma_{\boldsymbol{k}})}{3D^2} + \frac{g^4}{18D^2}\left(\frac{11}{10}-\gamma_{\boldsymbol{k}}-\frac{\gamma_{\boldsymbol{k}}^2}{10}\right). \tag{B.163}$$

Setting $\Gamma^{zz}_{\Lambda=1}(\boldsymbol{k}) = 0$ to compute the critical temperature, we find that a phase transition first occurs for $\gamma_{\boldsymbol{k}}^2 = 1$. This allows us to simplify the g^4 term so that we end up with the quartic equation

$$1 - g\gamma_{\boldsymbol{k}} + \frac{g^2(5+\gamma_{\boldsymbol{k}})}{6D} - \frac{g^3(1+\gamma_{\boldsymbol{k}})}{3D^2} + \frac{g^4}{18D^2}(1-\gamma_{\boldsymbol{k}}) = 0. \tag{B.164}$$

B.3.3 Second-order correction to Γ^{zz}_{Λ} for $S \to \infty$

First-order correction to the irreducible four-point vertex

Having derived the second-order correction to Γ^{zz}_{Λ} in Sec. B.3.2 for the quantum limit $S = 1/2$, it is only natural to also consider the classical limit $S \to \infty$.

Similar to the calculations for the Ising model in Sec. B.1, the classical limit implies that all irreducible vertices with an odd number of external legs vanish and that we do not need to introduce a temporal dependence. We start by considering the flow equation of the irreducible four-point vertex, which to leading order can be written as

$$\partial_\Lambda \left[\tilde{\mathbf{\Phi}}^{(4)}_\Lambda\right]_{\tilde\alpha_1\tilde\alpha_2\tilde\alpha_3\tilde\alpha_4} \approx \left[\mathbf{\Delta}^{(6)}_\Lambda\right]_{\tilde\alpha_1\tilde\alpha_2\tilde\alpha_3\tilde\alpha_4} - \mathcal{S}_{\tilde\alpha_1\tilde\alpha_2;\tilde\alpha_3\tilde\alpha_4}\left[\mathbf{\Delta}^{(4,4)}_\Lambda\right]_{\tilde\alpha_1\tilde\alpha_2\tilde\alpha_3\tilde\alpha_4}. \tag{B.165}$$

Here the tensors $\mathbf{\Delta}^{(6)}_\Lambda$ and $\mathbf{\Delta}^{(4,4)}_\Lambda$ are defined analogously to the $S = 1/2$ case in Sec. B.3.2,

$$\left[\mathbf{\Delta}^{(6)}_\Lambda\right]_{\tilde\alpha_1\tilde\alpha_2\tilde\alpha_3\tilde\alpha_4} \equiv \frac{1}{2}\mathrm{Tr}\left[\dot{\mathbf{F}}_\Lambda \tilde{\mathbf{\Phi}}^{(6)}_{\Lambda,\tilde\alpha_1\tilde\alpha_2\tilde\alpha_3\tilde\alpha_4}\right], \tag{B.166}$$

$$\left[\mathbf{\Delta}^{(4,4)}_\Lambda\right]_{\tilde\alpha_1\tilde\alpha_2\tilde\alpha_3\tilde\alpha_4} \equiv \frac{1}{2}\mathrm{Tr}\left[\dot{\mathbf{F}}_\Lambda \tilde{\mathbf{\Phi}}^{(4)}_{\Lambda,\tilde\alpha_1\tilde\alpha_2}\mathbf{F}_\Lambda\tilde{\mathbf{\Phi}}^{(4)}_{\Lambda,\tilde\alpha_3\tilde\alpha_4}\right]. \tag{B.167}$$

Note that, due to $S \to \infty$, the superindex $\tilde\alpha = (\alpha, i, \tau)$ can now effectively be taken as time independent, which suggests the notation

$$\left[\mathbf{\Delta}^{(x)}_\Lambda\right]_{\tilde\alpha_1\tilde\alpha_2\tilde\alpha_3\tilde\alpha_4} \to \delta(\boldsymbol{k}_1+\boldsymbol{k}_2+\boldsymbol{k}_3+\boldsymbol{k}_4)\Delta^{(x),\alpha_1\alpha_2\alpha_3\alpha_4}_\Lambda(\boldsymbol{k}_1,\boldsymbol{k}_2,\boldsymbol{k}_3) \tag{B.168}$$

for the tensor components in Fourier space. It is implied that these tensor components as well as the irreducible vertices are properly normalized with respect to β and S to render them dimensionless and finite; the last point also applies to derivatives of the Brillouin function so that, e.g.,

$$b' = \frac{S(S+1)}{3} \to \frac{1}{S^2}b' = \frac{1+1/S}{3} \sim \frac{1}{3}. \tag{B.169}$$

Contribution from $\mathbf{\Delta}^{(6)}_\Lambda$ We first consider $\mathbf{\Delta}^{(6)}_\Lambda$, for which we find

$$\begin{aligned}\sum_\alpha \Delta^{(6),\alpha\alpha zz}_\Lambda(\boldsymbol{q},-\boldsymbol{q},\boldsymbol{k}) &\approx \frac{1}{2}\sum_{\alpha\gamma}\int_{\boldsymbol{p}} \frac{\beta V_{\boldsymbol{p}}\tilde\Phi^{\gamma\gamma\alpha\alpha zz}_0(\boldsymbol{p},-\boldsymbol{p},\boldsymbol{q},-\boldsymbol{q},\boldsymbol{k})}{[1-\Lambda b'\beta V_{\boldsymbol{p}}]^2} \\ &\approx \frac{\Lambda g^2}{2b'D}\sum_{\alpha\gamma}\tilde\Phi^{\gamma\gamma\alpha\alpha zz}_0 = -\frac{8\Lambda g^2}{9D}.\end{aligned} \tag{B.170}$$

Here we have introduced the notation

$$\tilde\Phi^{\alpha_1\ldots\alpha_n}_0 \equiv \tilde\Phi^{\alpha_1\ldots\alpha_n}_0(\boldsymbol{k}_1=0,\ldots,\boldsymbol{k}_{n-1}=0). \tag{B.171}$$

Contribution from $\boldsymbol{\Delta}^{(4,4)}_{\Lambda}$ From our previous calculation (B.126) we already know that in general

$$\Delta^{(4,4),\alpha_1\alpha_2\alpha_3\alpha_4}_{\Lambda}(\boldsymbol{k}_1,\boldsymbol{k}_2,\boldsymbol{k}_3) \approx \frac{\Lambda g^2 \gamma_{\boldsymbol{k}_1+\boldsymbol{k}_2}}{4(b')^2 D} \sum_{\gamma\delta} \tilde{\Phi}^{\gamma\delta\alpha_1\alpha_2}_0 \tilde{\Phi}^{\delta\gamma\alpha_3\alpha_4}_0. \tag{B.172}$$

Specifying

$$\Delta^{(4,4),\alpha_1\alpha_2\alpha_3\alpha_4}_{\Lambda}(\boldsymbol{k}_1,\boldsymbol{k}_2,\boldsymbol{k}_3) = \Delta^{(4,4),\alpha\alpha zz}_{\Lambda}(\boldsymbol{q},-\boldsymbol{q},\boldsymbol{k}), \tag{B.173}$$

we find that the fully symmetrized contribution reads

$$\begin{aligned}
&\sum_{\alpha} \mathcal{S}_{\tilde{\alpha}_1\tilde{\alpha}_2;\tilde{\alpha}_3\tilde{\alpha}_4}\, \Delta^{(4,4),\alpha\alpha zz}_{\Lambda}(\boldsymbol{q},-\boldsymbol{q},\boldsymbol{k}) \\
\approx&\frac{\Lambda g^2}{2(b')^2 D} \sum_{\alpha\gamma\delta} \left[\tilde{\Phi}^{\gamma\delta\alpha\alpha}_0 \tilde{\Phi}^{\delta\gamma zz}_0 + (\gamma_{\boldsymbol{q}+\boldsymbol{k}} + \gamma_{\boldsymbol{q}-\boldsymbol{k}}) \tilde{\Phi}^{\gamma\delta\alpha z}_0 \tilde{\Phi}^{\delta\gamma\alpha z}_0 \right] \\
=&\frac{2\Lambda g^2}{9D} \left[1 + \frac{3}{5}(\gamma_{\boldsymbol{q}+\boldsymbol{k}} + \gamma_{\boldsymbol{q}-\boldsymbol{k}}) \right].
\end{aligned} \tag{B.174}$$

Second-order contribution to the flow of Π^{zz}_{Λ} from the leading correction to $\tilde{\boldsymbol{\Phi}}^{(4)}_{\Lambda}$ In total we thus find

$$\sum_{\alpha} \partial_{\Lambda} \tilde{\Phi}^{\alpha\alpha zz}_{\Lambda}(\boldsymbol{q},-\boldsymbol{q},\boldsymbol{k}) \approx -\frac{2\Lambda g^2}{9D} \left[5 + \frac{3}{5}(\gamma_{\boldsymbol{q}+\boldsymbol{k}} + \gamma_{\boldsymbol{q}-\boldsymbol{k}}) \right], \tag{B.175}$$

which integrates to

$$\sum_{\alpha} \left[\tilde{\Phi}^{\alpha\alpha zz}_{\Lambda}(\boldsymbol{q},-\boldsymbol{q},\boldsymbol{k}) - \tilde{\Phi}^{\alpha\alpha zz}_0 \right] \approx -\frac{\Lambda^2 g^2}{9D} \left[5 + \frac{3}{5}(\gamma_{\boldsymbol{q}+\boldsymbol{k}} + \gamma_{\boldsymbol{q}-\boldsymbol{k}}) \right]. \tag{B.176}$$

According to Eq. (B.122), the total second-order contribution to the flow of $\Pi^{zz}_{\Lambda}(\boldsymbol{k})$ from this first-order correction is then given by

$$\begin{aligned}
&-\frac{1}{2} \sum_{\alpha} \int_{\boldsymbol{q}} \beta V_{\boldsymbol{q}} \tilde{\Phi}^{\alpha\alpha zz}_{\Lambda}(\boldsymbol{q},-\boldsymbol{q},\boldsymbol{k}) - \Lambda b' \sum_{\alpha} \int_{\boldsymbol{q}} \beta^2 V^2_{\boldsymbol{q}} \left[\tilde{\Phi}^{\alpha\alpha zz}_{\Lambda}(\boldsymbol{q},-\boldsymbol{q},\boldsymbol{k}) - \tilde{\Phi}^{\alpha\alpha zz}_0 \right] \\
\approx&\frac{\Lambda^2 g^3 \gamma_{\boldsymbol{k}}}{10D^2} + \frac{5\Lambda^3 g^4}{6D^2}.
\end{aligned} \tag{B.177}$$

Second-order contribution from the denominator

It now remains to evaluate the contribution from the denominator of the first term in Eq. (B.103),

$$
\begin{aligned}
&-\frac{1}{2}\sum_{\alpha}\int_{\boldsymbol{q}}\frac{\beta V_{\boldsymbol{q}}\tilde{\Phi}_0^{\alpha\alpha zz}(\boldsymbol{q},-\boldsymbol{q},\boldsymbol{k})}{[1-\Lambda\beta V_{\boldsymbol{q}}\Pi_\Lambda^{\alpha\alpha}(\boldsymbol{q})]^2}\\
\approx&-\sum_{\alpha}\tilde{\Phi}_0^{\alpha\alpha zz}\int_{\boldsymbol{q}}\beta V_{\boldsymbol{q}}\left[\Lambda\beta V_{\boldsymbol{q}}\Pi_\Lambda^{zz}(\boldsymbol{q})+2(\Lambda b'\beta V_{\boldsymbol{q}})^3\right]\\
\approx&-\frac{2\Lambda b'}{9}\int_{\boldsymbol{q}}\beta^2V_{\boldsymbol{q}}^2\left[1-\frac{\Lambda^2g^2}{2D}+2(\Lambda b'\beta V_{\boldsymbol{q}})^2\right]\\
\approx&-\frac{\Lambda g^2}{3D}+\frac{\Lambda^3g^4}{6D^2}-\frac{\Lambda^3g^4}{D^2}=-\frac{\Lambda g^2}{3D}-\frac{5\Lambda^3g^4}{6D^2},
\end{aligned}
\tag{B.178}
$$

where we have used Eq. (B.67) as well as our first-order result (B.112).

Total second-order contribution to the flow of $\Pi_\Lambda^{zz}(\boldsymbol{k})$

The total second-order contribution to the flow of $\Pi_\Lambda^{zz}(\boldsymbol{k})$ thus reads

$$
\frac{\Lambda^2g^3\gamma_{\boldsymbol{k}}}{10D^2}+\frac{5\Lambda^3g^4}{6D^2}-\frac{5\Lambda^3g^4}{6D^2}=\frac{\Lambda^2g^3\gamma_{\boldsymbol{k}}}{10D^2},
\tag{B.179}
$$

so that the static, zero-field polarization function for $S=\infty$ is to second order in $1/D$ given by

$$
\Pi_{\Lambda=1}^{zz}(\boldsymbol{k})\approx b'\left[1-\frac{g^2}{2D}+\frac{g^3\gamma_{\boldsymbol{k}}}{10D^2}\right].
\tag{B.180}
$$

Inverting this expression and using the relation (3.135a) yields

$$
\Gamma_\Lambda^{zz}(\boldsymbol{k})+\beta V_{\boldsymbol{k}}=\frac{1}{b'}\left[1+\frac{g^2}{2D}-\frac{g^3\gamma_{\boldsymbol{k}}}{10D^2}+\frac{g^4}{4D^2}\right],
\tag{B.181}
$$

which together with the condition $\Gamma_\Lambda^{zz}(\boldsymbol{k})=0$ for a phase transition results in the quartic equation

$$
1-g\gamma_{\boldsymbol{k}}+\frac{g^2}{2D}-\frac{g^3\gamma_{\boldsymbol{k}}}{10D^2}+\frac{g^4}{4D^2}=0.
\tag{B.182}
$$

Appendix C

Deutsche Zusammenfassung

C.1 Renormierungsgruppe

Da sich die vorliegende Arbeit hauptsächlich mit der Anwendung der Renormierungsgruppe (RG) auf Spinsysteme beschäftigt, soll diese Methode hier kurz vorgestellt werden. Da die RG konzeptionell sehr stark durch die Arbeiten von Wilson geprägt wurde [19–22, 28, 29] und die in Kap. 2 und 3 benötigten Methoden der modernen funktionalen Renormierungsgruppe (FRG) dort konkret hergeleitet werden, soll im Folgenden insbesondere auf die Wilsonsche RG eingegangen werden. Die grundlegende Idee ist, ausgehend von einem mikroskopischen Modell iterativ Freiheitsgrade zu eliminieren. Dabei besteht eine Iteration jeweils aus zwei Schritten: Dezimierung und Reskalierung. Im ersten Schritt findet eine Reduktion der Freiheitsgrade statt, indem wir diese ausintegrieren oder eine partielle Spur berechnen. Intuitiv lässt sich dieser Vorgang so vorstellen, dass man das System mittels der RG durch ein Mikroskop betrachtet und schrittweise "herauszoomt", um schließlich Informationen über die makroskopische Eigenschaften des Systems zu erhalten. Nach der Dezimierung ist es nötig, alle Längenskalen so zu reskalieren, dass die Gitterkonstante wieder ihren ursprünglichen Wert annimmt. Durch diesen zweiten Schritt ist es möglich Fixpunkte zu finden, an denen sich das System invariant bezüglich der kombinierten Wirkung von Dezimierung und Reskalierung verhält. Eine anschauliche Darstellung dieser beiden Schritte im Ortsraum ist in Abb. C.1 gezeigt.

Allerdings hat sich gezeigt, dass es in der Praxis nützlicher ist, im Impulsraum zu arbeiten. In der einfachsten Variante eines harten Cutoffs unterteilt man die Fourierkomponenten der relevanten Felder φ in einen makroskopischen Teil $\varphi^{<}_{\Lambda_0}$ und einen mikroskopischen Teil $\varphi^{>}_{\Lambda_0}$,

$$\varphi(\boldsymbol{k}) = \varphi^{<}_{\Lambda_0}(\boldsymbol{k}) + \varphi^{>}_{\Lambda_0}(\boldsymbol{k}). \tag{C.1}$$

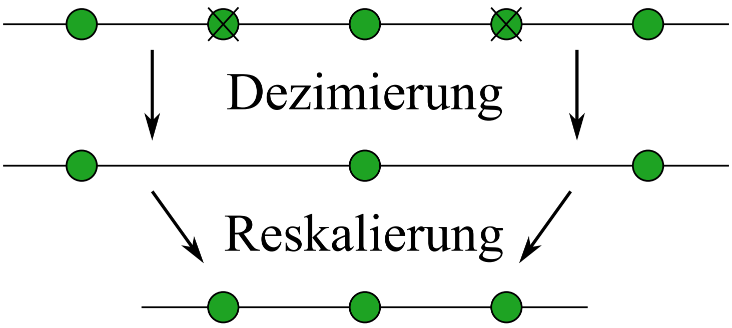

Abbildung C.1: Schematische Darstellung der beiden RG-Schritte im Ortsraum.

Die Unterteilung erfolgt dabei durch den Cutoff Λ_0 mittels der Heaviside-Funktion,

$$\begin{aligned} \varphi^{<}_{\Lambda_0}(\boldsymbol{k}) &= \Theta(\Lambda_0 - |\boldsymbol{k}|)\varphi(\boldsymbol{k}), \\ \varphi^{>}_{\Lambda_0}(\boldsymbol{k}) &= \Theta(|\boldsymbol{k}| - \Lambda_0)\varphi(\boldsymbol{k}). \end{aligned} \tag{C.2}$$

Indem wir zu Beginn nur über den mikroskopischen Teil $\varphi^{>}_{\Lambda_0}$ integrieren, erhalten wir eine Formulierung des Systems bezüglich der Impulsskala Λ_0; mathematisch drückt sich dies durch die Wirkung $S_{\Lambda_0}[\varphi^{<}_{\Lambda_0}, \boldsymbol{g}_{\Lambda_0}]$ aus, wobei der Vektor $\boldsymbol{g}_{\Lambda_0}$ alle vorkommenden Kopplungskonstanten beinhaltet. Der RG-Schritt der Dezimierung lässt sich nun dadurch definieren, dass wir eine zweite Impulsskala $\Lambda < \Lambda_0$ einführen und nur die Freiheitsgrade ausintegrieren, deren Impuls in das Intervall $[\Lambda, \Lambda_0]$ fällt, wodurch wir die neue Wirkung $S_\Lambda[\varphi^{<}_{\Lambda}, \boldsymbol{g}_\Lambda]$ erhalten. Grundsätzlich entspricht dies der in Kap. 2 verfolgten Strategie, wobei die dort verwendete technische Durchführung mittels eines Litim-Regulators eine effizientere Version des harten Cutoffs darstellt. Der Reskalierungsschritt lässt sich nun einfach durchführen, indem wir reskalierte Impulse

$$\tilde{\boldsymbol{k}} = b\boldsymbol{k} \tag{C.3}$$

und reskalierte Felder

$$\tilde{\varphi}(\tilde{\boldsymbol{k}}) = b^{D_\varphi}\sqrt{Z_b}\varphi(\boldsymbol{k}) \tag{C.4}$$

einführen mit $b = \Lambda_0/\Lambda > 1$. Während sich der Exponent D_φ aus einer einfachen Dimensionsanalyse ergibt, ist die Berechnung von Z_b nichttrivial, da in diesen Faktor Wechselwirkungseffekte einfließen. Zuletzt drücken wir die Wirkung $S_\Lambda[\varphi^{<}_{\Lambda}, \boldsymbol{g}_\Lambda]$ durch die reskalierten Größen aus und bringen die Wirkung in dieselbe Form, die sie vor der Dezimierung hatte. Diese Forderung definiert impliziert die reskalierten Kopplungskonstanten $\tilde{\boldsymbol{g}}_\Lambda$. Daher lässt sich eine einzelne Iteration der RG auch als Funktion darstellen, die Punkte im Raum aller möglichen Kopplungskonstanten aufeinander abbildet. Für infinitesimal kleine Schritte beschreibt die sukzessive Anwendung der RG daher eine Kurve in diesem Raum, was als Fluss der Kopplungskonstanten bezeichnet wird. Ein Beispiel für den Fluss in einem zweidimensionalen Unterraum ist im nächsten Abschnitt in Abb. C.4 dargestellt.

Der letzte wichtige Teil betrifft die Existenz von Fixpunkten. Diese zeichnen sich dadurch aus, dass die dazugehörigen Kopplungskonstanten $\boldsymbol{g}^*$ durch eine Iteration der RG auf sich selbst abgebildet werden. Da die reskalierte Korrelationslänge durch

$$\tilde{\xi} = \frac{\xi}{b} \tag{C.5}$$

gegeben ist und wir an einem Fixpunkt $\xi = \tilde{\xi}$ fordern, folgt sofort die wichtige Erkenntnis, dass die Korrelationslänge an einem Fixpunkt entweder verschwindet oder divergiert. Letzterer Fall tritt bei kontinuierlichen Phasenübergängen wie dem Berezinkskii-Kosterlitz-Thouless-Phasenübergang auf, der im nächsten Abschnitt betrachtet wird. Betrachtet man nun das Verhalten der Kopplungskonstanten in der Nähe eines solchen kritischen Fixpunktes, so findet man üblicherweise, dass fast alle Kopplungskonstanten gegen Null fließen; diese werden daher als irrelevant bezüglich des betrachteten Fixpunkts bezeichnet. Zur Berechnung der universellen Eigenschaften des kritischen Fixpunktes ist es daher ausreichend, nur eine kleine Untermenge an Kopplungskonstanten zu betrachten. Diese Tatsache wird explizit in Kap. 2 ausgenutzt, was dort eine analytische Betrachtung ermöglicht.

C.2 Berezinkskii-Kosterlitz-Thouless-Phasenübergang

Im zweiten Kapitel dieser Arbeit betrachten wir den BKT-Phasenübergang, der nach Berezinkskii, Kosterlitz und Thouless benannt ist [48–52]. Das einfachste Modell zur Beschreibung dieses kontinuierlichen Phasenübergangs ist das zweidimensionale XY-Modell

$$H_{XY} = -J \sum_{i,\mu} \boldsymbol{s}_i \cdot \boldsymbol{s}_{i+\mu} = -J \sum_{i,\mu} \cos(\theta_{i+\mu} - \theta_i). \tag{C.6}$$

Dieses besteht aus klassischen Spins $\boldsymbol{s}_i = \boldsymbol{e}_x \cos\theta_i + \boldsymbol{e}_y \sin\theta_i$ mit fester Länge, die auf den Gitterplätzen $\boldsymbol{r}_i$ eines quadratischen Gitters befestigt sind und die

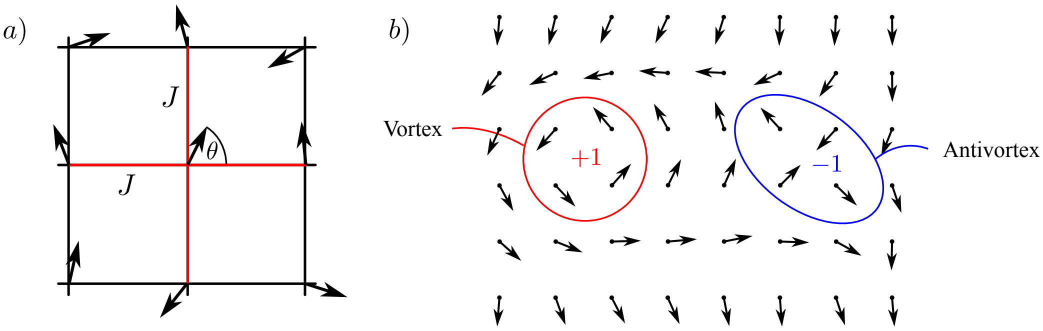

Abbildung C.2: (a) Schematische Darstellung des XY-Modells. Die durch den Polarwinkel θ parametrisierten klassischen Spins (schwarze Pfeile) wechselwirken über die Nächste-Nachbar-Wechselwirkung J (rote Linien, gezeigt für den zentralen Spin) miteinander. (b) Beispiel für eine Spinkonfiguration, die einen Vortex mit Vortizität $q = 1$ und einen Antivortex mit Vortizität $q = -1$ aufweist.

über eine Nächste-Nachbar-Wechselwirkung $J > 0$ miteinander wechselwirken. Eine graphische Darstellung dieses Systems ist in Abb. C.2a) gezeigt. Während das System offensichtlich einen ferromagnetischen Grundzustand besitzt, ist eine langreichweitige Ordnung bei endlichen Temperaturen aufgrund des Mermin-Wagner-Theorems [47] nicht möglich. Dies schließt jedoch nicht die Existenz eines kontinuierlichen Phasenübergangs aus, wie wir im Folgenden sehen werden. Dazu ist es nötig, das emergente Phänomen von Vortizes und Antivortizes zu betrachten.

Intuitiv bezeichnen diese eine spezielle Konfiguration der Spins, bei der diese kreisförmig um einen zentralen Punkt ausgerichtet sind [siehe Skizze in Abb. C.2b)]. Mathematisch ist es nützlich, die ganzzahlige Vortizität q einzuführen: Dabei entsprechen Vortizes einer positiven Vortizität, während für Antivortizes $q < 0$ gilt. Wie in Abb. C.2b) zu sehen ist, heben sich die Effekte von Vortizes und Antivortizes gleicher Vortizität für größere Abstände auf, was die Interpretation von q als Ladung nahelegt. Damit lässt sich nun der BKT-Phasenübergang qualitativ beschreiben: Für kleine Temperaturen $T < T_c$ liegen Vortizes und Antivortizes nur in eng gebundenen Paaren von verschwindender Vortizität vor. Diese Phase weist eine quasi-langreichweitige Ordnung auf, bei der die Spin-Spin-Korrelation für große Abstände mit einem Potenzgesetz abfällt [Abb. C.3a)]. Erst bei der kritischen Temperatur T_c werden die größten Vortex-Antivortex-Paare aufgebrochen, sodass für $T > T_c$ ungebundene Vortizes und Antivortizes energetisch möglich sind. Dies führt dazu, dass die Spin-Spin-Korrelation für große Distanzen exponentiell abfällt, was einer ungeordneten Phase entspricht [Abb. C.3b)].

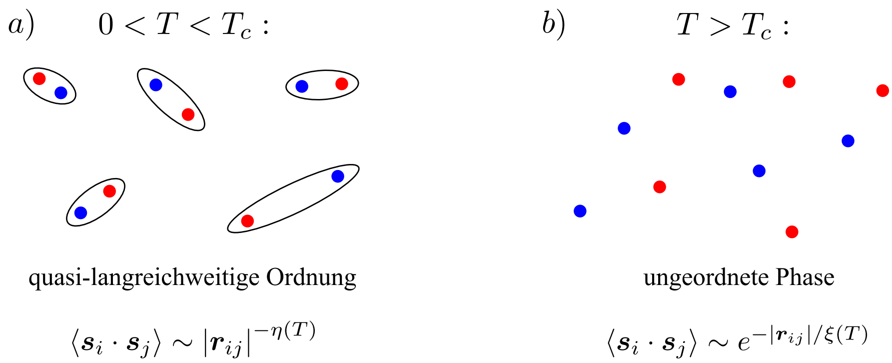

Abbildung C.3: Intuitive Darstellung des BKT-Phasenübergangs. (a) Bei hinreichend niedrigen Temperaturen liegen Vortizes (rote Punkte) und Antivortizes (blaue Punkte) nur in eng gebundenen Paaren vor. Das langreichweitige Verhalten der Spin-Spin-Korrelationsfunktion entspricht daher einem Potenzgesetz und wird durch die anomale Dimension $\eta(T)$ charakterisiert. (b) Für $T > T_c$ ist die Existenz von freien Vortizes und Antivortizes möglich. Dies führt zu einem exponentiellen Verhalten der Spin-Spin-Korrelationsfunktion mit einer endlichen Korrelationslänge $\xi(T)$.

In der Sprache der RG lässt sich dieser Phasenübergang durch das Verhalten der Kopplungskonstanten $\tilde{y}_l$ und τ_l charakterisieren, wobei erstere der reskalierten Vortex-Fugazität und letztere der dimensionslosen Temperatur entspricht. Deren Fluss wird durch die Kosterlitz-Thouless-Renormierungsgruppengleichungen

$$\partial_l \tilde{y}_l = (2 - \pi/\tau_l)\tilde{y}_l, \tag{C.7}$$

$$\partial_l \tau_l = \frac{\tilde{y}_l^2}{8\pi}, \tag{C.8}$$

beschrieben; das entsprechende Flussdiagramm in der Nähe des BKT-Phasenübergangs ist in Abb. C.4 gezeigt. Ursprünglichen wurden die Kosterlitz-Thouless-Flussgleichungen mithilfe einer spezifischen Formulierung der RG im Ortsraum hergeleitet [51–53]; dieser Zugang hat allerdings den Nachteil, dass er recht schwierig auf andere Probleme verallgemeinerbar ist. Der erste Teil von Kap. 2 beschäftigt sich daher mit der Herleitung dieser Flussgleichungen innerhalb der FRG, wozu wir im Impulsraum arbeiten und den weitverbreiteten Litim-Regulator [77] verwenden. Die Grundlage bildet dabei Abschn. 2.2, wo wir das XY-Modell durch das Villain-Modell [67] nähern und mittels mehrerer Transformationen eine duale Darstellung dessen herleiten. Das resultierende “Dual-Vortex”-Modell wird durch die

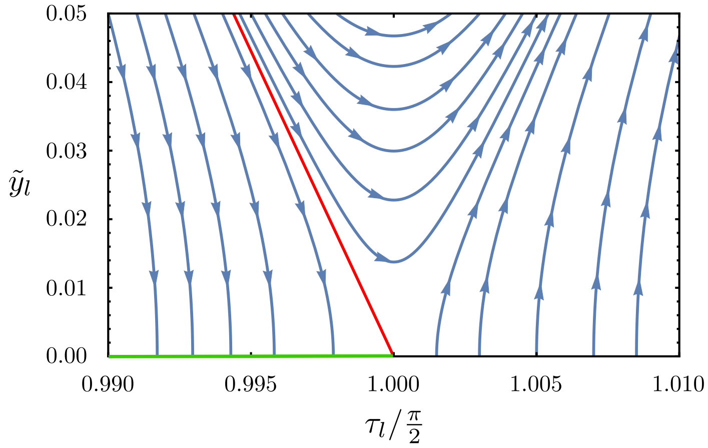

Abbildung C.4: Flussdiagramm für die Kosterlitz-Thouless-Renormierungsgruppengleichungen (C.7) und (C.8), die den Fluss der Vortex-Fugazität $\tilde{y}_l$ und der dimensionslosen Temperatur τ_l beschreiben. Auf der linken Seite der Separatrix (rote Linie) fließt das System in das Kontinuum an Gaußschen Fixpunkten (grüne Linie), was der quasi-langreichweitig geordneten Phase bei niedrigen Temperaturen entspricht. Die ungeordnete Phase bei hohen Temperaturen entspricht dem rechten Bereich, wo $\tilde{y}_l$ und τ_l divergieren. (Abbildung übernommen aus Ref. [54])

Zustandssumme

$$Z_{\text{Villain}} = \prod_i \left(\sum_{m_i=-\infty}^{\infty} \right) e^{-S_{\text{dual}}[m]} \tag{C.9}$$

mit der Wirkung

$$S_{\text{dual}}[m] = \frac{\tau}{2} \sum_{i,\mu} (\Delta_\mu m_i)^2 = \frac{1}{2} \sum_{\boldsymbol{k}} \omega_{\boldsymbol{k}} \left| m_{\boldsymbol{k}} \right|^2 \tag{C.10}$$

beschrieben. Das auffällige an dieser Darstellung ist, dass das Feld m_i nur ganzzahlige Werte annehmen kann, sodass wir die übliche Formulierung der FRG mittels Funktionalintegralen nicht anwenden können. Daher verwenden wir die von Machado und Dupuis entwickelte Gitter-FRG [76], die auch für ganzzahlige Felder gültig ist. Dazu regularisieren wir die Wirkung,

$$S_\lambda[m] = \frac{1}{2} \sum_{\boldsymbol{k}} \left[\omega_{\boldsymbol{k}} + R_\lambda(\boldsymbol{k}) \right] \left| m_{\boldsymbol{k}} \right|^2 , \tag{C.11}$$

wobei der Litim-Regulator gegeben ist durch

$$R_\lambda(\boldsymbol{k}) = (\lambda - \omega_{\boldsymbol{k}}) \Theta(\lambda - \omega_{\boldsymbol{k}}). \tag{C.12}$$

Diese Wahl hat den Vorteil, dass die Felder m_i bei der Anfangsskala

$$\lambda_0 = \max_{\boldsymbol{k}} \omega_{\boldsymbol{k}} = 8\tau \tag{C.13}$$

vollständig entkoppeln,

$$S_{\lambda_0}[m] = \frac{\lambda_0}{2} \sum_{\boldsymbol{k}} |m_{\boldsymbol{k}}|^2 = \frac{\lambda_0}{2} \sum_i m_i^2, \tag{C.14}$$

sodass wir für die Anfangsbedingung nur einen einzelnen isolierten Gitterpunkt betrachten müssen. Dies ermöglicht die analytische Herleitung der Kosterlitz-Thouless-Flussgleichungen (C.7) und (C.8), was wir in Abschn. 2.4 mittels der "vertex expansion" und in Abschn. 2.5 mittels der "derivative expansion" zeigen. Schließlich verallgemeinern wir unsere Methode in Abschn. 2.6 und 2.7 auf das $O(2)$-Modell sowie auf das stark anisotrope XXZ-Modell. Dies ermöglicht uns zu zeigen, dass schwache Amplitudenfluktuationen sowie schwache Auslenkungen aus der xy-Ebene in der Nähe des BKT-Phasenübergangs nur zu nicht-universellen Änderungen führen, sodass der Phasenübergang erhalten bleibt und in der gleichen Universalitätsklasse wie der des XY-Modells liegt.

C.3 Funktionale Renormierungsgruppe für Spinsysteme

Der letzte Teil der vorliegenden Arbeit beschäftigt sich mit der Entwicklung einer neuen Formulierung der FRG für Spinsysteme. Aufgrund der nichttrivialen Kommutationsrelation für quantenmechanische Spinoperatoren,

$$\left[S^\alpha, S^\beta\right] = i\epsilon^{\alpha\beta\gamma} S^\gamma, \tag{C.15}$$

lässt sich die übliche Formulierung der FRG für bosonische oder fermionische Felder nicht direkt auf diese übertragen. Bisher wurde dieses Problem dadurch gelöst, dass man die Spinoperatoren auf bosonische oder fermionische Freiheitsgrade abbildet und die FRG für das resultierende Modell löst, was in der Praxis allerdings mit verschiedenen Näherungen verbunden ist.

Einer der Hauptvorteile der in Kap. 3 vorgestellten Spin-FRG (SFRG) liegt daher in der Tatsache, dass diese direkt über die Spinoperatoren selbst formuliert ist. Möglich ist dies dadurch, dass Spinoperatoren an verschiedenen Gitterplätzen miteinander kommutieren, sodass die imaginärzeitgeordneten Spinkorrelationsfunktionen bosonische Kubo-Martin-Schwinger-Randbedingungen erfüllen. Die $\mathfrak{su}(2)$-Algebra der Spinoperatoren wird dabei komplett über die Anfangsbedingungen des FRG-Flusses berücksichtigt, welche daher eine vergleichsweise hohe Komplexität aufweisen. Indem wir einen Cutoff Λ in das generierende Funktional der zusammenhängenden imaginärzeitgeordneten Spinkorrelationsfunktionen einführen, welches durch eine Spur über den gesamten Spinraum definiert ist, können wir in Abschn. 3.2 durch einfaches Ableiten nach Λ eine exakte Flussgleichung für dieses generierende Funktional herleiten. Ausgehend davon folgen wir der üblichen Formulierung der FRG, um mittels Legendretransformation eine exakte Flussgleichung für das generierende Funktional der irreduziblen Vertizes zu erhalten,

$$\partial_\Lambda \tilde{\Gamma}_\Lambda[\boldsymbol{\eta}] = \frac{1}{2} \operatorname{Tr} \left\{ \left(\tilde{\mathbf{\Gamma}}''_\Lambda[\boldsymbol{\eta}] + \mathbf{R}_\Lambda \right)^{-1} \partial_\Lambda \mathbf{R}_\Lambda \right\} + \int_0^\beta \sum_i \frac{\delta \tilde{\Gamma}_\Lambda[\boldsymbol{\eta}]}{\delta \eta_i^z(\tau)} \partial_\Lambda \bar{M}_\Lambda. \quad \text{(C.16)}$$

Diese entspricht in ihrer Form exakt der Wetterichgleichung [34] für bosonische Felder. Um ein konkretes Beispiel für die Struktur der SFRG zu geben, wenden wir diese daraufhin auf das Spin-S Ising-Modell an und demonstrieren zwei verschiedene Methoden zur Berechnung der kritischen Temperatur T_c.

In Abschn. 3.3 zeigen wir, dass sich mittels einer Hubbard-Stratonovich-Transformation eine alternative Variante der SFRG herleiten lässt. Neben der Tatsache, dass diese eine einfachere Form der Anfangsbedingungen für quantenmechanische Spinsysteme erlaubt, stellt sie auch eine direkte Verbindung zum spindiagrammatischen Formalismus von Vaks, Larkin und Pikin (VLP) [1–3] her. Als Demonstration dessen zeigen wir explizit anhand der freien Energie und der longitudinalen Polarisationsfunktion, wie sich die von VLP berechneten führenden Korrekturen bezüglich einer Entwicklung in der inversen Wechselwirkungsreichweite innerhalb der SFRG herleiten lassen. Darüber hinausgehend nutzen wir die Hubbard-Stratonovich-SFRG außerdem, um die kritische Temperatur für das quantenmechanische Spin-S Heisenberg-Modell mit ferromagnetischer sowie antiferromagnetischer Austauschwechselwirkung zu erhalten.

Abschließend entwickeln wir in Abschn. 3.4 eine weitere Variante der SFRG, bei der die Hubbard-Stratonovich-Transformation nur im longitudinalen Kanal durchgeführt wird. Diese Hybrid-SFRG sollte insbesondere in der geordneten Phase von Vorteil sein, da in diesem Fall eine unterschiedliche Behandlung von transversalen und longitudinalen Fluktuationen naheliegt.

Bibliography

[1] V. G. Vaks, A. I. Larkin, and S. A. Pikin, Sov. Phys. JETP **26**, 188 (1968).

[2] V. G. Vaks, A. I. Larkin, and S. A. Pikin, Sov. Phys. JETP **26**, 647 (1968).

[3] Y. A. Izyumov and Y. N. Skryabin, *Statistical Mechanics of Magnetically Ordered Systems* (Consultants Bureau, New York, 1988).

[4] P. Dirac, Proc. Roy. Soc. **114**, 243 (1927).

[5] V. F. Weisskopf, Phys. Today **34**, 69 (1981).

[6] J. R. Oppenheimer, Phys. Rev. **35**, 461 (1930).

[7] W. E. Lamb and R. C. Retherford, Phys. Rev. **72**, 241 (1947).

[8] H. A. Bethe, Phys. Rev. **72**, 339 (1947).

[9] N. M. Kroll and W. E. Lamb, Phys. Rev. **75**, 388 (1949).

[10] J. B. French and V. F. Weisskopf, Phys. Rev. **75**, 1240 (1949).

[11] F. J. Dyson, Phys. Rev. **75**, 486 (1949).

[12] M. Gell-Mann, Phys. Lett. **8**, 214 (1964).

[13] G. Zweig, CERN preprint 8419/TH.412 (1964).

[14] N. N. Bogoljubov and D. V. Širkov, Nuovo Cimento **3**, 845 (1956).

[15] E. C. G. Stueckelberg and A. Petermann, Helv. Phys. Acta **24**, 317 (1951).

[16] E. C. G. Stueckelberg and A. Petermann, Helv. Phys. Acta **26**, 499 (1953).

[17] M. Gell-Mann and F. E. Low, Phys. Rev. **95**, 1300 (1954).

[18] D. J. Gross, Proc. Natl. Acad. Sci. U.S.A. **102**, 9099 (2005).

[19] K. G. Wilson, Phys. Rev. B **4**, 3174 (1971).

[20] K. G. Wilson, Phys. Rev. B **4**, 3184 (1971).

[21] K. G. Wilson and J. Kogut, Phys. Rep. **12**, 75 (1974).

[22] E. Brézin, J. Stat. Phys. **157**, 644 (2014).

[23] L. P. Kadanoff, Physics Physique Fizika **2**, 263 (1966).

[24] J. Polchinski, Nucl. Phys. B **231**, 269 (1984).

[25] D. J. Gross and F. Wilczek, Phys. Rev. Lett. **30**, 1343 (1973).

[26] H. D. Politzer, Phys. Rev. Lett. **30**, 1346 (1973).

[27] G. 't Hooft, Nucl. Phys. B Proc. Suppl. **74**, 413 (1999).

[28] K. G. Wilson, Adv. Math. **16**, 170 (1975).

[29] K. G. Wilson, Rev. Mod. Phys. **47**, 773 (1975).

[30] P. W. Anderson, G. Yuval, and D. R. Hamann, Phys. Rev. B **1**, 4464 (1970).

[31] P. W. Anderson, J. Phys. C **3**, 2436 (1970).

[32] F. J. Wegner and A. Houghton, Phys. Rev. A **8**, 401 (1973).

[33] P. Kopietz, L. Bartosch, and F. Schütz, *Introduction to the Functional Renormalization Group* (Springer, Berlin, 2010).

[34] C. Wetterich, Phys. Lett. B **301**, 90 (1993).

[35] B. Delamotte, Am. J. Phys. **72**, 170 (2004).

[36] A. Migdal, Sov. Phys. JETP **42**, 743 (1975).

[37] L. P. Kadanoff, Ann. Phys. **100**, 359 (1976).

[38] T. Matsubara, Prog. Theor. Phys. **14**, 351 (1955).

[39] J. A. Hertz, Phys. Rev. B **14**, 1165 (1976).

[40] F. Reinert and S. Hüfner, New J. Phys. **7**, 97 (2005).

[41] W. Nolting, *Grundkurs Theoretische Physik 7: Viel-Teilchen-Theorie* (Springer, Berlin, 2009).

[42] E. Fermi, *Nuclear Physics* (University of Chicago Press, Chicago, 1950).

[43] G. C. Wick, Phys. Rev. **96**, 1124 (1954).

[44] G. Baym and N. D. Mermin, J. Math. Phys **2**, 232 (1961).

[45] J. Rammer, *Quantum Field Theory of Non-equilibrium States* (Cambridge University Press, Cambridge, 2007).

[46] G. Cohen, D. R. Reichman, A. J. Millis, and E. Gull, Phys. Rev. B **89**, 115139 (2014).

[47] N. D. Mermin and H. Wagner, Phys. Rev. Lett. **17**, 1133 (1966).

[48] V. L. Berezinskii, Sov. Phys. JETP **32**, 493 (1971).

[49] V. L. Berezinskii, Sov. Phys. JETP **34**, 610 (1972).

[50] J. M. Kosterlitz and D. J. Thouless, J. Phys. C **5**, L124 (1972).

[51] J. M. Kosterlitz and D. J. Thouless, J. Phys. C **6**, 1181 (1973).

[52] J. M. Kosterlitz, J. Phys. C **7**, 1046 (1974).

[53] A. P. Young, J. Phys. C **11**, L453 (1978).

[54] J. Krieg and P. Kopietz, Phys. Rev. E **96**, 042107 (2017).

[55] I. Herbut, *A Modern Approach to Critical Phenomena* (Cambridge University Press, Cambridge, 2007).

[56] D. R. Nelson and J. M. Kosterlitz, Phys. Rev. Lett. **39**, 1201 (1977).

[57] D. J. Bishop and J. D. Reppy, Phys. Rev. Lett. **40**, 1727 (1978).

[58] D. J. Resnick, J. C. Garland, J. T. Boyd, S. Shoemaker, and R. S. Newrock, Phys. Rev. Lett. **47**, 1542 (1981).

[59] Z. Hadzibabic, P. Krüger, M. Cheneau, B. Battelier, and J. Dalibard, Nature **441**, 1118 (2006).

[60] V. Schweikhard, S. Tung, and E. A. Cornell, Phys. Rev. Lett. **99**, 030401 (2007).

[61] R. J. Fletcher, M. Robert-de-Saint-Vincent, J. Man, N. Navon, R. P. Smith, K. G. H. Viebahn, and Z. Hadzibabic, Phys. Rev. Lett. **114**, 255302 (2015).

[62] M. Gräter and C. Wetterich, Phys. Rev. Lett. **75**, 378 (1995).

[63] G. v. Gersdorff and C. Wetterich, Phys. Rev. B **64**, 054513 (2001).

[64] P. Jakubczyk, N. Dupuis, and B. Delamotte, Phys. Rev. E **90**, 062105 (2014).

[65] P. Jakubczyk and W. Metzner, Phys. Rev. B **95**, 085113 (2017). The final published version of this work substantially differs from the original preprint arXiv:1606.04547v1, where the possibility of the destruction of the BKT transition by amplitude fluctuations was discussed in more detail.

[66] N. Defenu, A. Trombettoni, I. Nándori, and T. Enss, Phys. Rev. B **96**, 174505 (2017).

[67] J. Villain, J. Phys. France **36**, 581 (1975).

[68] W. Janke and H. Kleinert, Nucl. Phys. B **270**, 135 (1986).

[69] P. Henrici, *Applied and Computational Complex Analysis*, Vol. 2 (Wiley Classics Library Edition, New York, 1991).

[70] J. V. José, L. P. Kadanoff, S. Kirkpatrick, and D. R. Nelson, Phys. Rev. B **16**, 1217 (1977).

[71] R. Savit, Phys. Rev. B **17**, 1340 (1978).

[72] P. Kopietz, Nucl. Phys. B **595**, 493 (2001).

[73] S. T. Chui and J. D. Weeks, Phys. Rev. B **14**, 4978 (1976).

[74] H. J. F. Knops, Phys. Rev. Lett. **39**, 766 (1977).

[75] W. Janke and K. Nather, Phys. Rev. B **48**, 7419 (1993).

[76] T. Machado and N. Dupuis, Phys. Rev. E **82**, 041128 (2010).

[77] D. F. Litim, Phys. Rev. D **64**, 105007 (2001).

[78] M. Abramowitz and I. A. Stegun, *Handbook of Mathematical Functions* (ninth printing, Dover, New York, 1972) page 576.

[79] J. Berges, N. Tetradis, and C. Wetterich, Phys. Rep. **363**, 223 (2002).

[80] L. Balents, Nature **464**, 199 (2010).

[81] A. Altland and B. Simons, *Condensed Matter Field Theory* (Cambridge University Press, Cambridge, 2010).

[82] H. Bethe, Z. Phys. **71**, 205 (1931).

[83] T. Holstein and H. Primakoff, Phys. Rev. **58**, 1098 (1940).

[84] F. J. Dyson, Phys. Rev. **102**, 1217 (1956).

[85] S. V. Maleev, Sov. Phys. JETP **6**, 776 (1958).

[86] D. P. Arovas and A. Auerbach, Phys. Rev. B **38**, 316 (1988).

[87] A. Auerbach, *Interacting Electrons and Quantum Magnetism* (Springer, Berlin, 1994).

[88] A. A. Abrikosov, Physics Physique Fizika **2**, 5 (1965).

[89] P. Coleman, *Introduction to Many-Body Physics* (Cambridge University Press, Cambridge UK, 2015).

[90] A. M. Tsvelik, Phys. Rev. Lett. **69**, 2142 (1992).

[91] A. Shnirman and Y. Makhlin, Phys. Rev. Lett. **91**, 207204 (2003).

[92] R. R. Biswas, L. Fu, C. R. Laumann, and S. Sachdev, Phys. Rev. B **83**, 245131 (2011).

[93] T. Herfurth, S. Streib, and P. Kopietz, Phys. Rev. B **88**, 174404 (2013).

[94] S. V. Maleev, Sov. Phys. JETP **38**, 613 (1974).

[95] Y. A. Izyumov, N. I. Chaschin, and V. Y. Yushankhai, Phys. Rev. B **65**, 214425 (2002).

[96] V. N. Krivoruchko, Phys. Rev. B **94**, 054434 (2016).

[97] S. G. Ovchinnikov and V. V. Val'kov, *Hubbard Operators in the Theory of Strongly Correlated Electrons* (Imperial College Press, London, 2004).

[98] D. Tarasevych, J. Krieg, and P. Kopietz, Phys. Rev. B **98**, 235133 (2018).

[99] J. Krieg and P. Kopietz, Phys. Rev. B **99**, 060403(R) (2019).

[100] W. Metzner, M. Salmhofer, C. Honerkamp, V. Meden, and K. Schönhammer, Rev. Mod. Phys. **84**, 299 (2012).

[101] J. M. Pawlowski, Ann. Phys. **322**, 2831 (2007).

[102] A. Rançon and N. Dupuis, Phys. Rev. B **83**, 172501 (2011).

[103] A. Rançon and N. Dupuis, Phys. Rev. B **84**, 174513 (2011).

[104] A. Rançon and N. Dupuis, Phys. Rev. A **85**, 063607 (2012).

[105] A. Rançon and N. Dupuis, Phys. Rev. A **86**, 043624 (2012).

[106] A. Rançon, Phys. Rev. B **89**, 214418 (2014).

[107] M. Kröger, J. Non-Newton. Fluid. Mech. **223**, 77 (2015).

[108] H. A. Kramers and G. H. Wannier, Phys. Rev. **60**, 252 (1941).

[109] A. M. Ferrenberg, J. Xu, and D. P. Landau, Phys. Rev. E **97**, 043301 (2018).

[110] P. H. Lundow and K. Markström, Phys. Rev. E **80**, 031104 (2009).

[111] P. Butera and M. Pernici, Phys. Rev. E **86**, 011139 (2012).

[112] W. J. Camp and J. P. Van Dyke, Phys. Rev. B **11**, 2579 (1975).

[113] A. J. Leggett, S. Chakravarty, A. T. Dorsey, M. P. A. Fisher, A. Garg, and W. Zwerger, Rev. Mod. Phys. **59**, 1 (1987).

[114] U. Weiss, *Quantum Dissipative Systems* (World Scientific, Singapore, 2012).

[115] J. Kondo, Prog. Theor. Phys. **32**, 37 (1964).

[116] J. Arnold, *Dimer initial condition for the exact renormalization group for the* Γ*-Heisenberg-Kitaev model*, Master's thesis, Johann Wolfgang Goethe-Universität Frankfurt am Main (2018).

[117] A. Cuccoli, R. Maciocco, and R. Vaia, J. Magn. Magn. Mater. **226-230**, 566 (2001).

[118] A. W. Sandvik, Phys. Rev. Lett. **80**, 5196 (1998).

[119] M. Troyer, F. Alet, and S. Wessel, Braz. J. Phys. **34**, 377 (2004).

[120] R. G. Brown and M. Ciftan, Phys. Rev. Lett. **76**, 1352 (1996).

List of publications

[P1] J. Krieg, P. Lange, L. Bartosch, and P. Kopietz, Phys. Rev. A **91**, 023612 (2015).

[P2] P. Lange, J. Krieg, and P. Kopietz, Phys. Rev. A **93**, 033609 (2016).

[P3] J. Krieg, D. Strassel, S. Streib, S. Eggert, and P. Kopietz, Phys. Rev. B **95**, 024414 (2017).

[P4] J. Krieg, and P. Kopietz, Phys. Rev. E **96**, 042107 (2017).

[P5] A. Sharma, A. Scammell, J. Krieg, and P. Kopietz, Phys. Rev. B **97**, 125113 (2018).

[P6] D. Tarasevych, J. Krieg, and P. Kopietz, Phys. Rev. B **98**, 235133 (2018).

[P7] J. Krieg, and P. Kopietz, Phys. Rev. B **99**, 060403(R) (2019).

The present thesis only covers Refs. [P4] and [P7], while Ref. [P6] is based on the formalism developed in Ch. 3.